



Forschungszentrum Karlsruhe
in der Helmholtz-Gemeinschaft

Wissenschaftliche Berichte
FZKA 7174

A Biomimetic Approach for Synthesizing Artificial Light-Harvesting Systems using Self-Assembly

A. D. Bhise

Institut für Nanotechnologie

Oktober 2005

Forschungszentrum Karlsruhe

in der Helmholtz-Gemeinschaft

Wissenschaftliche Berichte

FZKA 7174

**A Biomimetic Approach for Synthesizing
Artificial Light-Harvesting Systems
using Self-Assembly**

Anil Dnyanoba Bhise

Institut für Nanotechnologie

von der Fakultät für Chemie und Biowissenschaften
der Universität Karlsruhe (TH) genehmigte Dissertation

Forschungszentrum Karlsruhe GmbH, Karlsruhe

2005

Impressum der Print-Ausgabe:

**Als Manuskript gedruckt
Für diesen Bericht behalten wir uns alle Rechte vor**

**Forschungszentrum Karlsruhe GmbH
Postfach 3640, 76021 Karlsruhe**

**Mitglied der Hermann von Helmholtz-Gemeinschaft
Deutscher Forschungszentren (HGF)**

ISSN 0947-8620

urn:nbn:de:0005-071742

**A Biomimetic Approach for Synthesizing
Artificial Light-Harvesting Systems
using Self-Assembly**

Zur Erlangung des akademischen Grades eines

DOKTORS DER NATURWISSENSCHAFTEN

(Dr. rer. nat.)

Der Fakultät für Chemie und Biowissenschaften der

Universität Karlsruhe (TH)

genehmigte

DISSERTATION

von

Anil Dnyanoba Bhise

Aus Kalewadi (bei Pune), Indien

Dekan: Prof. Dr. Manfred Kappes

Referent: Prof. Dr. Dr. Clemens Richert

Korreferent: Prof. Dr. Joachim Podlech

Tag der mündlichen Prüfung: 14. Dezember 2004

Abstract

Photosynthesis is an extremely important process on Earth as it is the only natural source of food and fossil fuel, which fulfil our daily needs. After a certain period, the natural source of food and energy will decrease due to rapid consumption. Therefore, future generations will require alternative food and fuel sources. This represents a strong driving force to do research in construction of artificial light-harvesting (or antenna) systems. Synthetic antennas can be achieved either by covalent or non-covalent approaches by employing different strategies. This work throws light on the non-covalent approach *i. e.* a supramolecular approach in quest of artificial antenna systems wherein self-assembly and self-aggregation are at the focus. Furthermore this approach is biomimetic in nature as it is inspired by the antenna system which operates in green photosynthetic bacteria.

Bacteriochlorophyll-*c*, *d* and *e* we are selected as models for the syntheses of artificial mimics. The supramolecular interactions which are, the ligation of the central Mg atom by the 3¹-hydroxy group of another molecule; cooperative hydrogen bonding of the same OH group to the 13¹-carbonyl group of a third BChl-*c* molecule; and π - π interactions between the macrocycles are responsible for self-assembly of the building blocks or tectons. Well-defined architectures of self-assembling porphyrins find applications in mimicking the functions of light-harvesting. Porphyrins that are equipped with the same functional groups that are responsible for the self-assembly of bacteriochlorophylls-*c*, *d* and *e* within the chlorosomal antenna of some green photosynthetic bacteria, have been selectively synthesized from easily available and cheap starting materials, 10,20-Bis(3,5-di-*t*-butylphenyl)porphinato copper. All the target compounds were obtained after four to eight synthetic steps in good yields by employing different synthetic procedures involving also novel reactions. However, the four synthetic steps viz, the introduction of dicarbonyl functionality in the form of acyl or formyl groups into the periphery of starting porphyrin material, demetallation of the dicarbonyl compounds under highly acidic condition to obtain free base dicarbonyl compounds, monoreduction of only one of the carbonyl functionality to give chiral or achiral compound that posses carbonyl and hydroxyl group and zinc metallation of the monoreduced compounds were the general synthetic steps those were applied to synthesize the target compounds. These fully synthetic novel chromophores self-assemble in a similar way to the natural case and without the need of a protein-pigment complex acting as mechanical scaffold.

The architectures of the monomeric building blocks determine both the chirality and the optical properties of the supramolecular assembly achieving broad and bathochromically shifted absorption maxima. More importantly, due to highly ordered arrangements of the dye molecules, neither the self-assembly nor the chemisorption onto nanocrystalline titania (TiO₂) with different grain sizes quenches the fluorescence of the aggregates.

If light harvesting is to be harnessed in artificial devices, a broad absorption with high extinction coefficients over the entire spectral range is beneficial and some of the supramolecular assemblies reported herein are promising candidates for artificial antenna systems as they fulfil these requirements and thus lend hope for being useful in hybrid solar cells.

Ein biomimetischer Ansatz zur Synthese von artifiziellen lichtsammelnden Systemen durch Selbstassemblierung

Zusammenfassung

Die Photosynthese stellt als einzige natürliche Quelle für unseren täglichen Bedarf an Nahrungsmitteln und fossilen Brennstoffen weltweit einen außerordentlich wichtigen Prozess dar. Jedoch dürften aufgrund des raschen Verbrauchs die natürlichen Ressourcen an Nahrungsmitteln und fossilen Brennstoffen zunehmend knapper werden. Zukünftige Generationen werden daher auf alternative Nahrungsmittel- und Energiequellen angewiesen sein, woraus eine starke Motivation zur Erforschung und Herstellung künstlicher photonischer Antennensysteme erwächst. Diesem Ziel kann man sich durch unterschiedliche Synthesestrategien mit kovalentem oder nicht kovalentem Ansatz annähern. Auf der Suche nach künstlichen Antennensystemen beleuchtet die vorliegende Arbeit den nicht kovalenten Ansatz, d.h. einen supramolekularen Ansatz, bei dem die Selbstassemblierung und die Selbstaggregation die wichtigsten Prozesse darstellen. Weiterhin ist unser Ansatz biomimetisch, da er das Antennensystem von grünen photosynthetischen Bakterien nachahmt.

Als Modelle für die Synthese von künstlichen Systemen wurden Bacteriochlorophyll *c*, *d* und *e* ausgewählt. Folgende supramolekulare Wechselwirkungen zwischen den Makrozyklen sind für die Selbstassemblierung von Bausteinen oder Tektonen verantwortlich: (1) Die Ligation des zentralen Mg-Atoms eines Moleküls durch die 3¹-hydroxy-Gruppe eines zweiten Moleküls, (2) die Ausbildung einer kooperativen Wasserstoffbrückenbindung zwischen der 3¹-Hydroxy-Gruppe des zweiten Moleküls und der 13¹-Carbonyl-Gruppe eines dritten BChl-*c*-Moleküls und (3) π - π -Wechselwirkungen zwischen den Makromolekülen. Der wohldefinierte Aufbau von selbstassemblierten Porphyrinen findet bei der Nachahmung von biologischen lichtsammelnden Systemen seine Anwendung. Es wurden Porphyrine hergestellt, die jene funktionellen Gruppen besitzen, die innerhalb der chlorosomalen Antennen einiger grüner, photosynthetischer Bakterien für die Selbstassemblierung der Bacteriochlorophylle *c*, *d* und *e* verantwortlich sind. Die selektive Synthese dieser Porphyrine erfolgte mit hoher Ausbeute, unter Verwendung von leicht zugänglichen und billigen Ausgangsverbindungen und hatte die bathochrome Verschiebung des Absorptionsmaximums zum Ziel. Diese vollsynthetischen, neuartigen Chromophore sind – ähnlich wie die natürlichen Systeme – selbstassembliert, bilden jedoch keinen Protein-Pigment-Komplex.

Der Aufbau der monomeren Bausteine bestimmt sowohl die Chiralität als auch die optischen Eigenschaften des supramolekularen Ensembles. Noch bedeutender ist die Tatsache, dass auf Grund des hochgeordneten Arrangements der Farbstoffmoleküle die Fluoreszenz der Aggregate weder durch die Selbstassemblierung noch durch die Chemisorption auf nanokristallinem Titandioxid mit unterschiedlicher Korngröße gelöscht wird.

Falls die Lichtsammlung durch künstliche Systeme möglich wird, wäre eine breite Absorptionsbande mit hohen Extinktionskoeffizienten über den gesamten Spektralbereich vorteilhaft und einige der hier vorgestellten supramolekularen Assemblate stellen viel versprechende Vertreter für künstliche lichtsammelnde Systeme dar, da sie die notwendigen Anforderungen erfüllen und daher auf ihre Anwendung in hybride Solarzellen hoffen lassen

Contents

Chapter 1 Introduction

1.1	Photosynthesis	1
1.2	The Photosynthetic Unit/Reaction Centres	1
1.3	Natural Photosynthesis	2
1.3.1	Stages of Photosynthesis	3
1.4	Photosynthetic Pigments	3
1.4.1	Chlorophylls	3
1.4.1.1	Chlorophyll- <i>a</i>	3
1.4.1.2	Chlorophyll- <i>b</i>	4
1.4.1.3	Chlorophyll- <i>c</i>	5
1.4.2	Bacteriochlorophylls	6
1.4.2.1	Bacteriochlorophylls <i>a</i>	6
1.4.2.2	Bacteriochlorophylls <i>b</i>	6
1.4.2.3	Bacteriochlorophylls- <i>c</i> , <i>d</i> , and <i>e</i>	6
1.4.2.4	Bacteriochlorophylls <i>g</i>	6
1.4.3	Carotenoids	6
1.5	Self-Assembly and Self-Aggregation	7
1.6	Supramolecular Chemistry and its importance	8
1.7	Supramolecular Interactions in Bacteriochlorophyll Models	9
1.8	Current Status of Research	11
1.8.1	Light Harvesting Systems Constructed by a Covalent Bonding Approach	11
1.8.2	Optimization of the Photophysical Properties	12
1.8.2.1	Maximization of Absorbance Properties: With Windmill Like Porphyrin Arrays	12
1.8.2.2	Maximization of Energy Transfer- Properties with Niphaphyrins	13
1.8.3	Maximization of Spectral Coverage	13
1.8.3.1	Maximization of Spectral Coverage: With Star-Shaped Porphyrins- Phthalocyanine Pentad Array	14

1.8.4	Increase of the Charge Separated State Lifetime	14
1.8.4.1	Increase of the Charge Separated State Lifetime with Multiporphyrinic Rotaxanes	15
1.8.4.2	Increasing the Charge Separated State Lifetimes with Dyads, Triads, Tetrads, and Pentads	15
1.8.4.2.1	Triad.	16
1.8.5	Light Harvesting System by Non-Covalent Bonding/Supramolecular Approach	18
1.8.5.1	Metal Ligation	19
1.8.5.2	Hydrogen Bonding	21
1.8.5.3	Cooperative Interactions between Porphyrinic-Chromophores Using Metal ligation and Hydrogen Bonding	22

Chapter 2 Original Contribution

2.1	10,20-Di-(3,5-di- <i>t</i> -butylphenyl)porphinato copper (28)	24
2.2	Synthesis of (<i>rac</i>)-3,13-bis-acetyl-10,20-bis-(3,5-di- <i>t</i> -butylphenyl)-porphinato zinc (35) and (<i>rac</i>)-3,17-diacetyl-10,20-bis-(3,5-di- <i>t</i> -butylphenyl)porphinato zinc (36)	24
2.3	Synthesis of 5-formyl-15-hydroxymethyl-10,20-bis(3,5-di- <i>t</i> -butylphenyl)porphinato zinc (40)	26
2.4	Synthesis of 3-acetyl-15-hydroxymethyl-10,20-bis (3,5-di- <i>t</i> -butylphenyl)porphinato zinc (45)	27
2.5	Synthesis of (<i>rac</i>)-10,20-bis(3,5-di- <i>tert</i> -butylphenyl)-15-formyl-3-(hydroxyethyl)porphyrinato zinc (49)	28
2.6	Synthesis of Long Chain compounds (74-81)	29
2.7	Synthesis of 3,17-di-palmitoyl-10,20-bis (3,5-di- <i>t</i> -butylphenyl)porphinato zinc (79) and 3,13-di-palmitoyl-10,20-bis(3,5-di- <i>t</i> -butylphenyl)porphinato zinc (83)	34
2.8	Discussion	35
2.9	Characterization	42

Chapter 3

3.1	Detection of Self-assembly	51
3.2	Detection of Self-Assembly with the Long Alkyl Chain Compounds	53
3.3	Comparison between isomers 81 and 85	56
3.4	Absorption Properties of Self-Assembled 45 and 49	57
3.5	Comparison between the Wavelength Difference of the Aggregate Bands and Those of Zn-Methanol Adducts	58
3.6	Temperature Effect on the Aggregation of 49	59
3.7	CD-Spectroscopy and the Supramolecular Chirality of the Self-Assemblies	60
3.7.1	CD-Spectroscopy and the Supramolecular Chirality of 35 and 36 - Self-Assemblies	63
3.8	X-ray	65
3.9	Confocal Fluorescence Microscopy, Atomic Force Microscopy and Transmission Electron Microscopy of the Self-assemblies	66
3.9.1	Confocal Fluorescence Measurements	66
3.9.2	Atomic Force Microscopy (AFM) Measurements	69
3.9.3	Transmission Electron Microscopy (TEM) Observations	70
3.10	A New Synthetic Approach to Self-Assembled Chromophores	72
3.11	Factors Responsible for Self-Assembly	73
3.12	π -Stacking and the Nature of π - π Interactions in the Novel Porphyrins	74
3.13	Geometry Estimations of the Aggregates Based on Semiempirical Calculations	76
3.14	Outlook	77
3.14.1	Application of Self-Assembled Chromophores for Photovoltaic Cells	77
3.14.2	Silicon Cells	77
3.14.3	Thin Film Solar Cells	77
3.15	Conclusions	79

Chapter 4 Experimental Section

4.1	General Remarks	81
4.2	10,20-Di-(3,5-di- <i>t</i> -butylphenyl)-21,23 <i>H</i> -porphyrin [27]	82
4.3	10,20-Di-(3,5-di- <i>t</i> -butylphenyl)-porphinato copper [28]	82

4.4	3,13-Diacetyl-10,20-bis(3,5-di- <i>t</i> -butylphenyl)porphinato copper and 3,17-diacetyl-10,20-bis(3,5-di- <i>t</i> -butylphenyl)porphinato copper [29 and 30]	82
4.5	3,13-Diacetyl-10,20-bis(3,5-di- <i>t</i> -butylphenyl)-21,23 <i>H</i> -porphyrin [31]	83
4.6	3,17-Diacetyl-10,20-bis(3,5-di- <i>t</i> -butylphenyl) -21,23 <i>H</i> -porphyrin [32]	84
4.7	3-Acetyl-13-(1-hydroxyethyl)-10,20-bis(3,5-di- <i>t</i> -butylphenyl) -21,23 <i>H</i> -porphyrin [33]	85
4.8	3-Acetyl-17-(1-hydroxyethyl)-10,20-bis(3,5-di- <i>t</i> -butylphenyl) -21,23 <i>H</i> -porphyrin[34]	86
4.9	3-Acetyl-13-(1-hydroxyethyl)-10,20-bis(3,5-di- <i>t</i> -butylphenyl) porphinato zinc [35]	87
4.10	3-Acetyl-17-(1-hydroxyethyl)-10,20-bis(3,5-di- <i>t</i> -butylphenyl) porphinato zinc [36]	88
4.11	5,15-Diformyl-10,20-bis(3,5-di- <i>t</i> -butylphenyl)-porphinato copper[37]	88
4.12	5,15-Diformyl-10,20-bis(3,5-di- <i>t</i> -butylphenyl)-21,23 <i>H</i> -porphyrin [38]	89
4.13	5-Formyl-15-hydroxymethyl-10,20-bis(3,5-di- <i>t</i> -butylphenyl) -21,23 <i>H</i> -porphyrin [39]	90
4.14	5-Formyl-15-hydroxymethyl-10,20-bis-(3,5-di- <i>t</i> -butylphenyl) porphinato zinc [40]	91
4.15	5-Formyl-10,20-bis(3,5-di- <i>t</i> -butylphenyl)porphinato copper [41]	91
4.16	3-Acetyl-15-formyl-10,20-bis(3,5-di- <i>t</i> -butylphenyl) porphinato copper [42]	92
4.17	3-Acetyl-15-formyl-10,20-bis(3,5-di- <i>t</i> -butylphenyl) -21,23 <i>H</i> -porphyrin [43]	93
4.18	3-Acetyl-15-hydroxymethyl-10,20-bis(3,5-di- <i>t</i> -butylphenyl) -21,23 <i>H</i> -porphyrin [44]	94
4.19	3-Acetyl-15-hydroxymethyl-10,20-bis(3,5-di- <i>t</i> -butylphenyl) porphinato zinc [45]	95
4.20	3-Acetyl-10,20-bis(3,5-di- <i>tert</i> -butylphenyl) -15-(5,5-dimethyl-1,3-dioxan-2-yl)-porphyrin [46]	96
4.21	10,20- Bis(3,5-di- <i>tert</i> -butylphenyl) -15-(5,5-dimethyl-1,3-dioxan-2yl)-3(1-hydroxyethyl)-porphyrin [47]	97

4.22	10,20- Bis(3,5-di- <i>tert</i> -butylphenyl) -15-formyl-3-(1-hydroxyethyl)-porphyrin [48]	98
4.23	10,20- Bis(3,5-di- <i>tert</i> -butylphenyl) -15-formyl-3-(1-hydroxyethyl)-porphyrinato zinc [49]	99
4.24	General procedure for the synthesis of 3,17-diacyl-10,20-bis(3,5-di- <i>t</i> -butylphenyl) porphyrinato copper [50-57]	100
4.24.1	3,17-Diacyl-10,20-bis(3,5-di- <i>t</i> -butylphenyl) -21,23 <i>H</i> -porphyrin [58-65]	101
4.25	General procedure for the synthesis of 3-acyl-17-(1-hydroxyacyl)-10,20-bis(3,5-di- <i>t</i> -butylphenyl) -21,23 <i>H</i> -porphyrin [66-73]	102
4.26	General procedure for the synthesis of 3-acyl-17-(1-hydroxyacyl)-10,20-bis(3,5-di- <i>t</i> -butylphenyl) porphyrinato zinc [74-81]	103
4.27	3,17-Dibutyroyl-10,20-bis(3,5-di- <i>t</i> -butylphenyl) -21,23 <i>H</i> -porphyrin [58]	104
4.28	3,17-Divaleroyl-10,20-bis(3,5-di- <i>t</i> -butylphenyl) -21,23 <i>H</i> -porphyrin [59]	104
4.29	3,17-Dihexanoyl-10,20-bis(3,5-di- <i>t</i> -butylphenyl) -21,23 <i>H</i> -porphyrin [60]	105
4.30	3,17-Diheptanoyl-10,20-bis(3,5-di- <i>t</i> -butylphenyl) -21,23 <i>H</i> -porphyrin [61]	106
4.31	3,17-Dioctanoyl-10,20-bis(3,5-di- <i>t</i> -butylphenyl) -21,23 <i>H</i> -porphyrin [62]	107
4.32	3,17-Dilauroyl-10,20-bis(3,5-di- <i>t</i> -butylphenyl) -21,23 <i>H</i> -porphyrin [63]	108
4.33	3,17-Dimyristoyl-10,20-bis(3,5-di- <i>t</i> -butylphenyl) -21,23 <i>H</i> -porphyrin [64]	109
4.34	3,17-Dipalmitoyl-10,20-bis(3,5-di- <i>t</i> -butylphenyl) -21,23 <i>H</i> -porphyrin [65]	110
4.35	3-Butyroyl-17-(1-hydroxybutyl) -10,20-bis(3,5-di- <i>t</i> -butylphenyl)-21,23 <i>H</i> -porphyrin [66]	110

4.36	3-Valeroyl-17-(1-hydroxypentyl) -10,20-bis(3,5-di- <i>t</i> -butylphenyl)-21,23 <i>H</i> -porphyrin	[67]	111
4.37	3-Hexanoyl-17-(1-hydroxyhexyl) -10,20-bis(3,5-di- <i>t</i> -butylphenyl)-21,23 <i>H</i> -porphyrin	[68]	112
4.38	3-Heptanoyl-17-(1-hydroxyheptyl) -10,20-bis(3,5-di- <i>t</i> -butylphenyl)-21,23 <i>H</i> -porphyrin	[69]	113
4.39	3-Octanoyl-17-(1-hydroxyoctyl) -10,20-bis(3,5-di- <i>t</i> -butylphenyl)-21,23 <i>H</i> -porphyrin	[70]	114
4.40	3-Lauroyl-17-(1-hydroxydodecyl) -10,20-bis(3,5-di- <i>t</i> -butylphenyl)-21,23 <i>H</i> -porphyrin	[71]	115
4.41	3-Myristoyl-17-(1-hydroxytetradecyl) -10,20-bis(3,5-di- <i>t</i> -butylphenyl)-21,23 <i>H</i> -porphyrin	[72]	116
4.42	3-Palmitoyl-17-(1-hydroxyhexadecyl) -10,20-bis(3,5-di- <i>t</i> -butylphenyl)-21,23 <i>H</i> -porphyrin	[73]	117
4.43	3-Butyroyl-17-(1-hydroxybutyl) -10,20-bis(3,5-di- <i>t</i> -butylphenyl)porphinato zinc	[74]	118
4.44	3-Valeroyl-17-(1-hydroxypentyl) -10,20-bis(3,5-di- <i>t</i> -butylphenyl)porphinato zinc	[75]	118
4.45	3-Hexanoyl-17-(1-hydroxyhexyl) -10,20-bis(3,5-di- <i>t</i> -butylphenyl)porphinato zinc	[76]	119
4.46	3-Heptanoyl-17-(1-hydroxyheptyl) -10,20-bis(3,5-di- <i>t</i> -butylphenyl)-porphinato zinc	[77]	120
4.47	3-Octanoyl-17-(1-hydroxyoctyl) -10,20-bis(3,5-di- <i>t</i> -butylphenyl)porphinato zinc	[78]	120
4.48	3-Lauroyl-17-(1-hydroxydodecyl) -10,20-bis(3,5-di- <i>t</i> -butylphenyl)porphinato zinc	[79]	121
4.49	3-Myristoyl-17-(1-hydroxytetradecyl) -10,20-bis(3,5-di- <i>t</i> -butylphenyl)porphinato zinc	[80]	122
4.50	3-Palmitoyl-17-(1-hydroxyhexadecyl) -10,20-bis(3,5-di- <i>t</i> -butylphenyl)porphinato zinc	[81]	122
4.51	3,13-Dipalmitoyl-10,20-bis(3,5-di- <i>t</i> -butylphenyl) -21,23 <i>H</i> -porphyrin	[83]	123
4.52	(<i>Rac</i>)-3-(1-hydroxydecyl)13-palmitoyl -10,20-bis(3,5-di- <i>t</i> -butylphenyl)-21,23 <i>H</i> -porphyrin	[84]	124

4.53 3-(1-Hydroxyhexadecyl)-13-palmitoyl- -10,20-bis(3,5-di- <i>t</i> -butylphenyl)porphinato zinc [85]	125
--	-----

References	126
-------------------	-----

Chapter 1

Introduction

1.1 Photosynthesis

Solar energy is the principal energy source for almost all life on Earth. Photosynthesis is a complex succession of steps in the conversion of light energy into biochemical energy. All higher organisms on Earth receive their energy directly or indirectly from oxygenic photosynthesis performed by plants, green algae and different types of bacteria. In reaction centres light energy leads to charge separation which after a cascade of electron transfer steps stabilizes the hole and the electron on the opposite sides of the photosynthetic membrane. In antenna systems, light is captured and through rapid energy transfer step the energy is finally trapped within the reaction centre.

1.2 The Photosynthetic Unit/Reaction Centres

All reaction centres use light for electron transfer reactions, resulting in charge separation across the membrane. Some reaction centres pump protons which are coupled to the electron transfer reactions involving quinones. Different types of antenna complexes have been identified from various classes of photosynthetic organisms; however the basic principle of photosynthetic apparatus remains the same in natural as well as in artificial antenna systems.^[1] The coupling of an antenna system to a reaction center is shown in Figure 1.1.^[1, 2] The vast majority of photosynthetic pigment molecules in the antenna systems are arranged in such a way that the photons capturing process is greatly increased. Most of the pigments in a photosynthetic organism are not chemically active, but function primarily as an antenna.^[3-6] When photons strike pigment molecules the electrons are excited and leave the hole behind which is in turn filled up by next electron with a creation of yet another hole thus the photosynthetic molecules deliver excited state energy by means of excitation transfer to the reaction center complexes where charge separation takes place to generate chemical energy.

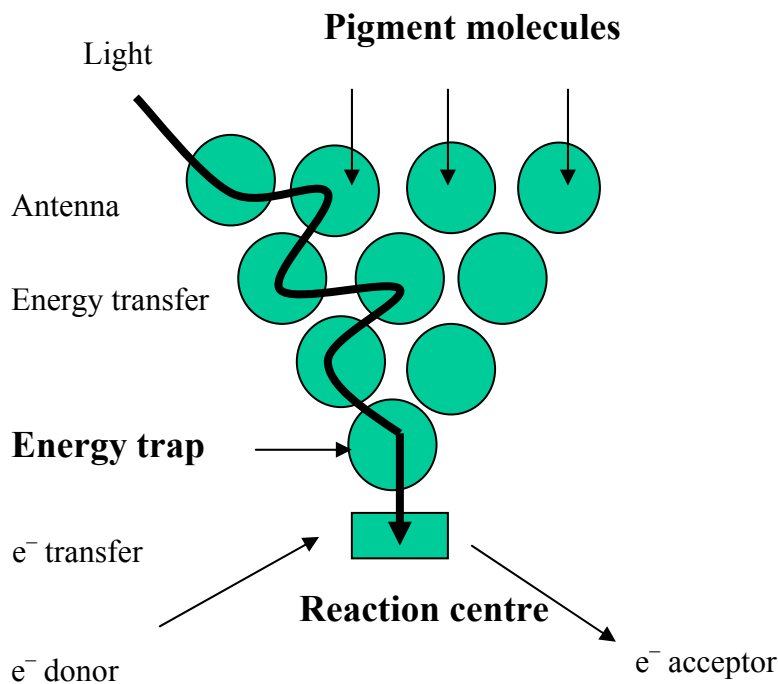


Figure 1.1: Basic concept of photosynthetic antenna and reaction center function. Adapted from Balaban, T. S. *Encyclopedia of Nanoscience and Nanotechnology* 2004, Vol. 4, p. 506.

1.3 Natural Photosynthesis

Photosynthesis is a natural biological process that nature has developed since 2.5 billions years ago. The photosynthetic organisms such as anoxygenic photosynthetic bacteria (e.g. purple bacteria, green sulfur bacteria, green nonsulfur bacteria, heliobacteria), the oxygenic bacteria (like cyanobacteria), and different kinds of algae and plants trap solar energy to convert water and carbon dioxide of the air. The typical overall chemical reaction of oxygenic photosynthesis is given below:



1.3.1 Stages of Photosynthesis

Photosynthesis is a two-stage process. The first process is the Light Dependent Process (Light Reaction), which requires the direct energy of light to make energy carrier molecules that are used in the second process. The Light Independent process (Dark Reaction) occurs when the products of the Light Reaction are used to form covalent C-C bonds of carbohydrates. The Dark Reactions can usually occur in the dark, if the energy carriers from the light process are present. Recent evidence suggests that a major enzyme of the Dark Reaction is indirectly stimulated by light, thus the term Dark Reaction is somewhat of a misnomer. The Light Reactions occur in the grana and the Dark Reactions take place in the stroma of the chloroplasts. In higher plants, the light-dependent portion of photosynthesis is carried out by two photosystems (photosystem I and photosystem II) in the thylakoid membrane of the chloroplasts which act in conjunction. Two special dimers of chlorophyll molecules, when photoexcited, drive the photosystems.

1.4 Photosynthetic Pigments

All photosynthetic organisms contain one or more organic pigments capable of absorbing visible radiation, which will initiate the photochemical reactions of photosynthesis. The three major classes of pigments found in plants and algae are the chlorophylls, the carotenoids and the phycobilins. Carotenoids and phycobilins are called accessory pigments since the quanta (packets of light) absorbed by these pigments can be transferred to chlorophyll. Different types of photosynthetic pigments, their structures and functions are described below.

1.4.1 Chlorophylls

Chlorophyll molecules contain a porphyrin 'head' and a phytol 'tail'. The polar (water-soluble) head is made up of a tetrapyrrole ring and a magnesium ion complexed by the four nitrogen atoms of the ring. The following four types of chlorophyll molecules are present in nature.

1.4.1.1 Chlorophyll-*a*

This is present in all higher plants and algae. Chlorophyll-*a* is present in all photosynthetic organisms that evolve O₂, although traces of minor variants of chlorophyll *a* are found in some anoxygenic bacteria, the green sulfur bacteria and heliobacteria. They perform an important function as an intermediate in the electron transport chain.

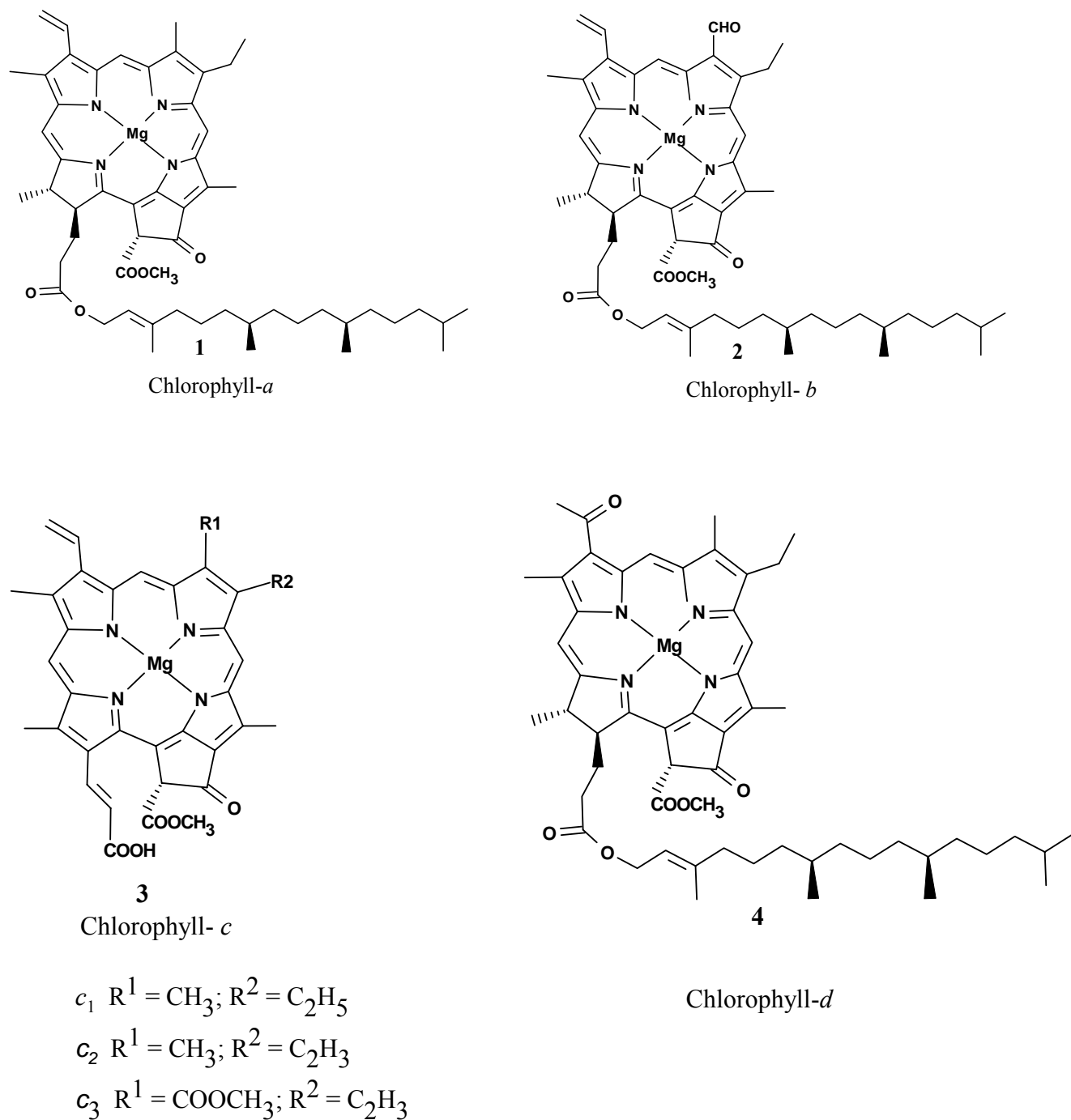


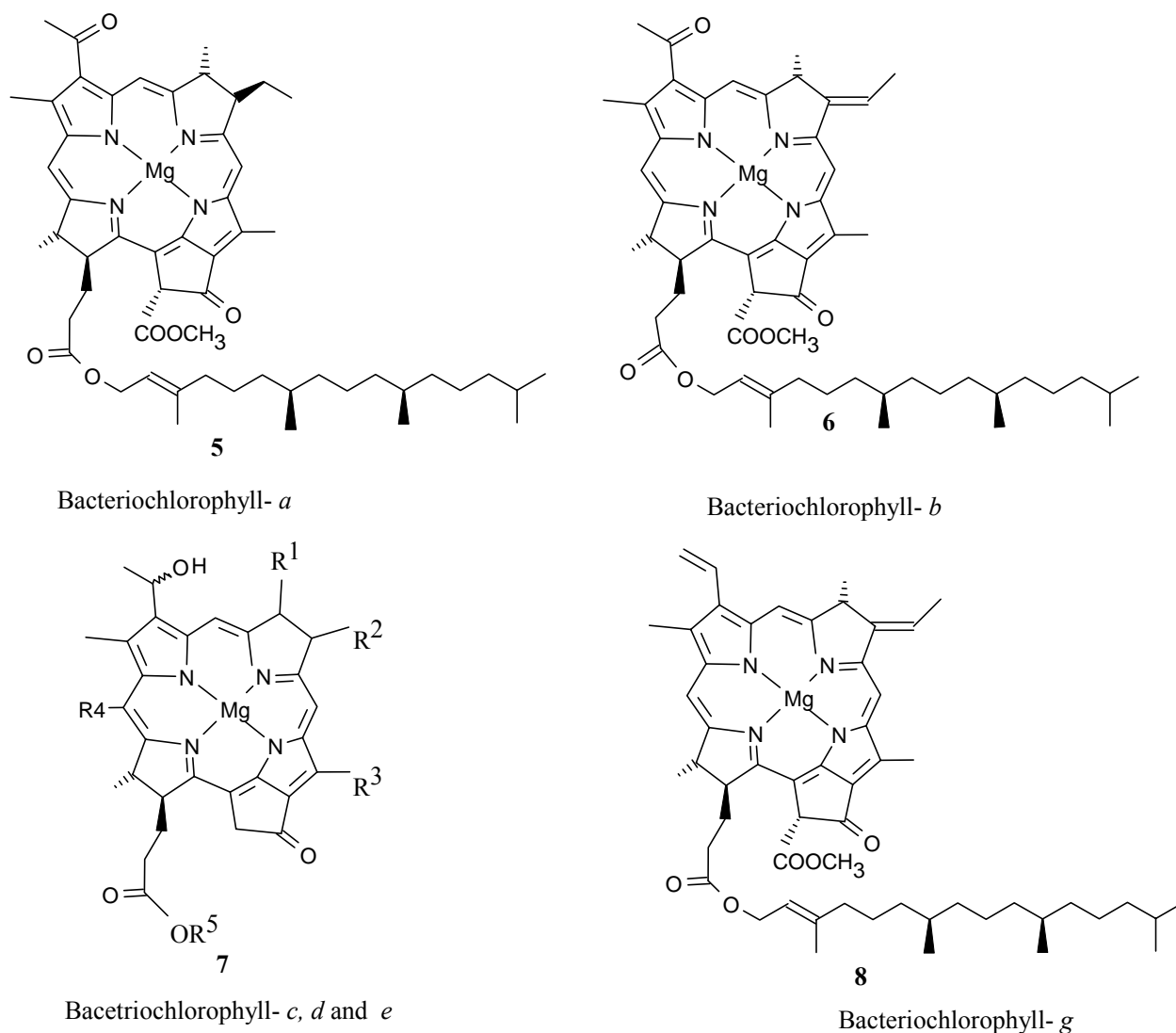
Figure 1.2: Chemical structures of chlorophyll *a*, *b*, *c* and *d*.

1.4.1.2 Chlorophyll-*b*

This is present in all higher plants and most green algae. Chlorophyll *b* is the major accessory light-absorbing pigment in the majority of eukaryotic photosynthetic organisms, with the exception of red and brown algae.

1.4.1.3 Chlorophyll-*c*

Chlorophyll-*c* is chemically classified as a porphyrin and is found exclusively in diatoms and brown algae. It functions as an accessory light-harvesting pigment, in pigment-protein complexes. There are several structural types of chlorophyll *c*, which differ by some of the peripheral ring substituents.



Bchl- *c* R¹ = Me; R² = Et, Pr, Bu, R³ = Me, Et; R⁴ = Me

R⁵ = stearyl, farnesyl, others

Bchl- *d* R¹ = Me; R² = Et, Pr, iso-Bu, neo-Pent; R³ = Me; R⁴ = H;

R⁵ = farnesyl, others

Bchl- *e* R¹ = CHO; R² = Et, Pr, iso-Bu, neo-Pent; R⁴ = Me;

R⁵ = farnesyl, others.

Figure 1.3: Chemical structures of bacteriochlorophylls- *a, b, c, d, e* and *g*

1.4.2 Bacteriochlorophylls

Different photosynthetic bacteria have different species of bacteriochlorophyll described as below:

1.4.2.1 Bacteriochlorophyll- *a*

It is the principal chlorophyll-type pigment in the majority of oxygenic photosynthetic bacteria. It has a reduced degree of conjugation and symmetry in the molecule in comparison with chlorophylls.

1.4.2.2 Bacteriochlorophyll- *b*

Bacteriochlorophyll *b* is found only in a few species of purple bacteria. It has the longest wavelength absorbance band of any known chlorophyll-type pigment. *In vivo* its absorbance maximum is at 960-1050 nm.

1.4.2.3 Bacteriochlorophylls- *c*, *d*, and *e*

These natural pigments are found only in green photosynthetic bacteria, in organisms that contain the antenna complex known as a chlorosome. The carbon atoms at position C-3¹ can have both *R* and *S* configuration. Because of other stereocenters in the molecule, the 3¹-epimers are diastereomers and can be thus easily separated by normal chromatography. The 3-hydroxyethyl group, carbonyl group, and Mg metal in the centre of bacteriochlorophyll *c*, *d*, and *e* are responsible for inducing self-assembly because in their absence, self-assembly does not occur.

1.4.2.4 Bacteriochlorophyll- *g*

This is the most recently discovered chlorophyll-type pigment. It is very unstable and isomerizes to chlorophyll *a* or closely related compounds.

1.4.3 Carotenoids

Carotenoids are found in all native photosynthetic organisms as well as in many non-photosynthetic organisms. There are two classes of carotenoids, the carotenes and the carotenols. All carotenoids have long isoprenoid chains, with alternating double and single bonds. Structurally, the carotenes are composed entirely of carbon and hydrogen, whereas the carotenols also contain oxygen in the form of hydroxyl or keto groups. Carotenoids perform two major roles in photosynthesis as partners of the usually more prevalent chlorophylls: light harvesting and photoprotection. Carotenoids absorb radiation in the visible region inaccessible to chlorophylls and transfer the absorbed energy to chlorophylls, which channel it into the photosynthetic reaction centre. Carotenoids perform photoprotection by rapidly

quenching triplet excited states of chlorophylls before they can react with oxygen to form the highly reactive and damaging excited singlet state of oxygen. Fig. 1.4 shows some carotenoids and carotenoids precursors important in photosynthetic systems. The absorbed energy can be transferred to chlorophylls, which channel it into the photosynthetic reaction centre. A third, more minor role of carotenoids, is structural: due to their rigidity they help assemble stable protein complexes. In carotenoidless mutants, some of the light-harvesting complexes are much more labile.

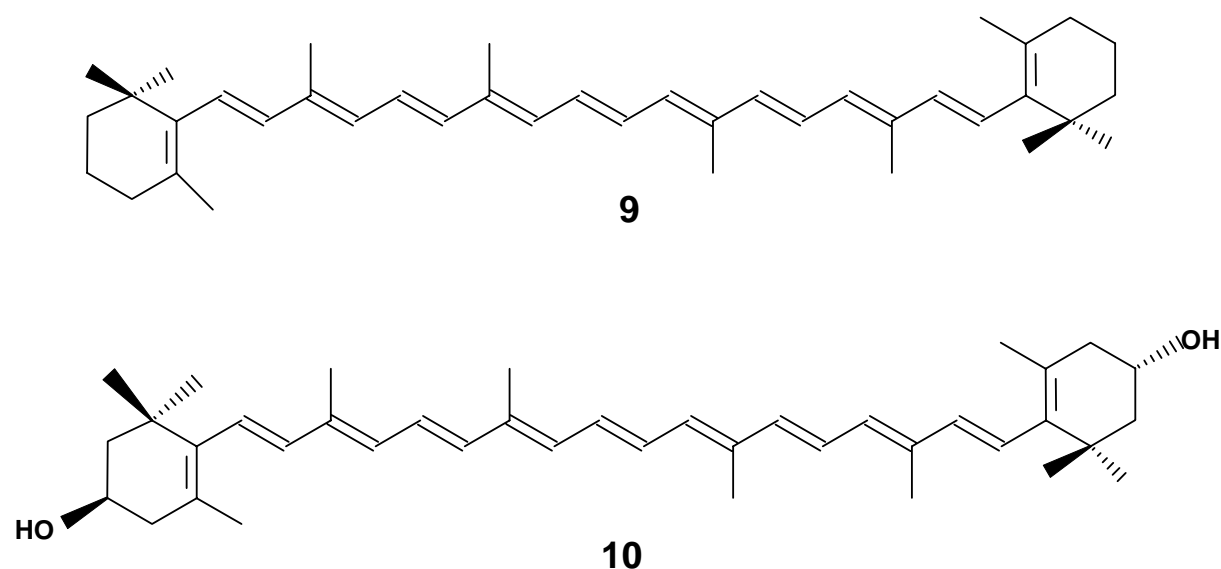


Fig 1.4: Chemical structures of β -carotene (9) and lutein (10)

1.5 Self-Assembly and Self-Aggregation

Biological systems provide many intricate and elegant examples of the use of self-assembly for engineering functional nanostructures. A typical case of natural biological self-assembly is observed in the antenna system of green photosynthetic bacteria. The term “self-assembly” has been applied to multimolecular systems to differentiate them from simpler host–guest complexes^[7]. Although the two terms self-assembly and self-aggregation are sometimes used as synonyms, there is a subtle difference in their meaning. Self-assembly conserves a specific and persistent pattern of monomeric building blocks (tectons) and thus permits predictability of the overall organization, while self-aggregation is less well defined leading to non-ordered structures. Self-assembly is a process in which components, either separated or linked, spontaneously form ordered aggregates. Self-assembly can occur with components having sizes from the molecular to the macroscopic levels, provided that appropriate conditions are

met. Although much of the work in self-assembly has focused on molecular components, many of the most interesting applications of self-assembling processes can be found at larger sizes (nanometers to micrometers). These larger systems also offer a level of control over the characteristics of the components and over the interactions among them that makes fundamental investigations especially tractable^[8]. Molecular self-assembly is a widespread phenomenon in both chemistry and biochemistry. Yet it was not until the rise of supramolecular chemistry that attention has increasingly been given to the designed self-assembly of a variety of synthetic molecules and ions. To a large extent, success in this area has reflected knowledge gained from nature. However, an increased awareness of the latent steric and electronic information implanted in individual molecular components has also contributed to this success.^[9]

The monomeric building blocks and the self-assembled species are remarkably different from each other and are exhibiting different properties. Thus, the self-assembling systems can be disassembled and assembled reversibly under appropriate conditions as shown in Fig. 1.5. The self-assembly can be programmed as in biological systems by mimicking the active molecular subunits (functional groups) which are responsible for the intermolecular interactions.

1.6 Supramolecular Chemistry and its Importance

Supramolecular chemistry encompasses the study of intermolecular bonding, *i.e.* a chemistry of weak interactions. Prof. J.-M. Lehn described supramolecular chemistry as “chemistry beyond the molecule” and is based on weak, reversible interactions such as hydrogen-bonding, electrostatic, aromatic stacking and Van der Waals or dispersive forces. Over the time the definition of supramolecular chemistry has been expanded to encompass any organized entity in which intermolecular forces hold two or more chemical species together. Supramolecular chemistry includes chemical, biological and physical processes. Supramolecular chemistry is a rapidly developing field of research that involves the use of non-covalent interactions to assemble molecules into stable well-defined structures. Self-assembly by the non-covalent approach generates large functional arrays of defined size and architecture while the bond-by-bond construction through covalent bonds places restriction on the size of the architectures that have to be generated. There are different ways in which molecules can be induced to self-assemble. Previously very difficult syntheses were required in order to covalently attach building blocks (such as porphyrins) into large assemblies. Even

if functionality is present in such an elaborate synthetic construct, due to immense fabrication costs, this construction is uneconomical if practical applications are envisaged.

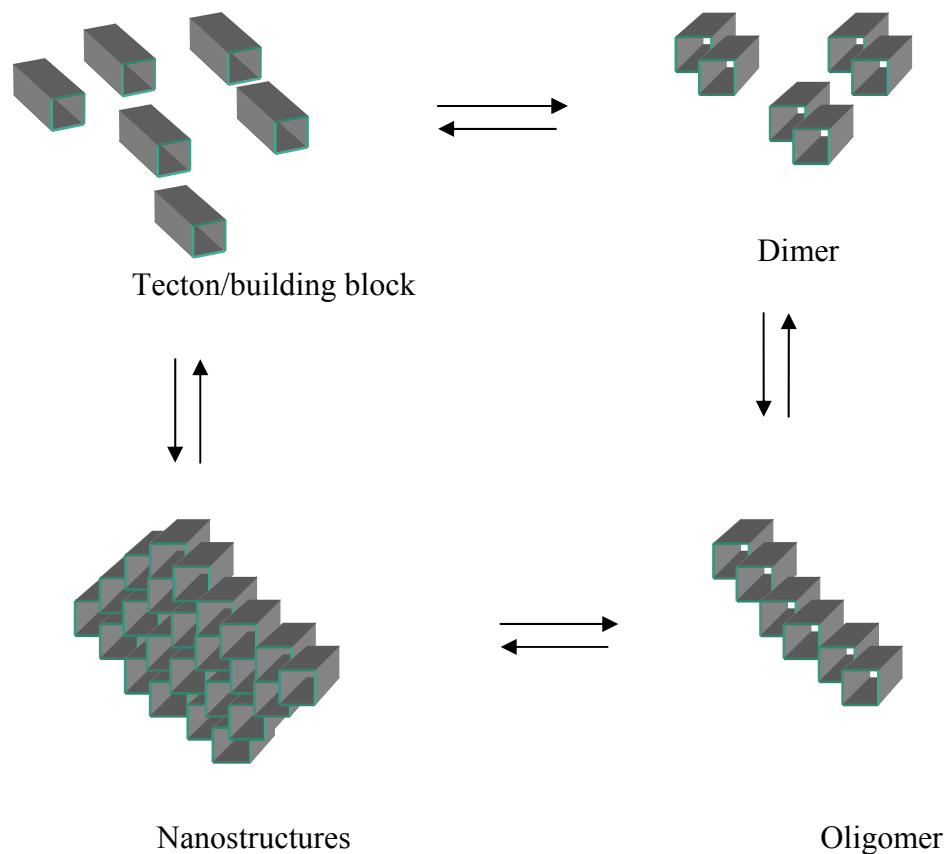
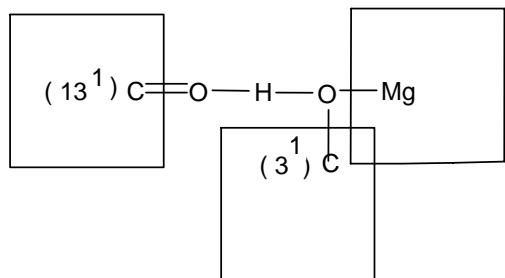


Figure 1.5: Illustration of a typical self-assembly process. Each 3D block represents a tecton/building block. Adapted from Balaban, T. S. Encyclopedia of Nanoscience and Nanotechnology. 2004, 4, 509.

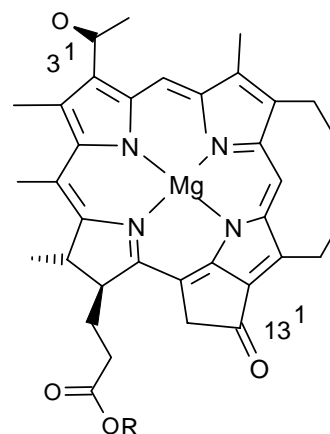
1.7 Supramolecular Interactions in Bacteriochlorophyll Models

The supramolecular interactions among the active parts of Bchl-*c* are responsible for self-assembly. The three main interactions are outlined below:

- 1) the ligation of the central magnesium atom by a hydroxy group;
- 2) cooperative hydrogen bonding of the same OH group to a carbonyl group of a third molecule;
- 3) π - π interactions between the conjugated molecules.^[10]



Supramolecular Interactions



3^1 S-[Et, Me] BChl c

Where R is a long chain

Figure 1.6: Schematic representation of the central building block formed by a bonding network interconnecting three BChl-c molecules (symbolized as rectangles): The 3^1 -hydroxy group of one BChl is bound to the magnesium of second through oxygen ligation and simultaneously to the 13^1 -keto group of a third BChl by hydrogen bonding (13^1).

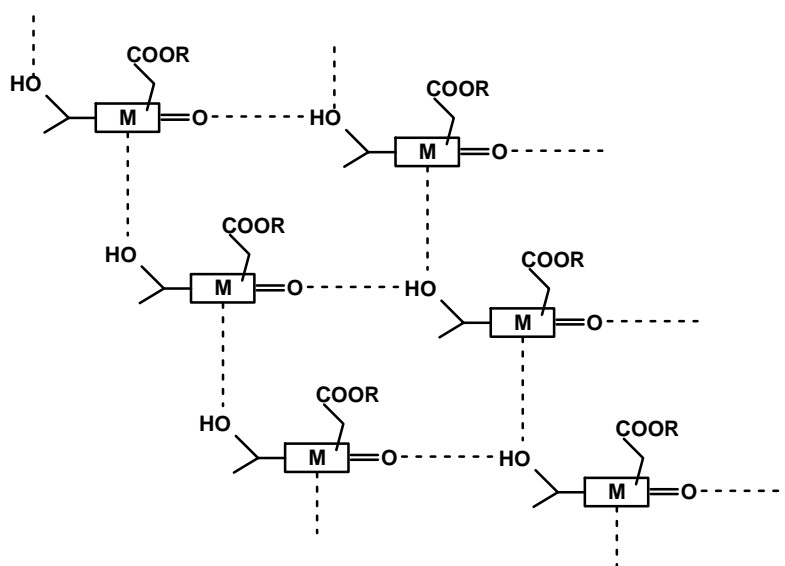


Figure 1.7: Proposed bonding network in the self-assembled species illustrating cooperative supramolecular interactions in BChl- c, d, and e. Adapted from T. S. Balaban, et.al., *J. Phys. Chem. B.* **2000**, 104, 1369.

The long future goal of this work would be to perform artificial light-harvesting antenna systems with the aid of self-assembling chromophores by using supramolecular chemistry.

The first step was to synthesize various self-assembling porphyrins mimicking the functionality of bacteriochlorophylls- *c*, *d*, or *e* suitably endowed for supramolecular interactions.

1.8 Current Status of Research

Various groups have focussed on the creation of artificial light-harvesting antenna systems either by using a covalent bonding approach or by using a supramolecular approach. Various kind of chromophores including phthalocyanines,^[11-14] perylene bis-imides,^[15-17] xanthenes,^[18-20] hemicyanines^[21-23] and porphyrins^[24-28] have been tested in quest of constructing artificial light-harvesting systems. This work especially addresses the utility of porphyrin chromophores to achieve this goal.

1.8.1 Light Harvesting Systems Constructed by a Covalent Bonding Approach

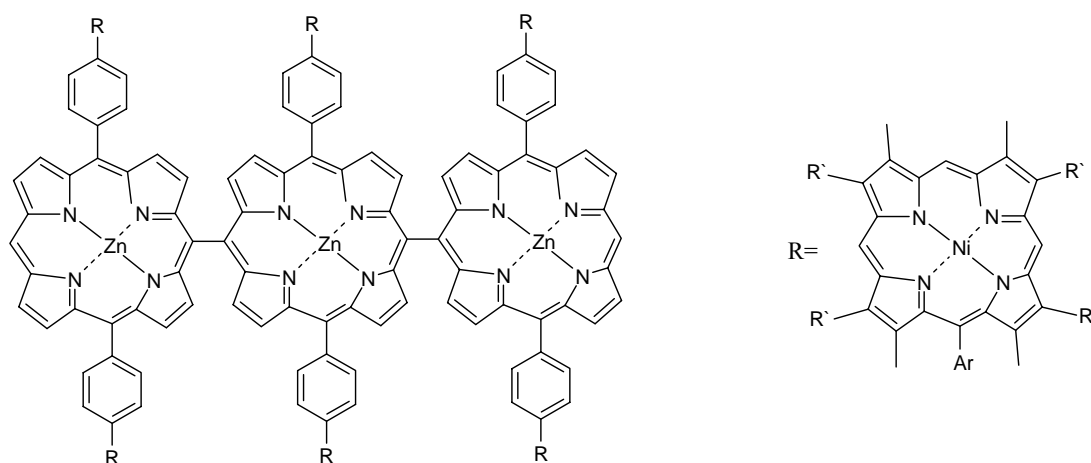
The prospect of realizing artificial photosynthesis to harvest solar energy has motivated many researchers. Design of artificial photosynthetic reaction centres requires several key factors. It refers to the tunability of the absorption wavelengths, energy transfer ability, redox potential, electronic coupling, and photoprotection. The selection of light-absorbing pigments and the choice of electron-donating and accepting functionalities within the system are of prime importance.^[29] The second major consideration is the organizational method through which the components will react. Many of the early efforts towards achieving such artificial systems used the covalent linkage of two porphyrins molecules,^[30-32] with the work of the last decade focused on the design of higher-ordered arrays of porphyrins including linear, cyclic and alkyne-separated arrays. Lindsey and co-workers contributed essentially to this early work in artificial light harvesting porphyrins arrays and has helped develop novel synthetic methods in porphyrin chemistry.^[33-34] In artificial photosynthetic reaction centres, researchers have focused primarily upon maximizing the absorbance and energy transfer processes between donating and accepting porphyrin centres by precisely controlling their geometry. Other approaches have been utilized in order to maximize the range of spectral coverage of the accepting functionalities, and more recent efforts have been made in order to maximize the lifetime of the charge separated state. All these aspects are important for developing an effective mimic of the photosynthetic reaction centre. Various groups have also used different types of the semisynthetic chlorophylls and porphyrins. Porphyrins are widely used compounds for artificial photosynthesis as they are thermally quite stable and show quite interesting photophysical properties. The extended conjugated π systems in chromophores

leads to a narrowing of the HOMO-LUMO gap so that electronic transitions are allowed at increased wavelengths.^[1]

1.8.2 Optimization of the Photophysical Properties

1.8.2.1 Maximization of Absorption Properties with Windmill-like Porphyrin Arrays

Osuka and coworkers have developed windmill-like porphyrin arrays that feature a *meso* linked diporphyrin as an energy sink.^[35] Upon irradiation with light a rapid energy transfer from the peripheral porphyrin rings to the diporphyrin core takes place.



11

Fig 1.8: Windmill-like porphyrin array

1.8.2.2 Maximization of Energy Transfer Properties with Niphaphyrins

Gossauer and co-workers reported the synthesis of a new class of snowflake-shaped porphyrin hexamers, termed niphaphyrin.^[36]

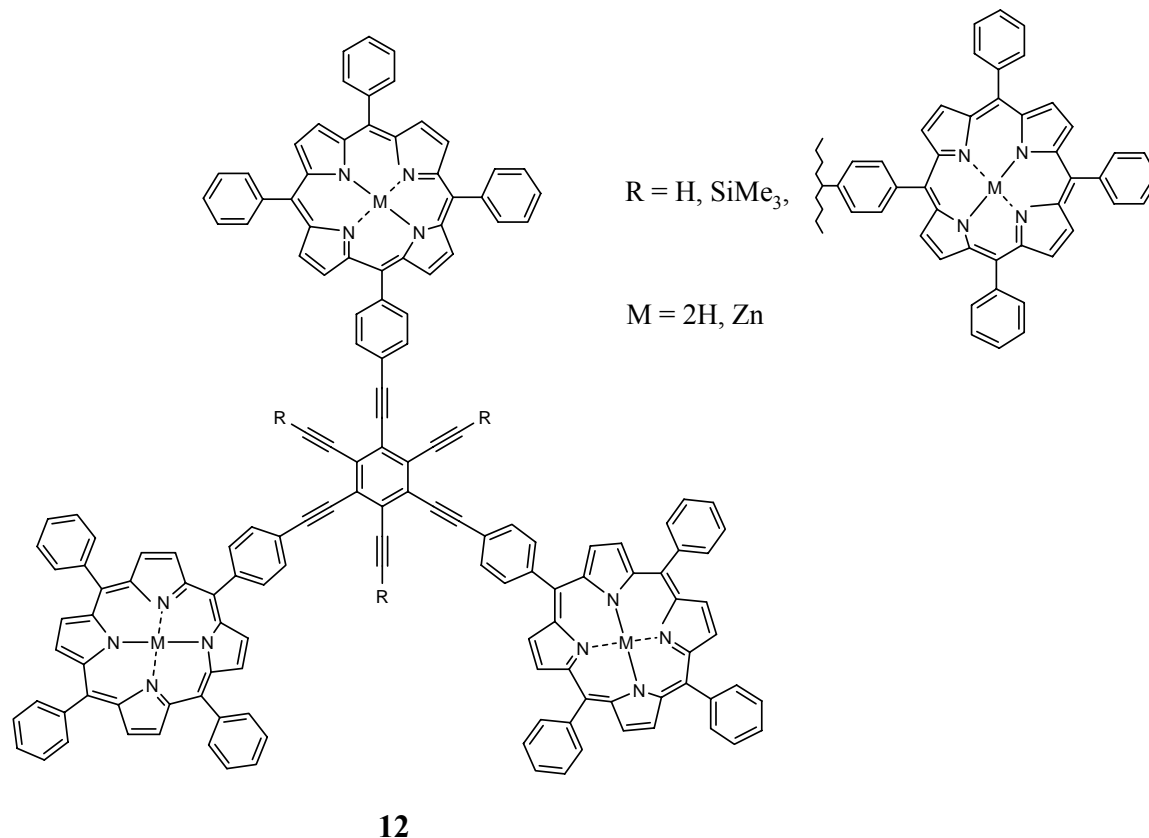


Fig 1.9 : Niphaphyrin

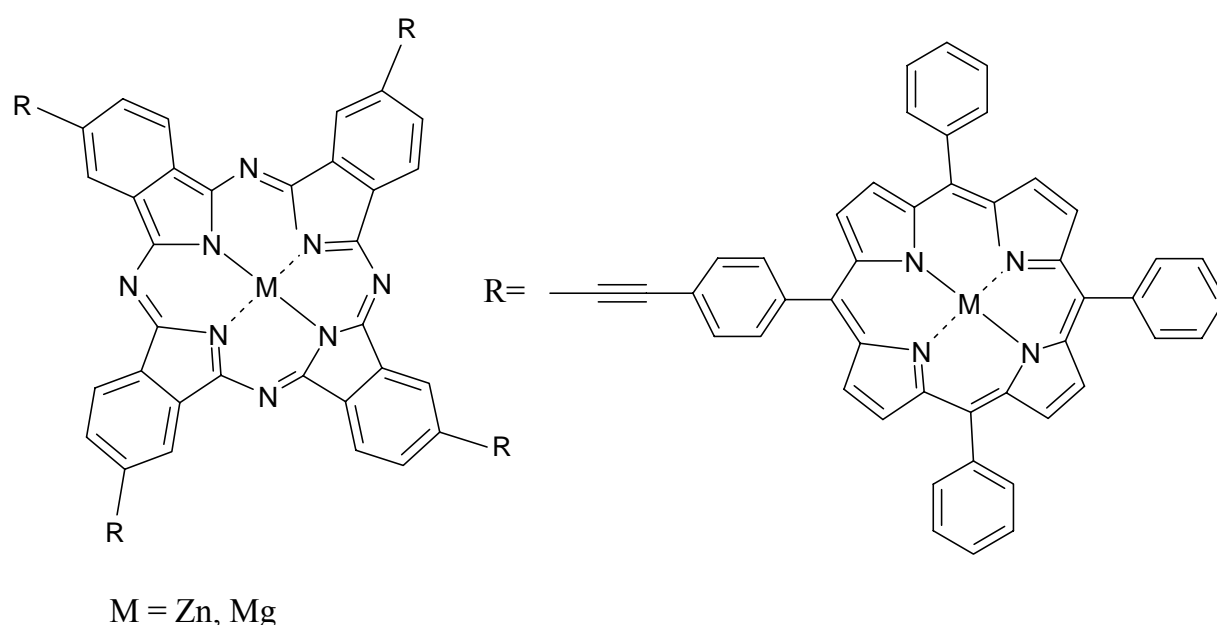
In these assemblies, six porphyrins cycles are covalently attached to the six positions of a benzene core through rigid ethynyl linkers. A very efficient singlet excited-state energy transfer has observed from the zinc chelates to the free base porphyrins chromophores in a niphaphyrin which three zinc porphyrins chelates alternating with three porphyrins free bases. The overall yield of energy transfer has been estimated as 98%.

1.8.3 Maximization of Spectral Coverage

Porphyrins absorb strongly in the blue. In contrast, phthalocyanine absorb strongly in the red region (600-700 nm). A mixed system of porphyrins and phthalocyanines that retains the essential electronic features of the respective pigments should absorb strongly both in the blue and in the red, thereby covering a large part of the solar spectrum.

1.8.3.1 Maximization of Spectral Coverage: with a Star-Shaped Porphyrins-Phthalocyanine Pentad Array

Lindsey and coworkers reported star-shaped porphyrin arrays that utilize a central phthalocyanine ring to form a pentad for maximization of the spectral range.^[37] These arrays have useful properties such as a reasonable solubility in organic solvents like toluene, THF, and CH₂Cl₂, strong absorption in the blue and red regions. The intramolecular singlet-excited-state energy transfer from the peripheral porphyrins to the phthalocyanine moiety is extremely rapid occurring within picoseconds. Thus they are efficient for light harvesting and other photonic applications.



13

Figure 1.10: Star-shaped porphyrins- phthalocyanine pentad array

1.8.4 Increase of the Lifetime of the Charge Separated State

In natural photosynthesis in photosynthetic bacteria, a very effective charge separation occurs with a lifetime of several microseconds over a large distance. Charge recombination is one of the problems in artificial systems and in order to increase the lifetime of the charge separated state large efforts have been devoted to designing artificial systems with charge separation implemented in molecular devices. Catenanes and rotaxanes arrays are particularly well adapted for the study of electron transfer in chromophores. Between the components of these systems there is no chemical bonding as they are mechanically interlocked.

1.8.4.1 Increase of the Charge Separated State Lifetime with Multiporphyrinic Rotaxanes

Electron transfer rates in porphyrins can be influenced greatly by the mutual arrangement of the chromophores. To study these effects, Sauvage and co-workers synthesized a multiporphyrinic rotaxane based on two porphyrin containing phenanthroline units **14** and **15**.^[38]

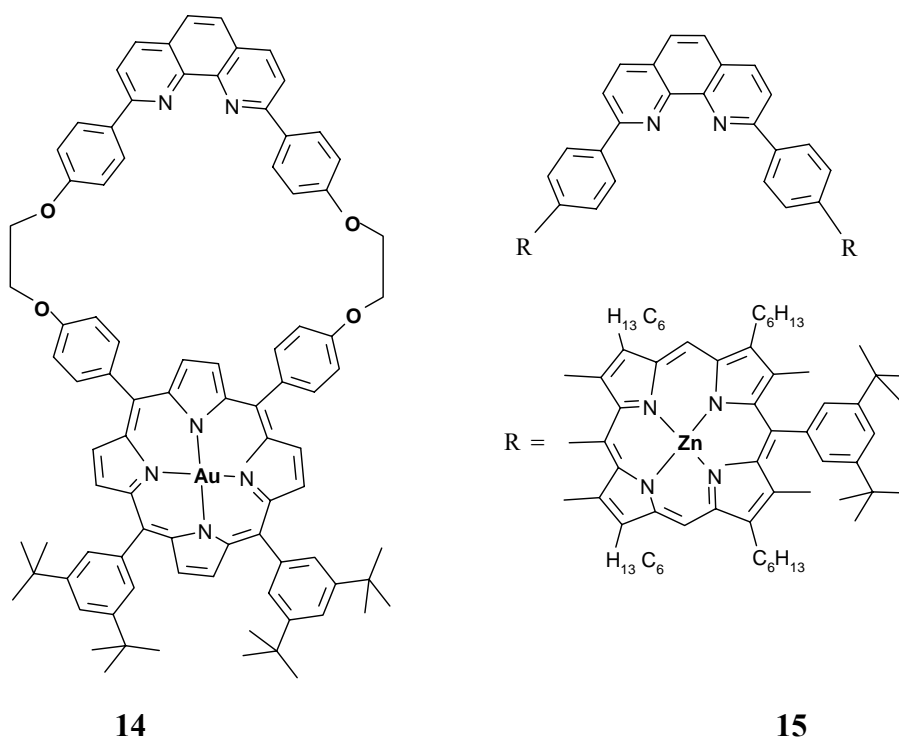


Figure 1.11: Multiporphyrinic rotaxanes

1.8.4.2 Increasing the Charge Separated State Lifetimes with Dyads, Triads, Tetrads, and Pentads

The dyads, triads, tetrads, and pentads molecules have a characteristic property of generating long-lived charge separated states upon photoexcitation and multistep electron transfer reactions. Devens Gust and coworkers synthesized a porphyrin quinone dyad.^[39] Although the spatial relationship between **16** and **17** is quite close, the two molecules show very different photoinduced electron-transfer characteristics which are attributed to the smaller separation of the ions in the P^+Q^- state in **16** relative to **17**.

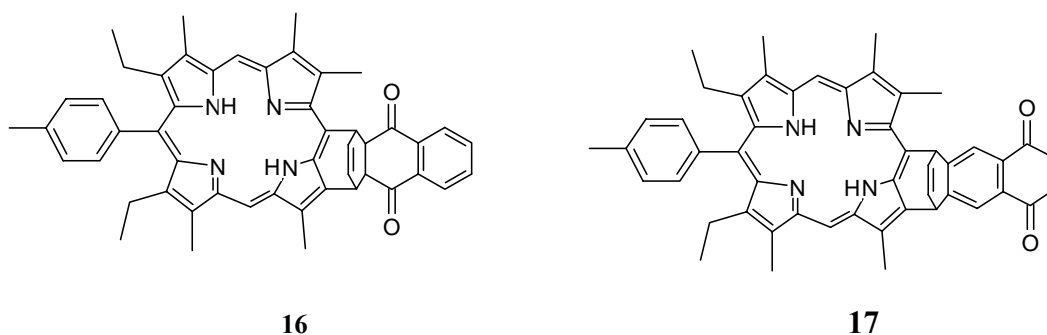


Figure 1.12: Porphyrin quinone dyad

Dyads **16** and **17** suffer charge recombination (<1 ns), so that the energy stored in the charge separated state is wasted as heat more rapidly than it can be used otherwise. The systems are strongly coupled, favouring both forward electron transfer and charge recombination.

1.8.4.2.1 Triad ^[40]

In this example a fullerene acts as the ultimate electron acceptor additionally to fullerene absorbs light over much of the visible spectrum. Flexible synthetic methodologies for fullerene modification permit their incorporation into a variety of structures. Importantly, they have been found to have small internal and solvent reorganization energies, and low sensitivity to solvent stabilization of their anions. These features lead to desirable forward electron transfer properties such as rapid photoinduced electron transfer and slow charge recombination. Thus fullerenes greatly increase the lifetime of the charge-separated state.

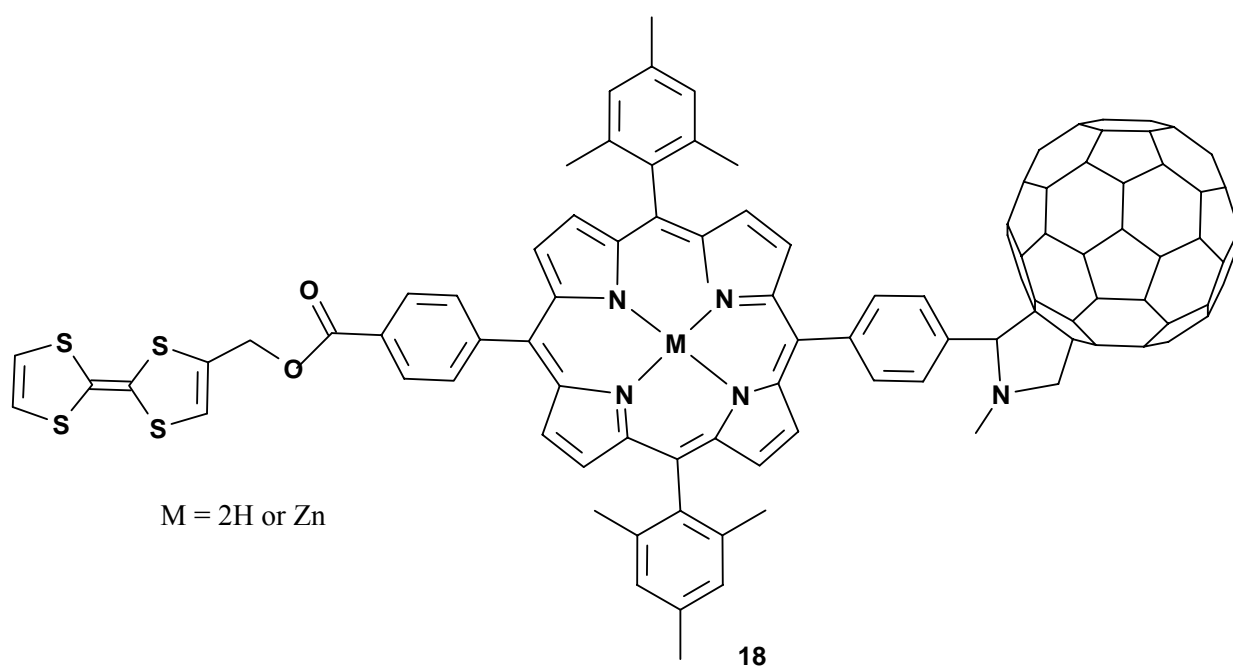
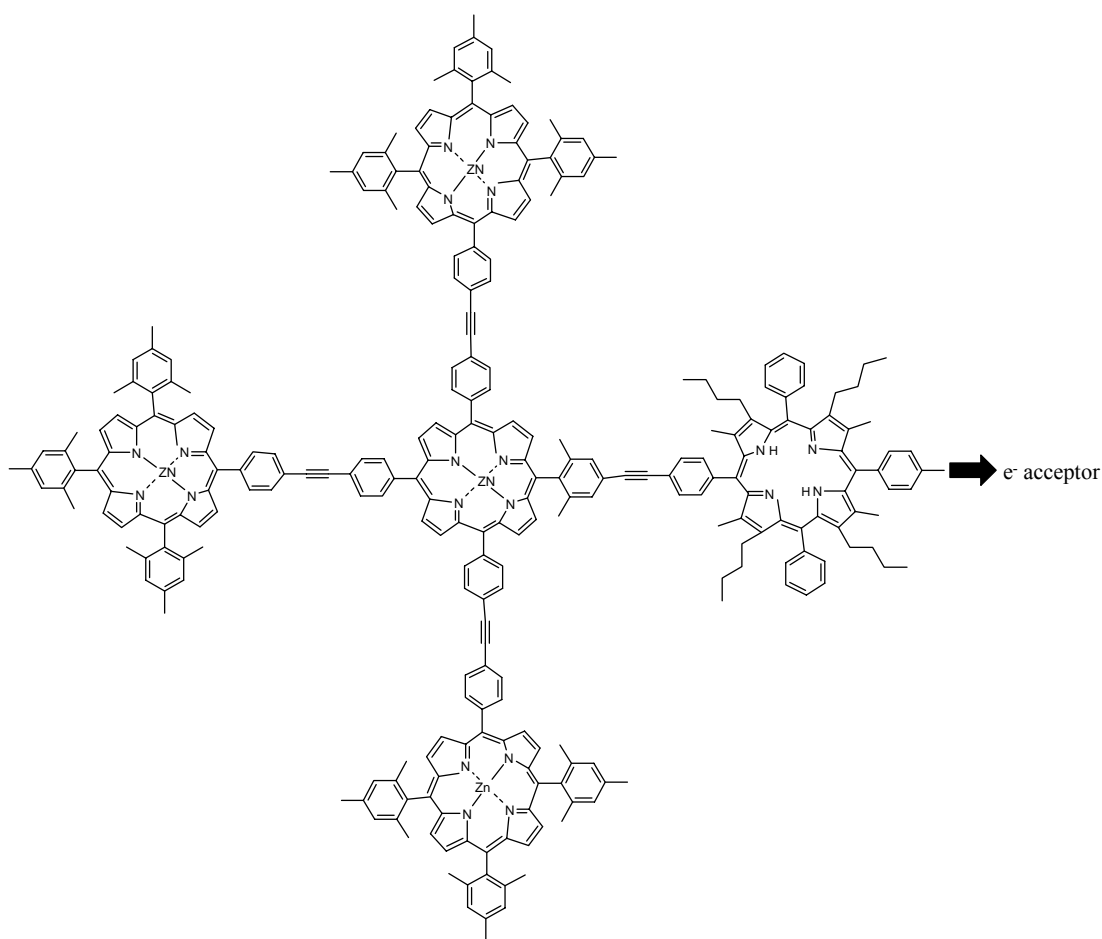


Fig 1.13: Tetrathiafulvalene-porphyrin-fullerene triad molecules

The design and properties of these systems are based upon substitution at the *meso* or β -pyrrolic position of the porphyrin ring and the choice of the metal incorporated into the porphyrin centre. To facilitate electron transfer in systems incorporating multiple porphyrin rings, a linker is incorporated which allows for unperturbed electron flow. Typically these linkers are alkene or alkynyl units, however some systems have been recently designed which feature porphyrins directly linked at the *meso* position^[40] or porphyrin rings joined at the β -pyrrolic position.^[41]

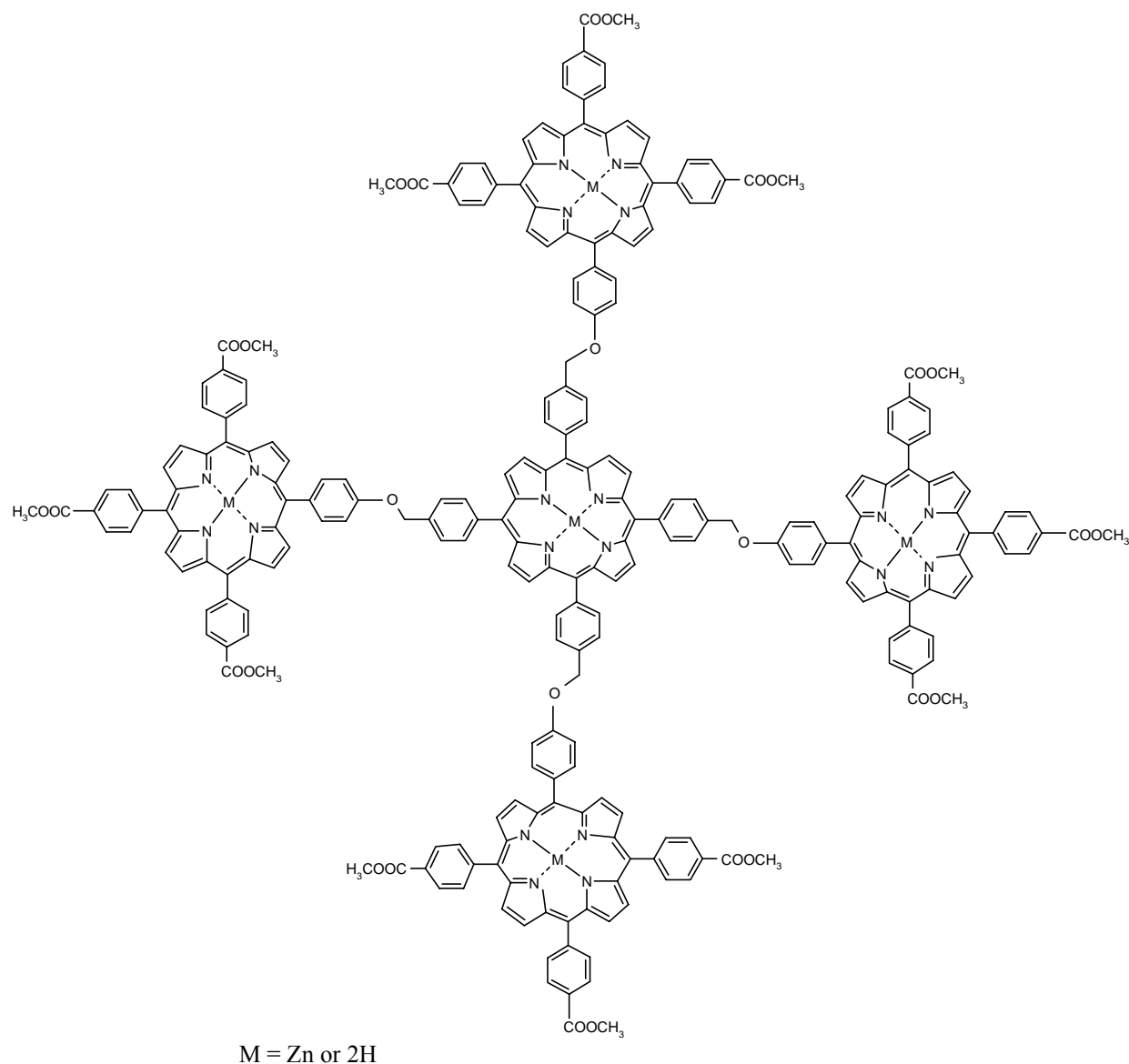


19

Figure 1.14

These arrays with alkyne linkers have a fluorescence quantum yield of almost unity if the free base P is excited and is about 0.7 if the antenna zinc porphyrins are excited. The major advantage of this molecule is that it has an increased light-gathering power^[42] through an increased photon capture cross section.

An elegant approach to construct covalent porphyrinic nanostructures is to use dendrimers. Repetitive chemical transformations with high yields could be used to access compounds of type **20** by Neil Branda.^[43]



20

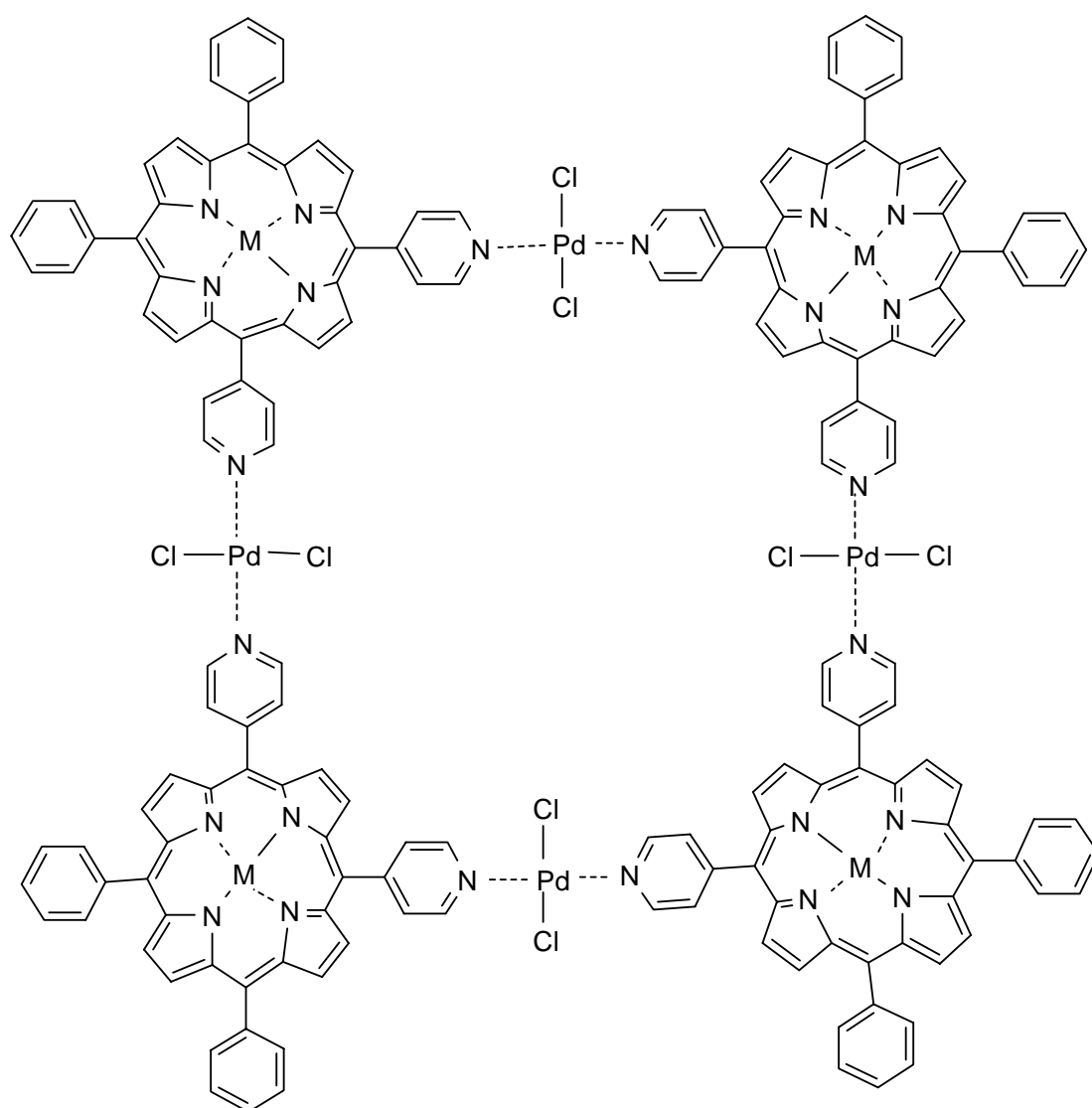
Figure 1.15

1.8.5 Light Harvesting Systems by Non-Covalent Bonding or Supramolecular Approach

This is an alternative way of constructing large light-harvesting antenna systems. In this method the small units called “tectons” are the building blocks which interact among themselves by applying the principles of supramolecular chemistry.^[44]

1.8.5.1 Metal Ligation

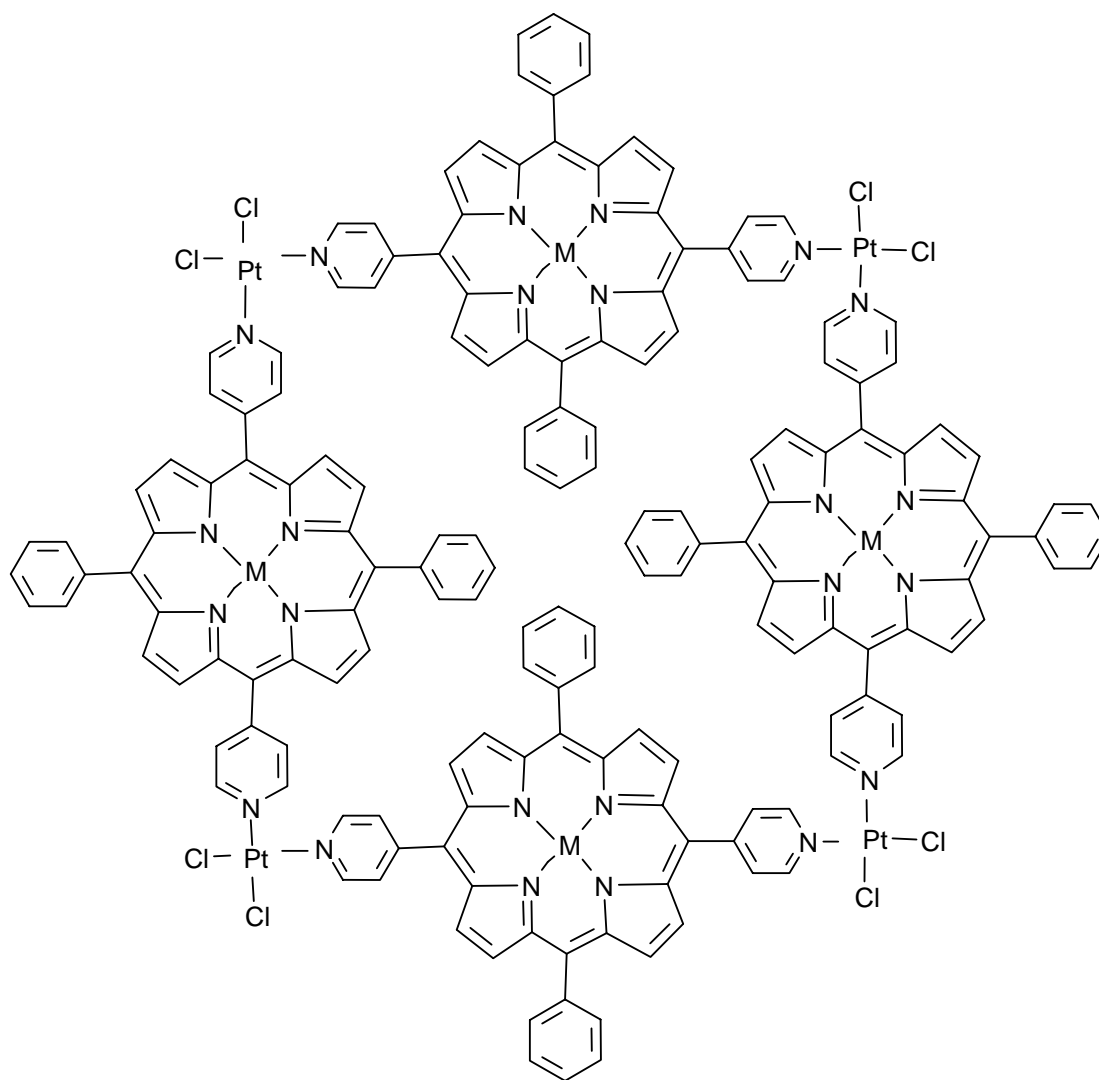
Different types of alkaline and transition metals have been widely used in construction of supramolecular assemblies. Lehn and Drain^[45] used palladium and platinum metals to bind together the *meso*-4-pyridyl substituted free base or Zn metallated porphyrins as shown in Figs. 1.16 and 1.17. The dimers and the tetramers of both the species have their Soret bands broadened.



21

Figure 1.16

M = 2H or Zn

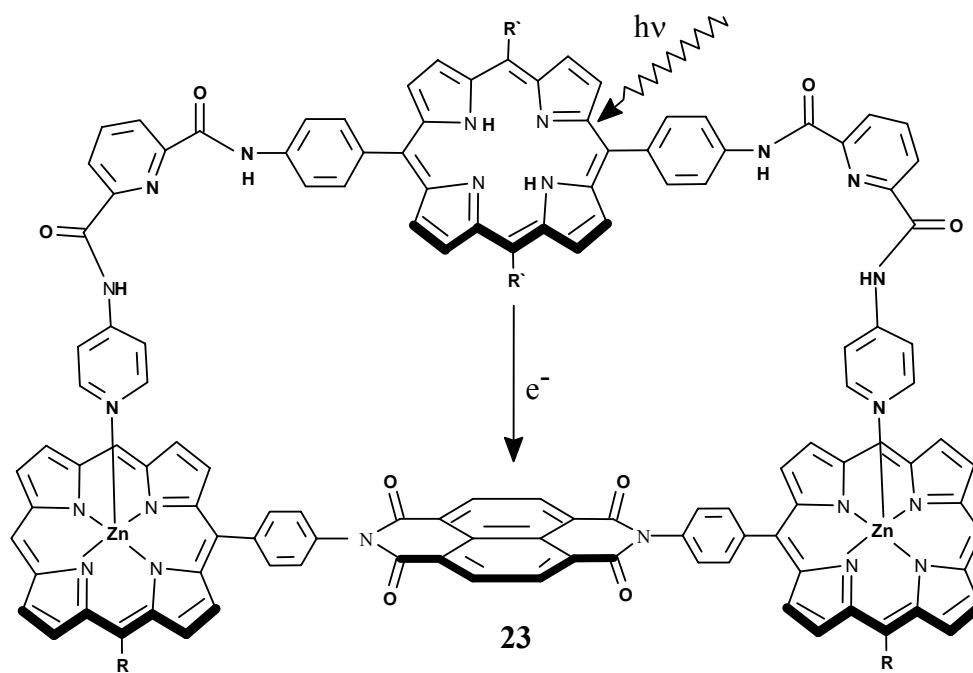


M = 2H or Zn

22

Figure 1.17

In Fig. 1.18 the naphthalenediamide spacer acts as an electron acceptor. The free base porphyrin fluorescence at ~ 650 nm is quenched up to 70% due to an intracomplex electron transfer process arising from the singlet state of the free base porphyrin to the electron acceptor.^[46]

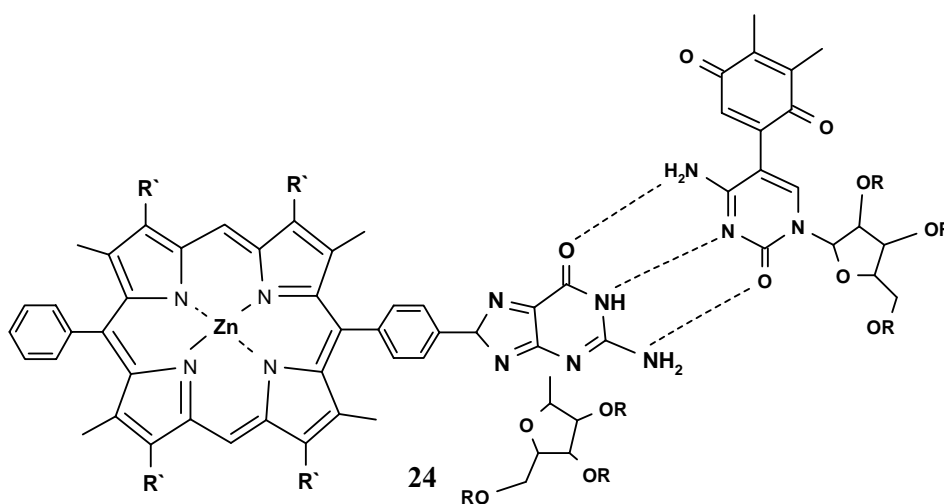


where R, R' = aryl substituents

Figure 1.18

1.8.5.2 Hydrogen Bonding

Jonathan Sessler and coworkers have reported an electron transfer process which occurs within 0.74 ns from the porphyrin which is triply hydrogen bonded to the quinone moiety.^[47]



Where R' = Bu and R = SiMe₂Bu^t

Figure 1.19

1.8.5.3 Cooperative Interactions between Porphyrinic Chromophores Using Metal ligation and Hydrogen Bonding

In order to induce self-assembly in bacteriochlorophyll type molecules, the three supramolecular interactions need to operate simultaneously.^[10] If the central metal atom is removed by demetallation or if either the hydroxyl and/or the carbonyl groups are removed or protected, the self-assembling ability and hence light-harvesting process is inhibited. Jesorka et al.^[48] have shown that the BChl-*c* and *d* can be induced to self-assemble, even after the positions of the 3¹-hydroxy groups and 13¹-carbonyl groups are interchanged. When these groups are removed or protected, self-assembly is inhibited, proving that the presence of a hydroxy group, a carbonyl group and of the central metal atom is the prerequisite condition that self-assembly occurs.

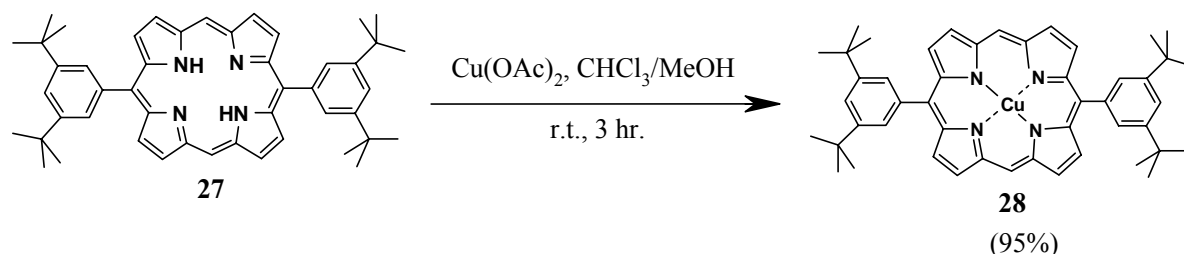
Chapter 2 – Original Contributions

Synthesis of Self-assembled Chromophores Starting from 10,20-Bis-(3,5-di-*tert*-butylphenyl)-porphinato copper

This chapter describes the novel syntheses of self-assembling porphyrinic chromophores. The new porphyrinic compounds were synthesised by employing a mild Friedel-Crafts-type diacylation reaction which is novel to porphyrin chemistry, and some Vilsmeier formylation reactions. The synthetic design is based on the incorporation within a porphyrin scaffold, that has an extended π -system and constitutes thus the chromophore of the three basic units needed for inducing self-assembly. These are two carbonyl groups, either as formyl or acyl residues into various desired positions of porphyrin periphery and a central metal atom. By very selective reduction of only one of the carbonyl groups a monoreduced hydroxy-porphyrin compound could be formed. This novel reaction provides a hydroxy substituent which serves as the metal chelating group, being also the strongest supramolecular interaction which governs the self-assembly. Finally, by zinc metallation of the monoreduced porphyrin the desired products could be obtained in preparatively useful yields. In the monoreduced porphyrin, the carbon atom bearing the hydroxy group can be either a chiral centre, as is the case for hydroxyalkyl groups, or achiral in the first member of this series, *i.e.* for the hydroxymethylene group.

2.1 10,20-Di-(3,5-di-*t*-butylphenyl)porphinato copper (28)

In order to synthesize compound **28** firstly the known free base **27** ^[49] was subjected to copper metallation ^[50] by optimizing known literature methods.



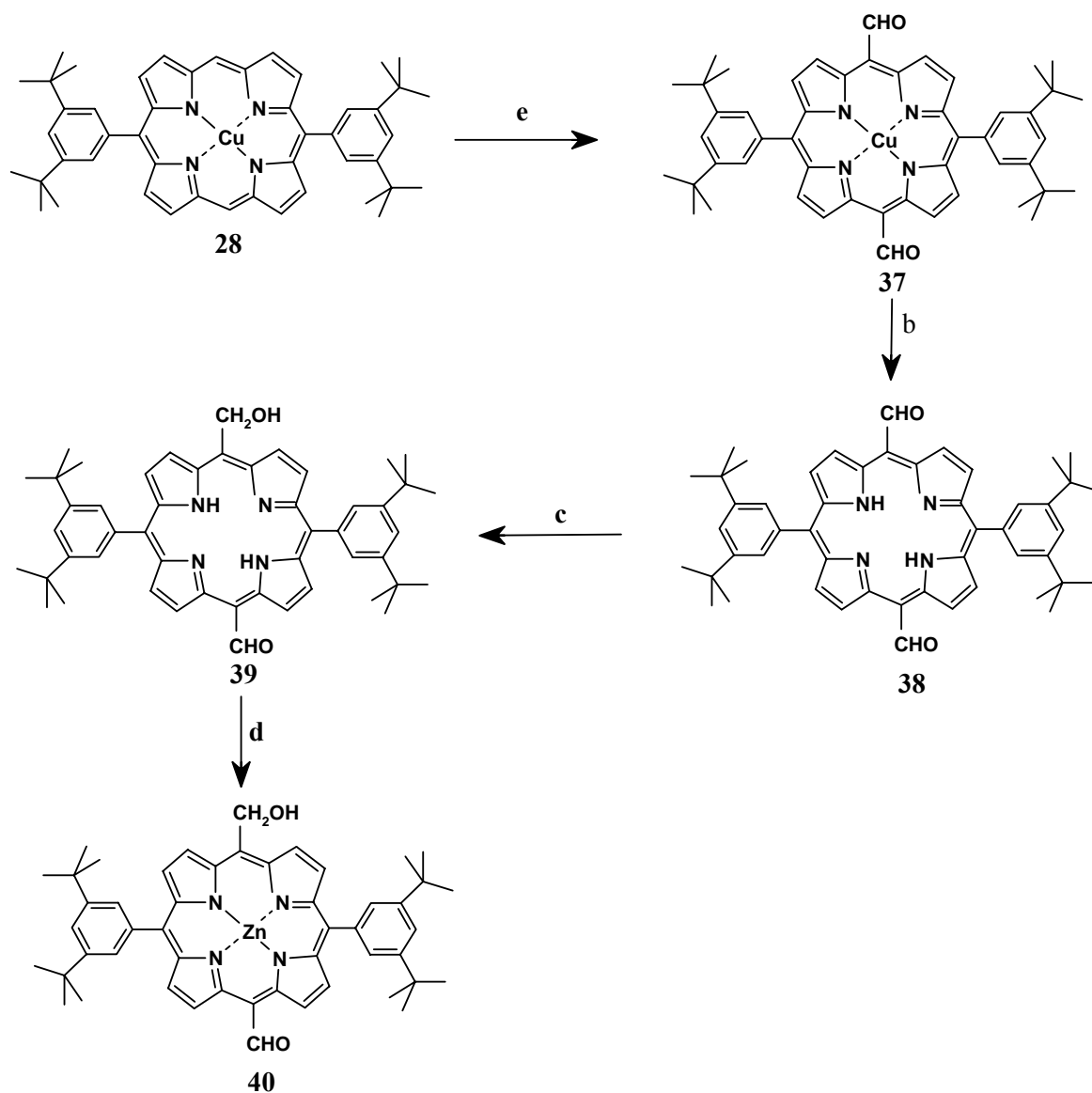
Scheme 2.1

2.2 Synthesis of (*rac*)-3,13-diacetyl-10,20-bis(3,5-di-*t*-butylphenyl)porphinato zinc (**35**) and (*rac*)-3,17-Di-acetyl-10,20-bis(3,5-di-*t*-butylphenyl)porphinato zinc (**36**)

Compounds **35** and **36** were synthesized by employing a very simple and selective novel synthetic procedure using a mild Friedel-Crafts acylation reaction. ^[51] The reaction conditions are similar to the Balaban-Nenitzescu-Praill synthesis ^[52] of pyrylium salts by olefin diacylation ^[53] and have been optimized for long chain pyrylium salts by T.S. Balaban and his coworkers. ^[54-59] After employing SnCl_4 as Lewis acid catalyst, ^[60] a pair of **29** and **30** diacetyl isomers was obtained in almost equimolar ratio (1:1, 34% yield). The side products of this reaction could not be identified each being probably in minute amounts under 5%. Monoacetyl, triacetyl and tetraacetyl porphyrines were formed as such minor side products in addition to the several other unidentified products as indicated by MALDI-TOF. The reduction of either acetyl groups of **31** and **32** with NaBH_4 gave the monoreduced products **33** and **34** respectively. In the final step, zinc metallation of the free base monohydroxy compounds **31** and **32** with $\text{Zn}(\text{Ac}_2\text{O})$ yielded **35** and **36** in almost quantitative yield, as shown in Scheme 2.2.

2.3 Synthesis of 5-formyl-15-hydroxymethyl-10,20-bis(3,5-di-*t*-butylphenyl)porphinato zinc (40)

Compound **40** was synthesised by employing a Vilsmeier-type diformylation reaction.



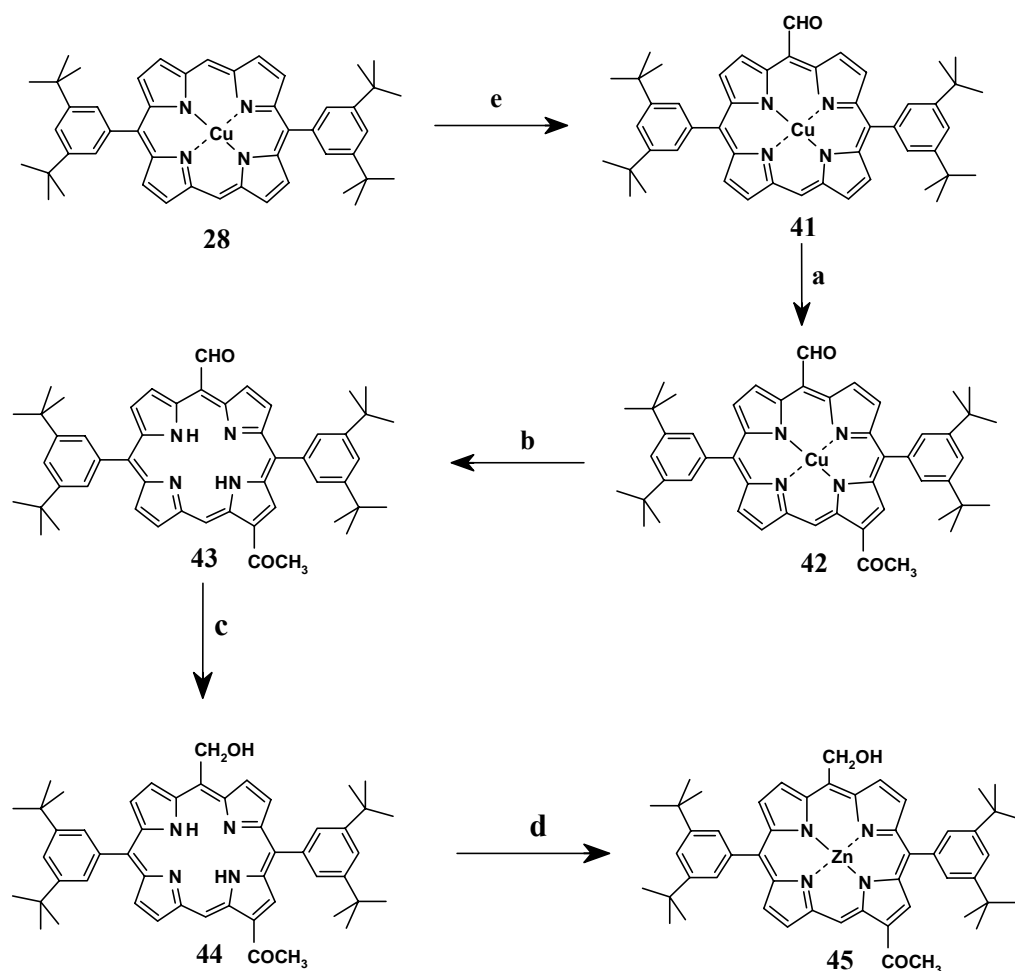
Scheme 2.3

Reaction conditions: **e** = POCl₃ / DMF, ClCH₂CH₂Cl, 60°C, 14h, 43%; **b** = TFA/H₂SO₄ (1/1 v/v), > 85%; **c** = NaBH₄ / MeOH/CHCl₃, r.t., 90%; **d** = anh. Zn(OAc)₂, MeOH/CHCl₃ > 90%.

The first step consists of the synthesis of *meso* disubstituted 5,15-diformyl porphyrin **37** followed by a demetallation process under acidic conditions employing a 1:1 mixture of sulfuric and trifluoroacetic acid to give the green protonated free base porphyrin **38**. The monoreduction of either formyl groups afforded **39**, which after zinc metallation produced **40** in good overall yield (30%) as shown in Scheme 2.3.

2.4 Synthesis of 3-acetyl-15-hydroxymethyl-10,20-bis (3,5-di-*t*-butylphenyl)-porphinato zinc (45)

This synthesis consisted of a combination of the previous two methods first by monoformylation of **28** under Vilsmeier condition to give **41** and the second one was a novel and selective monacylation reaction.



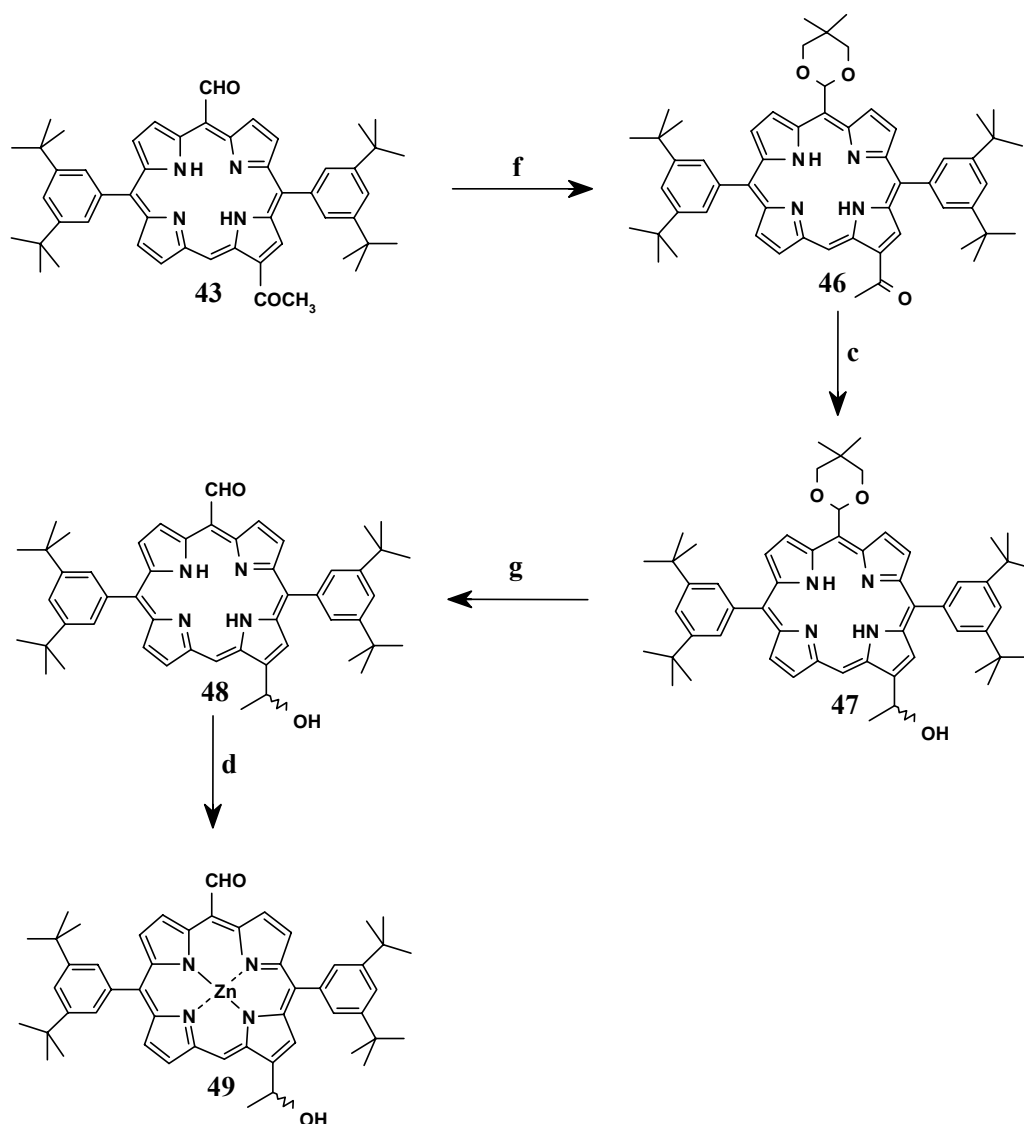
Scheme 2.4

Reaction conditions: **e** = POCl₃/DMF, ClCH₂CH₂Cl, 40°C, 45 min, 83%; **a** = Ac₂O, SnCl₄ / CS₂, 0°C, 3 min.; **b** = TFA/H₂SO₄ (1/1 v/v), 80%; **c** = NaBH₄ /MeOH/CHCl₃, r.t, 67%; **d** = Zn(OAc)₂, MeOH/CHCl₃ 92%.

This produced compound **42**, which after demetallation and selective reduction of the formyl group gave intermediate compounds **43** and **44** respectively. The final compound **45** was obtained after zinc metallation of the free base compound **44** as shown in Scheme 2.4.

2.5 Synthesis of (*rac*)-10,20-bis(3,5-di-*tert*-butylphenyl)-15-formyl-3-(hydroxyethyl)-porphyrinato zinc (49)

In order to obtain compound **49** having a *meso* formyl group, the acetyl group of **43** was selectively protected.



Scheme 2.5

Reaction conditions: **f** = 2,2-dimethyl-1,3-propanediol, PTSA, toluene, Δ , 65 min, 96%;

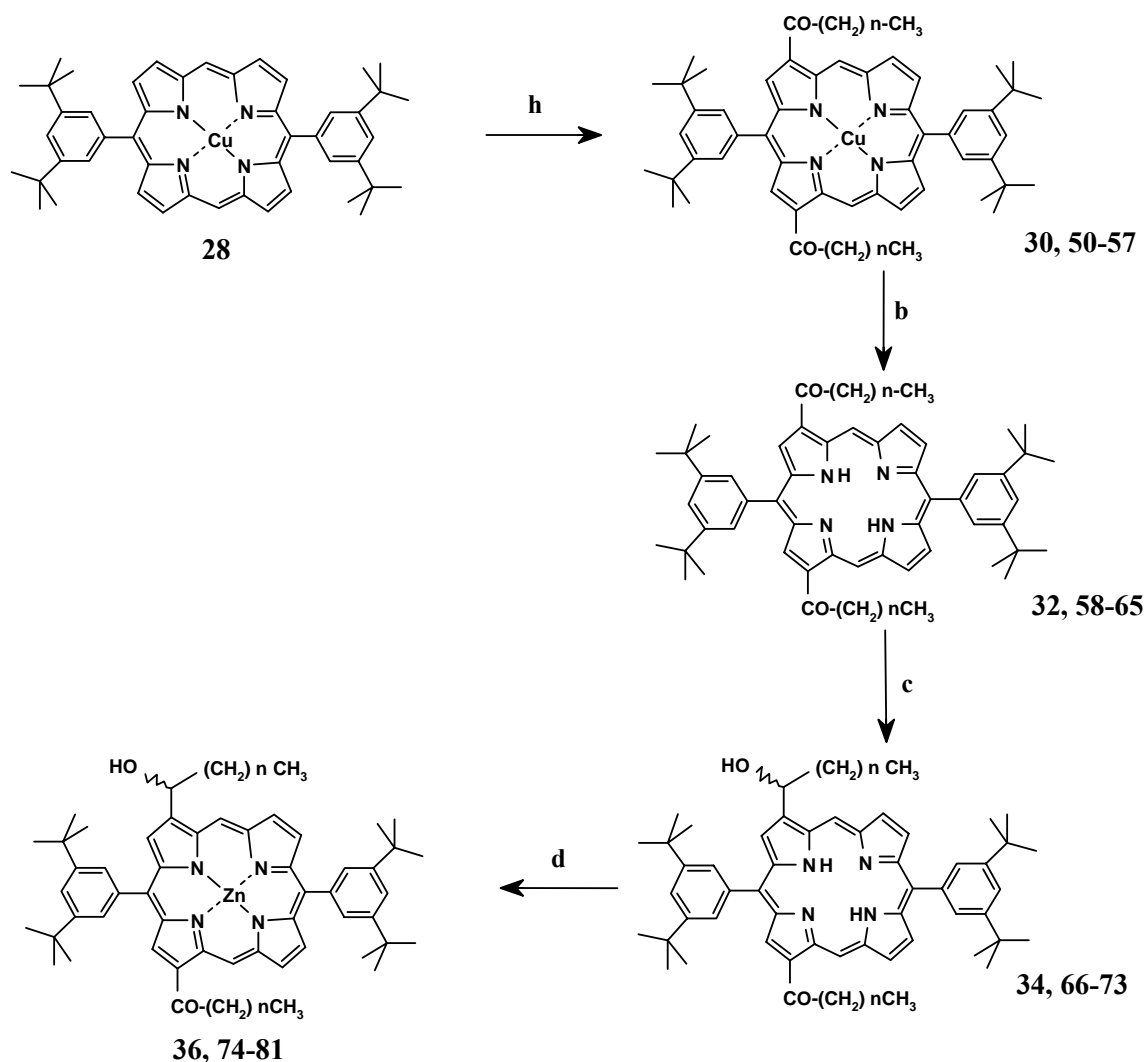
c = NaBH₄, MeOH, CH₂Cl₂, r.t., 19h, 72%; **g** = 0.5M HCl, 1,4-dioxane, Ar, r.t., 17h, 94%; **d**

Zn(OAc)₂, CHCl₃/MeOH (5:3, v/v), 3h, 93%.

The formyl group was protected according to Lindsey's procedure^[61] to give **46**. In the next step the acetyl group of **46** was then subjected to the reduction of the acetyl group with NaBH₄ to produce compound **47** as the racemate. Finally, compound **49** was obtained after zinc metallation of the free base intermediate compound **48** as shown in Scheme 2.5.

2.6 Synthesis of Long Chain Compounds (74-81)

Compounds **74-81** were synthesized by using AlCl_3 as an acid catalyst using Friedel-Crafts-type reaction developed for the diacetylation of **28** at low temperature ($0-5^\circ\text{C}$). Different types of acyl chlorides ranging from $n = 0-14$ were used to obtain long chain diacetylated Cu-compounds **50-57**.



Scheme 2.6

(For the values of n and the Formula numbers see next pages).

Reaction conditions: **h** = AlCl_3 / $\text{Cl-CO}-(\text{CH}_2)_n\text{CH}_3$, CS_2 , where $n = 0-14$: **b** = TFA/ H_2SO_4 (1:1, v/v), r.t., 1-2h, 44-79%: **c** = NaBH_4 / MeOH, r.t., 15-60 min, 38-75%: **d** = $\text{Zn}(\text{OAc})_2$, MeOH/ CHCl_3 , overnight, r.t., 77-96%.

The compounds **58-65** were obtained by the same synthetic route that applied for **44-45** in high yields as shown in Scheme 2.6 and in Table 1.

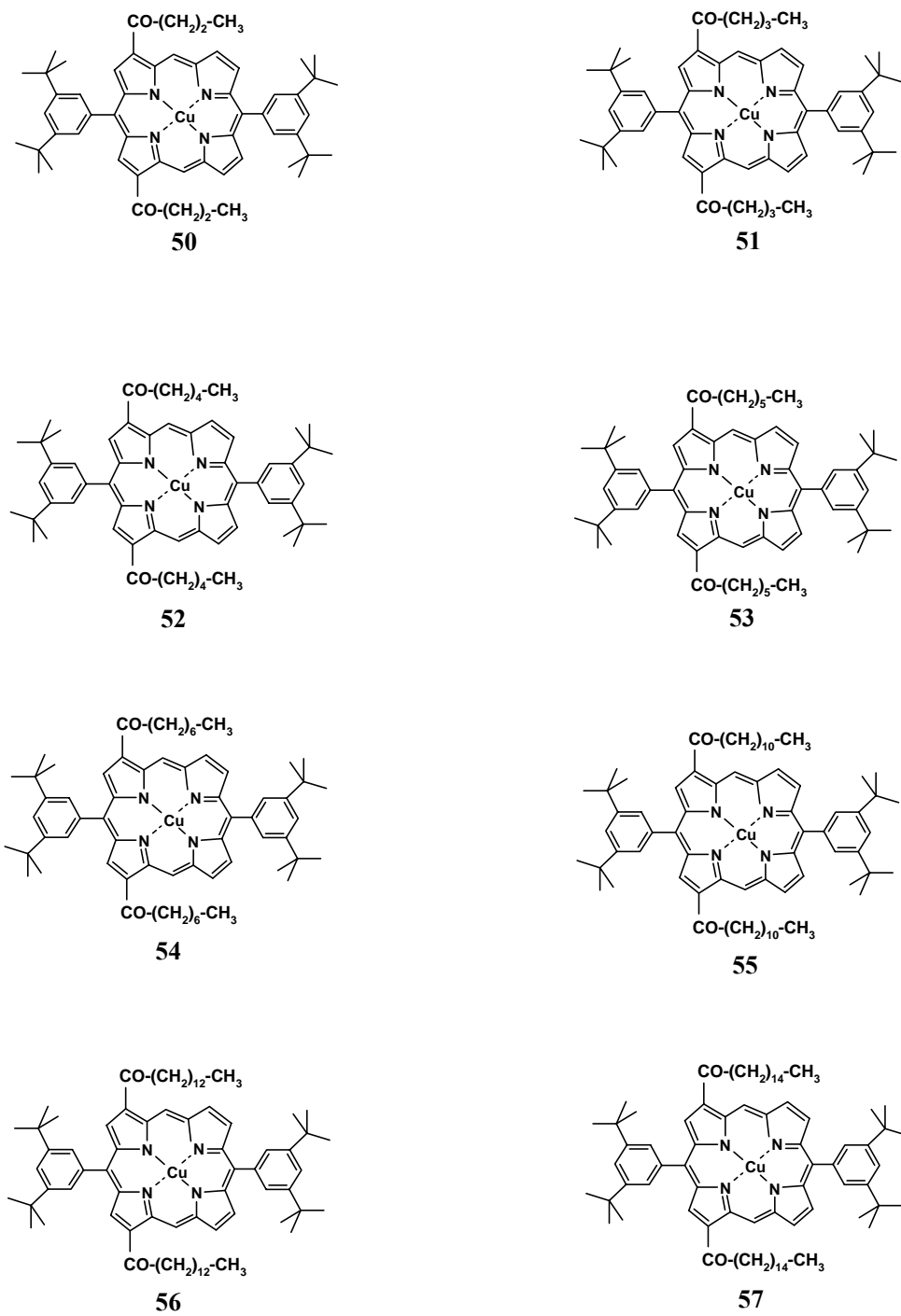


Figure 2.1: Intermediate 3,17-diacyl Cu-BTBPP compounds

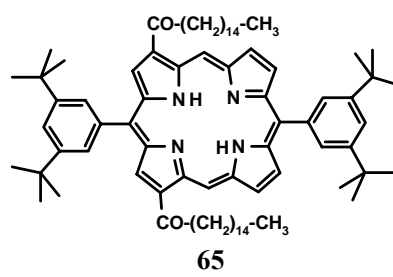
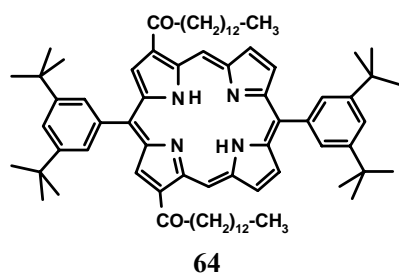
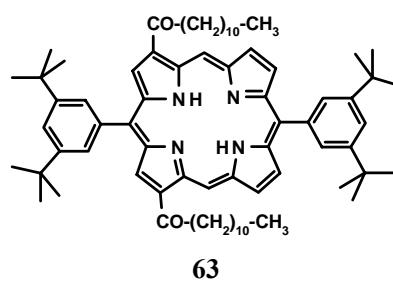
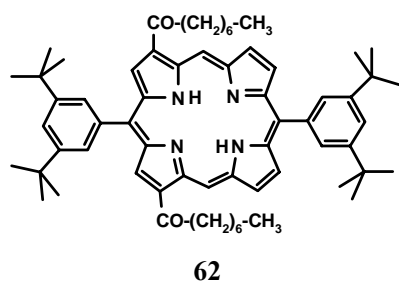
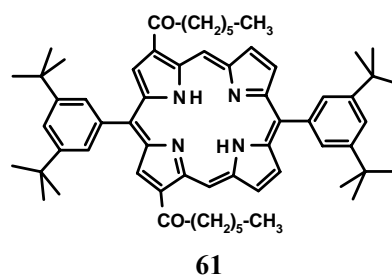
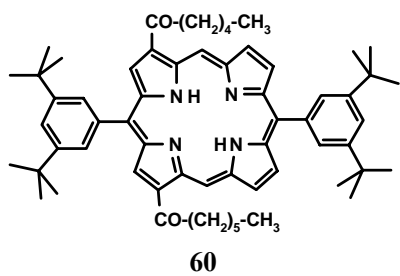
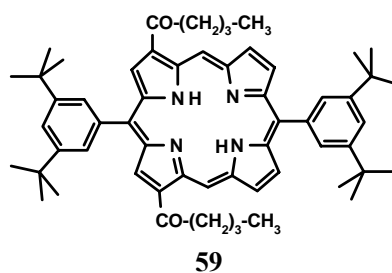
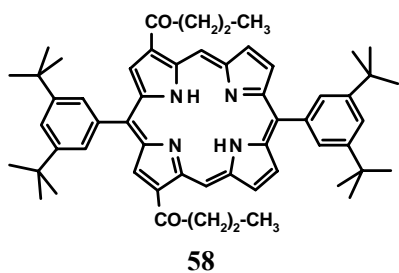


Figure 2.2: Intermediate 3,17-diacyl-BTBPP compounds (continued).

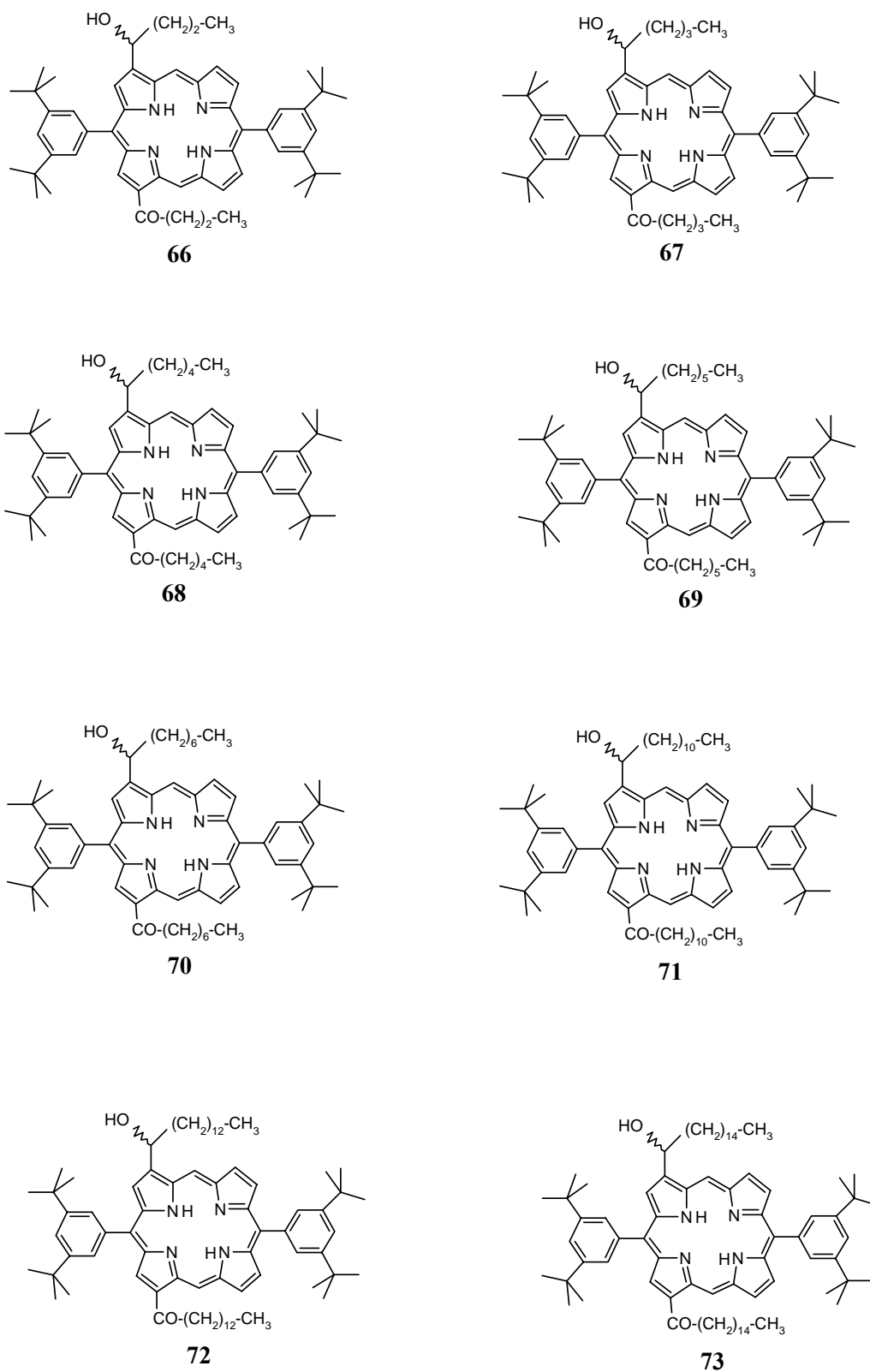


Figure 2.3: Intermediate monoreduced BTBPP compounds (continued).

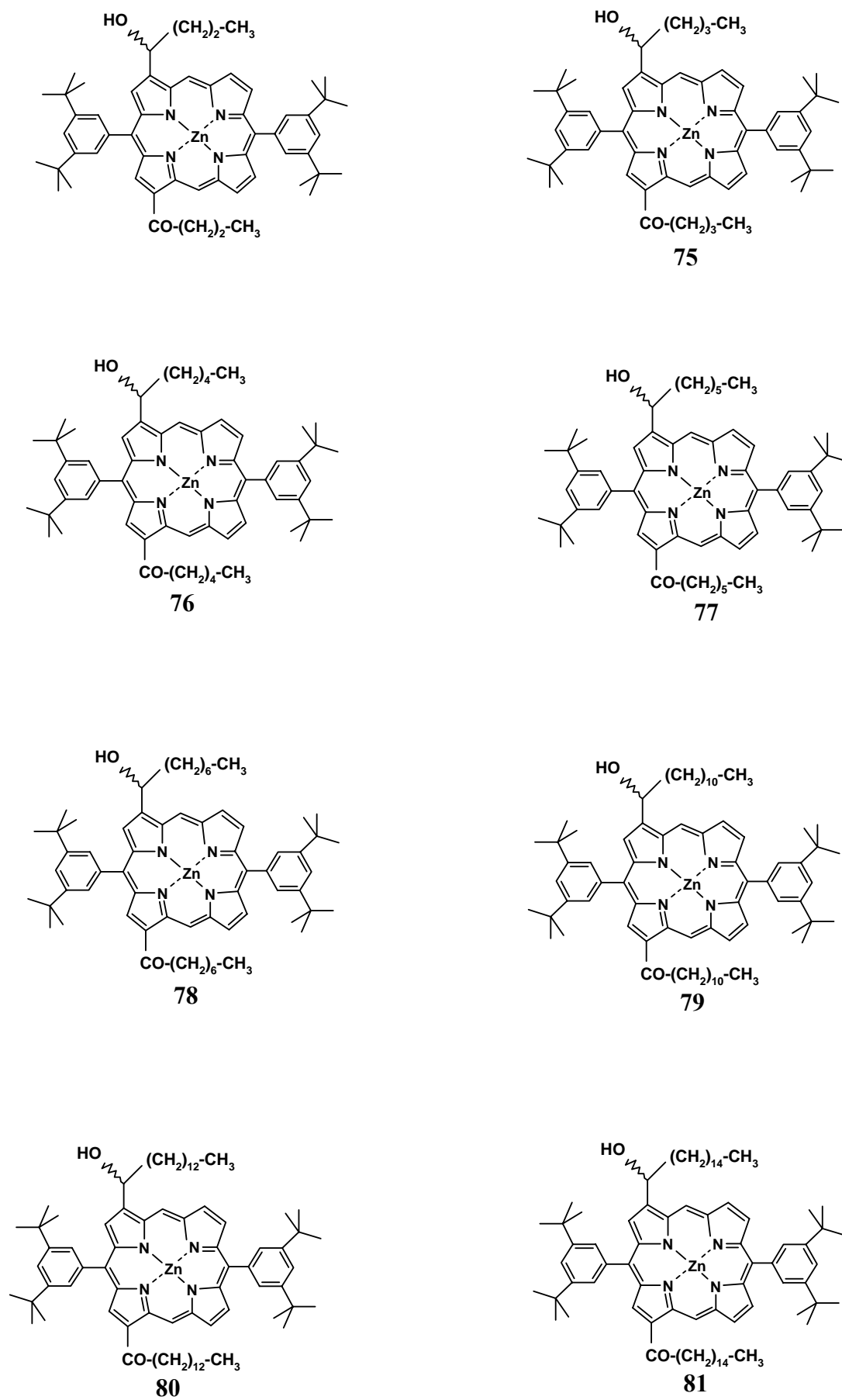
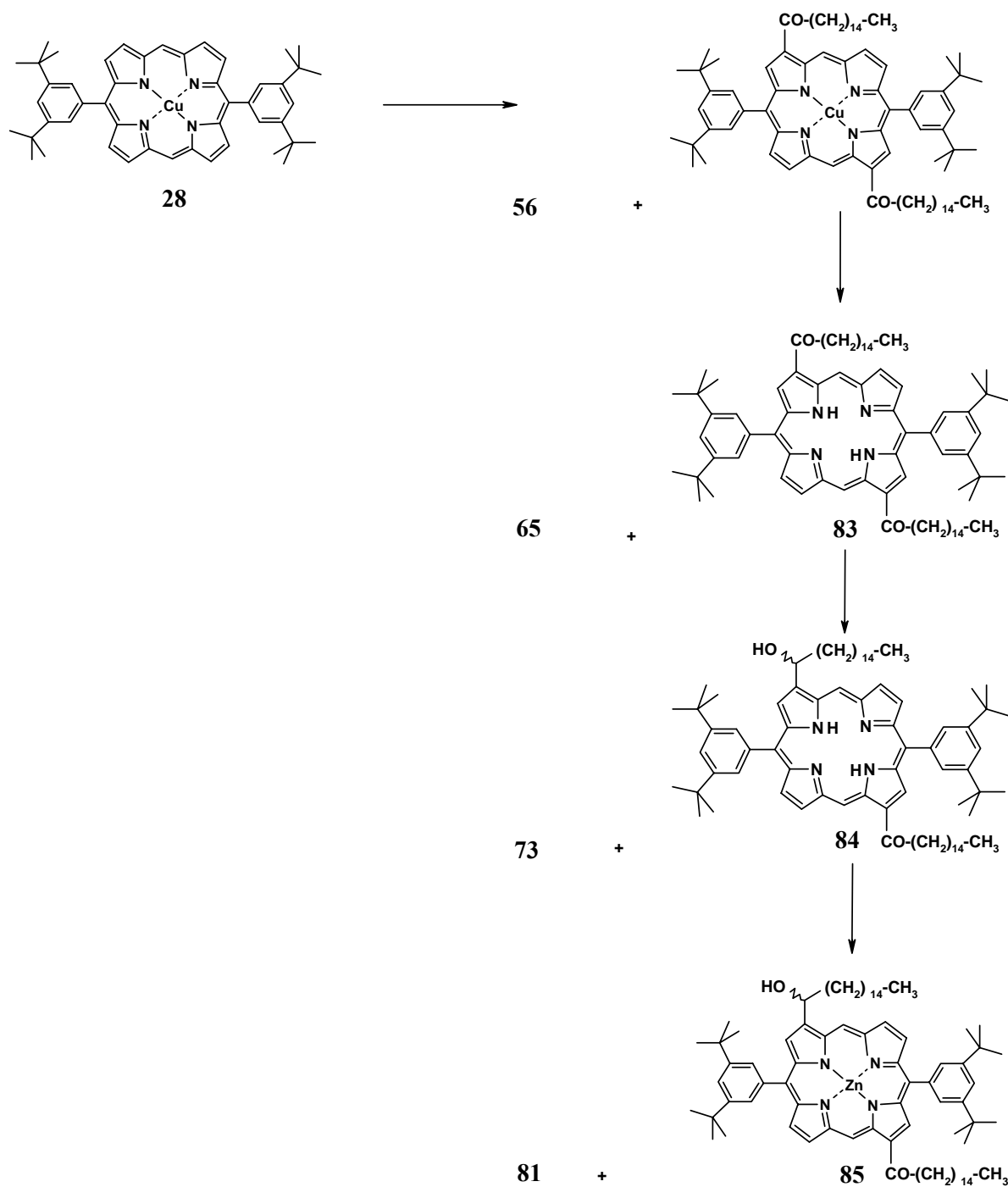


Figure 2.4: Intermediate Zn-ketol-BTBPP compounds

2.7 Synthesis of 3,17-Di-Palmitoyl-10,20-bis(3,5-di-*t*-butylphenyl)porphinato zinc (79) and 3,13-Di-Palmitoyl-10,20-bis(3,5-di-*t*-butylphenyl)porphinato zinc (83)

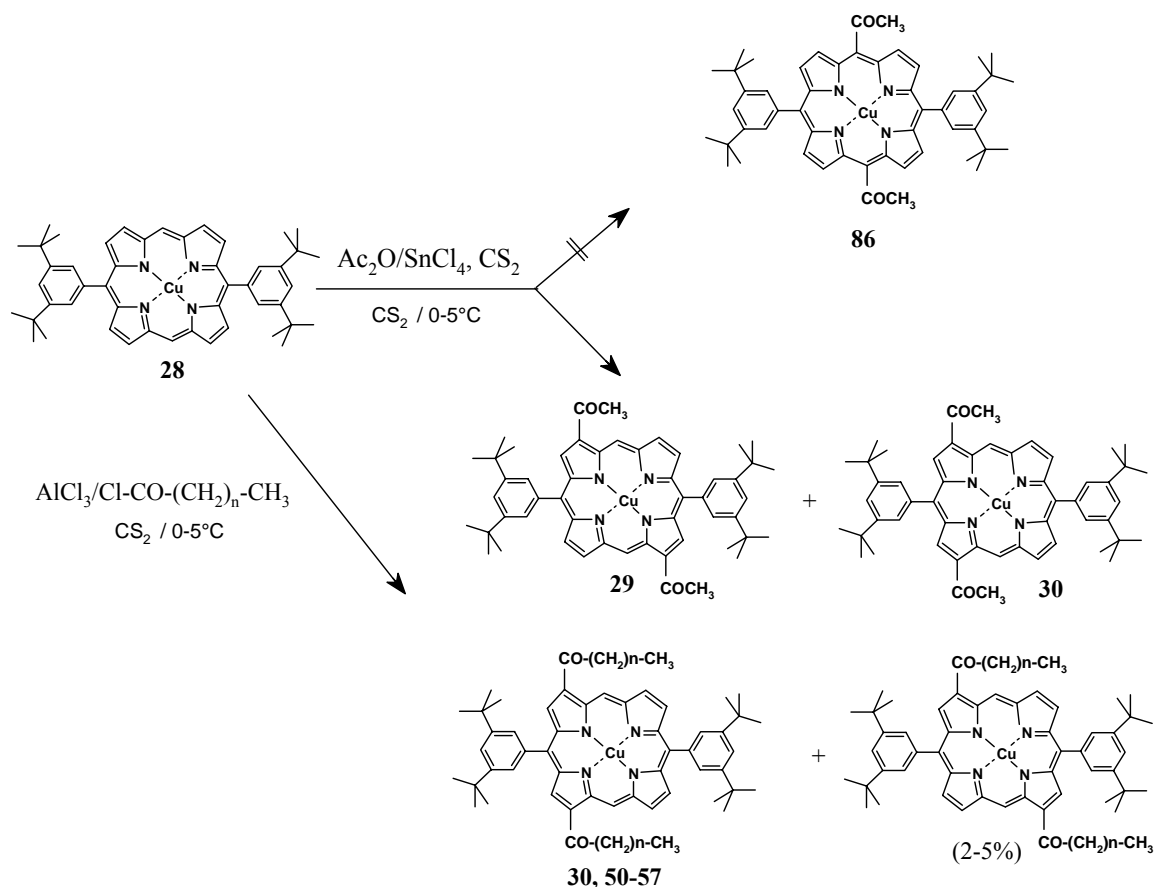
Compound **56** and **80** were synthesized by applying the same procedure that applied for the synthesis of compounds **29** and **30**. (See Scheme 2.2 and 2.7)



Scheme 2.7

2.8 Discussion

Even though different types of acid catalyst can be used in Friedel-Crafts type acylations, only two acid catalysts AlCl_3 and SnCl_4 were used to synthesize compounds **29**, **30**, **42**, **50-57** and **80**, as preliminary tests employing other ones such as FeCl_3 , ZnCl_2 etc. gave poor yields or no reaction. With AlCl_3 various acid chlorides were used as acylating agents, while with SnCl_4 , the much cheaper acetic anhydride was employed. Because the *meso* position of the porphyrin ring is more reactive, 5,15-diacetyl Cu BTBPP (**86**) would have been the expected product under Friedel-Crafts acylation conditions, just as is the case for the Vilsmeier formylations. However, after employing AlCl_3 as an acid catalyst **30**, **50-57** were selectively formed whereas with SnCl_4 the pair of **29** and **30** diacetyl isomers was formed instead of the expected isomer **86**. (Scheme 2.8).



Scheme 2.8

Where $n = 0-14$

Theoretically, twelve diacyl isomers (Figure 2.1) are possibly formed under Friedel-Crafts acylation condition, but only one pair of (3,13 and/or 3, 17) of diacyl isomers were found.

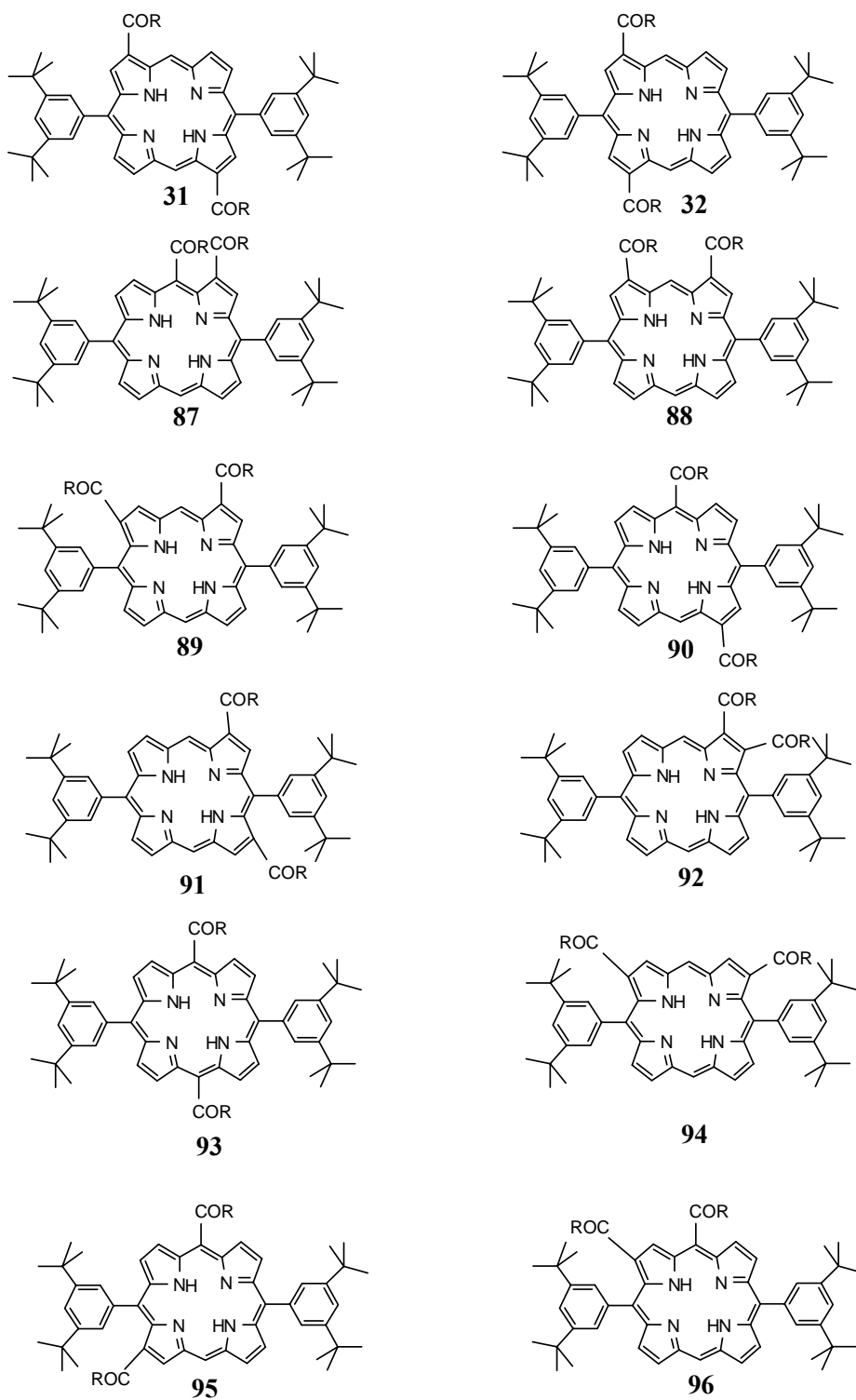


Figure 2.5: Twelve possible isomers in Friedel-Crafts diacylation reaction

Where, R = alkyl chains of the order, $n = 0-14$

When AlCl_3 was employed as Lewis acid catalyst in Friedel-Crafts acylation reaction, the 3,17-diacyl isomer (**30**) was the only product formed under kinetic control. Thus by reacting at low temperature, for less than 5 min, all 3,17-diacyl compounds could be obtained almost

pure. This represents a preparatively very useful novel reaction. At higher temperatures and at longer reaction times, in addition to the 3,17-diacyl compounds, the 3,13-diacyl isomers can be obtained as minor products summarizing, with both acid catalysts employed the 3,17-diacyl isomers were formed with higher selectivity. In order to explain the preferential formation of the 3,17-diacyl isomers over the 3,13-diacyl or any of the other isomers, a theoretical investigation on the geometry-optimized structure of a 3-formyl model compound was performed. This must be the initial acylation compound which suffers in a second step the diacylation. Because for molecule of this size, *ab initio* methods are time consuming, we performed semiempirical calculations for the monoacetyl compound **97** by applying the PM3 forcefield in combination with successive molecular mechanics calculations with the MM+ force field within the HyperChem® programme package.^[62]

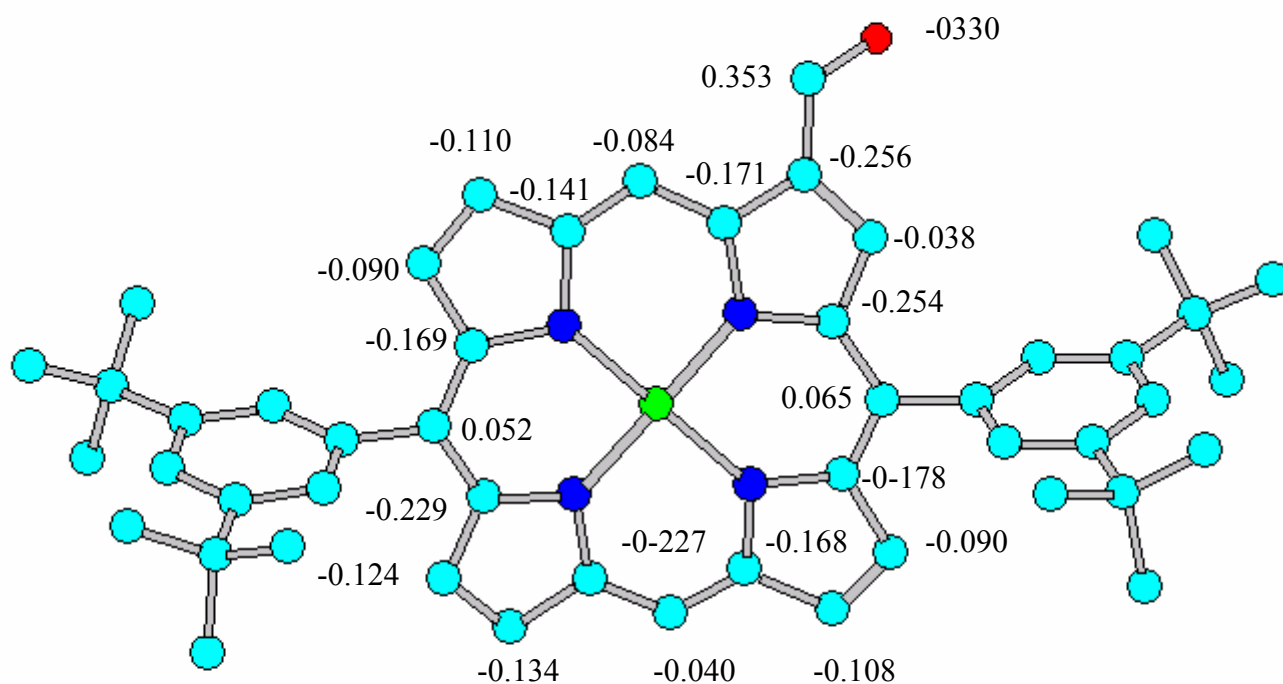
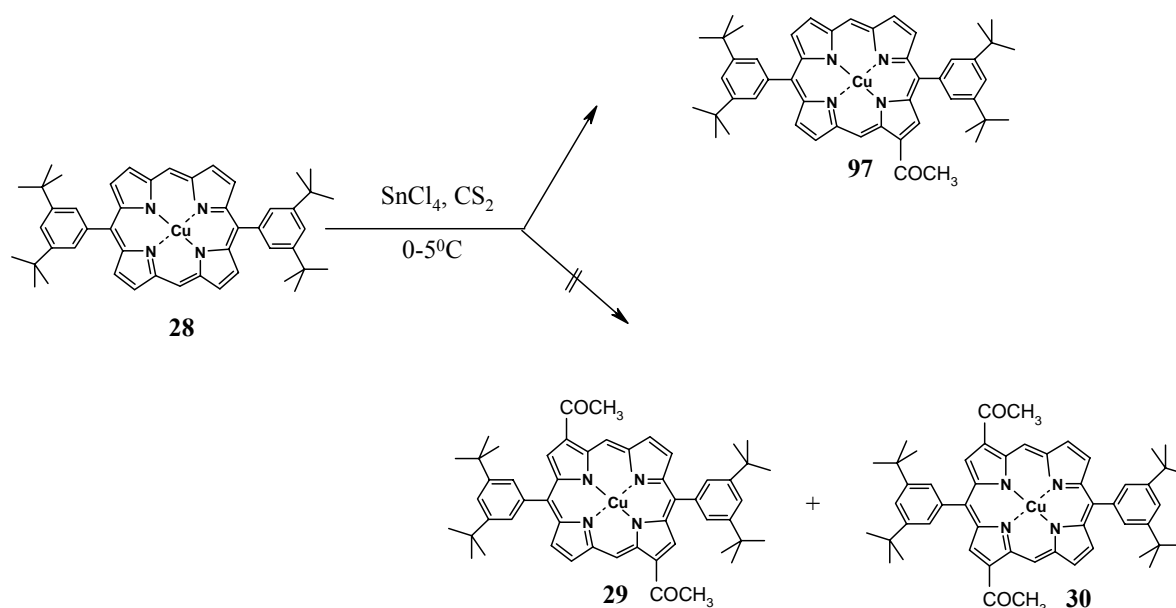


Figure 2.6 Calculated charge distribution in the 3-monoformyl model compound.
(PM3 and MM+ geometry optimization)

However, the information obtained from the charge distribution, as indicated in Figure 2.6, for each carbon of the porphyrin ring does not provide a satisfactory explanation for the preferential formation of the 3,17-diacetyl isomers over the 3,13-ones at this level of precision. It is however clear that the β -pyrrolic positions should be substituted more easily than the free 15-*meso* position. Due to the steric hindrance provided by the 3,5-di-*tert*-butylphenyl substituents, only the remote β -pyrrolic positions can be attacked by the acylation complexes.

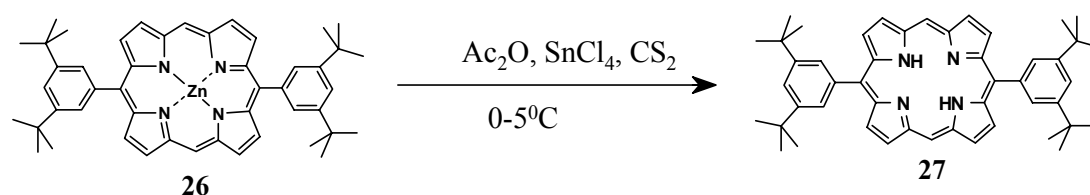
The separation of the 3,13 and 3,17-diacetyl isomers was very difficult on chromatography columns due to their similar R_f values. (0.54 and 0.52 for **29** and **30**, respectively in dichloromethane). Careful column chromatography on silica gel with 1:1 dichloromethane: n-hexane provided well-purified free base compounds (**31** and **32**) in quite high yields. Subsequent careful column chromatography on silica gel eluted firstly with dichloromethane gave the **29** isomer as the first fraction. Interestingly, in the preparative HPLC runs using 3% isopropanol in dichloromethane, the reverse elution order was encountered i. e **30** was eluted first. Furthermore, separation of **31** and **32** was more convenient than the separation of their copper complexes **29** and **30**, respectively, or of the monoreduced intermediates **33** and **34** from their mixtures. For the synthesis of diacylation products of porphyrins under Friedel-Crafts conditions, excess quantities of the acid catalyst and acid chlorides or acetic anhydrides are required. Presumably, this is because in the metallated porphyrins, the nucleophilic character of the porphyrin ring is reduced as the nitrogen atoms are engaged in metal bonding and hence excessive quantities of reagents are required in order for the reaction to take place. More importantly, the acylation reaction works well only on the metallated porphyrins as the free bases inhibit the Lewis acid reagent. When the acylation reaction was performed on the free base porphyrin instead of the copper porphyrin, the expected diacylated products were not formed.

When an attempt was made to perform the acylation reaction with smaller amounts of reagents, only the monoacylated compound **97** was obtained instead of **29** and **30** (Scheme 2.9). Also this acylation reaction does not work at equimolar ratio quantities. Furthermore, after diacylation of the porphyrin ring, the copper had to be removed in order to characterize the compound by NMR methods.



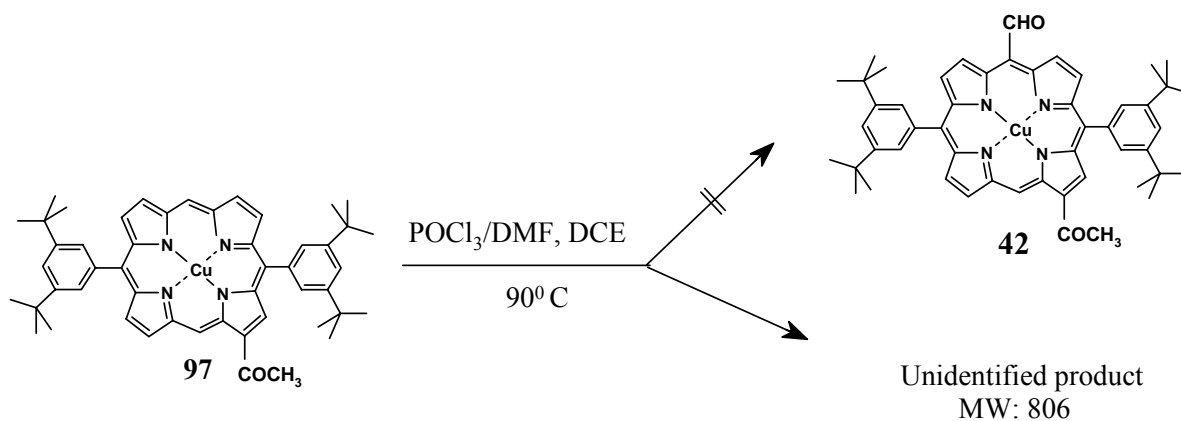
Scheme 2.9

Because the Zn metallated products were the desired final products of all the envisioned synthetic sequences, an attempt to perform the acylation reaction directly on the zinc porphyrin, under similar reaction conditions to those applied for the diacylation of the Cu porphyrin was performed. It was hoped that this would reduce the number of required steps but the attempt remained unfruitful because the zinc metal was very easily removed under the acidic reaction conditions to give only the unreactive free base porphyrin **27**. (Scheme 2.10)

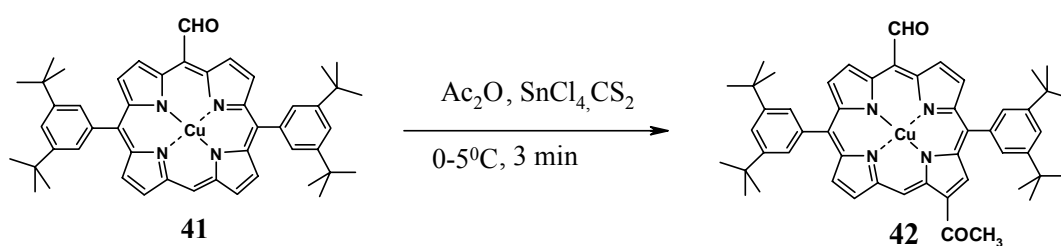


Scheme 2.10

In order to synthesize compound **42**, the isolated monoacetyl compound **97** was subjected to a formylation reaction under Vilsmeier condition. Unidentified products (MW = 806) were formed (Scheme 2.11). However the reverse order of reaction sequence i. e acetylation of the presynthesised monoformyl compound **41** under Friedel-Crafts conditions, yielded the desired product **42**. (Scheme 2.12).



Scheme 2.11



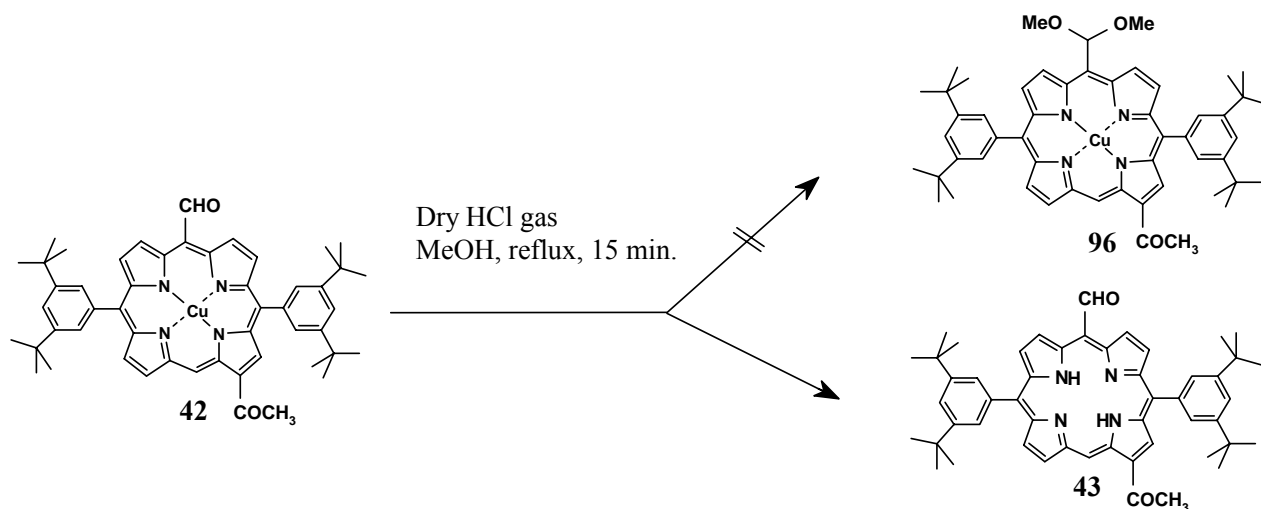
Scheme. 2.12

The diformylation of **28** required an excess of formylating reagent, an elevated reaction temperature (80°C at reflux in 1,2-dichloroethane) to produce **37**. On the other hand, in the monoformylation reaction to produce **41** smaller quantities of the Vilsmeier reagent were required. This is because once the monoformylated compound is formed the reactivity of **41** is reduced and hence much larger quantities of reagents were required for the diformylation.

When a formyl and an acetyl group substituted a porphyrin, monoreduction of the formyl group was possible with high selectivity leading to the achiral hydroxymethylene compound in 67% yield over 3 steps. For accessing the reversed functionalities with a reduced acetyl group (*i.e.* a chiral hydroxethyl group) and a formyl group as the carbonyl substituent, protective group strategies had to be devised.

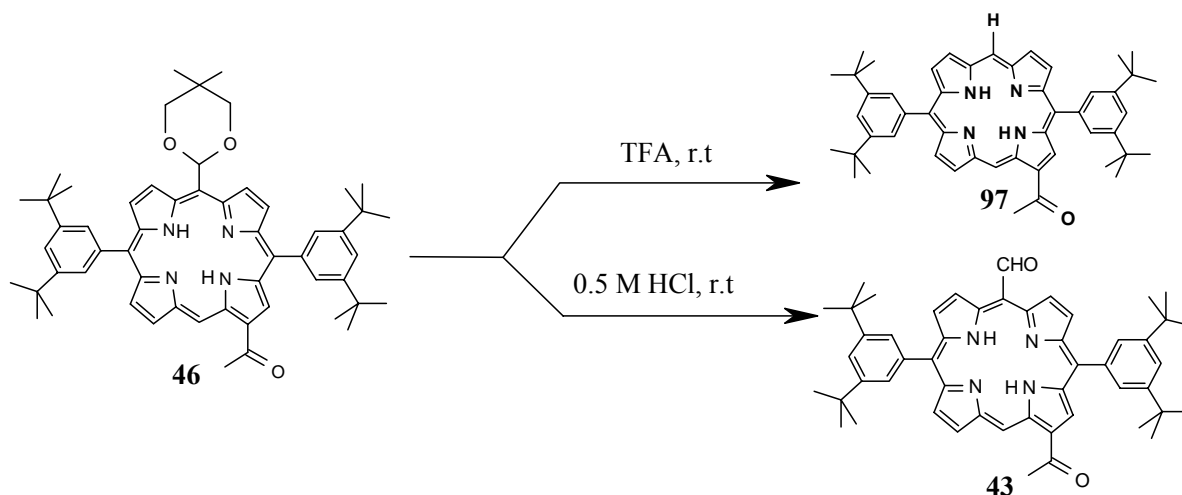
In order to protect the formyl group, several different protecting groups were tested. The attempted formyl group protection with dry HCl gas and methanol resulted in the formation of the free base product **43** rather than the expected one **96** (Scheme 2.13).^[54] Only the *gem*-dimethyl substituted dioxane group, which was introduced by Lindsey to porphyrin chemistry, worked well in the end to produce **46**. Although several acetals could be obtained, and the acetyl group could be reduced with sodium borohydride, the next step *i. e.* the deprotection of the acetal was challenging. When aqueous TFA was employed for

deprotection of various acetalic group, surprisingly a “decarbonylation” reaction occurred that actually replaced the formyl protected group by a *meso*-hydrogen atom to give compound **97**.



Scheme 2.13

On the other hand deprotection of the Lindsey acetal group was successful with a dilute (0.5 M) HCl solution (Scheme 2.14). The decarbonylation reaction presumably occurs due to the higher acidity of TFA (Scheme 2.14). This serendipitously found reaction sequence might prove of some synthetic interest in order to be able to remove selectively *meso*-substituted formyl groups.



Scheme 2.14

In addition to the diacetyl compounds other long chain isomeric compounds were also synthesized; however the separation of these long chain acyl isomeric compounds remained a difficult task because of their higher solubility even in nonpolar solvents like *n*-hexane and due to their similar R_f values in different solvents or mixtures thereof. With the many

mixtures that were tested to separate the isomers, only a pair of 3,13-dipalmitoyl (**81**) and 3,17-dipalmitoyl (**65**) compounds were successfully resolved in a very easy way by taking the advantage of their different solubility behavior in the dichloromethane/methanol (2:1, v/v) solvent combination. Compound **83** was insoluble in the above solvent combination where as **65** being much more polar, was soluble. On a similar line of thought, the separation attempts of other such long chain isomeric compounds 3,13 and 3,17 isomers, with different types of solvent combinations remained unsuccessful.

2.9 Characterization

All new compounds were adequately characterized in order to allow publication of the new results in high standard journals. Beside ^1H - and ^{13}C -NMR, 2D-NMR techniques such as COSY, NOESY and H-C COSY were routinely employed on a 300 MHz spectrometer by the author. Additionally, elemental analyses, MALDI-TOF-MS and HR-FAB MS were employed. For the characterization of the self-assemblies, UV-Vis and fluorescence were routinely used, as shown in Chapter 3. Advanced scanning probe techniques were also used in some cases. Only a few selected examples are given below, while the full characterization is given in Chapter 4 in the Experimental Section.

The structure of compound **31** was confirmed on the basis of NMR spectroscopy while the structure of compound **32** was also ascertained through an X-ray crystallographic structure.

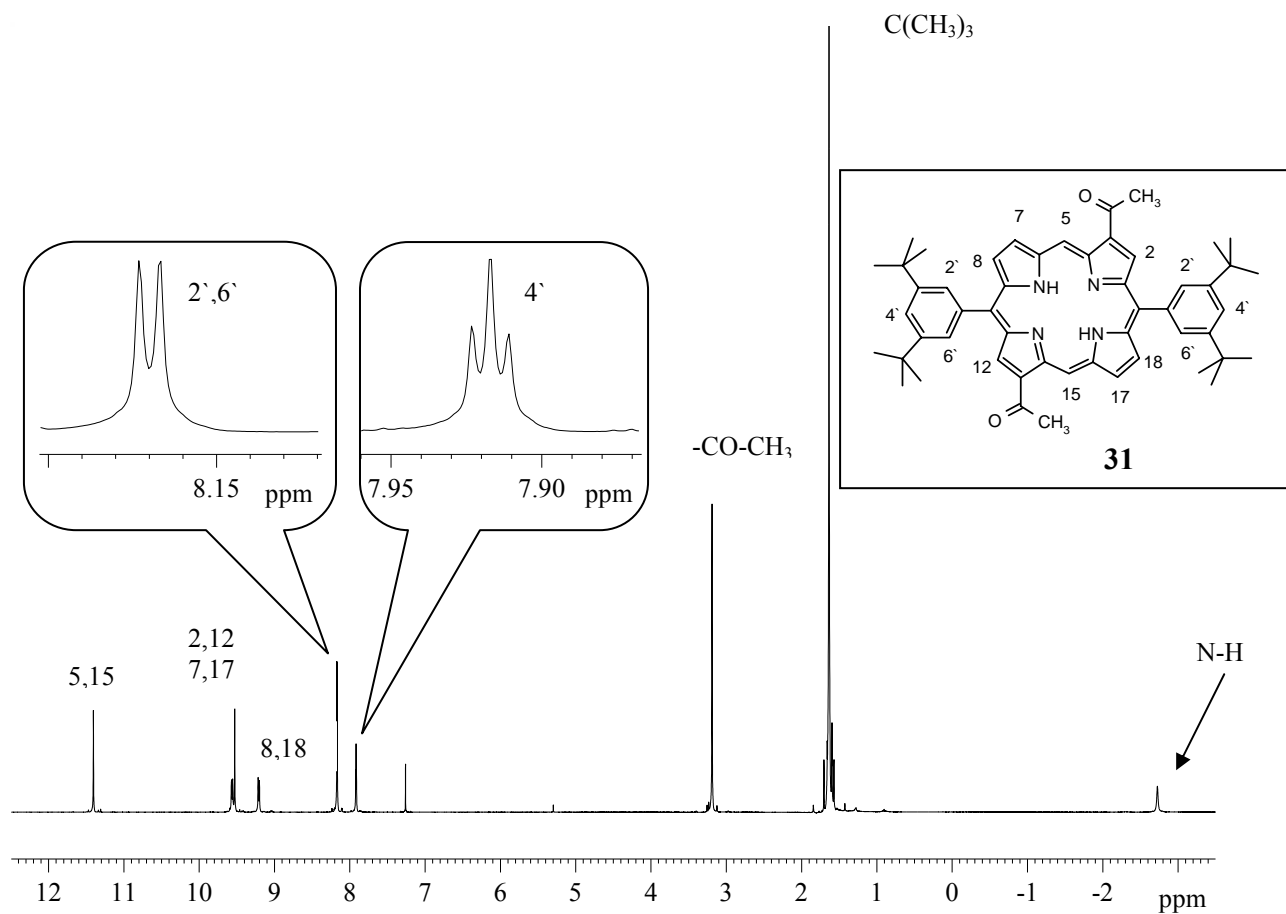


Figure 2.7: The $^1\text{H-NMR}$ spectrum (300 MHz in CDCl_3) for 3,13-diacetyl-10,20-bis-(3,5-di-*t*-butylphenyl)-21,23H-porphin (**31**) shows one doublet for the 2' and 6' protons while the 4' protons show a single triplet in the phenyl ring. Also the four *t*-butyl groups show a singlet indicating a symmetric structure.

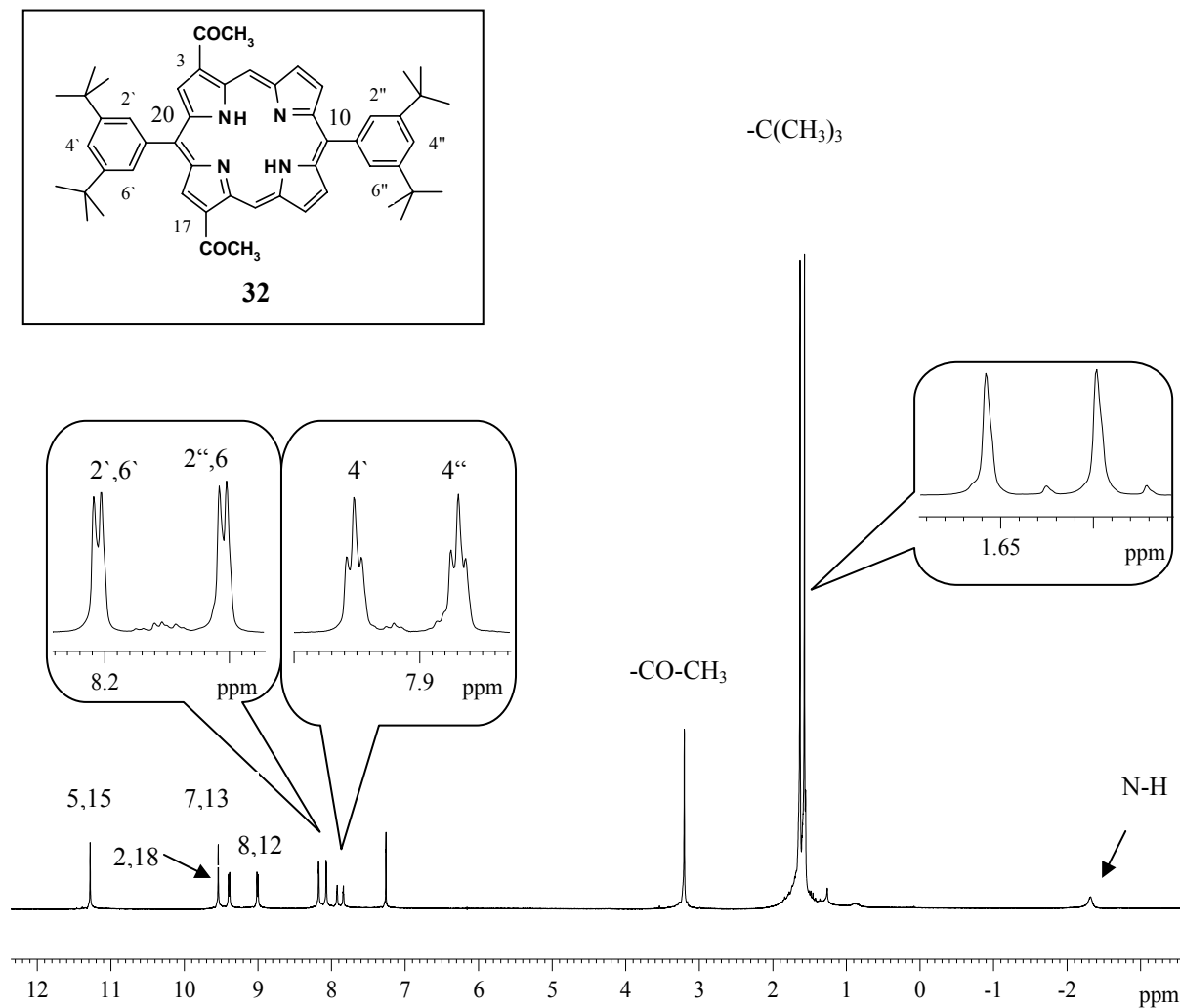


Figure 2.8: The $^1\text{H-NMR}$ spectrum (300 MHz in CDCl_3) for 3,17-diacetyl-10,20-bis-(3,5-di-*t*-butylphenyl)-21,23H-porphyrine (**32**) shows two doublets for the 2' & 6' and 2'' & 6'' protons while the 4' & 4'' protons show two triplets in the phenyl rings. Additionally the four *t*-butyl groups split into two different sharp singlets attributed to the 10- and 20-di-*t*-butylphenyl groups, respectively.

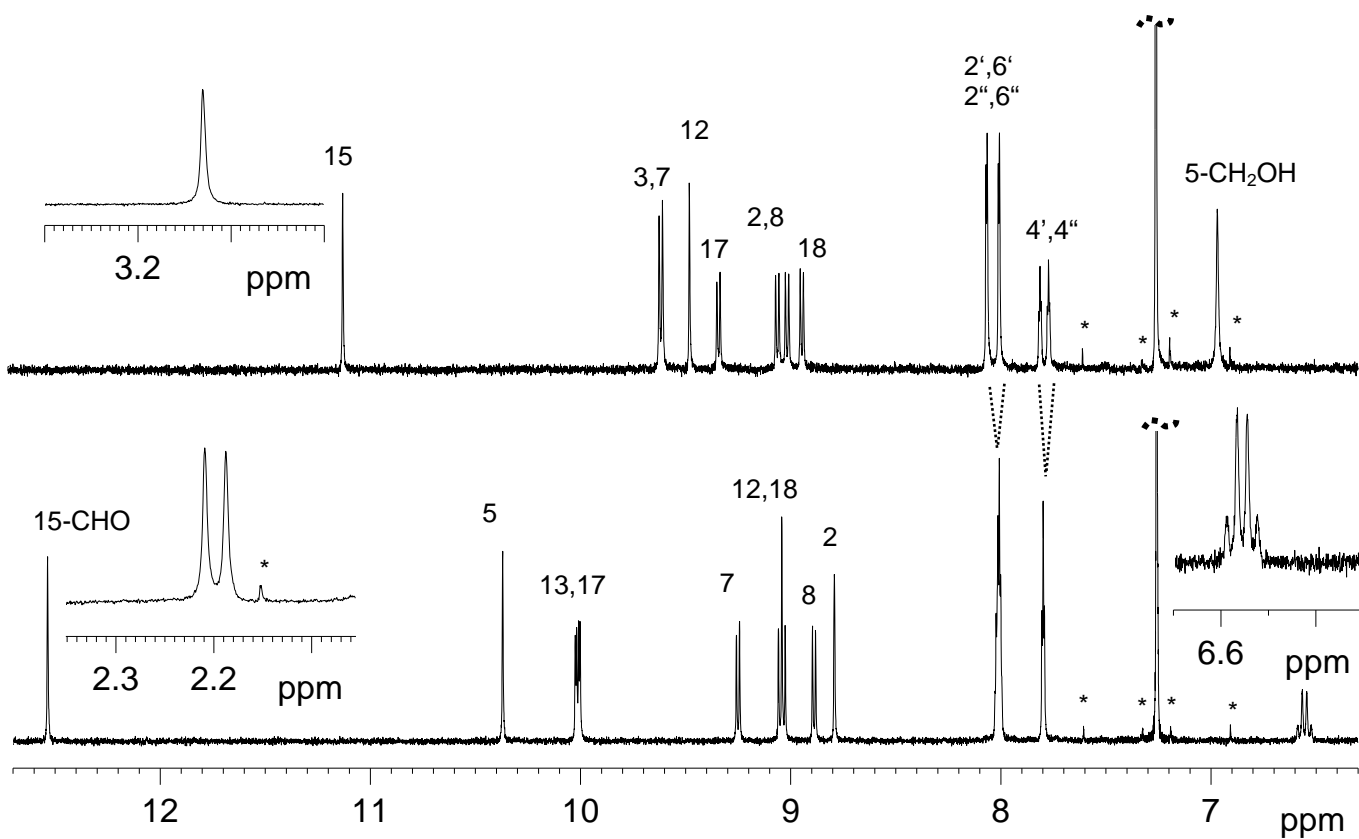


Figure 2.9. Low-field region of the 300 MHz NMR spectra of **49** (lower trace) and **45** (upper trace) in $\text{CDCl}_3:\text{CD}_3\text{OD}$ 10:1 (v/v). Assignments are based upon COSY and NOESY spectra. Insets show the 3-CHOHCH₃ signals (lower trace) and the 13-COCH₃ singlet (upper trace). The peaks indicated by asterisks do not belong to the sample being either ¹³C-satelites and spinning side bands of the CHCl₃ signal or a trace of acetone.

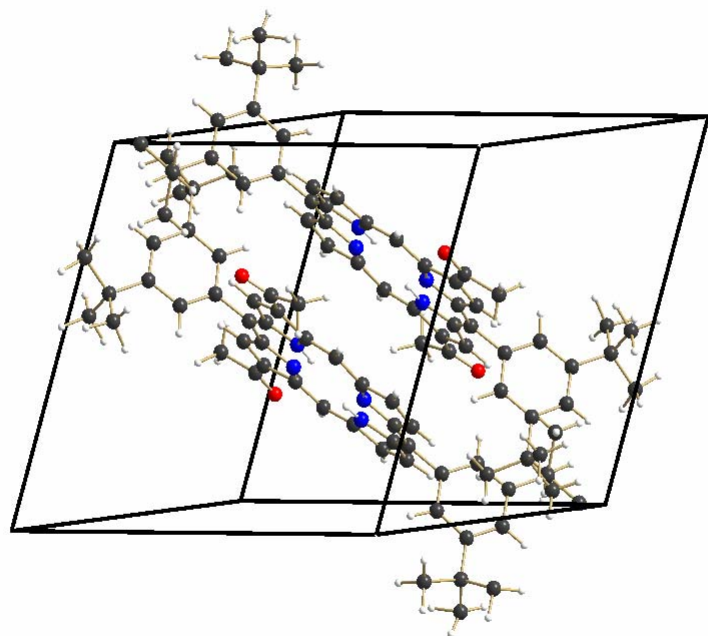


Figure 2.10 (a): X-ray crystal structure for 3,17-diacetyl-10,20-bis-(3,5-di-*t*-butylphenyl)-21,23H-porphyrine (**32**) Blue color indicates nitrogen atoms of the porphyrins ring whereas red color shows the oxygen atoms of the acetyl groups.

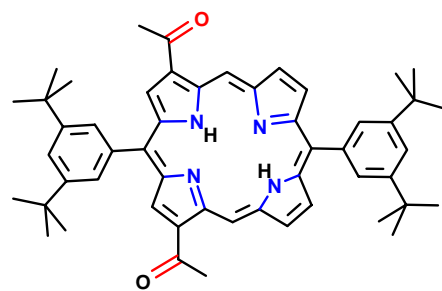
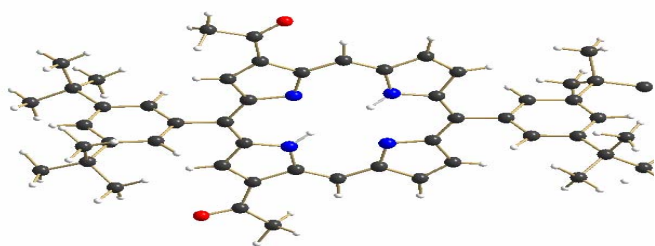


Figure 2.10(b): Molecular structure of 3,17-diacetyl-10,20-bis-(3,5-di-*t*-butylphenyl)-21,23H-porphyrin (**32**) with the same color indications.

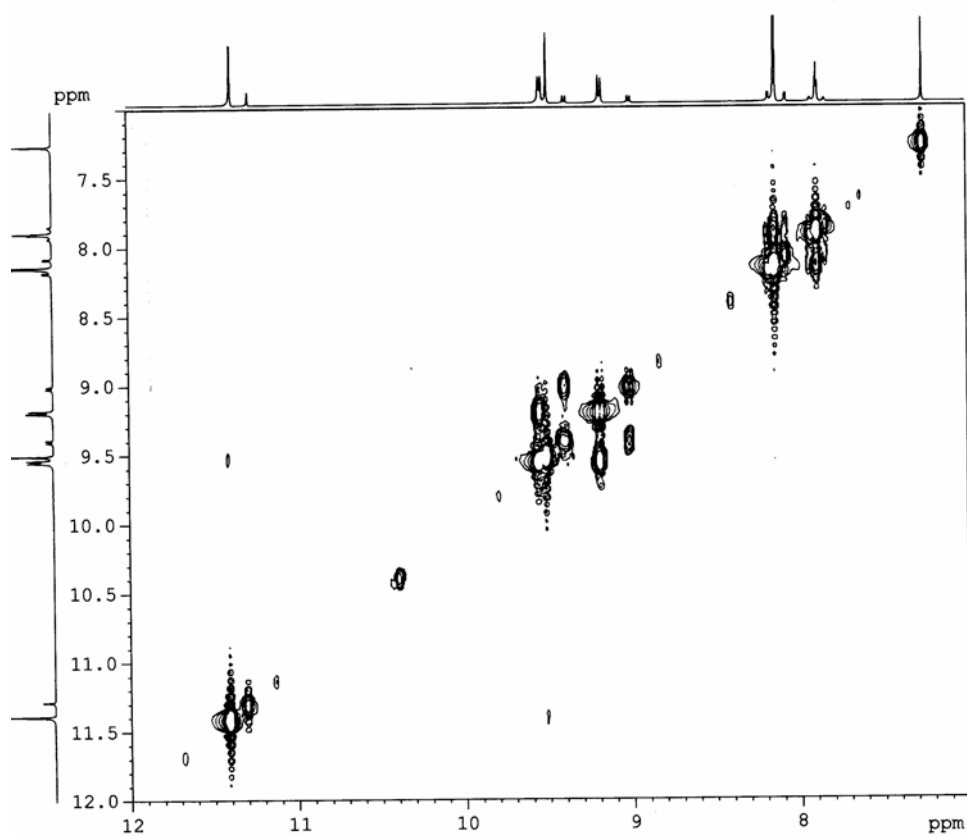


Figure 2.11: 3,13- diacetyl BTBPP (**31**): COSYGSTP in $CDCl_3$.
 GSTP stands for Gradient Shimming with Transfer of Polarization.

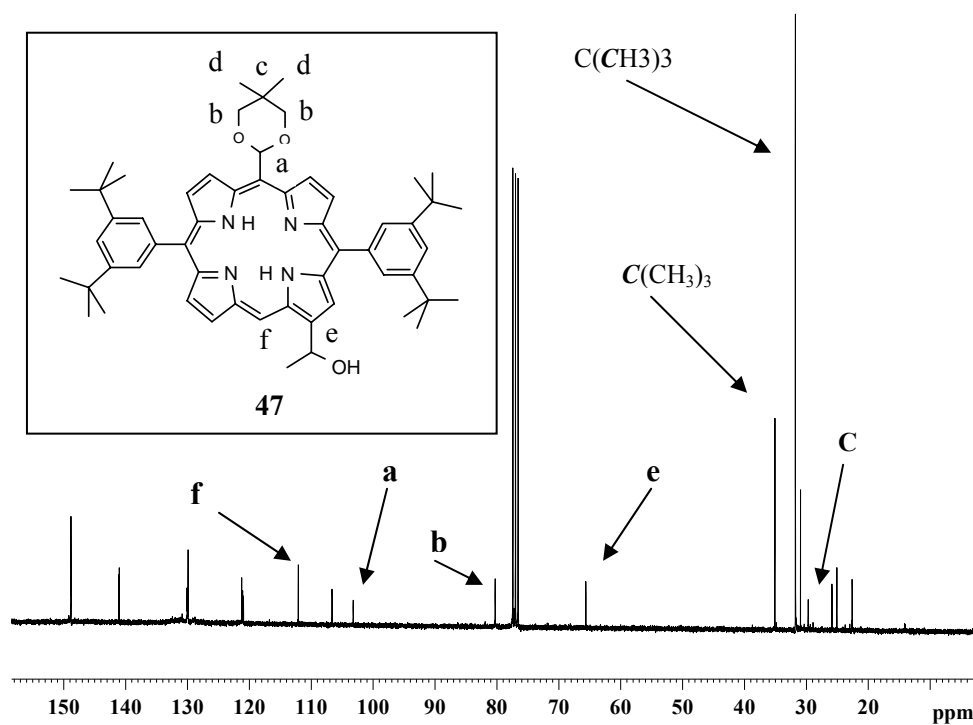


Figure 2.12: ^{13}C spectrum of **47** as a typical example.

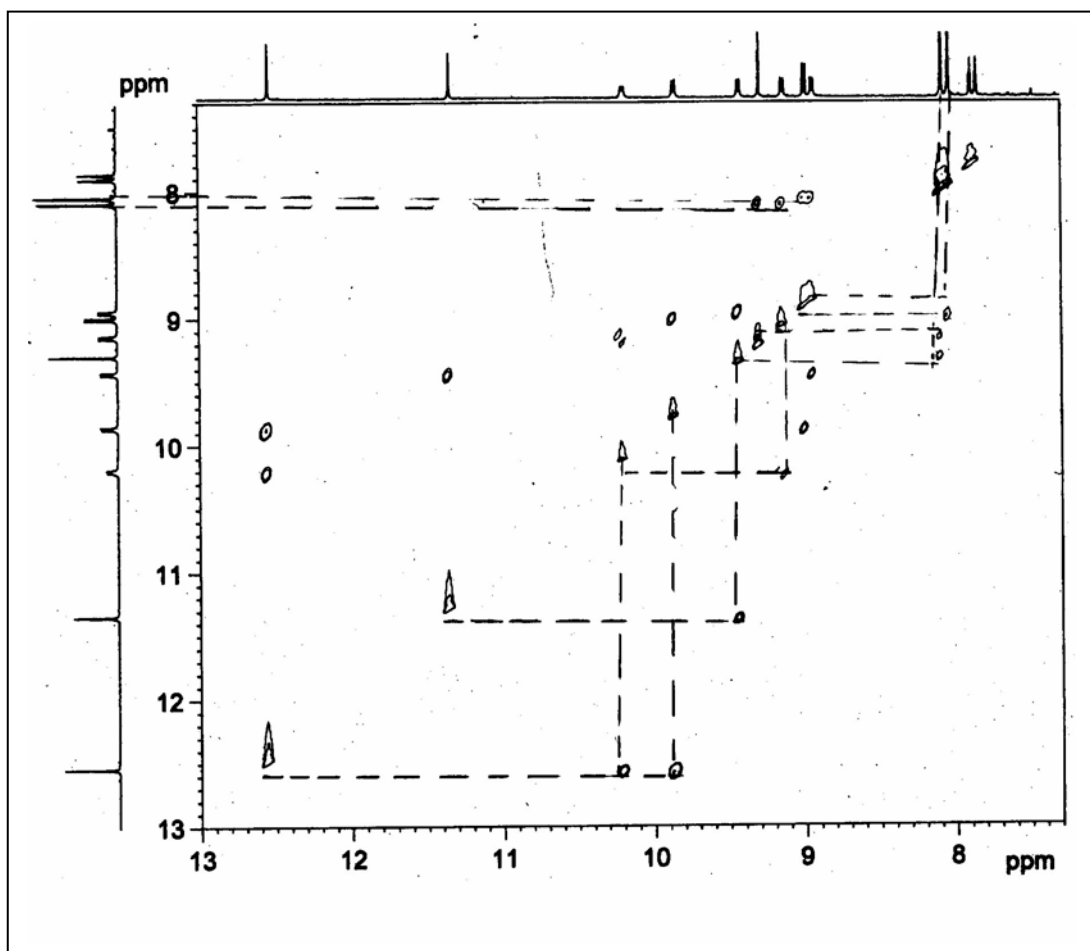


Figure 2.13: NOESYTP spectrum of 3-acetyl-15-formyl BTBPP in CDCl_3 (**43**) From the cross-correlations the 3-15 substitution pattern is clearly evident. TP stands for Transfer of Polarization.

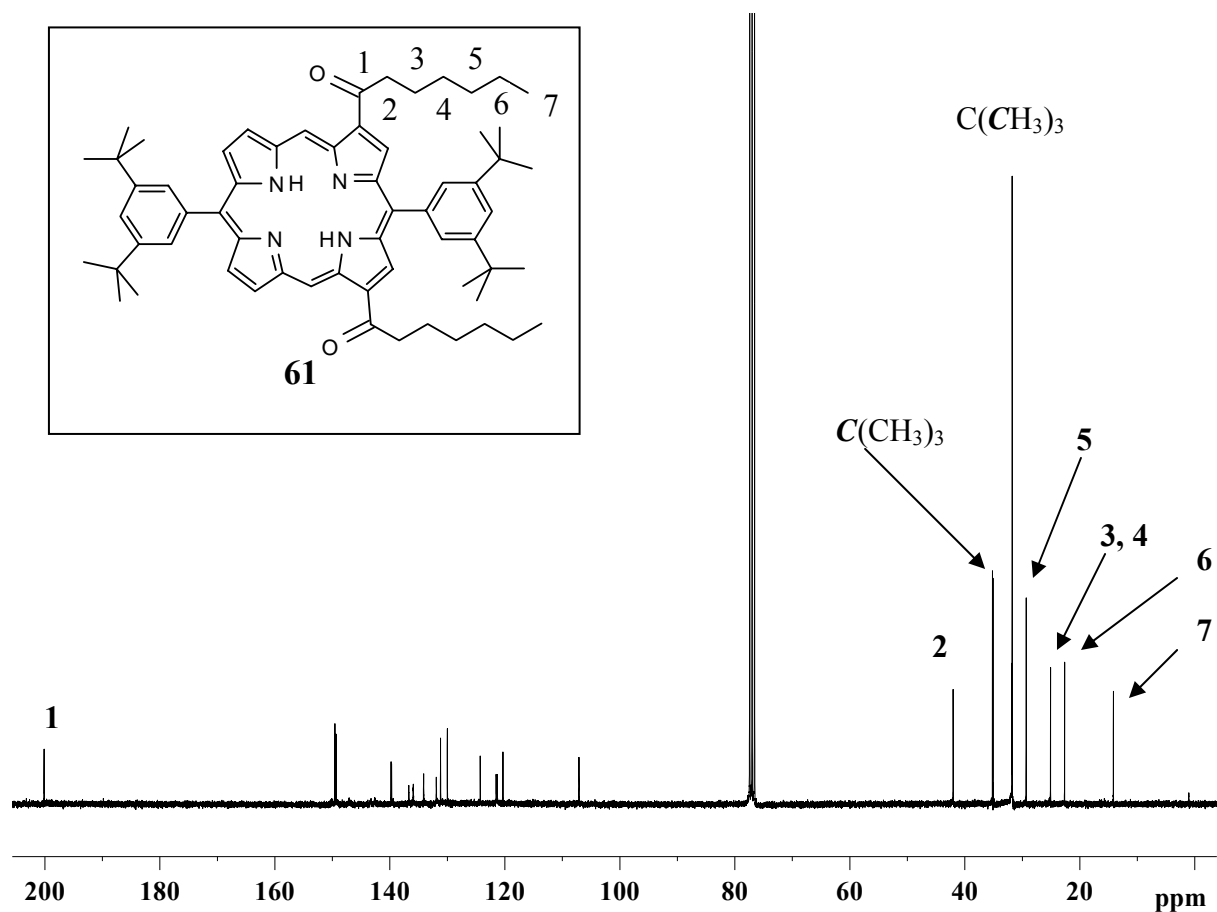
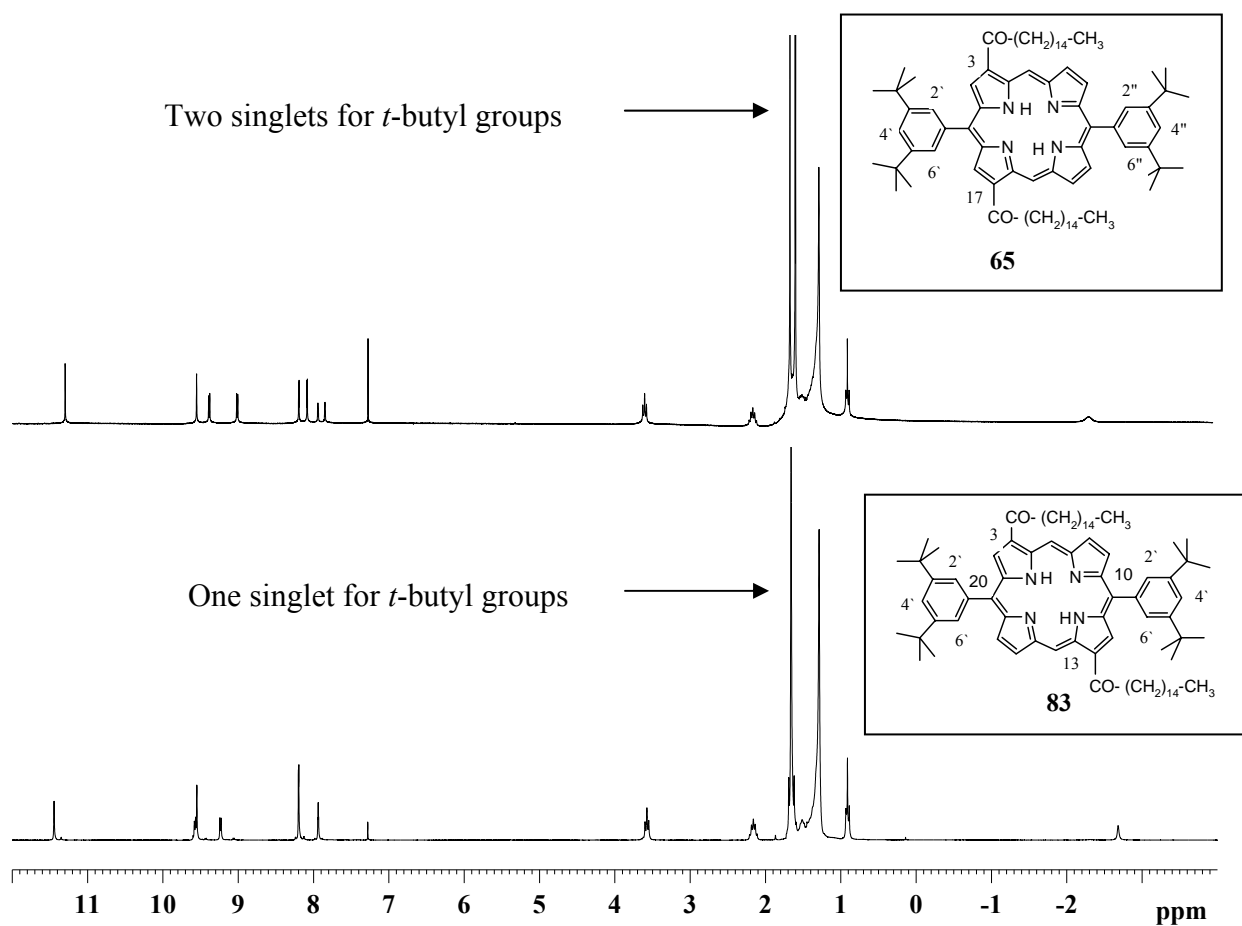


Fig. 2.14 Typical ¹H and ¹³C spectra of long chain substituted BTBPP

Chapter 3

In nature, a number of different pigments are found in a photosynthetic organism, and they perform a variety of functions during photosynthesis. Light absorption is a characteristic property of all photosynthetic apparatus and it is continuously being improved by different photosynthetic organisms by adaptation to different habitats. These pigments can be tetrapyrrolic chromophores like chlorophylls, bacteriochlorophylls or carotenoids depending on the type of organism. Usually proteins position these chromophores optimally for their function. These pigment-protein-complexes participate in energy and charge-transfer processes. In some early photosynthetic green bacteria, which live under the water surface at depths of over 50 m, a completely different antenna system is encountered than in purple bacteria or algae, which live at the surface, which in turn differ in their light-harvesting systems from terrestrial plants. While the latter, higher evolved species, have developed protein complexes to bind chromophores, in the early green photosynthetic bacteria, self-assembly of bacteriochlorophylls-*c*, *d*, and *e* is used. This much simpler architectural construct, which is fully functional, is worth mimicking with robust and easily available pigments, in the quest of construction of artificial antenna systems. The goal of present work is to mimic the functionality of bacteriochlorophylls-*c*, *d* and *e* and to self-assemble them in non-polar solvents by using supramolecular interactions in order to construct artificial antenna systems.

Well-ordered architectures of self-assembling porphyrins find applications in mimicking the functions of light-harvesting and charge-separation.^[63-65] The porphyrins and metalloporphyrins are self-assembled by a non-covalent approach by using hydrogen bonding,^[66-73] electrostatic interactions,^[74-75] and coordination using ligating porphyrins such as the oxoporphyrins.^[76-85]

The final Zn-compounds **35**, **36**, **40**, **45**, **49**, **74-81** were prepared in sufficient quantities on a 10-100 mg scale. These target compounds were characterized by different routine characterization techniques such as UV-Vis, circular dichroism, mass spectroscopy and X-ray. Modern instrumental characterization techniques such as Transmission Electron Microscopy (TEM), Atomic Force Microscopy (AFM), Confocal Fluorescence Microscopy (CFM) have also been used to analyse the target compounds and the self-assemblies that tend to form.

3.1 Detection of Self-assembly

Previous studies have shown that BChl-*c* self-aggregates in nonpolar solvents to form oligomers similar to those in native chlorosomes.^[86, 87] The monomeric compounds **35**, **36**, **40**, **45**, **49**, **74-81** and **83** self-assemble similarly in nonpolar solvents just as the natural BChls-*c*, *d* and *e* do. This fact is illustrated in Fig 3.1 for compound **35**. UV-Vis spectroscopy is a powerful technique to address self-assembly because of the interactions between chromophores. The sharp Soret band, characteristic for monomeric porphyrins, is spread out (i.e. considerably broadened) and red-shifted in nonpolar solvents. This can be seen by drastic changes in the absorption spectra spectra as indicated in Fig.3.1.

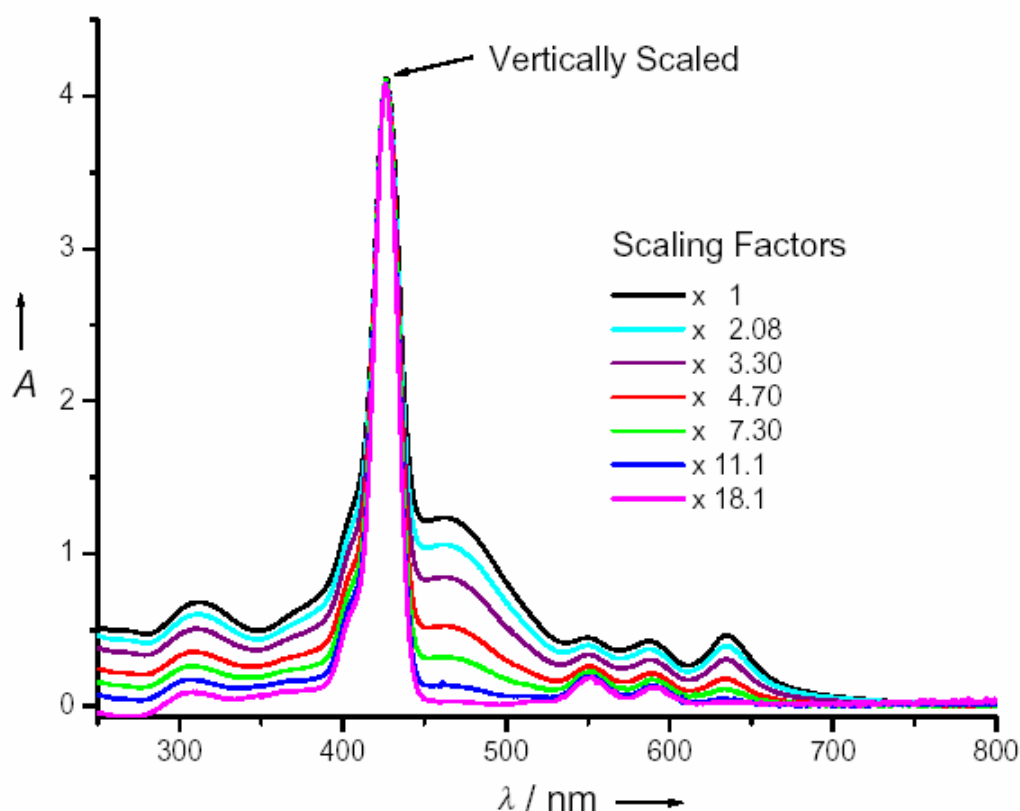
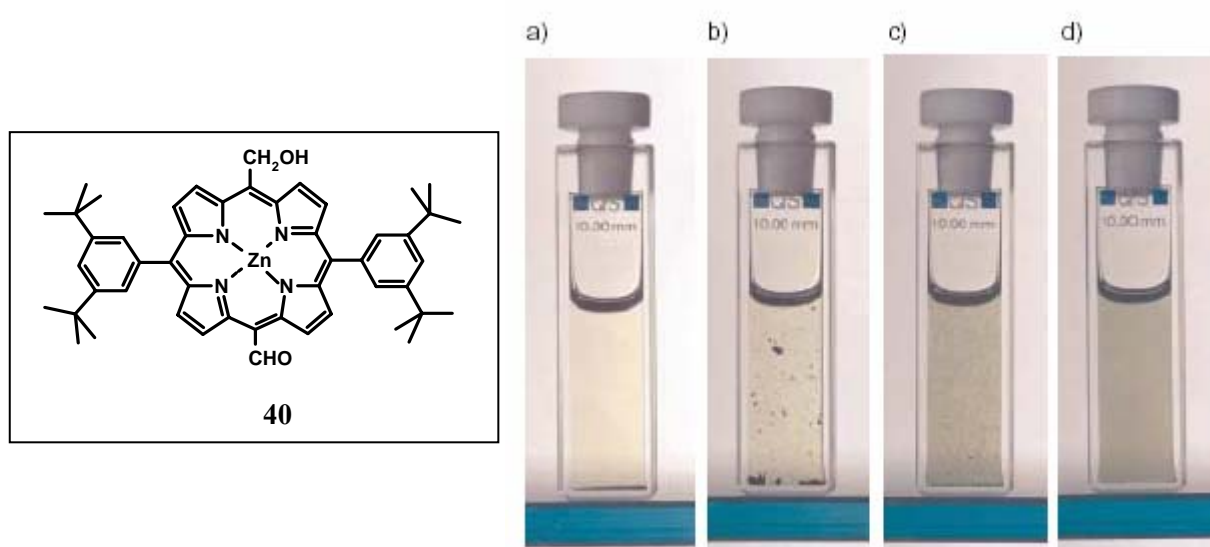


Figure 3.1 . Dilution of a dry, concentrated methylene chloride solution of **35**. The spectra have been scaled vertically at the Soret band by multiplying with the indicated scaling factors. The path length was 1 mm and the most dilute solution had a concentration of 0.9 μ molar. Note the decrease of the broad band at about 475 nm and the red-shifted Q band at 635 nm as the concentration is decreased.

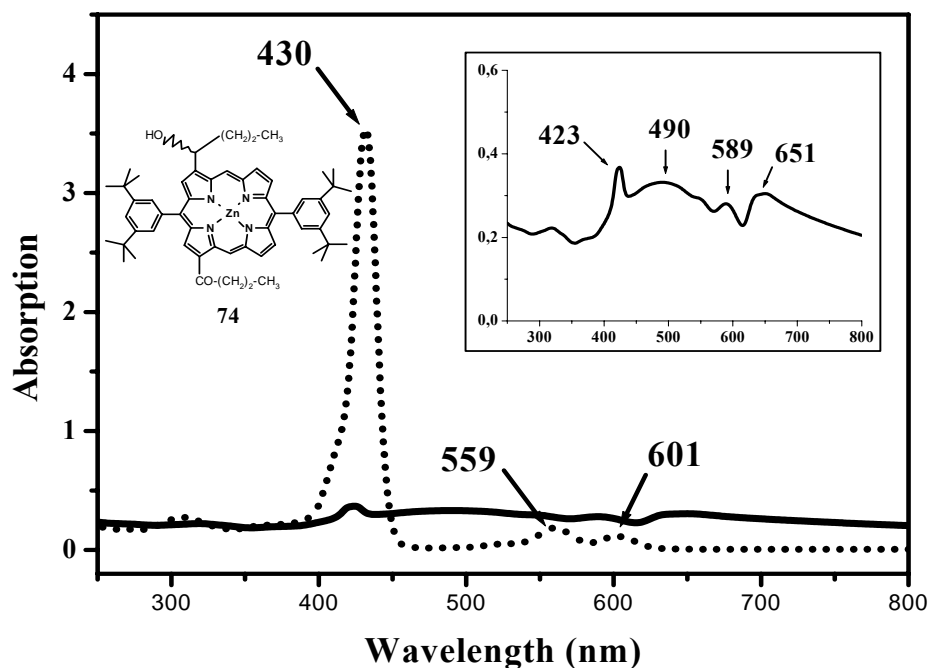
A new band in the absorption spectrum is produced due to the self-assembled species that is red-shifted compared to the monomeric absorption just as in J-aggregates.^[88-89] The Soret bands are red-shifted by about 50 nm and show partial overlap with the Q bands of the monomeric species and this provides a strong indication of nonzero absorption coefficient of self-assembled species in the range of 400-700 nm. In compound **45**, on the other hand, only a slight broadening and only a small red-shift is observed due to the limited π - π overlap of the macrocycles. When a polar solvent, such as methanol, is added in just over the stoichiometric amount to the self-assembled compounds **35**, **36**, **40** and **45**, a drastic change is observed in the Soret band, indicating the recovery of monomeric species. The characteristic sharp Soret band of the disassembled species due to zinc ligation by methanol. FT-IR spectra support this fact as the broad δ_{OH} vibrations between 3300 and 3200 cm^{-1} disappear upon methanol addition and the strong $\nu_{\text{C=O}}$ arising from the acetyl group appears at a very low frequency of 1639 cm^{-1} in this compound after self-assembly. As the concentration is decreased, molecules tend to be disrupted from the aggregate and disturb the π - π interactions and hence the shoulder adjacent to Soret band decreases as shown in Fig 3.1. If the critical micellar concentration is surpassed, self-assembly leads to the separation of thermodynamically stable fluffs which settle at the bottom of cuvettes as shown in Fig.3.2. These microaggregates are visible to the naked eye but upon gentle shaking they are disrupted by shearing forces to nanoaggregates of about 100 nm, as shown by dynamic light scattering and statistical analysis.



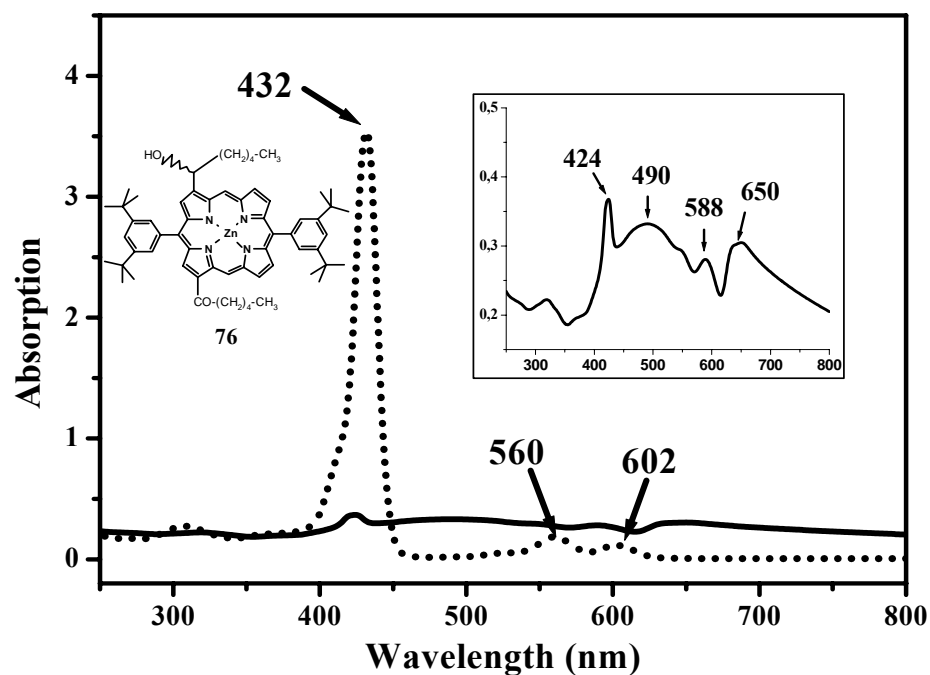
*Figure 3.2 A quartz cuvette with self-assembled **40** From left to right: a) the macro-aggregates have settled to the bottom and the solution is only weakly colored. b) Gentle heating of the bottom of the cuvette leads to convection; the fluffs circulate slowly and are visible to the eye.*

c) The same cuvette after a longer period of convection. d) The same cuvette after shaking—a homogeneous, strongly colored solution is obtained, which arises from shearing forces.

3.2 Detection of Self-Assembly with the Long Alkyl Chain Compounds



(continued on page next page)



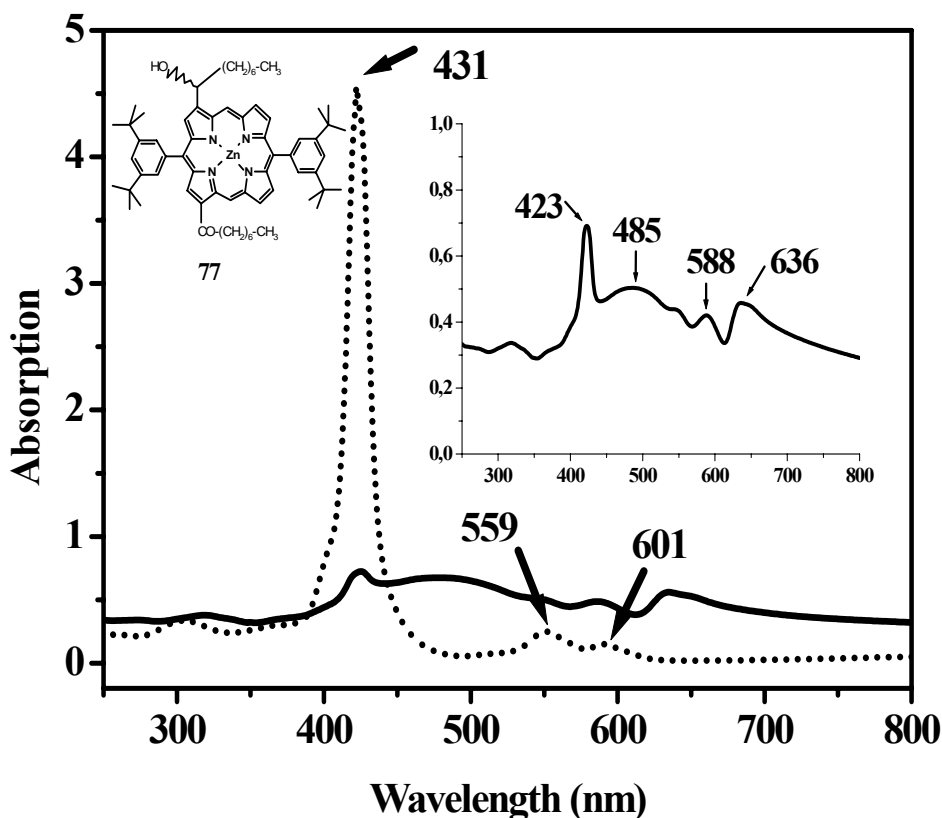


Figure 3.3: Self-assembled **74** (part **A**), **76** (part **B**) and **77**(part **C**) in dry *n*-heptane at room temperature (indicated by thick solid traces) with concentrations of $1.6 \times 10^{-4} \text{ M}$, $1.6 \times 10^{-4} \text{ M}$, $2.04 \times 10^{-4} \text{ M}$, The dotted traces of (A) and (B) are after addition of 0.05 mL of dry dichloromethane and the same quantity of methanol and $1/4^{\text{th}}$ and $1/2$, reduction of the total volume and dilution with *n*-heptane of the same samples, while the dotted traces of (C) was obtained after addition of 0.05 mL of dichloromethane and methanol to the same sample. Path length was 1 mm for all traces. Insets show enlargements of the self-assembled curves of (A), (B) and (C).

The compounds **74-81** possess long alkyl chains of various lengths that basically serve important functions like improving the solubility and increasing the hydrophobic character. The chiral centre in the hydroxyl substituted side chains controls the handedness of the self-assembly, which, in principle allows one to fine tune the architecture and consequently the macromolecular properties. The self-assembled supramolecular entities with long alkyl chains are promising dye molecules for artificial antenna systems as almost all of them exhibit useful UV-Vis spectroscopic properties due to a greater magnitude of the π - π interactions of

the porphyrin molecules in non polar solvents such as *n*-heptane and red shifted spectra. Typical spectra are shown in Fig.3.3.

The monomer molecules are normally induced to self-assembly by using a 1:99 % dichloromethane/*n*-heptane solvent combination. However, the long chain compounds **74-81**, they do not give self-assembly in this particular solvent combination. They do self-assemble merely in non-polar solvents like *n*-heptane. This is attributed to the higher solubility of long chain compounds into dichloromethane. More importantly, compounds **74-81** either show very weak Q bands or they completely disassemble in dichloromethane.

3.3 Comparison between isomers **81** and **85**

Fig.3.4 shows comparative absorption spectra of two isomers, **81** and **85**. Compound **85** has the same positions of the carbonyl and hydroxy groups like in the natural case while in compound **81** they have different positions.

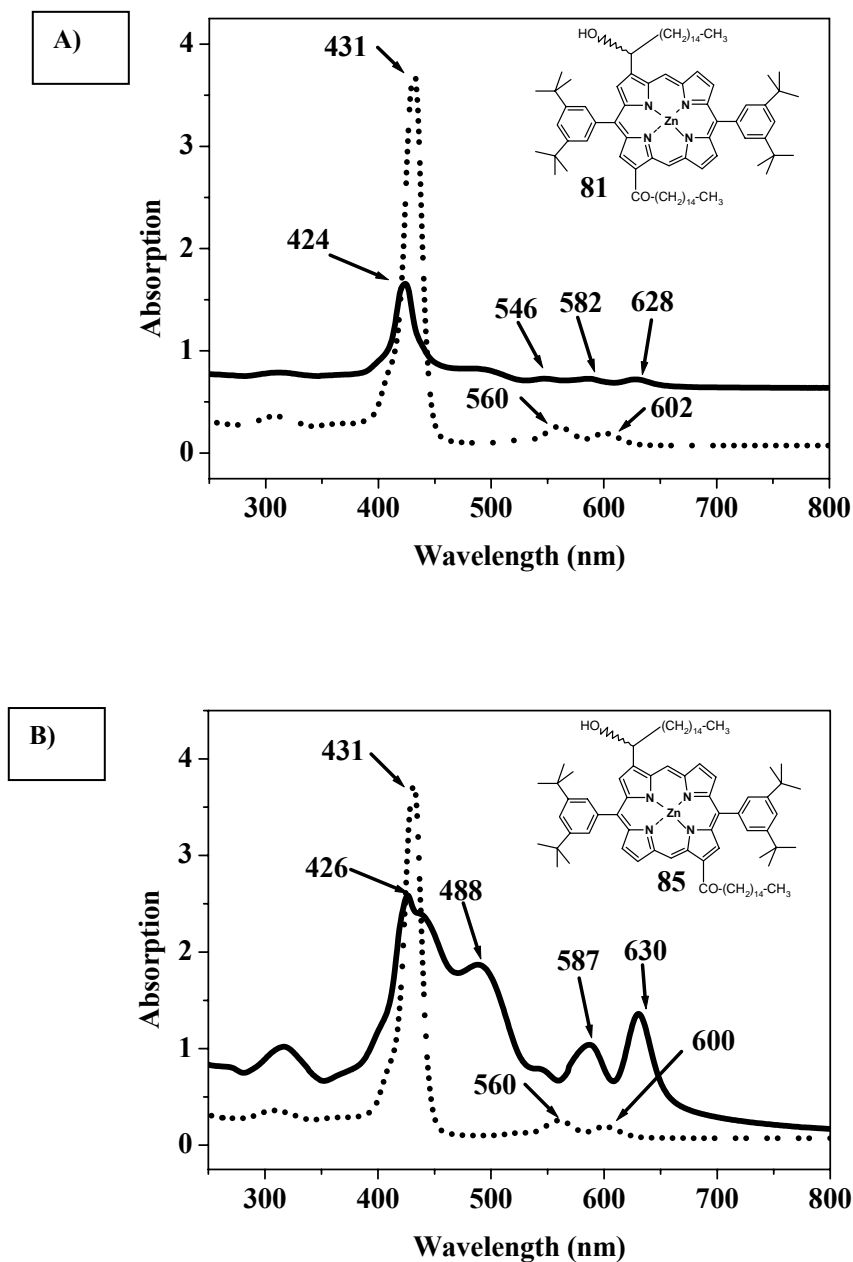


Figure 3.4: Self-assembled **81** (part A) and **85** (part B) in dry *n*-heptane at room temperature (thick solid traces) at the same concentration of 1.16×10^{-4} mM. The dotted traces of A and B are after addition of 0.05 mL of dry dichloromethane and the same quantity of methanol. Path length was 1 mm for all traces.

3.4 Absorption Properties of Self-Assembled **45** and **49**

The compounds **45** and **49** are isomeric and differ only by the positions of the carbonyl and hydroxy groups on the porphyrin ring. Fig.3.5 (part A and B) shows a direct comparison between the achiral hydroxymethylene group and the hydroxyethyl group as ligands for the zinc atoms in the self-assembled structures.

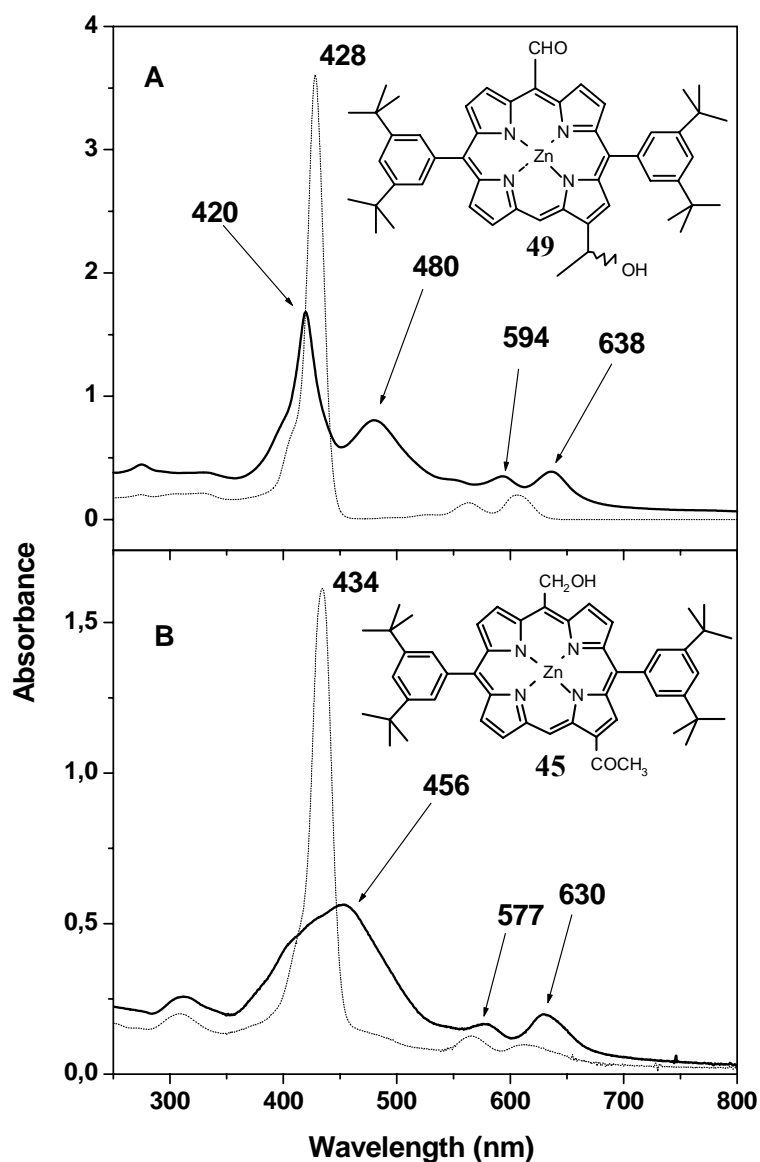


Figure 3.5: Self-assembled **49** (50 μ M, part A) and **45** (11 μ M, part B) in dry *n*-heptane at room temperature (full traces). The dotted traces are for the same samples after addition of suprastoichiometric amounts of methanol. Path length was 0.5 cm for all traces. For the **49**-MeOH adduct (part A, dotted trace), the solution was diluted with an equal volume of *n*-heptane.

That self-assembly is fully operational in **45** and **49** can be seen in nonpolar solvents by the broad and red-shifted absorption maxima of both the Soret and Q bands. Complete disassembly is ensured by adding minute (but suprastoichiometric) amounts of a competing solvent for the Zn-ligation, such as methanol, which is also expected to disrupt any intermolecular hydrogen bonding (Figure 3.5, part A, dotted traces). Furthermore, Fig 3.5 shows that almost no monomer **45** (shoulder at 405 nm) is present while on the other hand for **49** considerable amounts of monomers can be seen (sharp Soret band at 420 nm). The addition of MeOH to self-assembled species led to a sharpening of the Soret band which also becomes slightly red shifted (by ~8 nm) due to the formation of the Zn-CH₃OH adduct.

3.5 Comparison between the Wavelength Difference of the Aggregate Bands and Those of Zn-Methanol Adducts

The monomeric Zn-methanol adduct is formed by methanol addition to the self-assembled species as a result of complete disassembly. The aggregate bands in **49** and **45** appeared at 480 nm and 456 nm whereas the Soret band appears at 428 nm and 434 nm, respectively. Thus, the λ_{\max} difference between aggregate band and Zn-MeOH adducts is 52 nm and 22 nm for the **49** and **45**, respectively. The two Q bands have different intensities because of the different transition probabilities in these two desymmetrized porphyrins.

Interestingly, the most red-shifted Q_y band is the more intense one in **49** (638 nm) and **49**-Zn-MeOH adduct, while for **45** the red-shifted aggregate band at 630 nm is also more intense but a reversal occurs for the **45** MeOH adduct. This implies a $\Delta\lambda_{\max} = 75$ nm for this transition which allows to conclude that very similar self-assembled structures are actually obtained in both cases which give rise to red-shifted spectra as for J-aggregates.^[90-92] The anchoring group is hydroxy(m)ethyl which binds a zinc-atom of a neighboring porphyrin while the carbonyl group determines the direction of the Q_y transition and which must thus have slightly different relative orientations in the two supramolecules, as indicated by the molecular models presented in Scheme 3.1. Subtle variations in the π -overlap and/or optical properties of the assemblies can be engineered by varying the positions of attachment to the porphyrin macrocycle of the anchoring and carbonyl groups.

3.6 Temperature Effect on the Aggregation of 49

A self-assembled sample of **49** was heated from 25°C to 75°C and the absorption spectra were monitored to understand the temperature effect in the nonpolar solvent *n*-heptane. These spectra show that gradual disassembly (*vide supra*) occurs upon heating, but even at 75 °C, a considerable amount of aggregates still persists, only their size has been trimmed as observed from the step-wise decrease of light scattering. Only relatively large aggregates and small units, which could be for instance either monomers or dimers, seem to be present in equilibrium.

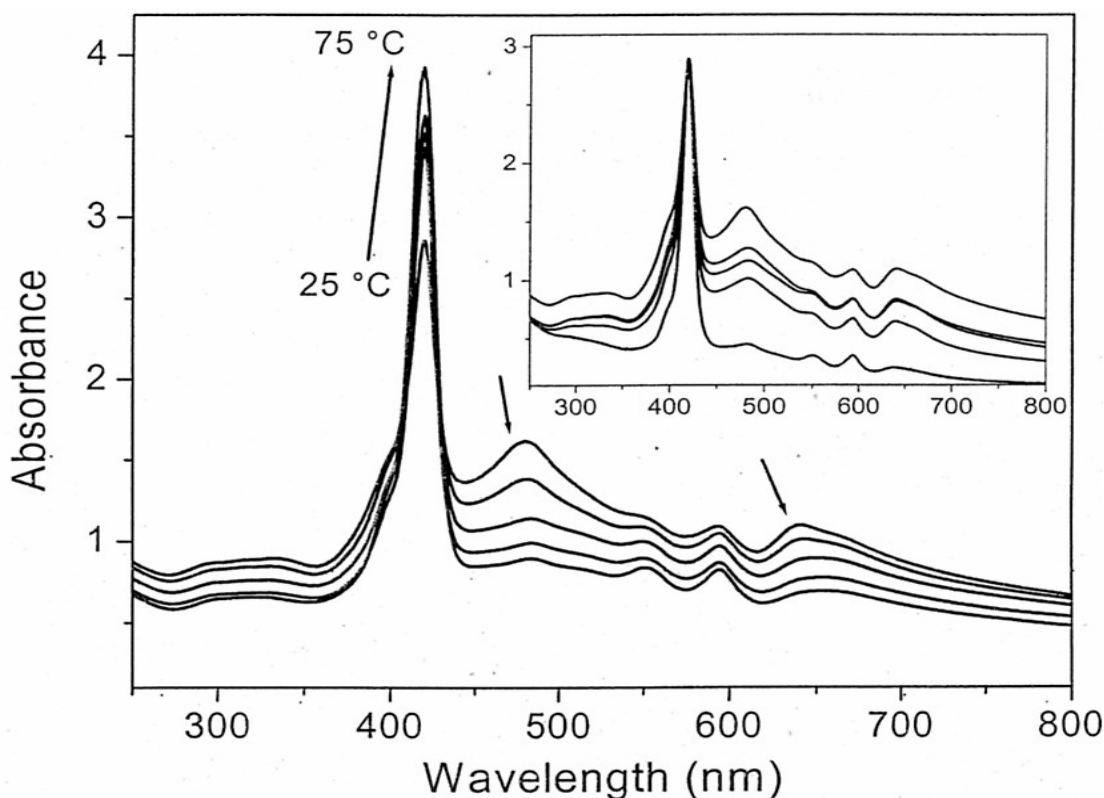


Figure 3.6. Variable temperature absorption spectra of self-assembled (*rac*)-**49** in *n*-heptane (70 μ M). The 1 cm path length cuvette was heated with a Peltier heating unit in 10° increments and the trace at 65°C is not shown. Note the gradual decrease of the scattering contribution, which usually leads to a shift of the baseline. Inset-Concentration dependence of the aggregation at 25°C. Traces have been scaled vertically at the Soret maximum of the monomer by multiplying with the following scaling factors (from the top trace to the bottom one): 1, 1.6, 2.3, 3.3, and 13.2. The samples were prepared by diluting a 3.7 mM CH_2Cl_2 solution of **49** with 2 mL dry *n*-heptane and had the following concentrations calculated for monomer species: 70, 40, 30, 20 and 10 μ M.

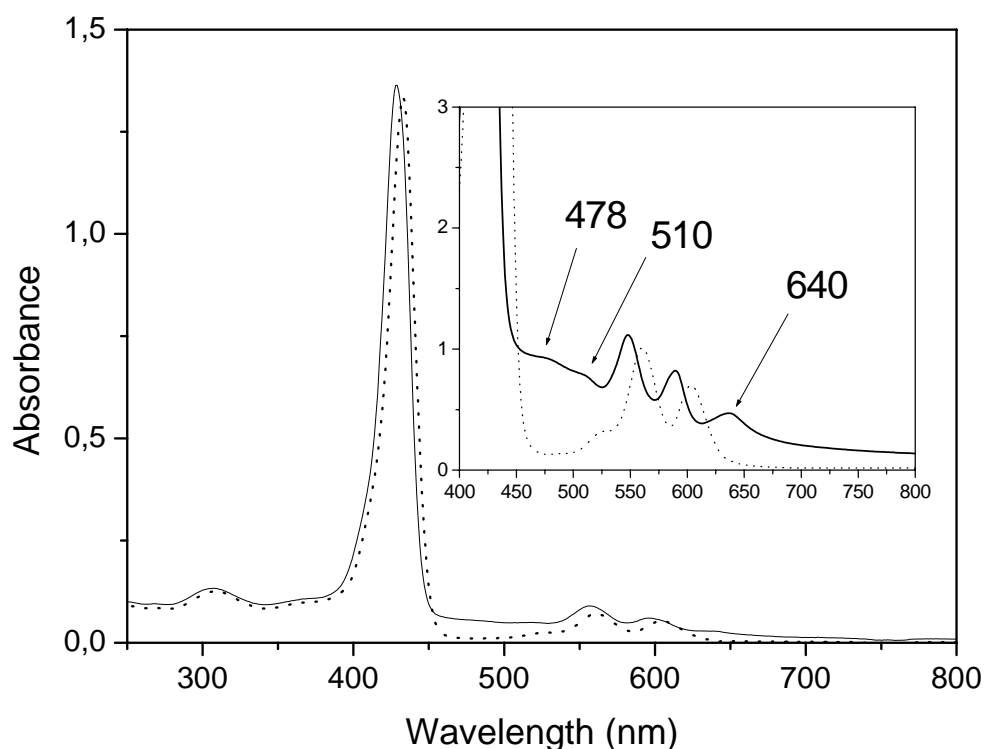


Figure 3.7. Absorption spectra of **36** under similar conditions as in Figs. 3.5 and 3.6, and a path length of 0.5 cm. Dotted lines: after disassembly with methanol. Inset: a five fold more concentrated sample (50 μ M) exhibiting more self-assembled species, which give the red shifted absorption maxima indicated by the arrows.

3.7 CD-Spectroscopy and the Supramolecular Chirality of the Self-Assemblies

Circular dichroism (CD) is a useful technique for the determination of chirality in enantiomerically enriched compounds.^[93-95] The racemate of free base **48** was resolved by chiral HPLC and zinc metalation of the two enantiomers was separately performed. Both enantiomers show self-assembly by their absorption spectra shown in Fig 3.8 and lead to helical superstructures (either M or P), which display giant (or PSI-type^[96] CD) as shown in Fig. 3.9. The two enantiomers after self-assembly, give mirror imaged exciton couplets in the region of the red-shifted Soret aggregate band. CD spectroscopy provides crucial information, as the sign of a CD couplet in the Soret region is indicative of the absolute configuration of the chiral substrate. From the positive or negative Cotton effect which appears at a longer wavelength, a clockwise or counterclockwise disposition of the transition dipole moments^[97, 98] in the π -stacked porphyrins can be assigned to the assemblies formed from the firstly and secondly eluted enantiomer, respectively (Figure 3.8). Upon addition of polar solvents, such

as methanol to the self-assembled species again leads to disassembly which is accompanied by a vanishing of the intense CD signals and a markedly increased, blue shifted Soret absorption band (Figure 3.8).

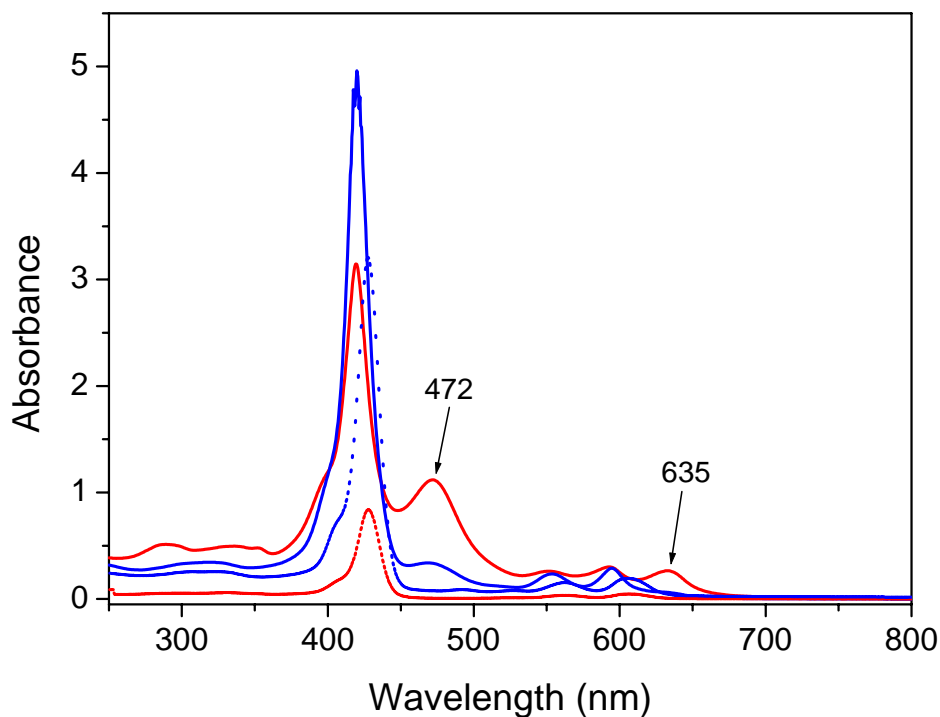


Figure 3.8. UV-Vis Spectra of self-assembled **49**. Red trace - first eluted enantiomer of free base compound of **48** after metallation with zinc acetate and self-assembly in *n*-heptane (28 μM solution). Blue trace - second eluted enantiomer of free base compound of **48** after Zn insertion and self-assembly in *n*-heptane (22 μM solution). The red trace contains more self-assembled species with maxima at 472 and 635 nm than the blue trace. The spectra were recorded at room temperature with a pathlength of 1 cm. Dotted traces are after disassembly with methanol. The red dotted trace was recorded with a 0.1 cm path length while the blue dotted trace was recorded with a 0.5 cm path length. Note the much smaller ratio between the aggregate maxima and the bands of the monomers in comparison with *rac*-**49**, shown in Fig 3.5, part A.

However, presently we can not tell whether the self-assembly using *rac*-**49** occurs equally well between the separated *R* and *S* enantiomers or if a hetero-enantiomeric process is energetically preferred. Nonetheless, it is informative that self-assembly of racemate sample is more prominent while it appears that the separated-enantiomers are less inclined to induce self-assembly under similar conditions. An experimental observation is that the size of the aggregates is strongly dependent on the initial concentration of the monomers. It has also

been recently shown,^[99] and theoretically explained^[100] that the CD signals are also strongly dependent on the size of the aggregates, and that even sign reversals of the longest wavelength Cotton effect may occur, by simply increasing the length of tubular aggregates of chromophores. Based upon ongoing work in Tamiaki's group, who has assigned the stereochemistry of 3-hydroxyethyl groups attached to porphyrins, bacteriochlorophylls and bacteriochlorins using the correlation of NMR chemical shifts in Mosher-type esters,^[101] it is tentatively possible to assign the configuration of the first eluted enantiomer as 3¹-*R* and the second eluted enantiomer as 3¹-*S* configuration. Assuming that no strange size effects occur in the CD spectra, the first and of the second eluted enantiomers lead to a *P*- and *M*-type helical suprastructures, respectively (Fig 3.9).

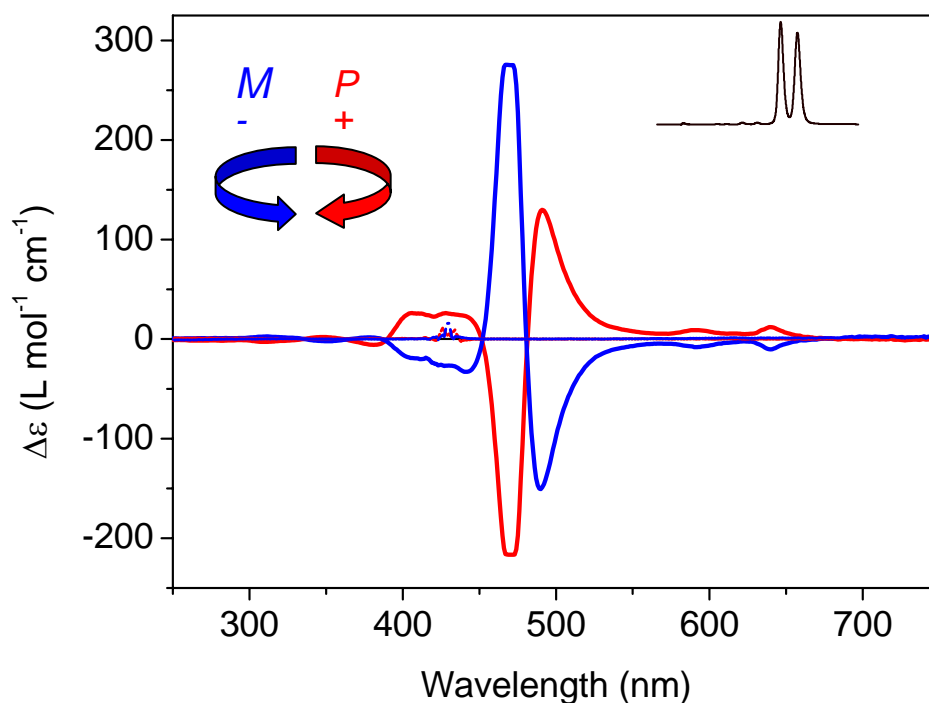


Figure 3.9. CD Spectra of self-assembled **49**. Red trace - first eluted enantiomer of **49** after metalation with zinc acetate and self-assembly in *n*-heptane (28 μ M solution). Blue trace - second eluted enantiomer of **49** after Zn insertion and self-assembly in *n*-heptane (22 μ M solution). The strongest Cotton effects are slightly truncated due to saturation of the detector. In more dilute solutions the self-assembly was less pronounced while with thinner cuvettes the Cotton effects of the *Q*-bands were less visible. Dotted traces, superimposing the zero line are after disassembly with methanol. In these cases, at \sim 430 nm, due to the intense Soret absorption of the monomers, practically no light passed through the sample anymore. The spectra were recorded at room temperature with a path length of 1 cm. The inset shows a typical preparative chiral HPLC trace.

3.7.1 CD-Spectroscopy and the Supramolecular Chirality of **35** and **36** Self-Assemblies

Racemates of **35** and **36** could be resolved satisfactorily on a chiral carbamate modified polysaccharide HPLC column (Chiralcel, OD-H), which provided fractions with enrichments varying between 78 and 95%. With both enantiomers of **35**, after the removal of any traces of 2-propanol and water (from the HPLC eluent), self-assembly was induced in n-heptane and in the CD spectra an excitonic couplet appears for the broadened Soret aggregate band. For the first fraction, which was more dilute and contained less self-assembled species, the couplet is not as symmetric as for the second fraction. In the latter case the longest wavelength Cotton effect of the couplet is positive, and has a maximum at 464 nm. The trough appears at 424 nm, thus indicating that indeed the rotary power stems from the red-shifted broad Soret band. The addition of methanol leads to complete disassembly, and the intense CD signals vanish, which indicates that the observed chirality is not due to the monomeric porphyrins. However, the different configurations (*R* or *S*) of the hydroxy bearing carbon atom induce different chirality in the self-assembled species. From the intense CD signals, this chirality appears to be helical in origin, and opposite helicities (*M* or *P*) are generated from the two enantiomers. Giant CD, sometimes referred to as Polymer and Salt Induced (PSI) CD may appear if the chiral objects (absorbing light at around 500 nm) are greater than 50 nm.^[99-100] This also affects the overall shape of the CD curves, which can vary widely because of the different sizes of self-assembled species and the scattering contribution to the CD. However, the application of the exciton chirality method^[102] leads to the assignments of the firstly eluted enantiomer to a self-assembled species in which the chirality of the transition dipole moments must be counter clockwise (defined as negative chirality). The second eluted enantiomer leads to an aggregate with positive chirality (i.e. a clockwise arrangement of the transition dipole moments) Fig. 3.10.

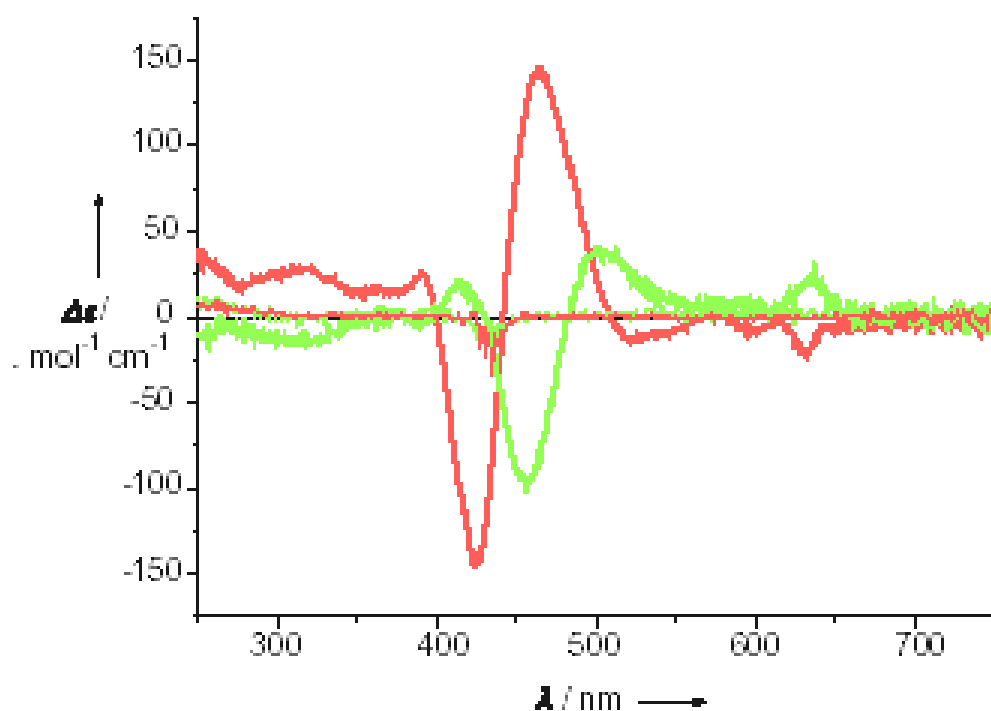


Figure 3.10. CD spectra of enantiomerically enriched **35** after self-assembly in *n*-heptane and after addition of methanol, which disrupts the assemblies. The concentrations were 2.7 mM for the fraction of the first eluting enantiomer (green lines) and 4.7 mM for the fraction containing the secondly eluting enantiomer (red lines), which contained more self-assembled species, as inferred from the absorption spectra. After addition of methanol the intense mirror imaged CD-signals disappear (thin red and green lines overlapping the 0 line). Pathlength was 1 cm and the averaging time was 2 s nm^{-1} . The spectra are corrected by subtracting the baseline, which was measured in the same cuvette with *n*-heptane alone.

3.8 X-ray

The single-crystal X-ray structure of Zn-compound has been reported by the Balaban group^[103] that adds very strong evidence for occurrence of self-assembly and it also indicates how the self-assembly in natural systems may operate. Fig. 3.11 shows also that supramolecular interactions act cooperatively.^[10]

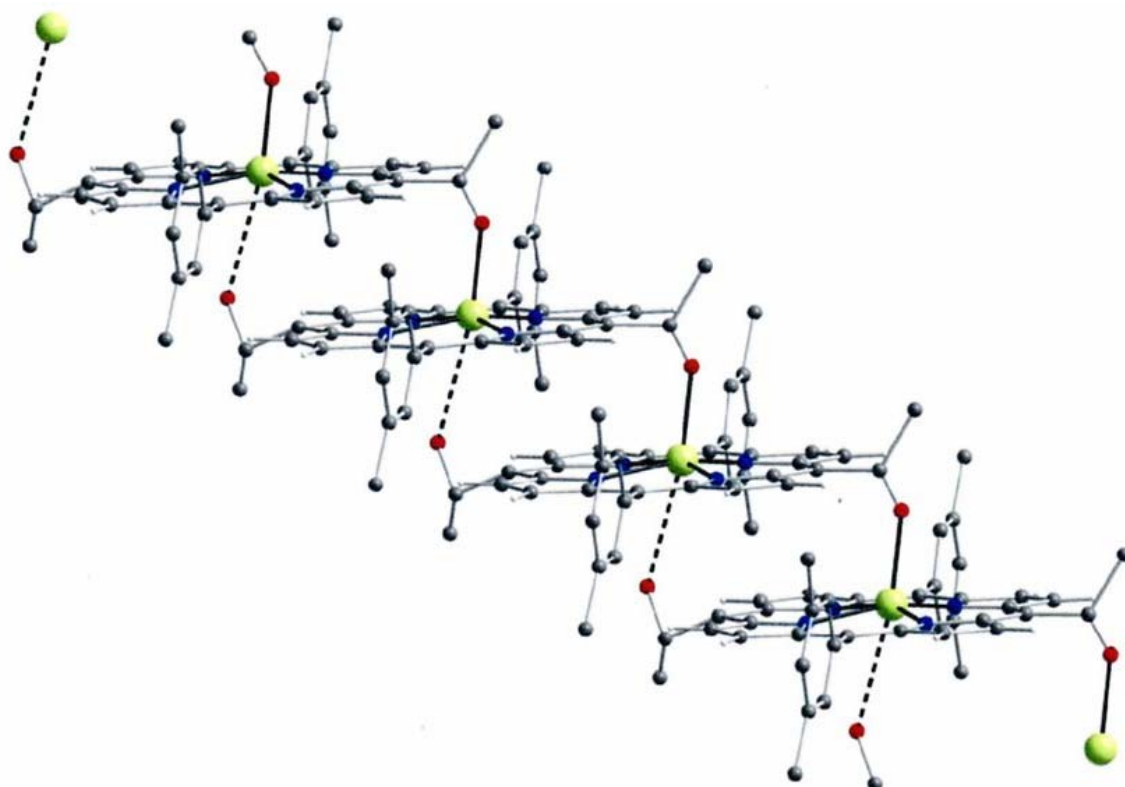


Figure 3.11. The single-crystal X-ray structure of 102 that shows, the ligation of zinc atoms within the porphyrin macrocycle by the hydroxyl group of the 1-hydroxyethyl groups and extensive π - π -stacking of the macrocycles are the dominant interactions which occur cooperatively.

3.9 Confocal Fluorescence Microscopy, Atomic Force Microscopy and Transmission Electron Microscopy of the Self-assemblies.

Confocal Fluorescence Microscopy, Atomic Force Microscopy and Transmission Electron Microscopy nanoscopic techniques are found to be very useful for studies of the supramolecular assemblies. The final compounds in the case of hydroxyethyl substituents have rod-like nanostructures (See on page 72) similar to those in natural case. The hydroxymethyl-substituted compounds lead to globular structures after self-assembly.

3.9.1 Confocal Fluorescence Measurements

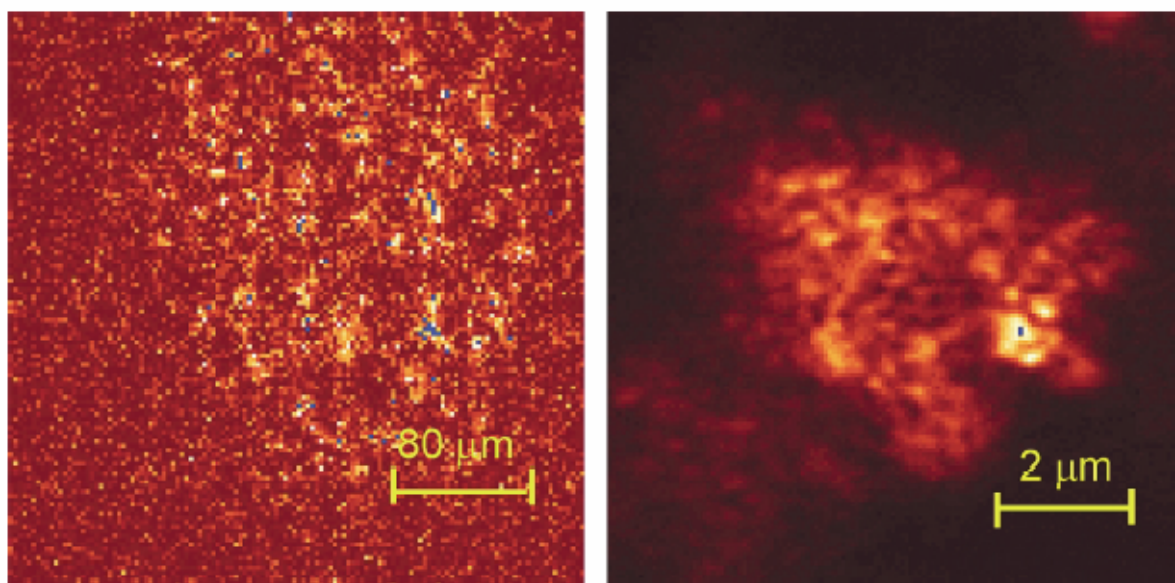
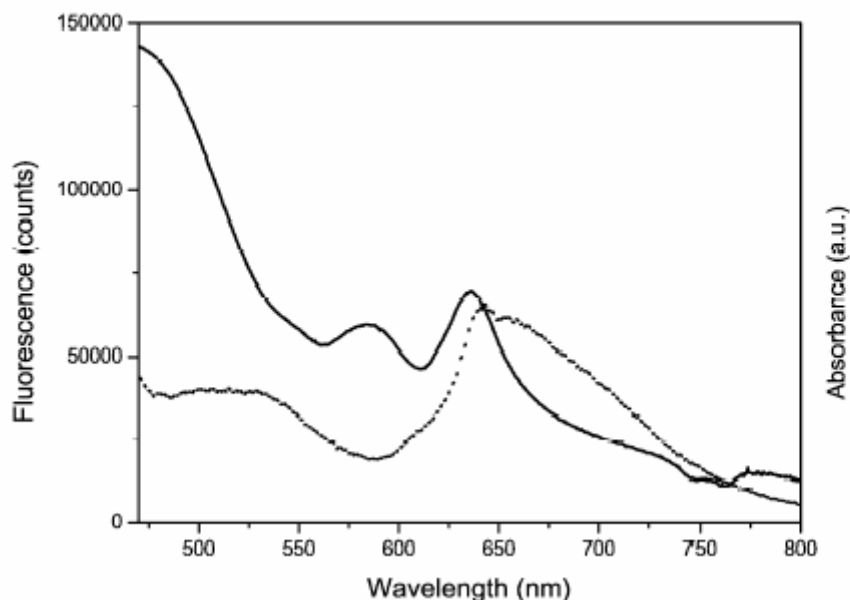


Fig.3.12. Confocal fluorescence intensity images of self-assembled 35, 36, 40, 45 and 49 on 7.8-nm nanocrystalline anatase(TiO₂), left image: scan size 340 x 340 μm; right image scan size 8.5 x 8.5 μm. Bright regions show strong fluorescence. The excitation wavelength was 458 nm. The detection wavelength was 650 nm.

In the mimics **35**, **36**, **40**, **45** and **49** the positions of carbonyl and hydroxyl groups differ and thus they lead to various degrees of overlap of the π -macrocylic system. Due to strong excitonic interactions, variously red-shifted absorption bands, as in J-aggregates, are encountered. The J-aggregates are characterized by a red-shifted and sharp absorption band in comparison with the monomer band, as result of exciton delocalisation over the aggregates.^[104-107] Probably because of inhomogeneous broadening, the absorption spectra are also broadened, a fact which is important for light harvesting. The usual narrow Soret band of the porphyrin [Full Width of the band at Half Maximum height (FWHM) of 20 nm] is decreased in intensity but broadened by a factor of more than 6, as shown in Fig.3.5.

Very interestingly, the fluorescence of these aggregates is not strongly quenched as is the case with most chromophores. Both in solution and in cast films (as shown in Fig. 3.13) one can observe strong fluorescence bands stemming from the aggregate. This lends hope for use of these aggregates in sensitizing wide band semiconductors, such as titanium dioxide, within solar cells.



*Fig. 3.13. Absorption spectrum (full line) of a self-assembled film of **49** on the walls of a 1-cm quartz cuvette and after decantation of the supernatant. Fluorescence spectrum (dotted line) from the same sample, the excitation wavelength was 458 nm.*

Fig. 3.13 show the absorption and fluorescence spectra for a film cast on the walls of a quartz cuvette and after decantation of the *n*-heptane solution used for inducing the self-assembly. At the same time, this film fluoresces, with a small Stokes shift, upon excitation of the Soret band. A similar film could be self-assembled from the same compound **49** onto a clean glass slide by dipping the slide vertically into *n*-heptane and injecting a concentrated dichloromethane solution of **49**. The formation of the monomeric species attributed to the formation of Zn-MeOH adducts, as MeOH is a polar solvent. It can compete for Zn ligation. Confocal fluorescence microscopy is a powerful tool for 3-D characterisation of complex surfaces in topographic representation. The topography of such a film is shown in Fig. 3.14. 3D-confocal fluorescence measurements show an average film thickness of 550 nm.

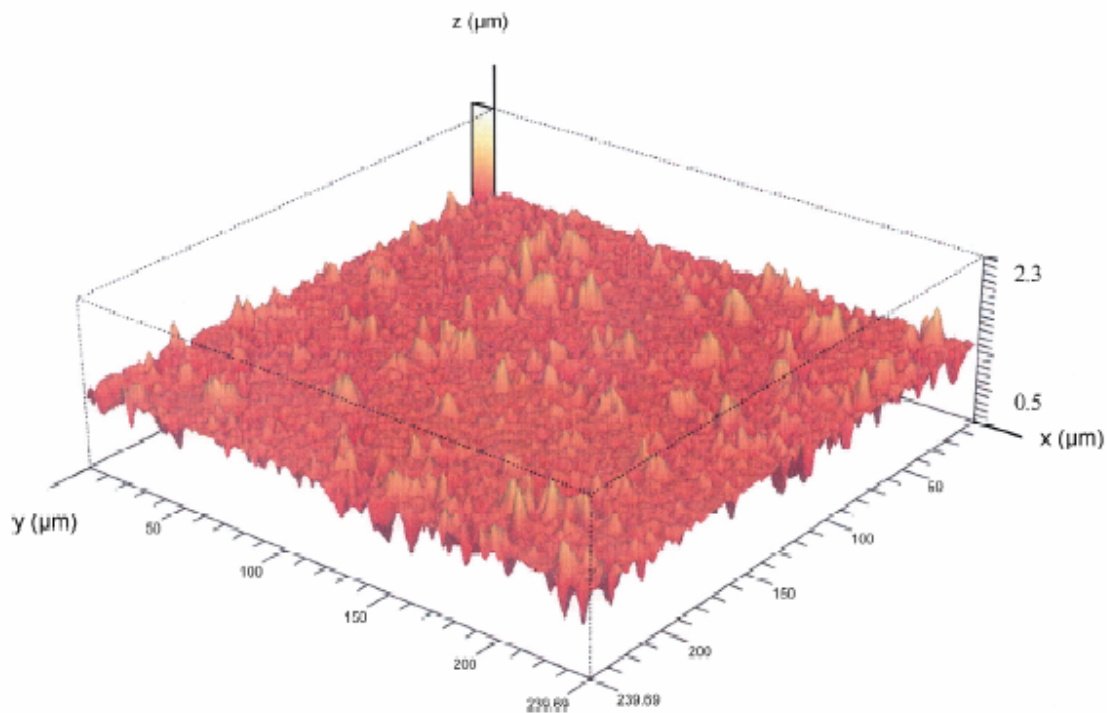


*Fig 3.14. 3D-confocal topographical image of a self-assembled film of **49** on a glass slide; scan size 240 X 240 mm; z-scale 2.3 μm. The image was taken in reflection mode. The laser wavelength was 458 nm.*

3.9.2 Atomic Force Microscopy (AFM) Measurements

AFM is yet another technique that provides nanometer-scale information about surface structures. The AFM intermittent contact image of the same sample of **49** is presented in Fig.3.15. The confocal microscopy and AFM experiments show almost the same surface morphology and quite agree in height measurements. By confocal microscopy technique a medium peak-valley distance of 550 nm was measured, whereas by the AFM technique, where height measurements are much more precise, it was measured in the range of 600 ± 50 nm (indicated by the cross-section example in Fig.3.17 (b)).

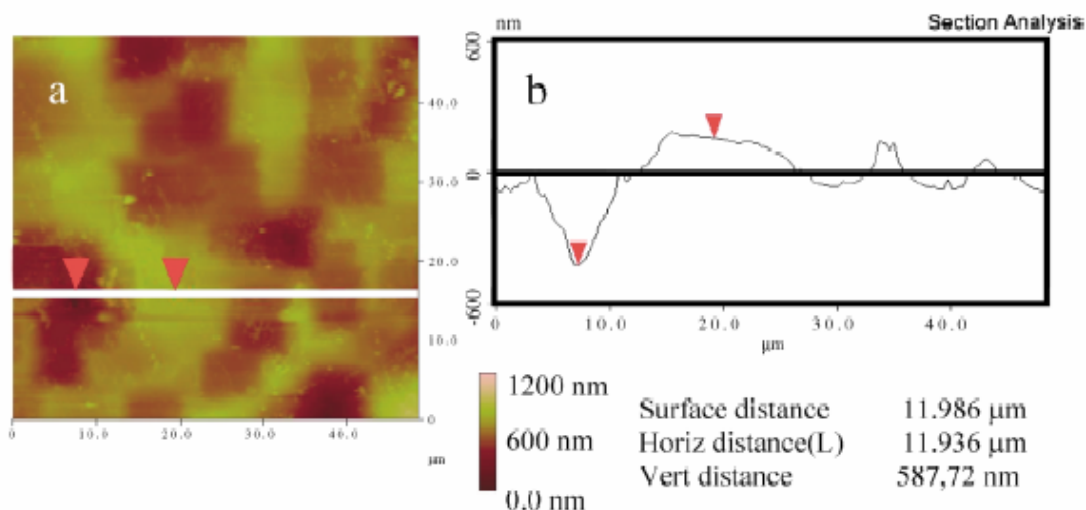


Fig 3.15 (a) AFM intermittent contact mode image of a self-assembled film of **49** on a glass slide; scan size $50 \times 50 \mu\text{m}$; z-scale $1.2 \mu\text{m}$. (b) Cross-section of the scan line indicated by the arrow heads in part (a). Average height between the peak and the trough was 600 ± 50 nm (same sample as in fig. 3.14).

From the results with the AFM technique it is evident that there are still some small free glass surface parts remaining and probably by nucleation of a few porphyrin molecules at certain defect sites of the glass film growth is initiated. Then a rapid growth *via* self assembly must occur. The above film thickness measurements lead to the conclusion that the average sizes of the cones thus formed is approximately 550 nm. Presumably, the hydroxy groups from water molecules adsorbed on the glass surface coordinate the zinc atom of the first layer of adsorbed porphyrins which then, by further metal ligation and π - π stacking self-assemble in a similar manner to the natural bacteriochlorophylls *c*, *d* and *e*. That such large structures are formed, which assuming a 3.4 \AA distance between molecules in two adjacent layers (similar

to the one encountered in graphite), must comprise over 1500 molecules in the vertical stacking direction. This shows that the nucleation process is the rate-limiting step and that once an anchoring site has been found, the molecules or small assemblies from the solution, tend to self-assemble at these sites. That water is responsible for film formation can be proven by heating glass slides in an oven at 110°C, for increasing periods of time. It is found that the film formation is gradually inhibited afterwards. Similar thin film formation could be observed onto nanocrystalline anatase (TiO₂) with various grain sizes (7.8, 9.4, 15.3 and 25 nm, as characterized by X-ray diffractometry). The films formed on nanocrystalline anatase have excellent stability even in the presence of light and air and could be suspended in dry *n*-heptane by stirring the suspension and injection of the concentrated dichloromethane solution of the porphyrins **35**, **36**, **40**, **45** and **49**. That self-assembly occurs, can be seen easily. As time passes the self-assembled molecules get adsorbed onto the TiO₂ surface by chemisorption process and lead to the gradual depletion of the molecules from the solution leaving behind a supernatant which is almost colorless. The coated nanoparticles which now are coloured, settle to the bottom of the reaction vessel and after decantation of the supernatant washing of the particles with *n*-heptane and drying them in vacuum, a free flowing greenish colored powder is obtained. Fig. 3.15 shows confocal fluorescence microscopy images of a sample of **49** self-assembled onto 7.8-nm anatase. Strongly fluorescent discrete nanoparticles can apparently be seen. The average island height measured by 3-D confocal fluorescence imaging again is on the order of 500±100 nm, however the spatial resolution in this case is much lower. This is presumably, because the titania nanoparticles do not aggregate and that on one nanoparticle a first adsorbed layer of zinc porphyrins forms which is then followed by rapid growth by self-assembly of the next layers. That fluorescence stemming from the self-assembled porphyrins can be observed in our case is due to the fact that there is no hole transport material present and no electrodes have been deposited. The much larger antenna assemblies than the core semiconductor nanoparticle, after photoexcitation still produce luminescence.

3.9.3 Transmission Electron Microscopy (TEM) Observations

The chiral compounds **36** and **49** show extended ordered structures of the self-assembled Zn-porphyrin molecules as evidenced by the TEM technique. The self-assembled chiral Zn-porphyrin molecules exhibit more ordered parallel stacks in comparison with its achiral counterpart. Furthermore, the racemates of compounds **36** and **49** show under high resolution ordered striations which are much more frequently seen than in the corresponding separated enantiomers.

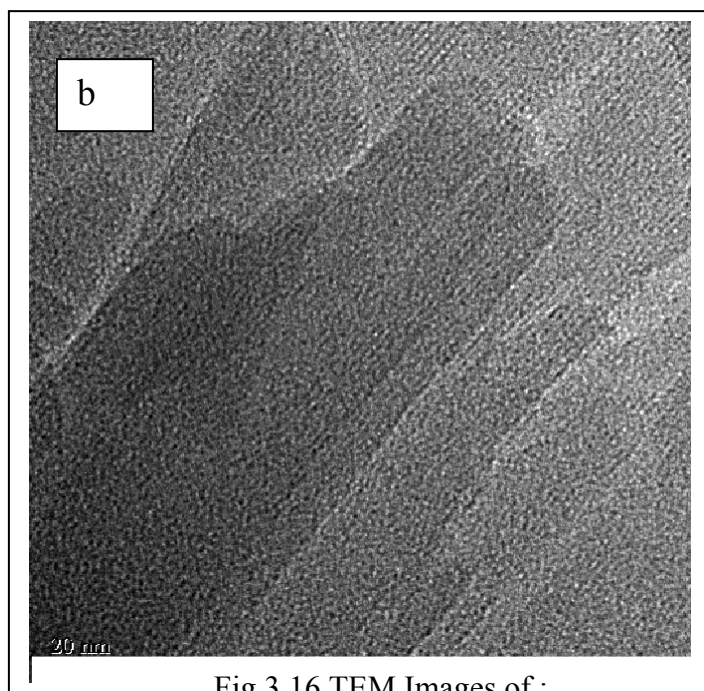
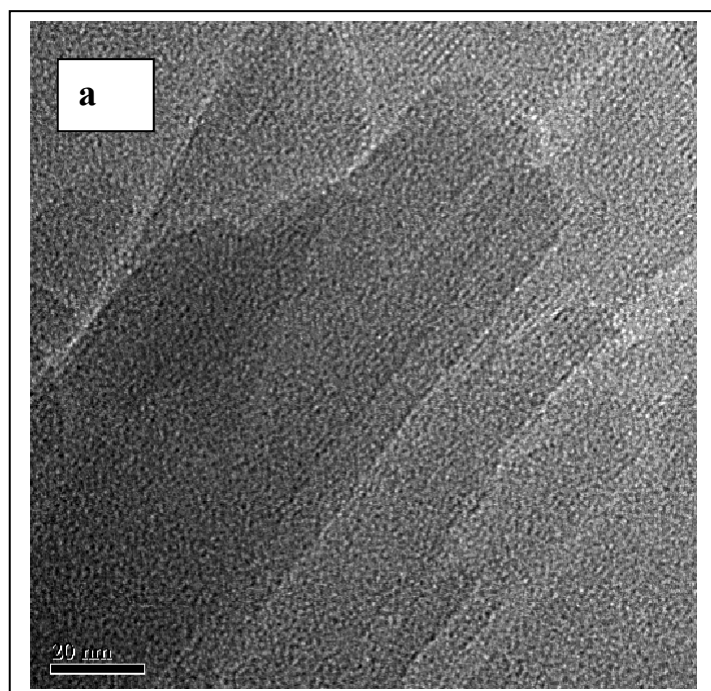
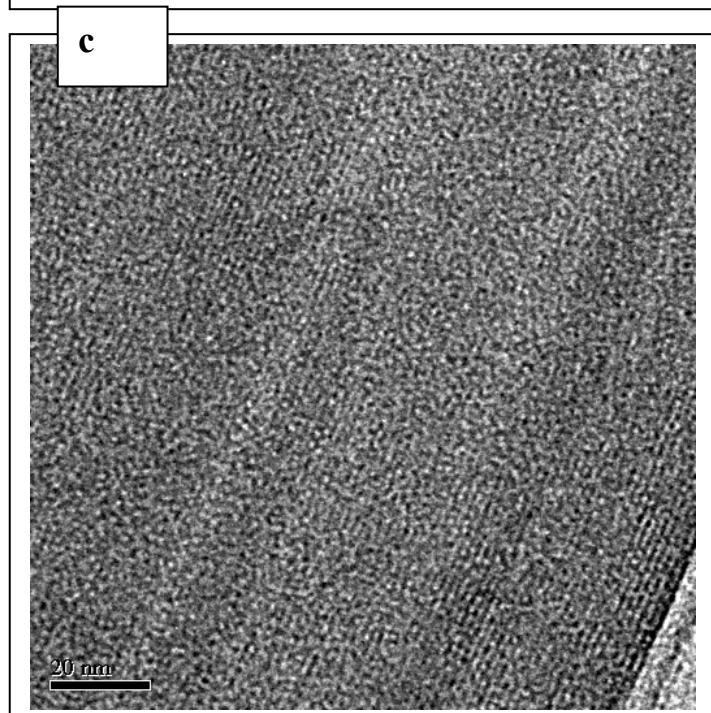


Fig 3.16 TEM Images of :

*a) 3-Acetyl-17-(1-hydroxyethyl)-10,20-bis-(3,5-di-*t*-butylphenyl)-porphinato zinc (36)*

*b) 3-Acetyl-15-hydroxymethyl-10,20-bis-(3,5-di-*t*-butylphenyl)-porphinato zinc (44)*

*c) 10,20-bis(3,5-di-*t*-butylphenyl)-15-formyl-3-(hydroxyethyl)-porphyrinato-zinc (49)*



3.10 A New Synthetic Approach to Self-Assembled Chromophores

While mimicking the functionality of bacteriochlorophyll-*c*, *d*, and *e* remarkable changes have been introduced in comparison to naturally occurring pigments in order to reduce the synthetic efforts. The changes included are

- 1) the use of 10,20-bis-(3,5-di-*tert*-butylphenyl) porphyrin instead of chlorin. Since porphyrins and metalloporphyrins reveal high versatility in their electron transfer, redox properties, photoactivity properties, incorporation of these species into the multicomponent arrays has proven to be an attractive strategy for the construction of functional arrays;
- 2) the second change is the use of Zn metal instead of Mg metal because of greater chemical stability and easier synthesis of Zn porphyrins,^[108]
- 3) the third change is that a carbonyl group has been appended into the porphyrins not as a isocyclic ring within the cyclopentanone ring which is very difficult to synthesize but as a simple acyl group;
- 4) the fourth change introduced was in the form of long saturated alkyl chains replacing the fatty alcohol esterifying the 17-propionic acid residue.

Furthermore, the 5,10-*meso*-substitution of the porphyrin moiety by bulky 3,5-di-*tert*-butylphenyl substituent proved to be helpful in five different ways:

- (i) the starting material 10,20-bis-(3,5-di-*tert*-butylphenyl) required to build-up basic porphyrins moiety is easily available in multigram quantities,^[49]
- (ii) it solubilizes complex architectures and minimizes π -stacking of *meso*-aryl porphyrins but still crystallizes so that single crystal diffraction studies can be performed. Due to its bulkiness it packs well especially in the presence of nonpolar solvents like *n*-hexane that act in the crystal lattice as a cement for self-assembling nanostructures,^[109]
- (iii) it prevents electrophilic substitution in the adjacent β -pyrrolic positions and on the benzene ring thus enabling very selective functionalization of the porphyrins;
- (iv) it induces enhanced solubility and allows growing crystals suitable for X-ray diffraction studies^[109] as mentioned before, but at the same time it enables visualization by scanning probe techniques^[110-111] for non-crystalline samples;
- (v) and finally, due to the sharp NMR *t*-butyl singlet, which is visible even at submicromolar concentrations, it allows easy identification of compounds and of their symmetry in order to allow monitoring of complex reaction mixtures. The final Zn-compounds **35**, **36**, **40**, **45**, **49**, **74-81** obtained by introducing all the above described changes show remarkable advantages over the semisynthetic mimics in terms of practical uses and synthetic procedures.

3.11 Factors Responsible for Self-Assembly

The complete genome sequence of *Chlorobium tepidum*, a photosynthetic, anaerobic, green-sulfur bacterium gives information for selective mutations to be performed.^[112] Evidence that self-assembly governs the antenna system was obtained by Donald Bryant and his co-workers, by deleting the genes expressing nine out of the ten proteins encountered in the chlorosome.^[113]

The chlorosome is the most efficient natural antenna system and is an organelle attached on the inner side of the cytoplasmic membrane of green bacteria.

By mimicking the functional groups from the natural self-assembling bacteriochlorophylls, the self-assembly can be induced for artificial molecules by using the same supramolecular interactions among the functional groups. However, the sole presence of these functional groups (Fig 1.6, chapter 1) is not the only the factor which accounts for the self-assembly. Among other factors, also the choice of central metal, the position of the carbonyl and hydroxyl functionality, the nature of hydrogen bonding, the chirality of the hydroxyl functionality, the aggregation type and the nature of π - π interactions are important factors, which determine the nature of the self-assembly. Single crystal X-ray crystallography is a way to judge the favourable and non-favourable interactions for self-assembly.^[114] Compounds **35**, **36**, **40**, **45**, **49**, **74-81**, **83**, **100** and **101**^[10, 49] are either chiral or achiral depending on the hydroxy substituents (hydroxyalkyl *versus* hydroxymethylene; respectively), the zinc atom and the carbonyl group collinearly arranged and they do self-assemble.

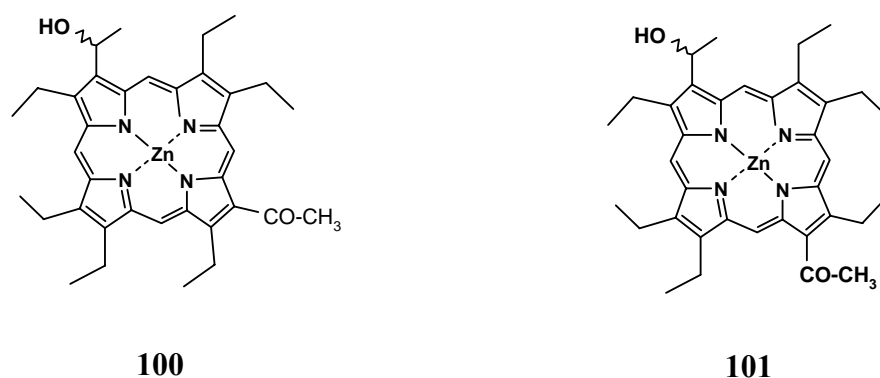


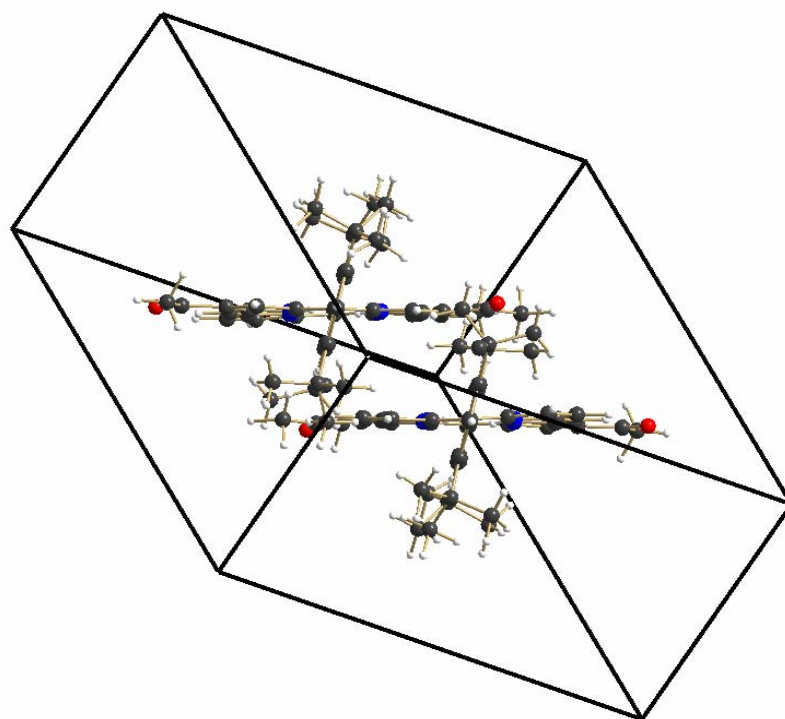
Figure 3.17

After our initial report,^[10] based on the same principle of obtaining functional antenna systems, synthesis of the Zn-compounds **100** and **101**^[115] was reported by Tamiaki and

coworkers (Fig. 3.17). When compounds **100** and **101** were induced to self-assembly in CH₂Cl₂/n-hexane (1:99%, v/v), a very intriguing result was that the zinc porphyrin **100** failed to give red-shifted and broad absorption spectra upon self-assembly despite availability of all the groups responsible for the self-assembly. The isomeric zinc porphyrin **101** self-assembles easily. This outcome has led the Japanese authors to state that collinearity of these three groups is an essential condition for the self-assembly to occur.^[115] This observation is at odds with the fact that both **45** and **36** could self-assemble despite their structural resemblance with **100**. Also **49** could self-assemble in spite of the angular disposition of the hydroxy group, central metal atom and carbonyl substituent. The collinearity of self-assembled groups is thus not a prerequisite for inducing self-organization, but that it is the amount of the π -overlap of the macrocycles in the self-assembled species which is responsible for the broadening and the red-shift of the absorption maxima in the UV-Vis spectra.

3.12 π -Stacking and the Nature of π - π Interactions in the Novel Porphyrins

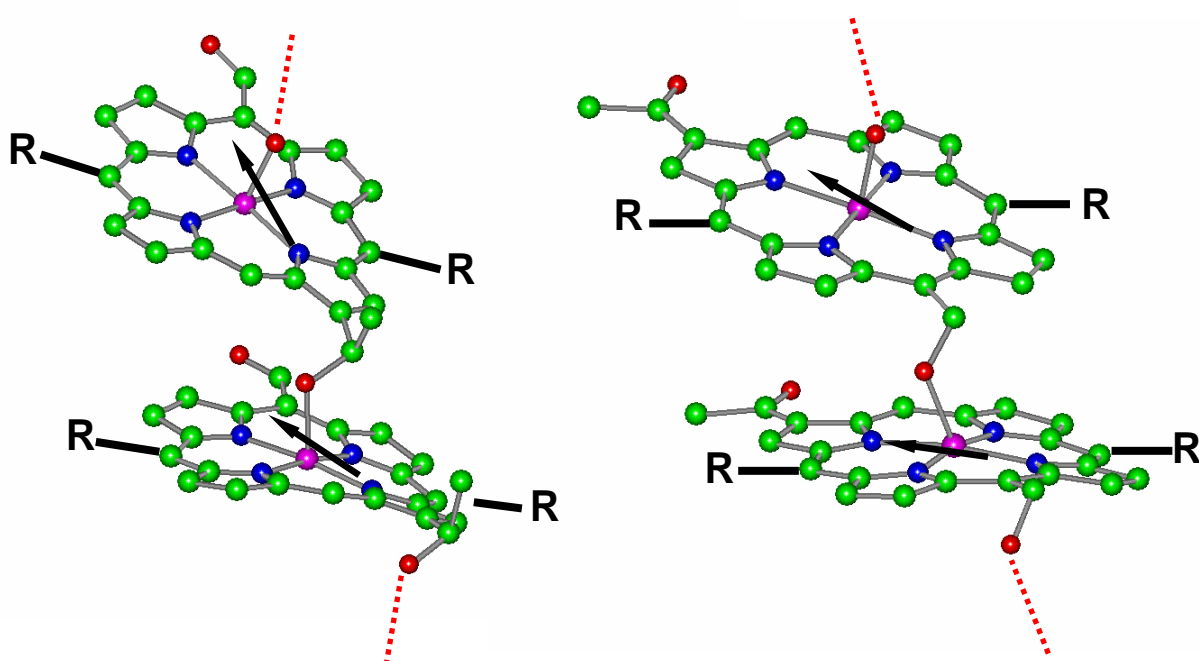
As discussed in the above section, π - π interactions and hence the amount of π -overlap of the macrocycles among the porphyrins is an important factor to induce self-assembly. Strong attractive interactions between the π systems control the aggregation of conjugated macrocycles such as porphyrins, phthalocyanines or polyacenes. A great amount of work has been devoted to identifying the role of π - π interactions which leads to either cofacial or perpendicular molecular arrangements. In the cofacial arrangement, the macrocycles are usually offsetted to minimize repulsion of the π orbitals with concomitant attraction of the π - π orbitals as described by Hunter and Sanders.^[116] The π - π interactions of porphyrins is not restricted only to metalloporphyrins, but it can be observed also in the free base porphyrins. The porphyrin rings normally do not lie exactly above each other, but are slightly slipped from each other in parallel direction. In our particular case, in the 3,17-diacetyl free base **32** the two porphyrins rings are exceptionally held exactly one above the other because of the electronegative acetyl groups which lower considerable the repulsion of the π orbitals in two neighbouring molecules in the crystal (Fig 3.18). The strong electron-withdrawing effect of the acetyl groups at 3,17 positions is also evident in their reactivity. Thus after monoreducing one group, the other carbonyl group becomes deactivated so that isolation of the monoreduced compounds can occur in high yields. Would the reverse situation be encountered (i.e. the monoreduced compound would have a more reactive carbonyl group, then the isolation of the monoreduced intermediate would have been extremely difficult. This is also supported partially by the semiempirical calculations (Scheme 3.1).



A similar type of π -stacking can be observed in the final self-assembled zinc compound **102** as shown in Fig 3.5. This compound could be crystallized and the structure could be solved in a collaborative effort involving Dr. Balaban's group.^[103]

3.13 Geometry Estimations of the Aggregates Based on Semiempirical Calculations

In accordance with detailed previous spectroscopic studies on the separated enantiomers of the methyl zincbacteriopheophorbide $d^{[117]}$, one can exclude the possibility that closed dimers are formed by double coordination of the zinc atoms by the hydroxy(m)ethyl groups which would also lead to parallel but opposing Q_y transition dipole moments and should thus be blue-shifted. More likely, the large assemblies are formed of extended stacks of different lengths, as implied by the dotted lines in Scheme 3.1. The different lengths account for the heterogeneity and thus the broad absorption maxima.



Scheme 3.1 Stacking interactions in 49 and 45 R stands for the 3,5-di-tert-butylphenyl groups. Only two porphyrin rings are shown in each case together with the direction of the Q_y transition dipole moments (indicated by arrows) The geometries were obtained by successive optimizations with the semiempirical force-field PM3 and molecular mechanics (MM+) within the HyperChem® programme package and should be regarded only as a crude approximation.

3.14 Outlook

In the following topics a possible application for self-assembled porphyrin is discussed.

3.14.1 Application of Self-Assembled Chromophores for Photovoltaic Cells

Solar cells are devices which convert solar energy into electricity, either directly *via* the photovoltaic effect, or indirectly by first converting the solar energy to heat or chemical energy. The most common form of solar cells is based on the photovoltaic (PV) effect. When sunlight is absorbed by semiconducting materials, the solar energy ejects electrons from their atoms, allowing the electrons to flow through the material to produce electricity. This process of converting light (photons) to electricity (voltage) is called the *photovoltaic (PV) effect*.

Silicon solar cells can consist of either single crystal, polycrystalline, or amorphous material.

3.14.2 Silicon Cells

Most solar cells are made of a single crystal of silicon. These efficient cells are called homojunctions, as both sides of the *p-n* junction are made of the same material. However, single crystal silicon is expensive and the size of the solar cells is limited to the size of the crystal. Thus, this type of cell is usually too expensive for large-scale use, except where price is not an issue, such as in space projects. Amorphous silicon based solar cells are much less efficient (< 10 %) but can be implemented in large area devices.

3.14.3 Thin Film Solar Cells

The thin film solar cells use layers of semiconductor materials only a few micrometers thick. Although thin film cells are less efficient than single crystal silicon cells they can now compete with the amorphous silicon cells and they have two important advantages. Firstly, the required thickness (only a few micrometers) of the active layer is small, being only two or three times the optical absorption length. Thus, the material cost will only be a small fraction of the total cell cost. Secondly, thin film devices can be produced on large and flexible area substrates in a continuous process, giving a high output with a low unit cost. The sensitised nanocrystalline injection solar cell employs organic dyes such as phthalocyanines, perylene bis-amides, xanthenes, hemicyanines and porphyrins. Transition metal complexes for spectral sensitisation of oxide semiconductors, such as TiO₂, ZnO, SnO₂, and Nb₂O₅^[118] have been tested. The incident light-to-electricity or Incident Photon to

Current Conversion Efficiency (IPCE) in organic dyes has been observed to be quite moderate in comparison with metal polypyridine complexes.^[119-123]

Among the known organic solar cells, the solid-state dye-sensitised mesoporous TiO₂ based Grätzel solar cell is the most efficient one up to now which also uses a ruthenium polypyridyl complex. Nanocrystalline TiO₂ is a high surface area wide-gap semiconductor that absorbs in the ultraviolet region and not in the visible region so that it has to be photosensitized with a chromophore which gives efficient collection of the solar spectrum. In Grätzel solar cells the charge separation can be directly used as a photocurrent and incident photon to electric current conversion has a yield as high as 33%. Ruthenium complexes having ligands such as polypyridine have been extensively studied as a photosensitizer for dye-sensitised nanocrystalline oxide semiconductor solar cells.^[124,-131]

Porphyrins are also important,^[132-136] e.g. for artificial photosynthetic reaction centres, as light-receptors in energy conversion and in the design of molecular-scale electronic devices^[137-138] in wide band gap semiconductors for solar energy conversion.^[139-140] The energy difference between the conduction band edge of an n-type semiconductor and the oxidation potential of the excited adsorbed dye, imparts a driving force for photoinduced charge injection.^[141-143] With porphyrins IPCE high values have been reported in various research groups.^[140-144] The mesoporous nanocrystalline films of the semiconductor considerably increase the effective surface area for dye adsorption. More recently, a great deal of research has focused on the photosensitising properties of porphyrins. Due to their photosensitising properties, the present work will hopefully contribute in setting up hybrid solar cell based on self-assembled chromophores for photosensitization of a wide band nanostructured semiconductor. A self-assembling chromophore molecule, that is able to bind to the surface of a nanostructured semiconductor and at the same time performs the function of a light-harvesting nanostructure has not been described before. The self-assembled artificial antenna system should have a broad absorption range and high extinction coefficients desirably over the whole visible region and into the near infrared. Most importantly, it must be able to pass on the excitation via rapid energy transfer processes and should not be hindered due to non-specific aggregation. Usually, due to concentration quenching, the fluorescence of aggregated dyes is strongly quenched and thus the excitation energy transfer is hindered. In natural photosynthesis, only a few pigment molecules are involved in the charge separation and subsequent electron transfer steps within the reaction centre. Most pigments are involved in light-harvesting by the antenna systems which perform following functions:

(i) increase the absorption cross-section and trapping efficiency of photons to a large extent;

- (ii) increase the absorption region so that a broader range of wavelengths from the solar spectrum can be filtered out and,
- (iii) the reaction centre can be cycled much more rapidly, with a frequency reaching almost 1 kHz.^[99-100]

3.15. Conclusions

Although absorption efficiency is not a limiting factor for silicon-based solar cells, for hybrid solar cells it is. In order to increase the overall efficiency of hybrid solar cells the antenna principles of the natural photosynthetic organisms could be followed. In chlorosomes bacteriochlorophylls *c*, *d* or *e* self-assemble^[145-147]. This very simple organization principle, which does not require a lot of genes for expressing proteins to bind the chromophores, is worth mimicking with fully synthetic and robust pigments which should be easy to synthesize and have a better stability than the natural (bacterio)chlorophylls. In this work, self-assembling porphyrins with the same functional groups like the natural bacteriochlorophylls *c*, *d* or *e* have been synthesized. More than 100 new compounds were synthesized, some of them by new synthetic methods, and characterized. The diacylation reaction of porphyrins is novel and could be optimized to occur regiospecifically under kinetic control. Thin films of self-assembled chromophores were deposited, either onto glass surfaces or on nanocrystalline titania of different grain sizes. These films and nanostructures were characterized using confocal microscopy in fluorescence and reflection mode, and atomic force microscopy. The very ordered structure of the self-assemblies ensures that the fluorescence is not quenched, thus giving hope that their luminescence is of use in future hybrid solar cells.

High surface area membrane-type films of semiconducting oxides are used in the design of dye-sensitised solar cells, which have a potential use in low-cost hybrid solar cells. The efficiency of dye sensitised wide band semiconductors solar cell is particularly hampered by non-specific aggregation of the dye molecules as it leads to a strong quenching of the dye fluorescence and as a consequence of low device efficiencies. A few number of the self-assembled chromophores dedcribed in this thesis show very broad absorption spectra, which is beneficial for efficient light collection over almost the entire visible spectrum. More importantly, it is also possible to control both the chirality and the optical properties through ordering of the transition dipole moments of the chromophores within the self-assembled nanostructures. Upon anchoring the self-assembled chromophores onto nanocrystalline titania with different grain sizes, remarkably the fluorescence was not quenched, presumably due to the very ordered arrangement of chromophores onto the TiO₂ surface. All these

findings together highlight the importance of the chromophores as they display tailored properties which might prove useful for low cost hybrid solar cells. Natural photosynthesis is fascinating and the new biomimetic approach described in this thesis implements the self-assembly ability to synthetic chromophores. In terms of efficiency, however, the natural photosynthesis occurs with much higher efficiencies than any artificial system. The large production cost of silicon-based solar cells puts restrictions on large-scale applications. Opportunities for research in organic or plastic solar cells, arise because of their potential cost effectiveness. Much cheaper devices can be constructed by using polymer techniques on large and flexible areas.

Chapter 4

Experimental Section

4.1 General Remarks

Solvents were dried and freshly distilled before use as follows: dichloromethane from calcium hydride; toluene and *n*-heptane from sodium metal; chloroform-*d* from phosphorous pentaoxide.

NMR Spectra were recorded at 300 MHz (^1H) with a Bruker DPX 300 Avance spectrometer. Chemical shifts are given in ppm relative to the signal of CHCl_3 which was taken as $\delta = 7.26$ (for ^1H) and 77.00 (for ^{13}C).

Preparative HPLC was performed on a Varian ProStar machine equipped with a normal phase column (250 x 25 mm). Details of the chiral separations can be learned from the CHIRBASE® database.

UV/Vis spectra were measured with a Varian Cary 500 instrument.

FT-IR spectra were obtained on a Perkin-Elmer Spectrum GX spectrometer as KBr pellets.

MALDI-TOFF mass spectra were obtained on a Voyager Instrument from Applied Biosystems either with anhydrous glycerol or 1,8,9- anthracenetriol matrices.

HR-FAB-MS were recorded using 3-nitro-benzylalcohol (NBA) as the matrix on a Finnigan MAT 90 machine.

CD Spectra were measured on an Aviv (Lakewood, N. J., USA) CD Spectrometer, model 62 A DS or on a JASCO J-180 CD spectrometer.

Fluorescence Spectra were measured on a Jobin Yvon SPEX Fluorolog spectrofluorimeter.

Confocal fluorescence microscopy was performed with a Leica TCS SP2-x1 Microscope.

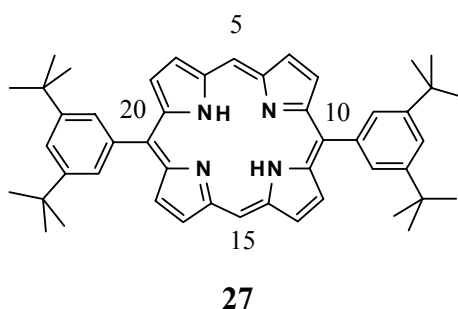
Elemental Analyses were performed with a CE Flash 400 Instrument. The metallated porphyrins gave consistently lower values for their carbon content (1-2%) than the theoretical values while the nitrogen and hydrogen contents were, within the usual experimental error, correctly reproduced.

Retention factors are given for silica gel TLC plates (Macherey-Nagel) which were eluted with dichloromethane stabilized with 0.2 % ethanol unless otherwise stated.

Column chromatography was performed with Merck silica gel 40-63 μm .

4.2 10,20-Di-(3,5-di-*t*-butylphenyl)-21,23*H*-porphyrin [27].

This known free base porphyrin was prepared in 10-15 g batches (after purification by column chromatography) by optimising known literature methods. Here for the first time is reported the ^{13}C spectrum.



^{13}C -NMR:

$\delta = 31.8$ ($\text{C}(\text{CH}_3)_3$), 35.1 ($\text{C}(\text{CH}_3)_3$), 105.1 (10, 20-C), 120.4 (5,15-C), 121.1 (4'-C), 130.2 (2',6'-C), 131.1 (3,7,13,17-C), 131.5 (2,8,12,18-C), 140.3 (1'-C), 145.0 (6 or 9-C), 147.4 (9 or 6-C), 149.1 (3',5'-C).

4.3 10,20-Di-(3,5-di-*t*-butylphenyl)-porphinato copper [28]

The previous free base porphyrin **27** (4 g, 5.82 mmol) dissolved in chloroform (130 mL) to which 100 mL methanol and 10 drops of water were added was metallated with anhydrous copper acetate (5.28 g, 29.1 mmol) by stirring at room temperature for 12 hrs under nitrogen atmosphere. Yields were 85-95% after purification by column chromatography on silica gel eluted with dichloromethane/methanol (99/1, v/v).

$R_f = 0.90$.

UV (CHCl_3) $\lambda_{\text{max}} = 405, 528$.

MALDI-TOFF-MS (Glycerol matrix): $m/z = 749.5$ (100)

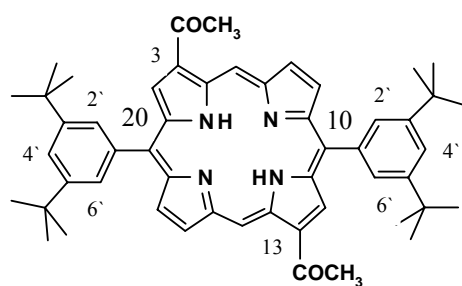
$[\text{M}+\text{H}^+]$; calc. for $\text{C}_{48}\text{H}_{52}\text{N}_4\text{Cu} = 747.35$

4.4 13-Diacetyl-10,20-bis(3,5-di-*t*-butylphenyl)porphinato copper and 3,17-diacetyl-10,20-bis(3,5-di-*t*-butylphenyl)porphinato copper [29 and 30]

Diacetylation of the copper porphyrin **28** (400 mg, 0.53 mmol) was performed by dissolving it in carbon disulfide (160 mL) in a 1L three-necked flask equipped with a rubber septum, a reflux condenser and thermometer under argon and then adding at 0-3 °C acetic anhydride (141 mL, 1.5 mol) followed by addition of tin tetrachloride via syringe (34.8 g, 15.6 mL, 134

mmol). After stirring at 0-2°C for 30 min the reaction mixture is diluted with 300 mL CS₂ and ice cold water (100 mL) was added dropwise within 35 min and stirred afterwards for another 40 min. After extraction into dichloromethane and washing with brine twice, the mixture was washed with aqueous sodium hydrogen carbonate and then again with brine. The organic layers were dried on sodium sulfate and after removal of the solvents in vacuum the mixture was chromatographed on silica gel eluted with dichloromethane. The fraction containing an almost equimolar mixture of the two isomeric diacetylated copper porphyrins weighed 154.8 mg (35 % yield). Over different runs yields over 27% were consistently obtained.

4.5 3,13-Diacetyl-10,20-bis(3,5-di-*t*-butylphenyl)-21,23*H*-porphyrin [31]



31

The above mixture of copper porphyrins **29** and **30** (53 mg) was demetallated using a 10 mL degassed mixture of trifluoroacetic and sulfuric acids (1:1 v/v) by stirring for 1.5 h at room temperature. The usual work-up consists in pouring on ice and extraction into dichloromethane, washing with brine, neutralization with aqueous sodium hydrogen carbonate and again washing with brine. After drying on sodium sulfate and evaporation to dryness a reddish-purple solid 47.2 mg (96 % yield) was obtained. Demetallation yields over different runs and scales (up to 1.5 g) gave consistently yields above 86%. Subsequent careful column chromatography on silicagel eluted first with dichloromethane gives the title porphyrine as the firstly eluted fraction. Careful column chromatography on silica gel of the above mixture after eluting with dichloromethane until the reddish isomer **32** is separated was followed by a second greenish fraction of the compound **31**.

$$R_f = 0.52$$

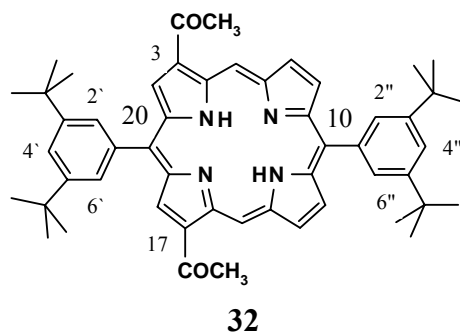
¹H-NMR:

δ = 11,42 (s, 2H, 5,15-H), 9.56 (s, 2H, 2,12-H), 9.56 (d, ³J = 4.8 Hz, 2H, 7,17-H), 9.21 (d, ³J = 4.8 Hz, 2H, 8,18-H), 8.17 (d, ⁴J = 1.8 Hz, 4H, 2',6'-H), 7.92 (t, ⁴J = 1.8 Hz, 2H, 4'-H), 3.20 (s, 6H, CO-CH₃), 1.64 (s, 36H, C(CH₃)₃), -2.72 (s, 2H, NH).

¹³C-NMR:

$\delta = 29.9$ (CO-CH₃), 31.8 (C(CH₃)₃), 35.16 (C(CH₃)₃), 107.7 (5,15-C), 121.5 (10,20-C), 122.11 (4'-C), 129.1 (8,18-C), 130.7 (2',6'-C), 138.9, 139.7, 140.2, 140.9, 149.5, 150.1 (2,12-C), 151.4, 197.4 (CO-CH₃).

4.6 3,17-Diacetyl-10,20-bis(3,5-di-*t*-butylphenyl)-21,23*H*-porphyrin [32]



$R_f = 0.54$

¹H-NMR:

$\delta = 11, 30$ (s, 2H, 5,15-H), 9.54 (s, 2H, 2,18-H), 9.40 (d, ³J = 4.8 Hz, 2H, 7,13-H), 9.02 (d, ³J = 4.8 Hz, 2H, 8,12-H), 8.19 and 8.09 (two d, ⁴J = 1.8 Hz, 2H each, 2',6'- and 2'',6''-H), 7.93 and 7.85 (two t, ⁴J = 1.8 Hz, 1H each, 4'- and 4''-H), 3.20 (s, 6H, CO-CH₃), 1.63 and 1.57 (two s, 18 H each, C(CH₃)₃), 2.32 (s, 2H, NH).

¹³C-NMR:

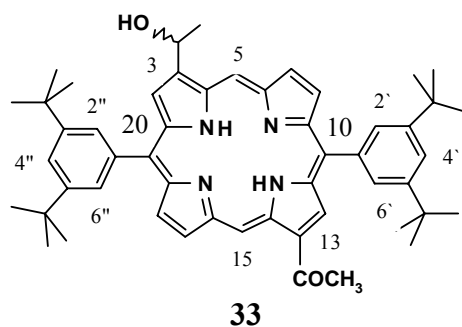
$\delta = 29.9$ (CO-CH₃), 31.7 (C(CH₃)₃), 35.09 and 35.18 (C(CH₃)₃), 107.1 (5,15-C), 120.4, 121.4, 121.6 (10,20-C), 124.4, 130.0 (2',6'-C), 131.1, 132.0, 134.2, 136.8, 139.67, 139.70, 149.4, 149.6, 196.8 (CO-CH₃).

MALDI-MS: 771.4.

HR-FAB-MS: 771.465 [M+H]⁺; Calc. for C₅₂H₅₉N₄O₂ = 771.4638.

Crystallization of 32: A solution of **32** in CH₂Cl₂ in the centrifuged bottle was concentrated and was diluted and centrifuged with *n*-hexane. After centrifugation and decantation, the supernatant was left in the refrigerator at -18^oC for 20 months. During this time, small crystals appeared which were left to grow until suitable for conventional X-ray crystallography.

4.7 3-Acetyl-13-(1-hydroxyethyl)-10,20-bis(3,5-di-*t*-butylphenyl)-21,23*H*-porphyrin [33]



The corresponding diacetyl free base porphyrine **31** was monoreduced using sodium borohydride as described for compound **34**.

$R_f = 0.28$

$^1\text{H-NMR}$:

$\delta = 11.40$ (s, 1H, 5-H), 10.44 (s, 1H, 15-H), 9.51 (s, 1H, 2-H), 9.51 (d, $^3J = 4.5$ Hz, 1H, 7-H), 9.41 (d, $^3J = 4.8$ Hz, 1H, 17-H), 9.17 (d, $^3J = 4.8$ Hz, 1H, 8-H), 9.10 (d, $^3J = 4.8$ Hz, 1H, 18-H), 8.88, (s, 1H, 12-H), 8.14 (d, $^4J = 1.8$ Hz, 2H, 2',6',-H), 8.08 (m, 2H, non-equivalent 2'',6''-H), 7.88 (t, $^4J = 1.8$ Hz, 1H, 4'-H), 7.84 (t, $^4J = 1.8$ Hz, 1H, 4''-H), 6.61 (q, $^3J \sim 6$ Hz, 1H, CH₃-CH-OH), 3.16 (s, 3H, CO-CH₃), 2.54 (broad s, 1H, CH₃-CH-OH), 2.25 (d, $^3J = 6.3$ Hz, 3H, CH₃-CH-OH), 1.60, 1.59, 1.57 and 1.57 (four s, 9 H each, C(CH₃)₃), -2.78 (broad s, 1H, NH).

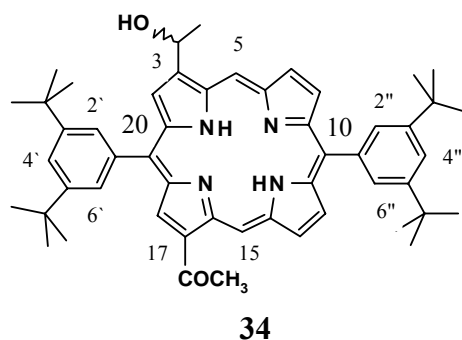
$^{13}\text{C-NMR}$:

$\delta = 13.70, 25.72, 29.69, 29.93$ (CO-CH₃), 31.77 (C(CH₃)₃), 35.10, 35.11 and 35.14 (C(CH₃)₃), 65.59 (HO-CH-CH₃), 102.67, 107.53 (5,15-C), 121.18 and 121.35 (10,20-C), 122.42 (4'-C), 128.32, 128.36, 130.67 (2',6'-C), 139.45, 139.980, 140.04, 149.26 and 149.36 (3',5'- and 3'',5''-C), 150.97 (2,12-C), 197.47 (CO-CH₃)

MALDI-MS (1,8,9-anthracene triol matrix): 772.8.

HR-FAB-MS: 773.4800 [M+H]⁺; Calc. for C₅₂H₆₁N₄O₂ = 772.4794.

4.8 3-Acetyl-17-(1-hydroxyethyl)-10,20-bis(3,5-di-*t*-butylphenyl)-21,23*H*-porphyrin [34]



Monoreduction of the corresponding 3,17-diacetyl compound **32** (55 mg, 0.07 mmol) was effected by dissolving it in 25 mL dichloromethane and 5 mL methanol and adding rapidly sodium borohydride (5.4 mg, 0.14 mmol). After stirring for 90 min. at room temperature the mixture was washed with brine, and the organic layer was dried on anhydrous sodium sulfate and chromatographed on silica gel eluted with dichloromethane. Recovered starting material (19 % yield) is eluted as the first fraction. The second band contains the monoreduced product (28 mg) and a final band with lower R_f consists of a mixture of the racemic and *meso*-dihydroxyethyl porphyrin (8 mg). The latter could be separated on a second column. Thus yields, over several runs, in the desired monoreduced compound were 51% depending on the reaction time and extent of over-reduction.

$R_f = 0.28$.

$^1\text{H-NMR}$:

$\delta = 11.40$ (s, 1H, 5-H), 10.38 (s, 1H, 15-H), 9.51 (s, 1H, 2-H), 9.51 (d, $^3J = 4.8$ Hz, 1H, 7-H), 9.29 (d, $^3J = 4.5$ Hz, 1H, 13-H), 9.11 (d, $^3J = 4.8$ Hz, 1H, 8-H), 9.11, (s, 1H, 18-H), 9.11 (d, $^3J = 4.5$ Hz, 1H, 12-H), 8.14 (d, $^4J = 1.8$ Hz, 2H, 2',6',-H), 8.10 (d, $^4J = 1.8$ Hz, 2H, 2'',6'',-H), 7.88 (t, $^4J = 1.8$ Hz, 1H, 4'-H), 7.84 (t, $^4J = 1.8$ Hz, 1H, 4''-H), 6.74 (q, $^3J = 6.3$ Hz, 1H, $\text{CH}_3\text{-CH-OH}$), 3.17 (s, 3H, CO-CH_3), 2.64 (broad s, 1H, $\text{CH}_3\text{-CH-OH}$), 2.31 (d, $^3J = 6.3$ Hz, 3H, $\text{CH}_3\text{-CH-OH}$), 1.61 and 1.57 (two s, 18 H each, $\text{C}(\text{CH}_3)_3$), -2.63 (broad s, 1H, NH), -2.89 (broad s, 1H, NH).

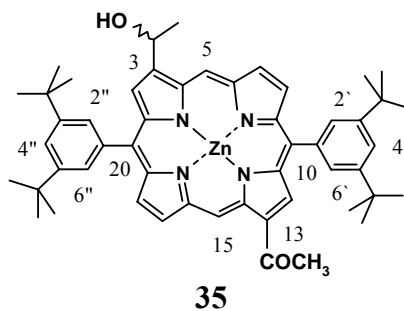
$^{13}\text{C-NMR}$:

$\delta = 25.88$ (CO-CH_3), 29.93 (HO-CH-CH_3) 31.75 ($\text{C}(\text{CH}_3)_3$), 35.09 and 35.14 ($\text{C}(\text{CH}_3)_3$), 65.52 (HO-CH-CH_3), 121.26 (10,20-C), 122.06 (4'-C), 130.06, 130.79, 139.98, 140.06, 149.25, 149.34, 197.42 (CO-CH_3).

MALDI-MS: 772.1.

HR-FAB-MS: 773.4811 [M+H]⁺; calc. for C₅₂H₆₀N₄O₂ = 773.4794.

4.9 3-Acetyl-13-(1-hydroxyethyl)-10,20-bis(3,5-di-*t*-butylphenyl)porphinato zinc [35]



The free base porphyrine **33** was metallated using zinc acetate as described above in over 80 % isolated yield. After column chromatography, the eluent was washed several times with brine to remove traces of methanol, evaporated in vacuum and was then thoroughly dried overnight (10^{-3} Torr) in order to perform self-assembly experiments.

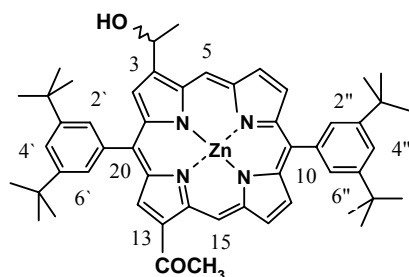
$R_f = 0.09$

¹H-NMR:

$\delta = 11.35$ (s, 1H, 5-H), 10.37 (s, 1H, 15-H), 9.59 (s, 1H, 2-H), 9.47 (d, $^3J = 4.5$ Hz, 1H, 7-H), 9.38 (d, $^3J = 4.5$ Hz, 1H, 17-H), 9.17 (d, $^3J = 4.5$ Hz, 1H, 8-H), 9.10 (d, $^3J = 4.5$ Hz, 1H, 18-H), 8.90 (s, 1H, 12-H), 8.14 (d, $^4J \sim 1.5$ Hz, 2H, 2',6'-H), 8.05 (m, 2H, nonequivalent 2'',6''-H), 7.87 (t, $^4J = 1.8$ Hz, 1H, 4'-H), 7.84 (t, $^4J = 1.8$ Hz, 1H, 4''-H), 6.63 (m, $^3J \sim 6.3$ Hz, 1H, CH₃-CH-OH), 3.18 (s, 3H, CO-CH₃), ~ 2.5 (broad d, CH₃-CH-OH), 2.23 (d, $^3J = 6.6$ Hz, 3H, CH₃-CH-OH), 1.60 , 1.57 and 1.53 (three s, 9, 9 and 18H respectively, nonequivalent C(CH₃)₃).

HR-FAB-MS: 834.3842; calc. For C₅₂H₅₈N₄O₂Zn = 834.3851.

4.10 3-Acetyl-17-(1-hydroxyethyl)-10,20-bis(3,5-di-*t*-butylphenyl)porphinato zinc [36]



36

Zinc metallation of **34** occurred with over 90 % yield as described above. After purification by column chromatography the eluent was washed several times with brine in order to remove methanol traces and subsequently dried. Self-assembly is possible only in dry solvents, in the absence of methanol. In such conditions NMR spectra give only broad lines. Upon addition of CD₃OD these give well resolved signals for the monomeric Zn-methanol adducts.

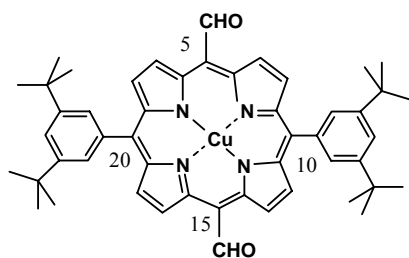
$R_f = 0.09$.

¹H-NMR:

$\delta = 11.30$ (s, 1H, 5-H), 10.30 (s, 1H, 15-H), 9.58 (s, 1H, 2-H), 9.47 (d, $^3J = 4.5$ Hz, 1H, 7- or 13-H), 9.37 (d, $^3J = 4.5$ Hz, 1H, 13- or 7-H), 9.12 and 9.11 (two overlapping d, $^3J \sim 4.2$ Hz, 2H, 12- and 8-H), 9.01 (s, 1H, 18-H), 8.15 and 8.11 (two t, $^4J = 1.8$ Hz, 2H, nonequivalent 2' or 6'-H and 2'' or 6''-H), 8.09 (dd, $^4J = 1.8$ Hz, 2H, nonequivalent 6' or 2'-H and 6'' or 2''-H), 7.87 and 7.84 (two t, $^4J = 1.8$ Hz, 2H, 4'- and 4''-H), 6.54 (q, $^3J \sim 6$ Hz, 1H, CH₃-CH-OH), 3.16 (s, 3H, CO-CH₃), 2.38 (broad s, 1H, CH₃-CH-OH), 2.24 (d, $^3J = 6.3$ Hz, 3H, CH₃-CH-OH), 1.60 , 1.59 , 1.57 and 1.57 (four s, 9 H each, nonequivalent C(CH₃)₃).

HR-FAB-MS: 834.3871; Calc. for C₅₂H₅₈N₄O₂Zn = 834.3851.

4.11 5,15-Diformyl-10,20-bis(3,5-di-*t*-butylphenyl)porphinato copper [37]



37

In a 4L three-necked flask equipped with a reflux condenser and dropping funnel, to

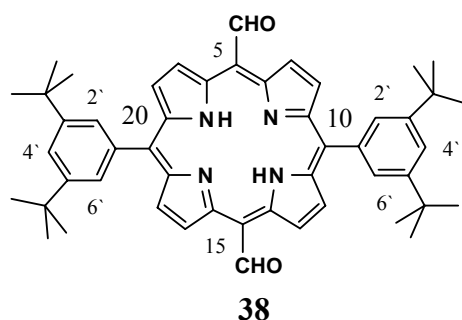
anhydrous DMF (200 mL) were added slowly, dropwise, POCl₃ (240 mL) at 0-2°C under nitrogen atmosphere. After some time the POCl₃-DMF complex solidified. After removal of the ice-bath, 1,2-dichloroethane (400 mL) was added and the solution was heated gently to 50 °C. From the dropping funnel which was protected from light with aluminum foil, a solution of the copper porphyrin (2.0 g) in 1L 1,2-dichloroethane was added slowly at 50 °C. After completion of addition the mixture was heated overnight under reflux. After cooling in an ice-bath, to the mixture were carefully added 1L of saturated aqueous sodium acetate solution and then the mixture was heated to 80°C for 3 hrs for completing the hydrolysis. Extraction into dichloromethane (3x), followed by washing once with water, twice with aqueous sodium hydrogen carbonate, and then finally twice with brine was followed by drying over anhydrous sodium sulfate and evaporation of the solvents in vacuum. After column chromatography on silica gel (H = 35 cm, Φ = 8 cm), a fraction containing pure product (0.915 g) 43 % yield, was obtained.

R_f = 0.72.

MALDI-MS (Glycerol matrix): *m/z* = 804.08 (100) [M+H]⁺.

HR-FAB-MS: 804.3452 [M+H]⁺; calc. for C₅₀H₅₃N₄O₂Cu = 804.3464 (for the main isotopomer).

4.12 5,15-Diformyl-10,20-bis(3,5-di-*t*-butylphenyl)-21,23*H*-porphyrin [38]



Demetallation of the above copper porphyrin **37** (800 mg, 0.99 mmol) was effected using a 120 mL mixture of trifluoroacetic and sulfuric acids (1.1 v/v) as described in the supporting informations.^[10] After the same work-up procedure 740 mg of product were obtained (99 % yield). In order to be sure that no contamination from green coloured chlorines occurred, a portion of the product was dissolved in chloroform and heated to reflux in the presence of 2,3-dichloro-5,6-dicyano-*p*-benzoquinone (DDQ). After work-up and column chromatography

the same spectral data were obtained for this pure product. Convenient recrystallization can be effected from boiling chloroform and *n*-hexane.

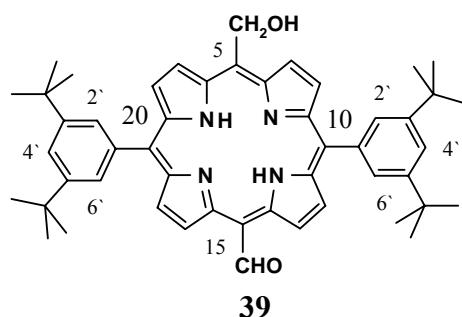
$R_f = 0.82$.

$^1\text{H-NMR}$:

$\delta = 12.58$ (s, 2H, CHO), 10.02 (broad d, $^3J = 5.1$ Hz, 4H, 3,7,13,17-H), 9.02 (sharp d, $^3J = 5.1$ Hz, 4H, 2,8,12,18-H), 8.04 (d, $^4J = 1.8$ Hz, 4H, 2',6'-H), 7.87 (t, $^4J = 1.8$ Hz, 2H, 4'-H), 1.57 (s, 36H, C(CH₃)₃), 2.27 (s, 2H, NH).

HR-FAB-MS: 741.4189 [M+H]⁺; calc. for C₅₀H₅₃N₄O₂ = 741.4168.

4.13 5-Formyl-15-hydroxymethyl-10,20-bis(3,5-di-*t*-butylphenyl)-21,23*H*-porphyrin [39]



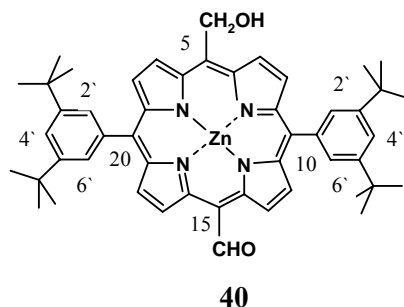
The corresponding 5,15-di-formyl free base porphyrin **38** (317 mg, 0.427 mmol) dissolved in 50 mL dichloromethane to which 5 mL methanol were added, was monoreduced with sodium borohydride (32.2 mg, 0.8 mmol). Yields varied between 28 and 35% over different runs. The reaction was stopped when by TLC the dihydroxymethyl compound with the lowest R_f value (0.2) starts to be formed (2-3 min). The reaction was quenched with brine, the organic layer was dried over sodium sulfate and after evaporation in vacuum purified by column chromatography. The first fraction consists of recovered starting material (45-40%) while the desired product elutes as the second band.

$R_f = 0.41$ or 0.15 (TLC eluted with dichloromethane – *n*-hexane (1:1 v/v)).

$^1\text{H-NMR}$:

$\delta = 12.49$ (s, 1H, CHO), 10.02 (broad d, $^3J = 4.8$ Hz, 2H, 3,7-H), 9.56 (sharp d, $^3J = 4.8$ Hz, 2H, 13,17-H) 9.01 (sharp d, $^3J = 4.8$ Hz, 2H, 12,18-H) 8.90 (sharp d, $^3J = 4.8$ Hz, 4H, 2,8-H), 8.03 (d, $^4J = 1.8$ Hz, 4H, 2',6'-H), 7.85 (t, $^4J = 1.8$ Hz, 2H, 4'-H), 6.91 (m, 2H, CH₂-OH), 2.68 (broad s, 1H, CH₂-OH), 1.56 (s, 36H, C(CH₃)₃), -2.15 (s, 2H, NH).

4.14 5-Formyl-15-hydroxymethyl-10,20-bis(3,5-di-*t*-butylphenyl)porphinato zinc [40]



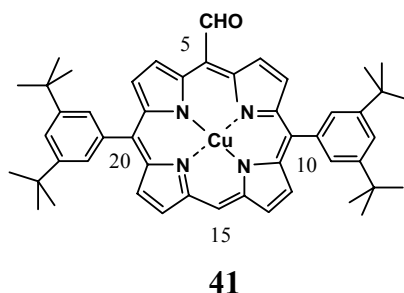
Zinc metallation of the above free base **39** (12 mg) with excess zinc acetate in a 28 mL chloroform/methanol mixture (2:1, v/v) after stirring for 3 hrs at room temperature the reaction was driven to completion (monitoring by UV-Vis). Washing with aqueous sodium hydrogen carbonate followed by washing with brine, drying over anhydrous sodium sulfate and evaporation of the solvent produced in quantitative yield the desired product. After column chromatography on silica gel with 3% methanol in dichloromethane, the eluent was washed twice with brine in order to remove the residual methanol. Recrystallization from dichloromethane and *n*-hexane followed by centrifugation and drying overnight in vacuum (10^{-3} Torr) produced samples which self-assembled in nonpolar solvents.

$^1\text{H-NMR}$:

δ = 12.50 (s, 1H, 5-CHO), 9.98 (d, $^3J = 4.8$ Hz, 2H, 13,17-H), 9.56 (d, $^3J = 4.8$ Hz, 2H, 3,7-H), 8.99 (d, $^3J = 4.8$ Hz, 2H, 12,18-H), 8.87 (d, $^3J = 4.8$ Hz, 2H, 2,8-H), 7.98 (d, $^3J = 1.8$ Hz, 4H, 2',6'-H), 7.80 (t, $^3J = 1.8$ Hz, 2H, 4'-H), 6.91 (s, 2H, CH₂-OH), 2.02 (broad s, CH₂-OH), 1.53 (s, 36H, C(CH₃)₃).

HR-FAB-MS: 807.3633 [M+H]⁺; calc. for C₅₂H₅₅N₄O₂Zn = 807.3616.

4.15 5-Formyl-10,20-bis-(3,5-di-*t*-butylphenyl)porphinato copper [41]



In a three necked 100 mL reaction flask equipped with a reflux condenser, the Vilsmeier complex was prepared by adding dropwise POCl₃ (5.12 g, 3.06 mL, 33.4 mmol) to DMF (2.54 g, 2.70 mL, 34.7 mmol) at 0-10 °C within 20 min under argon. When the complex solidified, small portions of 1,2-dichloroethane were added. A solution of the copper porphyrin (500 mg, 0.67 mmol) in 1,2-dichloroethane (70 mL total volume) was added dropwise at 5-10 °C within 5 min and then the mixture was heated under reflux for 45 min. The typical work-up consisted in cooling the reaction mixture in an ice bath, carefully adding a saturated solution of sodium acetate (8 ml) diluted with water (5 mL) and stirring overnight. Extraction into dichloromethane and washing first with brine, then with saturated aqueous sodium hydrogen carbonate and then finally again with brine produced after evaporation of the solvents a crude dark coloured solid. Column chromatography on silica gel eluted with dichloromethane gave the pure product as a second fraction (428 mg) in 82.6 % yield.

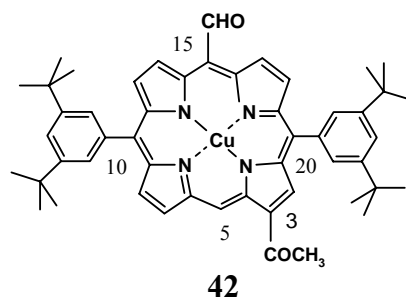
$R_f = 0.70$.

MALDI-MS (1,8,9-anthracenetriol matrix) $m/z = 774.9$ (100) [M+H⁺];

calc. for C₄₉H₅₂N₄OCu = 775.34 (for the main isotopomer).

HR-FAB-MS: 776.3527 [M+H⁺]; calc. for C₄₉H₅₃N₄OCu = 776.3515.

4.16 3-Acetyl-15-formyl-10,20-bis(3,5-di-*t*-butylphenyl)porphinato copper [42]

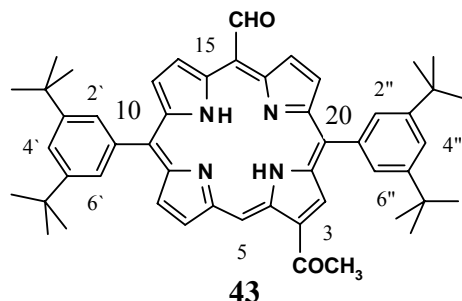


The monoformyl copper porphyrine **41** (200 mg) was dissolved in 50 mL carbon disulfide in a three-necked flask equipped with a rubber septum and a thermometer and degassed by passing a stream of argon. After cooling to 2°C acetic anhydride (6.1 mL, 64 mmol) was added via syringe. Then tin tetrachloride (3.0 mL, 6.71 g, 26 mmol) were added rapidly via syringe and the temperature rose to 7°C. The reaction was quenched rapidly thereafter (150 seconds after addition of SnCl₄) by pouring on ice. The mixture was stirred vigorously at room temperature for 45 min and then extracted into dichloromethane (2 x 20 mL) which was washed with aqueous sodium hydrogen carbonate and then with brine. After drying the organic layer on sodium sulfate, the solvents were evaporated in vacuum.

$R_f = 0.60$.

MALDI-MS (1,8,9-anthracenetriol matrix) = 818.07 [M+H]⁺; calc. for C₅₁H₅₄N₄O₂Cu = 817.35 (for the main isotopomer).

4.17 3-Acetyl-15-formyl-10,20-bis(3,5-di-*t*-butylphenyl)-21,23*H*-porphyrin [43]



The copper porphyrine **42** was demetallated as described above with a 10 mL mixture of sulfuric and trifluoroacetic acids (1/1 v/v). After a similar work-up and column chromatography on silica gel eluted with dichloromethane, the second fraction contained the pure product (154 mg), the yield over two steps (acetylation and demetallation) being thus 79 %.

R_f = 0.57.

¹H-NMR:

δ = 12.54 (s, 1H, 15-CHO), 11.34 (s, 1H, 5-H), 10.20, 12 (broad d, ³J = 5.1 Hz, 1H, 13-H), 9.86 (d, ³J = 4.8 Hz, 1H, 17-H), 9.43 (d, ³J = 4.5 Hz, 1H, 7-H), 9.30 (s, 1H, 2-H), 9.14 (d, ³J = 5.1 Hz, 1H, 12-H), 9.00 (sharp d, ³J = 4.8 Hz, 1H, 18-H), 8.95 (d, ³J = 4.5 Hz, 1H, 8-H), 8.11 and 8.05 (two d, ⁴J = 1.8 Hz, 4H, 2',6'- and 2'',6''-H), 7.90 and 7.86 (two t, ⁴J = 1.8 Hz, 2H, 4'- and 4''-H), 3.12 (s, 3H, CO-CH₃), 1.60 (s, 18H, C(CH₃)₃), 1.57 (s, 18H, C(CH₃)₃), 2.05 (s, 2H, NH).

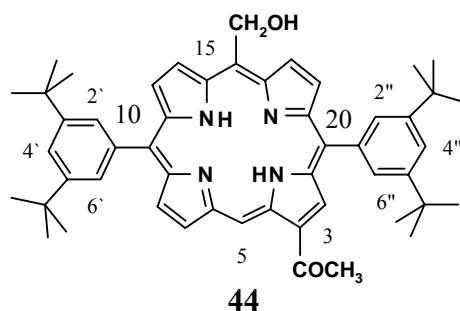
¹³C-NMR:

δ = 29.8 (CO-CH₃), 31.7 (C(CH₃)₃), 35.10 and 35.14 (C(CH₃)₃), 108.1 (10,20-C), 112.5 (5-C), 121.66 and 121.76 (4' and 4''-C), 123.0 (15-C), 125.6, 127.1 (broad, 13-C), 129.3 (broad, 8-C), 129.7 and 130.4 (2',6'- and 2'',6''-C), 130.5 (broad, 17-C), 131.8 (broad), 132.9 (broad, 12-C), 136.4 (broad, 18-C), 139.9 and 140.0 (1' and 1''-C), 149.30 and 149.36 (3',5'- and 3'',5''-C), 195.0 (15-CHO), 197.1 (3-CO-CH₃).

MALDI-MS (1,8,9-anthracenetriol matrix) *m/z* = 757.12 (100%) [M+H]⁺.

HR-FAB-MS: 757.4498 [M+H]⁺. calc. for C₅₁H₅₆N₄O₂ = 757.03

4.18 3-Acetyl-15-hydroxymethyl-10,20-bis(3,5-di-*t*-butylphenyl)-21,23*H*-porphyrin
[44]



The corresponding 3-acetyl-15-formyl free base porphyrine **43** (100 mg, 0.13 mmol) was dissolved in dichloromethane (30 mL) and methanol (10 mL) under argon after which sodium borohydride (10 mg, 2 eq.) were added. The mixture was stirred at room temperature in the dark for 8 min after which it was washed with brine. The organic layer was dried on sodium sulfate and evaporated in vacuum. Purification by column chromatography on silica gel eluted with dichloromethane gave the desired product (67.6 mg) as the second eluted fraction in 67.4 % yield.

$R_f = 0.27$

$^1\text{H-NMR}$:

$\delta = 11.32$ (s, 1H, 5-H), 9.71 (d, $^3J = 5.1$ Hz, 1H, 13-H), 9.60 (d, $^3J = 4.8$ Hz, 1H, 17-H), 9.46 (d, $^3J = 4.8$ Hz, 1H, 7-H), 9.45 (s, 1H, 2-H), 9.17 (d, $^3J = 5.1$ Hz, 1H, 12-H), 9.05 (d, $^3J = 4.8$ Hz, 16 1H, 8-H), 9.00 (sharp d, $^3J = 4.8$ Hz, 1H, 18-H), 8.13 and 8.08 (two d, $^4J = 1.8$ Hz, 4H, 2',6'- and 2'',6''-H), 7.89 and 7.85 (two t, $^4J = 1.8$ Hz, 2H, 4'- and 4''-H), 7.01 (broad d, $^3J = 5.7$ Hz 2H, $\underline{\text{CH}_2\text{-OH}}$), 3.16 (s, 3H, CO-CH_3), 2.66 (broad t, $^3J = 5.4$ Hz, $\underline{\text{CH}_2\text{-OH}}$), 1.60 (s, 18H, $\text{C}(\underline{\text{CH}_3})_3$), 1.57 (s, 18H, $\text{C}(\underline{\text{CH}_3})_3$), -2.78 (s, 2H, $\underline{\text{NH}}$).

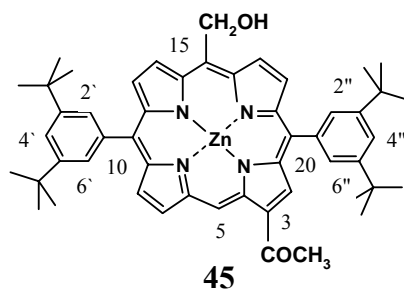
$^{13}\text{C-NMR}$:

$\delta = 29.87$ ($\text{CO-}\underline{\text{CH}_3}$), 31.74 ($\text{C}(\underline{\text{CH}_3})_3$), 35.07 and 35.12 ($\underline{\text{C}}(\text{CH}_3)_3$), 64.71 ($\text{HO-}\underline{\text{CH}_2\text{-CH}_3}$), 107.88, 115.06, 120.87, 121.41, 123.02, 129.90, 130.51, 140.33, 149.08 and 149.16 ($3',5'$ - and $3'',5''\text{-C}$), 197.35 ($\underline{\text{CO-CH}_3}$).

MALDI-MS (1,8,9-anthracenetriolmatrix) $m/z = 759.13$ (100%) $[\text{M}+\text{H}]^+$.

HR-FAB-MS: 759.4630 $[\text{M}+\text{H}]^+$; calc. for $\text{C}_{51}\text{H}_{59}\text{N}_4\text{O}_2 = 759.46$.

4.19 3-Acetyl-15-hydroxymethyl-10,20-bis(3,5-di-*t*-butylphenyl)porphinato zinc [45]



Zinc metallation of the above free base **44** (10 mg) could be effected in over 85 % isolated yield after the typical work-up described above.

¹H-NMR:

δ = 11.27, (s, 1H, 5-H), 9.64 (dd, ³J ~ 4 Hz, 1H), 9.52 (s, 1H, 2-H), 9.44 (d, ³J = 4.5 Hz, 1H), 9.14 (d, ³J = 4.5 Hz, 1H), 9.09 (d, ³J = 5.1 Hz, 1H), 9.05 (d, ³J = 4.8 Hz, 1H), 8.12 and 8.07 (two d, ⁴J = 1.8 Hz, 4H, 2',6'- and 2'',6''-H), 7.86 and 7.83 (two t, ⁴J = 1.8 Hz, 2H, 4'- and 4''-H), 6.72 (s, 2H, CH₂-OH), 3.15 (s, 3H, CO-CH₃), 1.58 (s, 18H, C(CH₃)₃), 1.55 (s, 18H, C(CH₃)₃). The spectrum changes with different CD₃OD amounts.

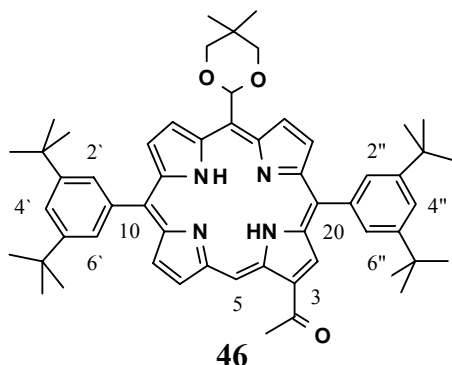
¹³C-NMR:

30.30 (CO-CH₃), 32.16 (C(CH₃)₃), 35.50 and 35.54 (C(CH₃)₃), 65.13 (CH₂-OH), 108.30, 115.48, 121.29, 121.73, 121.84, 123.44, 130.33, 130.94, 140.76, 140.50, 149.50 and 149.59 (3', 5' and 3'', 5''-C), 197.78 (CO-CH₃).

MALDI-MS (1,8,9-anthracenetriol matrix): 820.02 (100%) [M]⁺.

HR-FAB-MS: 821.3759 [M+H]⁺, Calc. for C₅₁H₅₇N₄O₂Zn = 821.37.

4.20 3-Acetyl-10,20-bis(3,5-di-*tert*-butylphenyl)-15-(5,5-dimethyl-1,3-dioxan-2-yl)-porphyrin [46]



The 3-acetyl-10,20-bis(3,5-di-*tert*-butylphenyl)-15-formyl-porphyrin **43** (0.200 g, 0.26 mmol), neopentyl glycol (0.255 g, 2.44 mmol), *p*-toluenesulfonic acid (0.018 g, 0.094 mmol) and toluene (140 mL) and were placed in a 250 mL flask equipped with a Dean-Stark trap and a reflux condenser and the mixture was heated to reflux for 65 min. The reaction mixture was then cooled and was washed with a saturated NaHCO₃ solution and then with water. The organic layer then was dried over Na₂SO₄. After solvent evaporation **46** is obtained as a purple solid (0.215 mg, 96 %)

¹H NMR:

δ = 11.30 (s, 1H, 5-H), 10.10 (d, 1H, ³J = 4.8 Hz, 13-H), 9.80 (d, 1H, ³J = 4.8 Hz, 17-H), 9.45 (d, 1H, ³J = 4.8 Hz, 7-H), 9.40 (s, 1H, 2-H), 9.11 (d, 1H, ³J = 5.1 Hz, 12-H), 9.01 (d, 1H, ³J = 4.5 Hz, 18-H), 8.94 (d, 1H, ³J = 4.8 Hz, 8-H), 8.10 (d, 2H, ⁴J = 1.8 Hz, 2', 6'), 8.06 (d, 2H, ⁴J = 1.8 Hz, 2'', 6''), 7.97 (s, 1H, 2-H_{acetal}), 7.87 (t, 1H, ⁴J = 1.5 Hz, 4'), 7.83 (t, 1H, ⁴J = 1.8 Hz, 4''H), 4.33 (s, 4H, OCH₂_{acetal}), 3.13 (s, 3H, CO-CH₃), 1.93 (s, 3H, CH₃_{eq-acetal}), 1.12 (s, 3H, CH₃_{ax-acetal}), -2.83 (s, 2H, NH).

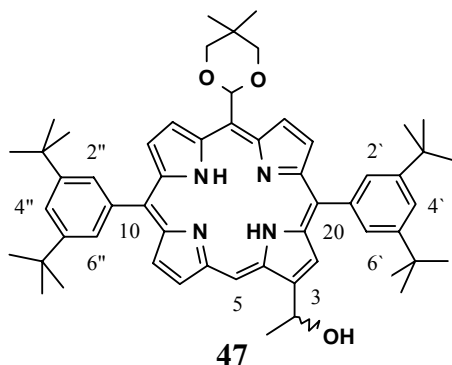
¹³C-NMR:

δ = 22.58, 25.06, 29.69, 29.87, 30.94 (CO-CH₃), 31.76 (C(CH₃)₃), 35.08 and 35.12 (C(CH₃)₃), 106.43, 108.23, 112.97, 120.77, 121.21, 121.31, 122.94, 129.87, 130.42, 140.70, 140.73, 148.96 and 149.01 (3', 5' and 3'', 5''-C), 197.32 (CO-CH₃).

UV-Vis (CH₂Cl₂), λ_{\max} (nm): 428, 534, 576, 603, 661.

HR-FAB-MS: found m/z = 843.5195 [M+H]⁺; calc. for C₅₆H₆₇N₄O₃ = 843.5213

4.21 10,20-Bis(3,5-di-*tert*-butylphenyl)-15-(5,5-dimethyl-1,3-dioxan-2-yl)-3(hydroxyethyl)-porphyrin [47]



Compound **46** (160 mg, 0.1897 mmol), NaBH₄ (143.5mg, 0.379 mmol), methanol (12 mL) and dichloromethane (25 mL) were stirred in a 100 mL single neck flask at r.t. for 19 hrs. The reaction mixture was then washed with brine twice and dried over Na₂SO₄ after which the solvents were evaporated to leave a crude product which was then purified by column chromatography (SiO₂, eluted with CH₂Cl₂) to give 115 mg (72 %) of pure purple compound

¹H NMR:

δ = 10.42 (s, 1H, 5-H), 10.02 and 9.97 (two d, 2H, ³J = 4.5 Hz, 1H, 13- and 17-H), 9.34 (d, ³J = 4.5Hz, 1H, 7-H), 9.03 (two partially overlapping d, 3H, 12, 18 and 8-H), 8.91 (s, 1H, 2-H), 8.09 and 8.08 (two d, 4H, ⁴J = 1.8 Hz, 4H, 2', 6' and 2'', 6''-H), 8.03 (s, 1H, 2-H_{acetal}), 7.84 (t, 2H, ⁴J = 1.8 Hz, 4', 4''-H), 6.65 (quintet, 1H, HO-CH-CH₃), 4.34 (s, 4H, CH₂-acetal), 2.59 (d, ³J = 4.5 Hz, 1H, OH), 2.26 (d, ³J = 6.3 Hz, 3H, 6.6Hz, HO-CH-CH₃), 1.95 (s, 3H, CH₃ *eq*-acetal), 1.57 (two s, 2x18H, C(CH₃)₃), 1.13 (s, 3H, CH₃ *ax*-acetal), -3.05 (s, 2H, N-H).

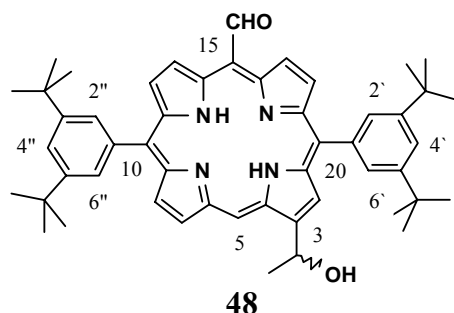
¹³C-NMR:

δ = 22.60, 25.07, 25.86, 29.69, 30.95 (CO-CH₃), 31.78 (C(CH₃)₃), 35.08 (C(CH₃)₃), 65.63 (CH₃-CH-OH), 103.21, 106.64, 112.10, 120.05, 120.95, 121.10, 121.25, 129.90, 130.01, 130.07, 141.01, 141.07, 148.80 and 148.82 (3', 5' and 3'', 5''-C).

UV-Vis (CH₂Cl₂), λ_{\max} (nm): 414, 510, 573, and other two less intense Q bands.

HR-FAB-MS: m/z = 845.5357 [M+H]⁺; calc. for C₅₆H₆₉N₄O₃ = 845.5370

4.22 10,20- Bis(3,5-di-*tert*-butylphenyl)-15-formyl-3-(1-hydroxyethyl)-porphyrin [48]



Aqueous HCl (20 mL, 0.5M) was added to a solution of compound **47** (100 mg, 0.118 mmol) in 1,4-dioxane (30 mL) under inert atmosphere and stirred at r.t. for 17 hrs. After completion of the reaction (TLC monitoring), the mixture was washed with brine and neutralized with a saturated aqueous NaHCO₃ solution. The organic layer was extracted with dichloromethane and dried over Na₂SO₄. The solvent was evaporated to get a crude product which after column chromatography on SiO₂ eluted with CH₂Cl₂ afforded 83.4 mg, (94 % yield) of green compound **48**.

¹H NMR:

δ = 12.58 (s, 1H, 15-CHO), 10.49 (s, 1H, 5-H), 10.08 (d, 1H, ³J = 4.5 Hz, 2H, 13-H), 10.04 (d, ³J = 4.5 Hz, 2H, 17-H), 9.31 (d, ³J = 4.8 Hz, 1H, 7-H), 9.09 (two d, 2H, ³J = 4.5 Hz, 12-H and 18-H), 8.93 (d, ³J = 4.5 Hz, 1H, 8-H), 8.82 (s, 1H, 2-H), 8.08 (m, 4H, 2', 6' and 2'', 6''-H), 7.88 (t, ⁴J = 1.8 Hz, 2H, 4', 4''-H), 6.59 (q, ³J = 6.3 Hz, 1H, HO-CH-CH₃), 2.58 (s, 1H, OH), 2.24 (d, ³J = 6.6 Hz, 3H, HO-CH-CH₃), 1.56 (m, 36H, C(CH₃)₃), -2.36 (s, 2H, NH).

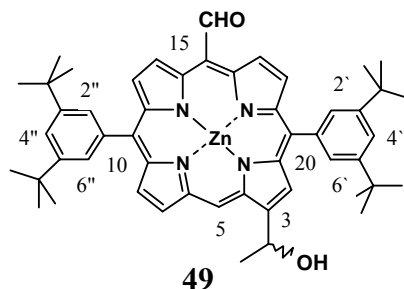
¹³C-NMR:

δ = 25.94 (CH₃-CH-OH), 31.72 (C(CH₃)₃), 35.09 (C(CH₃)₃), 65.56(CH₃-CH-OH), 108.04, 121.48, 129.77, 129.91, 129.95, 140.20, 140.26, 149.11 and 149.13 (3', 5' and 3'', 5''-C), 195.35 (CHO)

UV-Vis (CH₂Cl₂), λ_{\max} (nm): 424, 525, 565, 596, 653.

HR-FAB-MS: found m/z = 759.4653 [M+H]⁺, calc. for. C₅₁H₅₉N₄O₂ = 759.4638

4.23 10,20- Bis(3,5-di-*tert*-butylphenyl)-15-formyl-3-(1-hydroxyethyl)-porphinato-zinc [49]



Zinc acetate (43 mg, 0.023 mmol) was added to a solution of compound **48** (25 mg, 0.0329 mmol) in CHCl_3 (20 mL) and MeOH (12 mL) and the reaction mixture was stirred at r.t. for 3 hrs, under inert atmosphere. The reaction mixture was then washed with brine and extracted with dichloromethane. The organic layer was dried over Na_2SO_4 and was evaporated to leave the green compound **49** in high purity and yield (25.2 mg, 93 %).

^1H NMR:

δ = 12.54 (s, 1H, 15-CHO), 10.37 (s, 1H, 5-H), 10.02 and 10.01 (two d, 2H, $^3J = 4.9$ Hz, 13- and 17-H), 9.25 (d, 1H, $^3J = 4.5$ Hz, 7-H), 9.05 and 9.03 (two d, 2H, $J = 4.7$ and 4.9 Hz, 12- and 18-H), 8.89 (d, 1H, $J = 4.3$ Hz, 8-H), 8.79 (s, 1H, 2-H), 8.01 (m, 4H, 2', 6', 2'', 6''-H), 7.57 (t, 2H, $^4J = 1.8$ Hz, 4', 4''-H), 6.55 (q, 1H, $^3J = 6.5$ Hz, HO-CH-CH₃), 3.40 (s, 1H, OH), 2.20 (d, 3H, $^3J = 6.4$, Hz, HO-CH-CH₃), 1.53 (two s, 36H, C(CH₃)₃).

UV-Vis ($\text{CH}_2\text{Cl}_2 + n$ -heptane), λ_{max} , (nm): 638, 594, 480, 420. After methanol addition: 607, 563, 428.

UV-Vis (CH_2Cl_2 , 0.23 mM), λ_{max} , [$\lg(\lambda_{\text{max}})$]: 600 (4.19), 557 (4.05), 424 (5.47)

HR-FAB-MS: found $m/z = 821.3782$, $[\text{M}+\text{H}]^+$; calc. for $\text{C}_{51}\text{H}_{56}\text{N}_4\text{O}_2\text{Zn} = 821.3773$

4.24 General procedure for the synthesis of 3,17-di-acyl-10,20-bis(3,5-di-*t*-butylphenyl)porphinato copper [50-57]

Diacylation of the copper porphyrin **28** (300 mg, 0.40 mmol) was performed by dissolving it in carbon disulfide (10 mL) in a 100 mL three-necked flask equipped with a rubber septum, nitrogen bubbler and thermometer then adding at 2-4°C the corresponding long chain acyl chlorides (3.5 equivalents, 1.4 mol) and then the reaction mixture was allowed to stir for 2-3 min followed by addition in one shot of anhydrous aluminium chloride (240 mg, 1.80 mmol, 4.5 equivalents). After stirring at 2-4 °C for 4-6 min ice cold water(10 mL) was added to the reaction mixture and stirred afterwards for another 1hr. After extraction into dichloromethane and washing with brine twice, the mixture was washed with aqueous sodium hydrogencarbonate and then again with brine. The organic layers were dried on sodium sulfate and after removal of the solvents in vacuum the crude products were obtained. [**30, 50-57**]. When the reaction period was prolonged more than 6 minutes to 1 hr, some 3,13-diacyl isomers were also obtained in 2-5% yields.

4.24.1 3,17-Diacyl-10,20-bis(3,5-di-*t*-butylphenyl)-21,23*H*-porphyrin [58-65]

The above crude products of the corresponding long chain copper porphyrins [50-57] were demetallated by using a 10 mL degassed mixture of trifluoroacetic and sulfuric acids (1:1 v/v) by stirring for overnight at room temperature. The usual work-up consists in pouring on ice and extraction into dichloromethane, washing with brine, neutralization with aqueous sodium hydrogencarbonate and again washing with brine. After drying on sodium sulfate and evaporation to dryness the solid products were obtained. Demetallation yields gave consistently yields in the range of 60-80%. Subsequent careful column chromatography on silica gel eluted first with dichloromethane : *n*-hexane (1:1.v/v) gives the corresponding monoacylated products as the firstly eluted fraction and the second fraction of respective title porphyrins [58-65]. This is summarized in Table 4.1.

Comp. No.	Acyl chlorides	Molecular Formula	Reaction Time (min)	Yields
58	Butyroyl Chloride	CH ₃ -(CH ₂) ₂ -CO-Cl	5	60 %
59	Valeroyl Chloride	CH ₃ -(CH ₂) ₃ -CO-Cl	5	63 %
60	Hexanoyl Chloride	CH ₃ -(CH ₂) ₄ -CO-Cl	4	68 %
61	Heptanoyl chloride	CH ₃ -(CH ₂) ₅ -CO-Cl	5	76 %
62	Octanoyl Chloride	CH ₃ -(CH ₂) ₆ -CO-Cl	6	72 %
63	Lauroyl Chloride	CH ₃ -(CH ₂) ₁₀ -CO-Cl	4	69 %
64	Myristoyl Chloride	CH ₃ -(CH ₂) ₁₂ -CO-Cl	4	78 %
65	Palmitoyl Chloride	CH ₃ -(CH ₂) ₁₄ -CO-Cl	4	79 %

Table: 4.1

4.25 General procedure for the synthesis of 3-acyl-17-(1-hydroxyacyl)-10,20-bis(3,5-di-*t*-butylphenyl)-21,23*H*-porphyrin [66-73]

Monoreduction of the corresponding 3,17-diacyl compound (1 eq) was effected by dissolving it in 25 mL dichloromethane and 5 mL methanol and adding rapidly sodium borohydride (2 eq). After stirring for 15-150 min. at room temperature the mixture was washed with brine, and the organic layer was dried on anhydrous sodium sulfate and chromatographed on silica gel eluted with dichloromethane. Recovered starting material (16-47%) is eluted as the first fraction. The second band contains the monoreduced product (38-75%) [66-73] and a final band with lower *R_f* consists of a mixture of the racemic and *meso*-dihydroxyalkyl porphyrin (mg). The latter could be separated on a second column.

Comp. No.	3,17-diacyl BTBPP	ReactionTime (min)	Yields
66	3,17-dibutyroyl BTBPP	60	52 %
67	3,17-divaleroyl BTBPP	15	75 %
68	3,17-dihexanoylBTBPP	15	52 %
69	3,17-diheptanoyl BTBPP	20	38 %
70	3,17-dioctanoyl BTBPP	25	60 %
71	3,17-dilauroyl BTBPP	30	50 %
72	3,17-myristoyl BTBPP	30	52 %
73	3,17-palmitoyl BTBPP	40	41 %

Table: 4.2

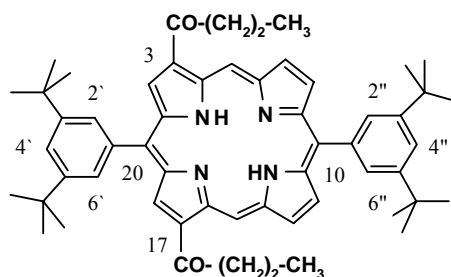
4.26 General procedure for the synthesis of 3-acyl-17-(1-hydroxyacyl)-10,20-bis(3,5-di-*t*-butylphenyl)porphinato zinc [74-81]

Zinc metallation of the above free base [66–73] (1 eq) with excess zinc acetate in a 28 mL chloroform/methanol mixture (2:1, v/v) after stirring for overnight at room temperature the reaction was driven to completion (monitoring by UV-Vis). Washing with aqueous sodium hydrogen carbonate followed by washing with brine, drying over anhydrous sodium sulfate and evaporation of the solvent produced in quantitative yield the desired product. After column chromatography on silica gel with 3% methanol in dichloromethane, the eluent was washed twice with brine in order to remove the residual methanol. Recrystallization from dichloromethane and *n*-hexane followed by centrifugation and drying overnight in vacuum (10^{-3} Torr) produced samples [74–81] which self-assembled in nonpolar solvents.

Comp. No.	3,17-Ketol BTBPP	Reaction Time (hr)	Yields
74	3,17-butyroyl	16	77 %
75	3,17-valeroyl	15	97 %
76	3,17-hexanoyl	15	93 %
77	3,17-heptanoyl	17	89 %
78	3,17-octanoyl	14	96 %
79	3,17-lauroyl	15	83 %
80	3,17-myristoyl	16	96 %
81	3,17-palmitoyl	17	92 %

Table: 4.3

4.27 3,17-Dibutyroyl-10,20-bis(3,5-di-*t*-butylphenyl)-21,23*H*-porphyrin [58]



58

$R_f = 0.74$ (CH_2Cl_2 : n-Hexane, 1:1, v/v).

$^1\text{H-NMR}$:

$\delta = 11.33$ (s, 2H, 5,15-H), 9.57 (s, 2H, 2,18-H), 9.41 (d, $^3J = 4.8$ Hz, 2H, 7,13-H), 9.03 (d, $^3J = 4.5$ Hz, 2H, 8,12-H), 8.20 and 8.10 (two d, $^4J = 1.8$ Hz, 2H each, 2',6'- and 2'',6''-H), 7.94 and 7.85 (two t, $^4J = 1.8$ Hz, 1H each, 4'- and 4''-H), 3.59 (t, $^3J = 7.2$ Hz, 4H, $\text{CO-CH}_2\text{-CH}_2\text{-CH}_3$), 2.19 (sextet, 4H, $\text{CO-CH}_2\text{-CH}_2\text{-CH}_3$), 1.65 and 1.59 (two s, 18 H each, $\text{C}(\text{CH}_3)_3$), 1.25 (t, $^3J = 4.2$ Hz, 6H, CH_3), -2.32 (s, 2H, NH).

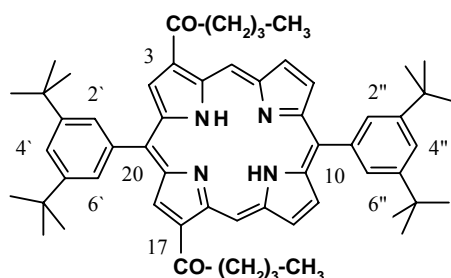
MALDI-MS: 826.8

HR-FAB-MS: $[\text{M}+\text{H}]^+ 827.5273$; calc. for $\text{C}_{56}\text{H}_{66}\text{N}_4\text{O}_2 = 826.5185$

$^{13}\text{C-NMR}$: [58]

$\delta = 14.20$ ($\text{CO-CH}_2\text{-CH}_2\text{-CH}_3$), 18.54 ($\text{CO-CH}_2\text{-CH}_2\text{-CH}_3$), 31.74 ($\text{C}(\text{CH}_3)_3$), 35.09 and 35.19 ($\text{C}(\text{CH}_3)_3$), 43.91, ($\text{CO-CH}_2\text{-CH}_2\text{-CH}_3$), 107.09 (5 and 15-C), 120.30, 121.32, 121.51 (10 and 20 - C), 124.28, 126.38, 127.14, 130.09 (2',6'-C), 131.20, 131.94, 134.15, 135.99, 136.69, 139.67, 139.76, 149.35 and 149.53 (3', 5' and 3'', 5''-C), 200.02 ($\text{CO-CH}_2\text{-CH}_2\text{-CH}_3$).

4.28 3,17-Divaleroyl-10,20-bis(3,5-di-*t*-butylphenyl)-21,23*H*-porphyrin [59]



59

$R_f = 0.79$ (CH_2Cl_2 : n-Hexane, 1:1, v/v).

¹H-NMR:

δ = 11.33 (s, 2H, 5,15-H), 9.58 (s, 2H, 2,18-H), 9.41 (d, ³J = 4.8 Hz, 2H, 7,13-H), 9.04 (d, ³J = 4.8 Hz, 2H, 8,12-H), 8.21 and 8.10 (two d, ⁴J = 1.8 Hz, 2H each, 2',6'- and 2'',6''-H), 7.95 and 7.86 (two t, ⁴J = 1.8 Hz, 1H each, 4'- and 4''-H), 3.61 (t, ³J = 7.5 Hz, 4H, CO-CH₂-CH₂-CH₂-CH₃), 2.15 (m, 8H, CO-CH₂-CH₂-CH₂-CH₃), 1.66 and 1.59 (two s, 18 H each, C(CH₃)₃), 1.12 (t, 6H, CH₃), -2.67 and -2.91 (two s, 2H, NH).

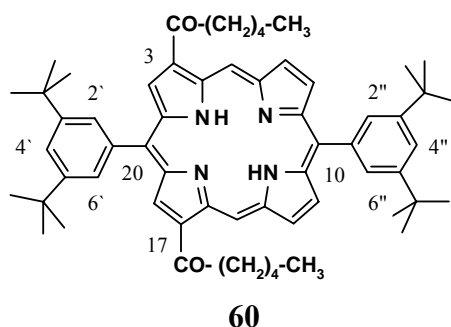
¹³C-NMR:

δ = 14.08 (CO-(CH₂)₃-CH₃), 22.76 (CO-CH₂-CH₂-CH₂-CH₃), 27.23, (CO-CH₂-CH₂-CH₂-CH₃), 31.75 (C(CH₃)₃), 35.10 and 35.19 (C(CH₃)₃), 41.74 (CO-CH₂-CH₂-CH₂-CH₃), 107.10 (5 and 15-C) 120.31, 121.32, 121.52, (10,20-C) 124.27, 130.00, 130.44, 130.70, (2',6'-C), 131.16, 131.91, 134.10, 135.93, 136.69, 139.69, 139.77, 149.36, 149.46, 149.55 (3', 5' and 3'', 5''-C), 200.13 (CO-CH₂-CH₂-CH₂-CH₃)

MALDI-MS: 854.9

HR-FAB-MS: [M+H]⁺: 855.5588; calc. for C₅₈H₇₀N₄O₂ = 854.5498

4.29 3,17-Di-hexanoyl-10,20-bis(3,5-di-*t*-butylphenyl)-21,23H-porphyrin [60]



R_f = 0.86 (CH₂Cl₂ : n-Hexane, 1:1,v/v).

¹H-NMR:

δ = 11.30 (s, 2H, 5,15-H), 9.54 (s, 2H, 2,18-H), 9.38 (d, ³J = 4.8 Hz, 2H, 7,13-H), 9.00 (d, ³J = 4.5 Hz, 2H, 8,12-H), 8.18 and 8.07 (two d, ⁴J = 2.1 and 1.8 Hz, 2H each, 2', 6'- and 2'', 6''-H), 7.92 and 7.83 (two t, ⁴J = 1.8 Hz, 1H each, 4'- and 4''-H), 3.57 (t, ³J = 7.5 Hz, 4H, CO-CH₂-CH₂-CH₂-CH₂-CH₃), 2.14 (m, 4H, CO-CH₂-CH₂-CH₂-CH₂-CH₃), 1.48-1.70 (m, 8H, CO-CH₂-CH₂-CH₂-CH₂-CH₃), 1.63 and 1.59 (two s, 18 H each, C(CH₃)₃), 1.00 (t, 6H, CH₃), -2.37 (broad s, 2H, NH)

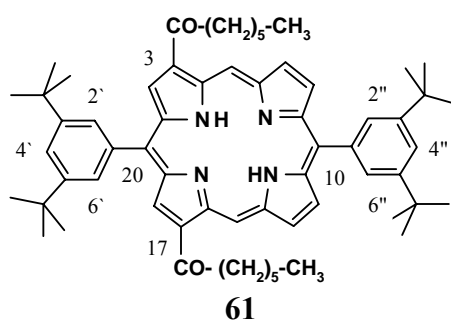
¹³C-NMR:

$\delta = 14.05$ (CO-(CH₂)₄-CH₃), 31.74 (C(CH₃)₃), 35.10 and 35.19 (C(CH₃)₃), 41.97 (CO-CH₂-(CH₂)₃-CH₃), 107.10 (5 and 15-C), 120.33, 121.32 and 121.52 (10 and 20-C), 124.27, 130.00 (2',6'-C), 131.14, 131.93, 134.11, 135.95, 136.69, 139.69, 139.78, 149.36 and 149.55 (3', 5' and 3'', 5''-C), 200.16 (CO-(CH₂)₄-CH₃),

MALDI-MS: 883.3

HR-FAB-MS: [M+H]⁺.883.5878; calc. for C₆₀H₇₄N₄O₂ = 882.5811

4.30 3,17-Diheptanoyl-10,20-bis(3,5-di-*t*-butylphenyl)-21,23*H*-porphyrin [61]



$R_f = 0.63$ (CH₂Cl₂ : n-Hexane, 1:1, v/v).

¹H-NMR:

$\delta = 11, 34$ (s, 2H, 5,15-H), 9.59 (s, 2H, 2,18-H), 9.42 (d, ³J = 4.5 Hz, 2H, 7,13-H), 9.05 (d, ³J = 4.5 Hz, 2H, 8,12-H), 8.23 and 8.12 (two d, ⁴J = 1.8 Hz, 2H each, 2', 6'- and 2'', 6''-H), 7.97 and 7.87 (two t, ⁴J = 1.2 Hz, 1H each, 4'- and 4''-H), 3.61 (t, 4H, CO-CH₂-CH₂-CH₂-CH₂-CH₂-CH₃), 2.17 (m, 4H, CO-CH₂-CH₂-CH₂-CH₂-CH₂-CH₃), 1.68-1.44 (m, 12H, CO-CH₂-CH₂-CH₂-CH₂-CH₂-CH₃) 1.68 and 1.61 (two s, 18 H each, C(CH₃)₃), 0.99 (t, 6H, CH₃), -2.31 (broad s, 2H, NH).

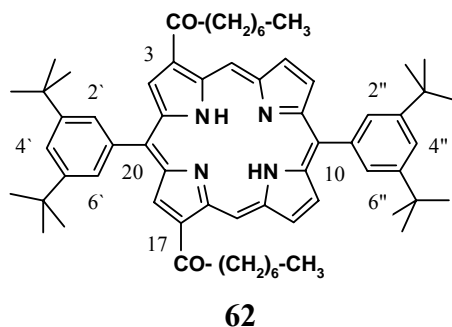
¹³C-NMR:

$\delta = 14.15$ (CO-(CH₂)₅-CH₃), 31.76 (C(CH₃)₃), 35.10 and 35.20 (C(CH₃)₃), 42.02 (CO-CH₂-(CH₂)₄-CH₃), 107.11, 120.34, 121.34, 121.52, 124.28, 128.39, 130.01, 131.19, 131.93, 134.13, 135.94, 136.72, 139.70, 149.36 and 149.56 (3', 5' and 3'', 5''-C), 200.46 (CO-(CH₂)₅-CH₃).

MALDI-MS: 913.2

HR-FAB-MS: [M+H]⁺.913.6345; calc. for C₆₂H₇₈N₄O₂ = 912.6281

4.31 3,17-Di octanoyl-10,20-bis(3,5-di-*t*-butylphenyl)-21,23*H*-porphyrin [62]



$R_f = 0.86$ (CH_2Cl_2 : n-Hexane, 1:1, v/v).

$^1\text{H-NMR}$:

$\delta = 11.30$ (s, 2H, 5,15-H), 9.54 (s, 2H, 2,18-H), 9.37 (d, $^3J = 4.8$ Hz, 2H, 7,13-H), 9.00 (d, $^3J = 4.5$ Hz, 2H, 8,12-H), 8.18 and 8.07 (two d, $^4J = 1.8$ Hz, 2H each, 2',6'- and 2'',6''-H), 7.92 and 7.83 (two t, $^4J = 1.8$ Hz, 1H each, 4'- and 4''-H), 3.57 (t, $^3J = 7.5$ Hz, 4H, $\text{CO-CH}_2\text{-CH}_2\text{-CH}_2\text{-CH}_2\text{-CH}_2\text{-CH}_2\text{-CH}_3$), 2.13 (m, 4H, $\text{CO-CH}_2\text{-CH}_2\text{-CH}_2\text{-CH}_2\text{-CH}_2\text{-CH}_2\text{-CH}_3$), 1.35 - 1.70 (m, 16H, $\text{CO-CH}_2\text{-CH}_2\text{-CH}_2\text{-CH}_2\text{-CH}_2\text{-CH}_2\text{-CH}_3$) 1.65 and 1.57 (two s, 18 H each, $\text{C}(\text{CH}_3)_3$), 1.25(t, 6H, CH_3), -2-36 (s, 2H, NH).

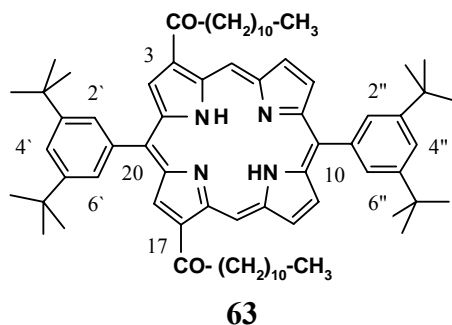
$^{13}\text{C-NMR}$:

$\delta = 14.15$ ($\text{CO-}(\text{CH}_2)_6\text{-CH}_3$), 31.76 ($\text{C}(\text{CH}_3)_3$), 35.10 and 35.20 ($\text{C}(\text{CH}_3)_3$), 42.03 ($\text{CO-CH}_2\text{-}(\text{CH}_2)_5\text{-CH}_3$), 107.12, 120.33, 124.28, 130.01, 131.19, 139.71, 139.81, 136.74, 135.93, 134.13, 131.95, 149.36 and 149.56 (3',5'- and 3'',5''-C), 200.14 ($\text{CO-}(\text{CH}_2)_6\text{-CH}_3$)

MALDI-MS: 939.

HR-FAB-MS: $[\text{M}+\text{H}]^+ .939.6503$; calc. for $\text{C}_{64}\text{H}_{82}\text{N}_4\text{O}_2$: 938.6437.

4.32 3,17-Dilauroyl-10,20-bis(3,5-di-*t*-butylphenyl)-21,23*H*-porphyrin [63]



$R_f = 0.88$ (CH_2Cl_2 : n-Hexane, 1:1, v/v).

$^1\text{H-NMR}$:

$\delta = 11.38$ (s, 2H, 5,15-H), 9.63 (s, 2H, 2,18-H), 9.46 (d, $^3J = 4.5$ Hz, 2H, 7,13-H), 9.09 (d, $^3J = 4.5$ Hz, 2H, 8,12-H), 8.27 and 8.16 (two d, $^4J = 1.8$ Hz, 2H each, 2',6'- and 2'',6''-H), 8.00 and 7.90 (two t, $^4J = 1.5$ & 1.8 Hz, 1H each, 4'- and 4''-H), 3.64 (t, $^3J = 7.2$ Hz, 4H, CO-CH₂-CH₂-CH₂-CH₂-CH₂-CH₂-CH₂-CH₂-CH₂-CH₂-CH₃), 2.19 (m, 4H, CO-CH₂-CH₂-CH₂-CH₂-CH₂-CH₂-CH₂-CH₂-CH₂-CH₃), 1.33-1.44 (broad m, 32H, CO-CH₂-CH₂-CH₂-CH₂-CH₂-CH₂-CH₂-CH₂-CH₂-CH₃), 1.65 and 1.59 (two s, 18 H each, C(CH₃)₃), 0.93(t, 6H, CH₃), -2.27 (s, 2H, NH).

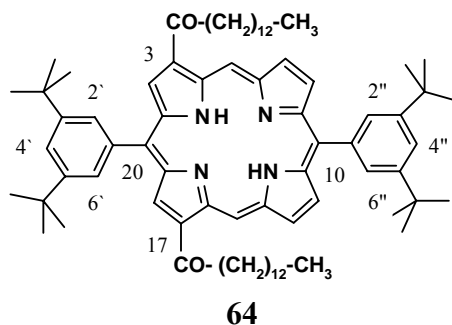
$^{13}\text{C-NMR}$:

$\delta = 14.52$ (CO-(CH₂)₁₀-CH₃), 31.77 (C(CH₃)₃), 35.11 (C(CH₃)₃), 42.39 (CO-CH₂-(CH₂)₉-CH₃), 107.49, 111.95, 121.68, 121.87, 124.65, 126.75, 127.48, 130.40, 131.62, 132.30, 134.51, 136.33, 137.05, 140.73, 140.18, 149.59, 149.36 and 149.92(3',5'- and 3'',5''-C), 152.37, 200.14 (CO-(CH₂)₁₀-CH₃)

MALDI-MS: 1051.3

HR-FAB-MS: $[\text{M}+\text{H}]^+$.1051.4, calc. for $\text{C}_{72}\text{H}_{98}\text{N}_4\text{O}_2 = 1050.7689$

4.33 3,17-Dimyristoyl-10,20-bis(3,5-di-*t*-butylphenyl)-21,23*H*-porphyrin [64]



$R_f = 0.90$ (CH_2Cl_2 : n-Hexane, 1:1, v/v).

$^1\text{H-NMR}$:

$\delta = 11.29$ (s, 2H, 5,15-H), 9.54 (s, 2H, 2,18-H), 9.37 (d, $^3J = 4.8$ Hz, 2H, 7,13-H), 8.99 (d, $^3J = 5.1$ Hz, 2H, 8,12-H), 8.17 and 8.06 (two d, $^4J = 1.5$ Hz, 2H each, 2',6'- and 2'',6''-H), 7.92 and 7.83 (two t, $^4J = 1.8$ Hz, 1H each, 4'- and 4''-H), 3.57 (t, $^3J = 7.2$ Hz, 4H, $\text{CO-CH}_2\text{-(CH}_2\text{)}_{11}\text{-CH}_3$), 2.13 (m, 4H, $\text{CO-CH}_2\text{-CH}_2\text{-(CH}_2\text{)}_{10}\text{-CH}_3$), 1.25-1.32 (44 H broad s, $\text{CO-CH}_2\text{-(CH}_2\text{)}_{11}\text{-CH}_3$) 1.63 and 1.56 (two s, 18 H each, $\text{C(CH}_3\text{)}_3$), 0.86 (t, 6H, CH_3), -2.37 (s, 2H, NH).

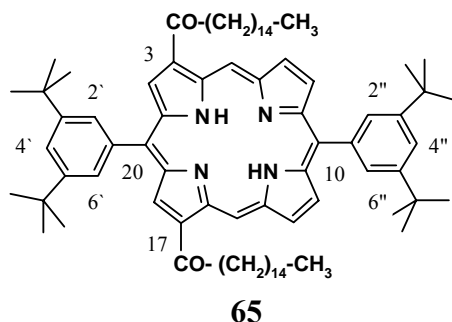
$^{13}\text{C-NMR}$:

$\delta = 14.16$ ($\text{CO-CH}_2\text{-CH}_3$), 31.77 ($\text{C(CH}_3\text{)}_3$), 31.93, 35.11 and 35.22 ($\text{C(CH}_3\text{)}_3$), 42.03, ($\text{CO-CH}_2\text{-(CH}_2\text{)}_{11}\text{-CH}_3$), 107.13, 120.33, 121.33, 121.52, 124.28, 126.39, 128.80, 130.04, 131.27, 131.93, 134.15, 135.95, 136.69, 139.71, 139.82, 149.36 and 149.56 ($3',5'$ - and $3'',5''$ -C), 200.16 ($\text{CO-CH}_2\text{-CH}_3$).

MALDI-MS: 1107.4

HR-FAB-MS: $[\text{M}+\text{H}]^+$; calc. for $\text{C}_{76}\text{H}_{106}\text{N}_4\text{O}_2 = 1106.8315$

4.34 3,17-Dipalmitoyl-10,20-bis(3,5-di-*t*-butylphenyl)-21,23*H*-porphyrin [65]



$R_f = 0.92$ (CH_2Cl_2 : n-Hexane, 1:1, v/v).

$^1\text{H-NMR}$:

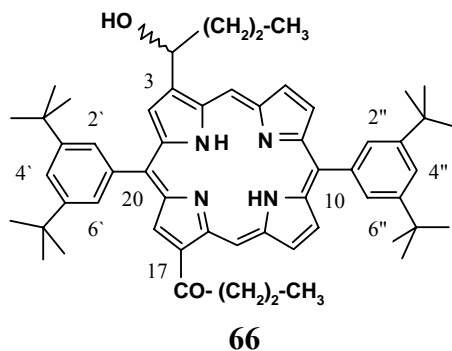
$\delta = 11.34$ (s, 2H, 5,15-H), 9.59 (s, 2H, 2,18-H), 9.42 (d, $^3J = 4.5$ Hz, 2H, 7,13-H), 9.05 (d, $^3J = 4.5$ Hz, 2H, 8,12-H), 8.23 and 8.12 (two d, $^4J = 1.5$ and 1.8 Hz, 2H each, 2',6'- and 2'',6''-H), 7.97 and 7.87 (two t, $^4J = 1.8$ Hz, 1H each, 4'- and 4''-H), 3.61 (t, $^3J = 7.5$ Hz, 4H, $\text{CO-CH}_2\text{-(CH}_2\text{)}_{13}\text{-CH}_3$), 2.19 (m, 4H, $\text{CO-CH}_2\text{-CH}_2\text{-(CH}_2\text{)}_{12}\text{-CH}_3$), 1.21-1.39 (broad m 48H, $\text{CO-CH}_2\text{-CH}_2\text{-(CH}_2\text{)}_{12}\text{-CH}_3$), 1.68 and 1.60 (two s, 18 H each, $\text{C(CH}_3\text{)}_3$), 0.90 (t, 6H, CH_3), -2.33 (s, 2H, NH).

$^{13}\text{C-NMR}$:

$\delta = 14.11, 22.67, 25.13, 29.35, 29.63, 29.64, 29.67, 29.69, 31.74$ ($\text{C(CH}_3\text{)}_3$), 31.75, 31.90, 35.08 and 35.19 ($\text{C(CH}_3\text{)}_3$), 42.38, 107.07, 119.88, 120.31, 129.99, 131.84, 134.13, 139.66, 139.78, 149.34 and 149.54 (3',5'- and 3'',5''-C), 200.17 ($\text{CO-(CH}_2\text{)}_{14}\text{-CH}_3$).

MALDI-MS: 1163.5; calc. for $\text{C}_{80}\text{H}_{114}\text{N}_4\text{O}_2 = 1162.8941$

4.35 3-Butyroyl-17-(1-hydroxybutyroyl)-10,20-bis(3,5-di-*t*-butylphenyl)-21,23*H*-porphyrin [66]



$R_f = 0.46$ (CH_2Cl_2 : n-Hexane, 1:1, v/v).

¹H-NMR:

δ = 11.43 (s, 1H, 5-H), 10.36 (s, 1H, 15-H), 9.53 (s, 1H, 2-H), 9.51(d, ³J = 5.1 Hz, 1H, 7-H), 9.30 (d, ³J = 4.5 Hz, 1H, 13-H), 9.13 (overlapped d, 1H, 8-H), 9.11, (s, 1H, 18-H), 9.04 (d, ³J = 4.5 Hz, 1H, 12-H), 8.11-8.17 (m, 4H, 2',6' and 2'',6'',-H), 7.89 (t, ⁴J = 1.8 Hz, 1H, 4'-H), 7.84 (t, ⁴J = 1.8 Hz, 1H, 4''-H), 6.52 (t, ³J = 6.3 Hz, 1H, CH₃-CH₂-CH₂-CH-OH), 3.54 (t, 2H, CO-CH₂-CH₂-CH₃), 2.60 (m, 4H, CH₃-CH₂-CH₂-CH-OH), 2.16 m, ³J = 6.3 Hz, 2H, CO-CH₂-CH₂-CH₃), 1.62 and 1.61 (two s, 18 H each, C(CH₃)₃), -1.24 (t, ³J = 7.5 Hz, 3H, CO-CH₂-CH₂-CH₃), 1.15 (t, ³J = 7.5 Hz, 3H, CH₃-CH₂-CH₂-CHOH), -2.67 and -2.91 (two s, 2H, NH)

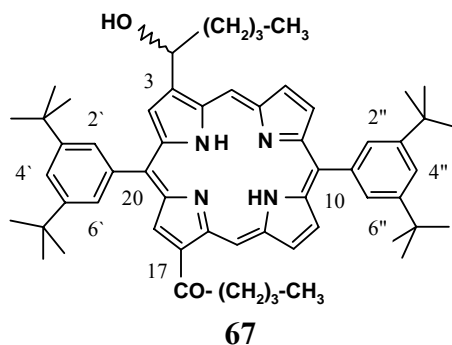
¹³C-NMR:

δ = 14.15 (CO-CH₂-CH₂-CH₃), 18.68 (HO-CH-CH₂-CH₂-CH₃), 19.60 (CO-CH₂-CH₂-CH₃), 42.01 (HO-CH-CH₂-CH₂-CH₃), 43.97 (CO-CH₂-CH₂-CH₃), 31.75 (C(CH₃)₃), 35.09 and 35.14 (C(CH₃)₃), 42.01 (HO-CH-CH₂-CH₂-CH₃), 69.33 (HO-CH-CH₂-CH₂-CH₃), 102.32, 107.61, 120.60, 121.24, 122.00, 126.57, 126.58, 129.34, 130.08, 131.43, 134.41, 134.84, 134.41, 139.21, 139.88, 139.99, 140.11, 144.89, 149.23, 149.29, 149.32, 181.17, 200.32 (CO-CH₂-CH₂-CH₃)

MALDI-MS: 829.0

HR-FAB-MS: [M+H]⁺ 429.5403; calc. for C₅₆H₆₈N₄O₂ = 828.5342

4.36 3-Valeroyl-17-(1-hydroxypentyl)-10,20-bis(3,5-di-*t*-butylphenyl)-21,23H-porphyrin [67]



R_f = 0.53 (CH₂Cl₂ : n-Hexane, 1:1, v/v).

¹H-NMR:

δ = 11.42 (s, 1H, 5-H), 10.36 (s, 1H, 15-H), 9.52 (s, 1H, 2-H), 9.50 (d, ³J = 4.8 Hz, 1H, 7-H), 9.29 (d, ³J = 4.5 Hz, 1H, 13-H), 9.12 (overlapped d, 1H, 8-H), 9.11, (s, 1H, 18-H), 9.02 (d, ³J = 4.5 Hz, 1H, 12-H), 8.14-8.17 (m 4H, 2', 6' and 2''6''-H), 7.88 (t, ⁴J = 1.8 Hz, 1H, 4'-H),

7.84 (t, $^4J = 1.8$ Hz, 1H, 4''-H), 6.51 (q, $^3J = 6.9$ Hz, 1H, CH₃-CH₂-CH₂-CH₂-CH-OH), 3.55 (t, 2H, CO-CH₂-CH₂-CH₂-CH₃), 2.62 (broad m, 4H, CH₃-CH₂-CH₂-CH₂-CH-OH), 2.11 (m, $^3J = 6.3$ Hz, 3H, CO-CH₂-CH₂-CH₂-CH₃), 1.55 (broad s, 4H, CO-CH₂-CH₂-CH₂-CH₃ and CH₃-CH₂-CH₂-CH₂-CHOH), 1.08 (t, 3H, CO-CH₂-CH₂-CH₂-CH₂-CH₃), 0.95 (CH₃-CH₂-CH₂-CH₂-CH-OH) 1.57-1.61 (d and s, 18 H each, C(CH₃)₃), -2.67 (broad s, 1H, NH), -2.91 (broad s, 1H, NH).

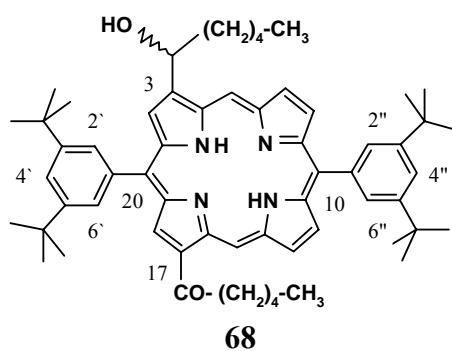
¹³C-NMR:

$\delta = 14.09$ (CO-(CH₂)₃-CH₃) and (HO-CH-CH₂-CH₂-CH₂-CH₃), 31.75 (C(CH₃)₃), 35.09 and 35.14 (C(CH₃)₃), 39.64 (CO-CH₂-CH₂-CH₂-CH₃), 41.81 (HO-CH-CH₂-CH₂-CH₂-CH₃), 69.60 (HO-CH-CH₂-CH₂-CH₂-CH₃), 102.38, 107.63, 120.60, 122.24, 126.59, 128.39, 128.57, 129.34, 130.07, 130.82, 131.42, 133.84, 134.40, 138.28, 139.22, 140.01, 140.14, 144.93, 149.24 and 149.30 (3',5'- and 3'',5''-C), 200.43 (CO-(CH₂)₃-CH₃).

MALDI-MS: 857.0

HR-FAB-MS: [M+H]⁺ 857.5743; Calc. for C₅₈H₇₂N₄O₂ = 856.5655.

4.37 3-Hexanoyl-17-(1-hydroxyhexyl)-10,20-bis(3,5-di-*t*-butylphenyl)-21,23H-porphyrin [68]



$R_f = 0.60$ (CH₂Cl₂ : n-Hexane, 1:1, v/v).

¹H-NMR:

$\delta = 11.48$ (s, 1H, 5-H), 10.36 (s, 1H, 15-H), 9.57 (s, 1H, 2-H), 9.56 (d, $^3J = 5.1$ Hz, 1H, 7-H), 9.32 (d, $^3J = 4.5$ Hz, 1H, 13-H), 9.17 (d, $^3J = 4.5$ Hz, 1H, 8-H), 9.14 (s, 1H, 18-H), 9.07 (d, $^3J = 4.5$ Hz, 1H, 12-H), 8.21 (d, $^4J = 1.8$ Hz, 2H, 2',6'-H), 8.16 (d, $^4J = 0.9$ Hz, 2H, 2'',6''-H), 7.93 (t, $^4J = 1.8$ Hz, 1H, 4'-H), 7.89 (t, $^4J = 1.5$ Hz, 1H, 4''-H), 6.74 (q, $^3J = 6.3$ Hz, 1H, CH₃-CH₂-CH₂-CH₂-CH₂-CH-OH), 3.59 (t = 6.6 Hz, 2H, CO-CH₂-(CH₂)₃-CH₃), 2.67-2.60 (m, 4H, HO-CH-CH₂-CH₂-(CH₂)₂-CH₃), 2.18 (q, 2H, CO-CH₂-(CH₂)₂-CH₂-CH₃), 1.30-1.55 (broad m,

6H, CO-(CH₂)-CH₂-CH₂-CH₂-CH₃ & HO-CH-(CH₂)₂-CH₂-CH₂-CH₃) 1.66 and 1.62 (two s, 18 H each, C(CH₃)₃), -2.63 (broad s, 1H, NH), -2.89 (broad s, 1H, NH).

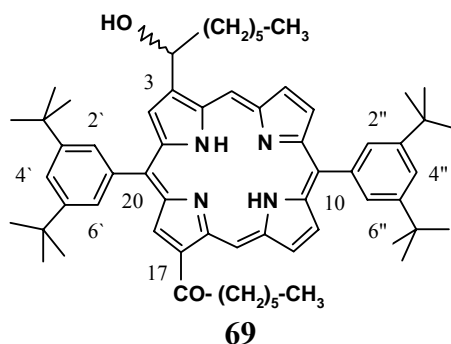
¹³C-NMR:

δ = 14.05 (CO-(CH₂)₄-CH₃), 31.76, (C(CH₃)₃), 35.10 and 35.14, (C(CH₃)₃), 39.88 (HO-CH-CH₂-CH₂-CH₂-CH₂-CH₃), 42.04 (CO-CH₂-CH₂-CH₂-CH₂-CH₃), 69.59, (HO-CH-CH₂-CH₂-CH₂-CH₂-CH₃), 120.60, 121.24, 130.07, 130.82, 140.01, 140.14, 149.24 and 149.30 (3',5'- and 3'',5''-C), 200.43 (CO-(CH₂)₄-CH₃).

MALDI-MS: 885.1

HR-FAB-MS: [M+H]⁺ 885.6033; calc. for C₆₀H₇₆N₄O₂ = 884.5958

4.38 3-Heptanoyl-17-(1-hydroxyheptyl)-10,20-bis(3,5-di-*t*-butylphenyl)-21,23H-porphyrin [69]



R_f = 0.63 (CH₂Cl₂ : n-Hexane, 1:1, v/v).

¹H-NMR:

δ = 11.43 (s, 1H, 5-H), 10.36 (s, 1H, 15-H), 9.53 (s, 1H, 2-H), 9.51 (d, ³J = 4.8 Hz, 1H, 7-H), 9.30 (d, ³J = 4.5 Hz, 1H, 13-H), 9.13 (overlapped d, 1H, 8-H), 9.12, (s, 1H, 18-H), 9.03 (d, ³J = 4.5 Hz, 1H, 12-H), 8.11-8.17 (m, 4H, 2',6'-H and 2'',6'' -H), 7.89 (t, ⁴J = 1.8 Hz, 1H, 4'-H), 7.85 (t, ⁴J = 1.8 Hz, 1H, 4''-H), 6.74 (q, ³J = 6.6 Hz, 1H, CH₃-CH₂-CH₂-CH₂-CH₂-CH₂-CH₂-OH), 3.55 (t = 7.2 Hz, 2H, CO-CH₂ (CH₂)₄-CH₃), 2.63-2.60 (broad m, 4H, HO-CH-CH₂-CH₂-CH₂-CH₂-CH₃), 2.13 (q, 2H, CO-CH₂ (CH₂)₃-CH₂-CH₃), 1.62 and 1.58 (two s, 18 H each, C(CH₃)₃), 1.26-1.55 (broad m, 12H, CO-CH₂-CH₂-CH₂-CH₂-CH₂-CH₃ & HO-CH-(CH₂)₂-CH₂-CH₂-CH₂-CH₃), 0.95 (t, 6.9 Hz, 3H, CO-CH₂-(CH₂)₄-CH₃), 0.87 (t, 6.9 Hz, 3H, HO-CH-(CH₂)₅-CH₃), -2.63 (broad s, 1H, NH), -2.89 (broad s, 1H, NH).

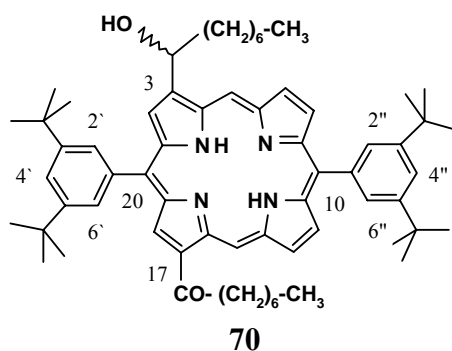
¹³C-NMR:

δ = 14.14 (HO-CH-CH₂-CH₂-CH₂-CH₂-CH₂-CH₂-CH₃), 14.70 (CO-CH₂-CH₂-CH₂-CH₂-CH₂-CH₃), 31.75 (C(CH₃)₃), 35.09 and 35.14 (C(CH₃)₃), 42.09(CO-CH₂-CH₂-CH₂-CH₂-CH₂-CH₃), 69.59 (HO-CH-CH₂-CH₂-CH₂-CH₂-CH₂-CH₃), 102.37, 107.62, 120.60, 121.23, 121.98, 126.57, 128.39, 129.00, 129.32, 130.08, 130.83, 130.86, 131.42, 133.83, 134.40, 138.30, 139.9, 140.12, 144.92, 149.23, 149.28, 149.32, 200.46 (CO-CH₂-CH₂-CH₂-CH₂-CH₂-CH₃).

MALDI-MS: 913.2

HR-FAB-MS: [M+H]⁺ 913.6345; calc. for C₆₂H₇₈N₄O₂ = 912.6281

4.39 3-Octanoyl-17-(1-hydroxyoctyl)-10,20-bis(3,5-di-*t*-butylphenyl)-21,23H-porphyrin [70]



R_f = 0.66 (CH₂Cl₂ : n-Hexane, 1:1, v/v).

¹H-NMR:

δ = 11.47 (s, 1H, 5-H), 10.36 (s, 1H, 15-H), 9.57 (s, 1H, 2-H), 9.55 (d, ³J = 4.8 Hz, 1H, 7-H), 9.31 (d, ³J = 4.8 Hz, 1H, 13-H), 9.13 (d, ³J = 4.8 Hz, 1H, 8-H), 9.14 (s, 1H, 18-H), 9.07 (d, ³J = 4.5 Hz, 1H, 12-H), 8.20 (two overlapped t, 4H, 2',6'-H and, 2'',6'' -H), 8.16 (t, ⁴J = 0.9Hz, 1H, 4''-H), 7.93 (t, ⁴J = 1.8 Hz, 1H, 4'-H), 7.88 (t, ⁴J = 1.8 Hz, 1H, 4''-H), 6.49 (q, ³J = 6.6 Hz, 1H, CH₃-(CH₂)₆-CH-OH), 3.58 (t = 6.9 Hz, 2H, CO-CH₂-(CH₂)₅-CH₃), 2.60-2.67 (broad m, 4H, HO-CH-CH₂-CH₂-(CH₂)₄-CH₃), 2.16 (q, 2H, CO-CH₂-(CH₂)₄-CH₂-CH₃), 1.65 and 1.61 (two s, 18 H each, C(CH₃)₃), 1.46-1.59 (broad m, 16H, CO-CH₂-CH₂-CH₂-CH₂-CH₂-CH₂-CH₃ and HO-CH-(CH₂)₂-CH₂-CH₂-CH₂-CH₂-CH₃), 0.95 (t, 3H, 6.9 Hz, CH₃-(CH₂)₆-CH-OH), 0.87 (t, 3H, CH₃, 6.6 Hz), -2.64 and 2.89 (two broad s, 2H, NH),

¹³C-NMR:

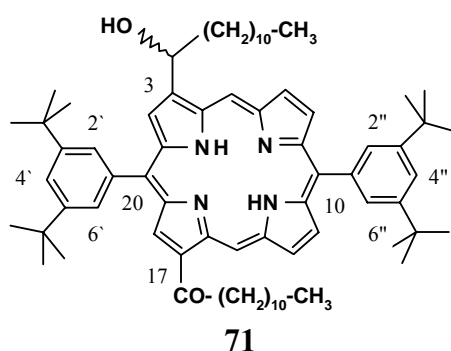
δ = 14.05 (CO-(CH₂)₆-CH₃), 14.13 (HO-CH-CH₂-CH₂-CH₂-CH₂-CH₂-CH₂-CH₃), 31.77 (C(CH₃)₃), 35.10 and 35.15 (C(CH₃)₃), 42.11 (CO-CH₂-(CH₂)₅-CH₃), 69.61 (HO-CH-CH₂-

CH₂-CH₂-CH₂-CH₂-CH₂-CH₃), 102.38, 107.64, 120.61, 121.24, 121.99, 126.58, 129.33, 130.08, 130.84, 130.86, 131.43, 133.81, 134.39, 138.26, 139.24, 140.33, 140.16, 144.96, 149.25, 149.30, 149.34, 200.45 (CO-(CH₂)₆-CH₃).

MALDI-MS:941.4

HR-FAB-MS: [M+H]⁺ 941.6684; calc. for C₆₄H₈₄N₄O₂ = 940.6594

4.40 3-Lauroyl-17-(1-hydroxydodecyl)-10,20-bis(3,5-di-*t*-butylphenyl)-21,23H-porphyrin [71]



R_f = 0.70 (CH₂Cl₂ : n-Hexane, 1:1, v/v).

¹H-NMR

δ = 11.48 (s, 1H, 5-H), 10.36 (s, 1H, 15-H), 9.57 (s, 1H, 2-H), 9.56 (d, ³J = 5.1 Hz, 1H, 7-H), 9.32 (d, ³J = 4.5 Hz, 1H, 13-H), 9.17 (d, ³J = 4.8 Hz, 1H, 8-H), 9.15 (s, 1H, 18-H), 9.07 (d, ³J = 4.5 Hz, 1H, 12-H), 8.21 (t, ⁴J = 2.1 Hz, 2H, 2',6'-H), 8.17 (t, ⁴J = 1.5 Hz, 2H, 2'',6''-H), 7.94 (t, ⁴J = 1.8 Hz, 1H, 4''-H), 7.89 (t, ⁴J = 1.8 Hz, 1H, 4'-H), 6.49 (q, ³J = 6.3 Hz, 1H, CH₃-(CH₂)₁₀-CH-OH), 3.59 (t = 6.3 Hz, 2H, CO-CH₂-(CH₂)₇-CH₃), 2.53-2.67 (broad m, 4H, HO-CH-CH₂-CH₂-(CH₂)₆-CH₃), 2.17 (q, 2H, CO-CH₂-(CH₂)₆-CH₂-CH₃), 1.67 and 1.62 (two s, 18 H each, C(CH₃)₃), 1.25-1.41 (broad m, 16H, CO-CH₂-CH₂-CH₂-CH₂-CH₂-CH₂-CH₂-CH₃ & HO-CH-(CH₂)₂-CH₂-CH₂-CH₂-CH₂-CH₃), 0.95 (t, 3H, 6.9 Hz, CH₃-(CH₂)₆-CH-OH), 0.87 (t, 3H, 6.6 Hz), -2.63 and 2.88 (two broad s, 2H, NH),

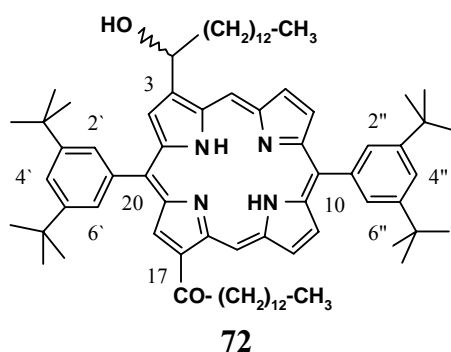
¹³C-NMR:

δ = 14.07 (CO-(CH₂)₁₀-CH₃) and (CH-OH-(CH₂)₁₀-CH₃), 31.76 (C(CH₃)₃), 35.09, 35.15 (C(CH₃)₃), 39.95, (HO-CH-CH₂-(CH₂)₉-CH₃), 42.11 (CO-CH₂-(CH₂)₉-CH₃), 69.62 (HO-CH-(CH₂)₁₀-CH₃), 102.38, 107.65, 120.60, 121.23, 121.99, 126.58, 129.33, 130.07, 130.87, 131.43, 133.82, 134.39, 139.22, 140.01, 140.15, 144.95, 149.24, 149.30, 149.33, 200.45 (CO-(CH₂)₁₀-CH₃).

MALDI-MS: 1053.5

HR-FAB-MS:[M+H]:1052.780; calc. for C₇₂H₁₀₀N₄O₂ = 1052.7846.

4.41 3-Myristoyl-17-(1-hydroxytetradecyl)-10,20-bis(3,5-di-*t*-butylphenyl)-21,23*H*-porphyrin [72]



R_f = 0.74 (CH₂Cl₂ : n-Hexane, 1:1, v/v).

¹H-NMR:

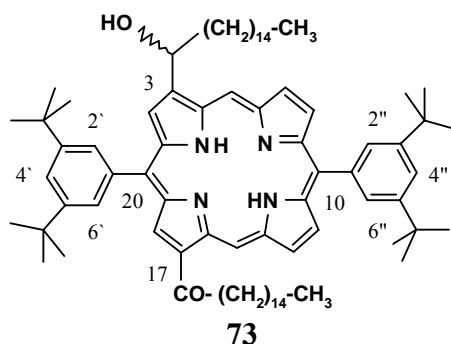
δ = 11.47 (s, 1H, 5-H), 10.37 (s, 1H, 15-H), 9.57 (s, 1H, 2-H), 9.55 (d, ³J = 4.8 Hz, 1H, 7-H), 9.31 (d, ³J = 4.5 Hz, 1H, 13-H), 9.16 (d, ³J = 4.8 Hz, 1H, 8-H), 9.14 (s, 1H, 18-H), 9.07 (d, ³J = 4.5 Hz, 1H, 12-H), 8.15-8.21 (m, 4H, 2', 6'-H and 2'', 6'' -H), 7.93 (t, ⁴J = 1.8 Hz, 1H, 4''-H), 7.88 (t, ⁴J = 1.8 Hz, 1H, 4'-H), 6.50 (t, ³J = 6.9 Hz, 1H, CH₃-(CH₂)₁₂-CH-OH), 3.59 (t = 6.3 Hz, 2H, CO-CH₂-(CH₂)₁₀-CH₃), 2.61-2.68 (broad m, 4H, HO-CH-CH₂-CH₂-(CH₂)₁₀-CH₃), 2.16 (q, 2H, CO-CH₂-(CH₂)₁₀-CH₂-CH₃), 1.65 and 1.72 (two s, 18 H each, C(CH₃)₃), 1.24-1.46 (broad m, 38H, CO-CH₂-(CH₂)₁₀-CH₂-CH₃ and HO-CH-(CH₂)₂-CH₂-CH₂-CH₂-CH₂-CH₂-CH₂-CH₂-CH₂-CH₃), 0.86-0.98 (two overlapped t, 6H, CO-(CH₂)₁₂-CH₃ & CH₃-(CH₂)₁₂-CH-OH), -2.64 to -2.88 (s, 2H, NH).

¹³C-NMR:

δ = 14.10, 14.12, 22.65, 22.69, 25.31, 26.34, 29.31, 29.36, 29.60, 29.65, 29.70, 31.58, 31.77, (C(CH₃)₃), 31.88, 31.92, 35.10 and 35.15 (C(CH₃)₃), 39.93, 42.11 (CO-CH₂-(CH₂)₁₁-CH₃), 69.59 (HO-CH-(CH₂)₁₂-CH₃), 102.37, 107.64, 120.60, 121.98, 130.09, 130.89, 131.42, 133.81, 134.40, 138.30, 139.24, 140.02, 140.16, 144.96, 149.25, 149.30, 149.34, 200.46 (CO-(CH₂)₁₂-CH₃).

MALDI-MS: 1109.6

4.42 3-Palmitoyl-17-(1-hydroxyhexadecyl)-10,20-bis(3,5-di-*t*-butylphenyl)-21,23H-porphyrin [73]



$R_f = 0.76$ (CH_2Cl_2 : n-Hexane, 1:1, v/v).

$^1\text{H-NMR}$:

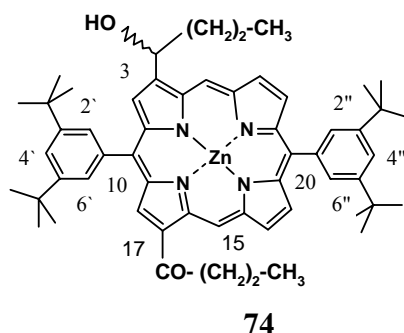
$\delta = 11.43$ (s, 1H, 5-H), 10.36 (s, 1H, 15-H), 9.52 (s, 1H, 2-H), 9.51 (d, $^3J = 4.5$ Hz, 1H, 7-H), 9.30 (d, $^3J = 4.5$ Hz, 1H, 13-H), 9.13 (overlapped d, 1H, 8-H), 9.12 (s, 1H, 18-H), 9.03 (d, $^3J = 4.8$ Hz, 1H, 12-H), 8.11-8.18 (m, 4H, 2',6'-H and 2'',6''-H), 7.89 (t, $^4J = 1.8$ Hz, 1H, 4''-H), 7.84 (t, $^4J = 1.8$ Hz, 1H, 4'-H), 6.51 (q, $^3J = 6.3$ Hz, 1H, $\text{CH}_3\text{-(CH}_2\text{)}_{14}\text{-CHOH}$), 3.56 (t, $^3J = 6.3$ Hz, 2H, $\text{CO-CH}_2\text{-(CH}_2\text{)}_{13}\text{-CH}_3$), 2.53-2.63 (broad m, 4H, $\text{HO-CH-CH}_2\text{-CH}_2\text{-(CH}_2\text{)}_{12}\text{-CH}_3$), 2.12 (q, 2H, $\text{CO-CH}_2\text{-(CH}_2\text{)}_{12}\text{-CH}_2\text{-CH}_3$), 1.61 and 1.57 (two s, 18 H each, $\text{C(CH}_3\text{)}_3$), 1.20-1.25 (broad d, 46H, $\text{CO-CH}_2\text{-(CH}_2\text{)}_{12}\text{-CH}_2\text{-CH}_3$ and $\text{HOCH-(CH}_2\text{)}_2\text{-CH}_2\text{-CH}_2\text{-CH}_2\text{-CH}_2\text{-CH}_2\text{-CH}_2\text{-CH}_2\text{-CH}_2\text{-CH}_2\text{-CH}_2\text{-CH}_3$), 0.83-0.89 (m, 6H, $\text{CO-(CH}_2\text{)}_{14}\text{-CH}_3$ and $\text{CH}_3\text{-(CH}_2\text{)}_{14}\text{-CH-OH}$), -2.67 and 2.92 (two broad s, 2H, NH),

$^{13}\text{C-NMR}$:

$\delta = 14.12, 14.14, 22.67, 22.69, 25.29, 29.33, 29.36, 29.65, 29.71, 31.77$ ($\text{C(CH}_3\text{)}_3$), 31.89, 31.92, 35.10 and 35.15 ($\text{C(CH}_3\text{)}_3$), 39.93, 42.10, 69.56 ($\text{HO-CH-(CH}_2\text{)}_{14}\text{-CH}_3$), 102.37, 107.62, 120.59, 121.22, 121.97, 126.56, 129.31, 130.11, 130.91, 131.41, 133.85, 134.42, 138.35, 139.21, 140.03, 140.13, 144.92, 149.23, 149.28, 149.31, 200.47 ($\text{CO-(CH}_2\text{)}_{14}\text{-CH}_3$).

MALDI-MS: 1164.5

4.43 3-Butyroyl-17-(1-hydroxybutyl)-10,20-bis(3,5-di-*t*-butylphenyl)porphinato zinc
[74]



$R_f = 0.20$ (CH_2Cl_2 : n-Hexane, 1:1, v/v).

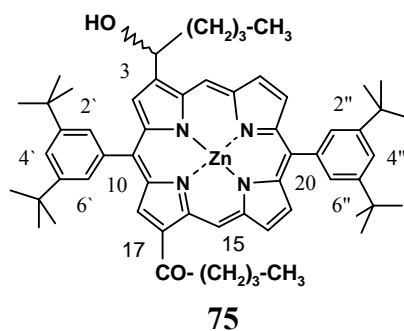
$^1\text{H-NMR}$:

$\delta = 11.10$ (s, 1H, 5-H), 10.20 (s, 1H, 15-H), 9.48 (s, 1H, 2-H), 9.30 (d, $^3J = 4.5$ Hz, 1H, 7-H), 9.24 (d, $^3J = 4.8$ Hz, 1H, 13-H), 8.97 (d, $^3J = 4.2$ Hz, 1H, 8-H), 8.95 (d, $^3J = 4.8$ Hz, 1H, 12-H), 8.91 (s, 1H, 18-H), 7.99 – 8.05 (4H, 2', 6'-H & 2'', 6''-H), 7.77 (t, $^4J = 1.8$ Hz, 1H, 4'-H), 7.73 (t, $^4J = 1.8$ Hz, 1H, 4''-H), 6.33 (t, $^3J = 6.6$ Hz, 1H, $\text{CH}_3\text{-CH}_2\text{-CH}_2\text{-CH-OH}$), 3.46 (t, 2H, $\text{CO-CH}_2\text{-CH}_2\text{-CH}_3$), 2.48 (m, 2H), 2.08 (m, $^3J = 6.3$ Hz, 2H, $\text{CH}_3\text{-CH}_2\text{-CH}_2\text{-CH-OH}$), 1.51 and 1.48 (two s, 18 H each, $\text{C}(\text{CH}_3)_3$), 1.15 (t, $\text{CH}_3\text{-CH}_2\text{-CH}_2\text{-CH-OH}$), 1.03 (t, $\text{CO-CH}_2\text{-CH}_2\text{-CH}_3$).

MALDI-MS: 891.0

HR-FAB-MS: $[\text{M}+\text{H}]^+$. 891.4555; calc. for $\text{C}_{56}\text{H}_{66}\text{N}_4\text{O}_2\text{Zn} = 892.55$

4.44 3-Valeroyl-17-(1-hydroxypentyl)-10,20-bis(3,5-di-*t*-butylphenyl)porphinato zinc
[75]



$R_f = 0.24$ (CH_2Cl_2 : n-Hexane, 1:1, v/v).

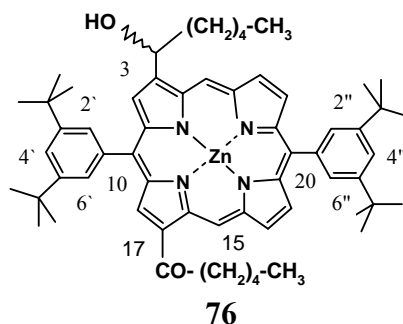
¹H-NMR:

δ = 11.14 (s, 1H, 5-H), 10.22 (s, 1H, 15-H), 9.50 (s, 1H, 2-H), 9.33 (d, 3J = 4.8 Hz, 1H, 7-H), 9.26 (d, 3J = 4.5 Hz, 1H, 13-H), 8.99 (d, 3J = 4.5 Hz, 1H, 8-H), 8.97 (d, 3J = 4.5 Hz, 1H, 12-H), 8.94 (s, 1H, 18-H), 8.01-8.08 (m 4H, 2', 6' and 2'', 6''-H), 7.80 (t, 4J = 0.9 Hz, 1H, 4'-H), 7.76 (t, 4J = 0.9 Hz, 1H, 4''-H), 6.35 (q, 3J = 6.9 Hz, 1H, CH₃-CH₂-CH₂-CH₂-CH₂-OH), 3.51 (t 2H, CO-CH₂-CH₂-CH₂-CH₃), 2.62 (broad m, 4H, CH₃-CH₂-CH₂-CH₂-CH-OH), 2.04 (m, 3J = 6.9 Hz, 3H, CO-CH₂-CH₂-CH₂-CH₃), 1.57-1.61 (d and s, 18 H each, C(CH₃)₃), 1.55 (broad s, 4H, CO-CH₂-CH₂-CH₂-CH₃ and CH₃-CH₂-CH₂-CH₂-CH-OH), 1.02 (t, 3J = 6.3 Hz, 3H, CO-CH₂-CH₂-CH₂-CH₂-CH₃), 0.89 (t, 3J = 7.5 Hz, 3H, CH₃-CH₂-CH₂-CH₂-CHOH)

MALDI-MS: 920.6

HR-FAB-MS: [M+H]⁺: 919.4857; calc. for C₅₈H₇₂N₄O₂ = 918.4790

4.45 3-Hexanoyl-17-(1-hydroxyhexyl)-10,20-bis(3,5-di-*t*-butylphenyl)porphinato zinc [76]



R_f = 0.28 (CH₂Cl₂ : n-Hexane, 1:1, v/v).

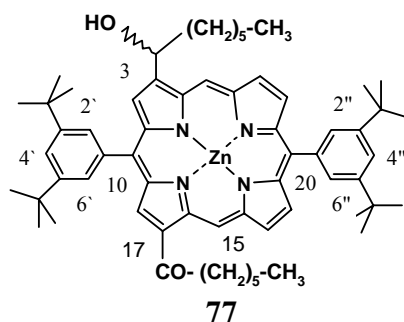
¹H-NMR:

δ = 11.12 (s, 1H, 5-H), 10.21 (s, 1H, 15-H), 9.41 (s, 1H, 2-H), 9.32 (d, 3J = 4.5 Hz, 1H, 7-H), 9.25 (d, 3J = 4.5 Hz, 1H, 13-H), 8.98 (d, 3J = 4.8 Hz, 1H, 8-H), 8.96 (d, 3J = 4.5 Hz, 1H, 12-H), 8.93 (s, 1H, 18-H), 8.05 – 8.06 (m, 4H, 2', 6'-H and 2'', 6''-H), 7.78 (t, 4J = 1.5 Hz, 1H, 4'-H), 7.74 (t, 4J = 1.8 Hz, 1H, 4''-H), 6.34 (q, 3J = 6.6 Hz, 1H, CH₃-CH₂-CH₂-CH₂-CH₂-OH), 3.59 (t = 6.6 Hz, 2H, CO-CH₂-(CH₂)₃-CH₃), 2.67-2.60 (m, 4H, HOCH-CH₂-CH₂-(CH₂)₂-CH₃), 2.05 (q, 2H, CO-CH₂-(CH₂)₂-CH₂-CH₃), 1.30-1.55 (broad m, 6H, CO-CH₂-CH₂-CH₂-CH₂-CH₃ and HO-CH-(CH₂)₂-CH₂-CH₂-CH₃) 1.66 and 1.62 (two s, 18 H each, C(CH₃)₃).

MALDI-MS: 945.8

HR-FAB-MS: [M+H]⁺ 947.5198; calc. for C₆₀H₇₄N₄O₂Zn = 946.5103

4.46 3-Heptanoyl-17-(1-hydroxyheptyl)-10,20-bis(3,5-di-*t*-butylphenyl)porphinato zinc [77]



$R_f = 0.3$ (CH_2Cl_2 : n-Hexane, 1:1, v/v).

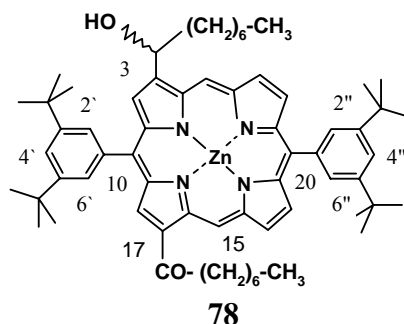
$^1\text{H-NMR}$:

$\delta = 11.43$ (s, 1H, 5-H), 10.36 (s, 1H, 15-H), 9.53 (s, 1H, 2-H), 9.51 (d, $^3J = 4.8\text{Hz}$, 1H, 7-H), 9.30 (d, $^3J = 4.5\text{ Hz}$, 1H, 13-H), 9.13 (overlapped d, 1H, 8-H), 9.12, (s, 1H, 18-H), 9.03 (d, $^3J = 4.5\text{ Hz}$, 1H, 12-H), 8.11-8.17 (m, 4H, 2'',6'-H and, 2'',6''-H), 7.89 (t, $^4J = 1.8\text{ Hz}$, 1H, 4'-H), 7.85 (t, $^4J = 1.8\text{ Hz}$, 1H, 4''-H), 6.74 (q, $^3J = 6.6\text{ Hz}$, 1H, $\text{CH}_3\text{-(CH}_2\text{)}_5\text{-CH-OH}$), 3.55 (t = 7.2 Hz, 2H, $\text{CO-CH}_2\text{-(CH}_2\text{)}_4\text{-CH}_3$), 2.63-2.60 (broad m, 4H, $\text{HO-CH-CH}_2\text{-CH}_2\text{-(CH}_2\text{)}_3\text{-CH}_3$), 2.13 (q, 2H, $\text{CO-CH}_2\text{-(CH}_2\text{)}_3\text{-CH}_2\text{-CH}_3$), 1.62 and 1.58 (two s, 18 H each, $\text{C(CH}_3\text{)}_3$), 1.26-1.55 (broad m, 12H, $\text{CO-CH}_2\text{-CH}_2\text{-CH}_2\text{-CH}_2\text{-CH}_2\text{-CH}_3$ & $\text{HO-CH-(CH}_2\text{)}_2\text{-CH}_2\text{-CH}_2\text{-CH}_2\text{-CH}_3$), 0.95 (t, 6.9 Hz, 3H, $\text{CO-CH}_2\text{-(CH}_2\text{)}_4\text{-CH}_3$), 0.87 (t, 6.9 Hz, 3H, $\text{HO-CH-(CH}_2\text{)}_5\text{-CH}_3$).

MALDI-MS: 974.1

HR-FAB-MS: $[\text{M}+\text{H}]^+ .975.5484$; calc. for $\text{C}_{62}\text{H}_{78}\text{N}_4\text{O}_2\text{Zn} = 974.5416$

4.47 3-Octanoyl-17-(1-hydroxyoctyl)-10,20-bis(3,5-di-*t*-butylphenyl)porphinato zinc [78]



$R_f = 0.34$ (CH_2Cl_2 : n-Hexane, 1:1, v/v).

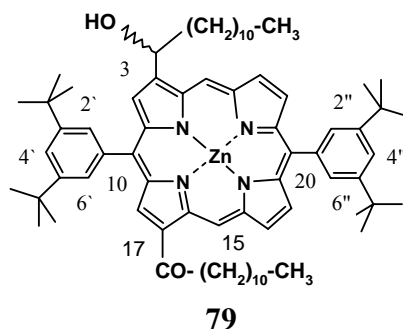
¹H-NMR:

δ = 11.08 (s, 1H, 5-H), 10.18 (s, 1H, 15-H), 9.46 (s, 1H, 2-H), 9.28 (d, 3J = 4.8 Hz, 1H, 7-H), 9.22 (d, 3J = 4.5 Hz, 1H, 13-H), 8.95 (d, 3J = 4.5 Hz, 1H, 8-H), 8.93 (d, 3J = 4.5 Hz, 1H, 12-H), 8.90 (s, 1H, 18-H), 7.97-8.04 (m, 4H, 2',6'-H and 2'',6''-H), 7.76 (t, 4J = 1.8 Hz, 1H, 4''-H), 7.71 (t, 4J = 1.8 Hz, 1H, 4'-H), 6.30 (q, 3J = 6.6 Hz, 1H, CH₃-(CH₂)₆-CH-OH), 3.58 (t, 3J = 6.9 Hz, 2H, CO-CH₂-(CH₂)₅-CH₃), 2.48 (broad m, 4H, HO-CH-CH₂-CH₂-(CH₂)₄-CH₃), 2.02 (q, 2H, CO-CH₂-(CH₂)₄-CH₂-CH₃), 1.50 and 1.46 (two s, 18 H each, C(CH₃)₃), 1.16-1.28 (broad m, 16H, CO-CH₂-CH₂-CH₂-CH₂-CH₂-CH₂-CH₃ and HO-CH-(CH₂)₂-CH₂-CH₂-CH₂-CH₂-CH₃), 0.81 (t, 3H, 6.9 Hz, CH₃-(CH₂)₆-CO), 0.74 (t, 3H, 6.6 Hz CH₃-(CH₂)₆-CH-OH).

MALDI-MS: 1002.1

HR-FAB-MS: [M+H]⁺+1003.580; calc. for C₆₄H₈₂N₄O₂Zn = 1002.5729

4.48 3-Lauroyl-17-(1-hydroxydodecyl)-10,20-bis(3,5-di-*t*-butylphenyl)porphinato zinc [79]



R_f = 0.38 (CH₂Cl₂ : n-Hexane, 1:1, v/v).

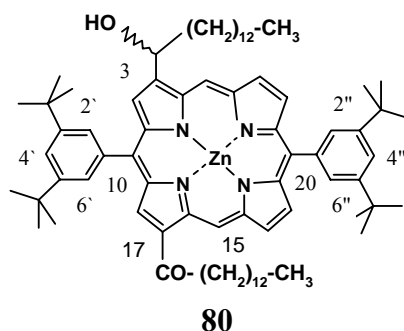
¹H-NMR:

δ = 11.07 (s, 1H, 5-H), 10.17 (s, 1H, 15-H), 9.46 (s, 1H, 2-H), 9.27 (d, 3J = 4.8 Hz, 1H, 7-H), 9.21 (d, 3J = 4.5 Hz, 1H, 13-H), 8.94 (d, 3J = 4.5 Hz, 1H, 8-H), 8.92 (d, 3J = 4.5 Hz, 1H, 12-H), 8.89 (s, 1H, 18-H), 7.96-8.034 (m, 4H, 2',6',-H and 2'',6''-H), 7.75 (t, 4J = 1.8 Hz, 1H, 4''-H), 7.71 (t, 4J = 1.8 Hz, 1H, 4'-H), 6.28 (q, 3J = 6.6 Hz, 1H, CH₃-(CH₂)₁₀-CH-OH), 3.45 (t = 6.3 Hz, 2H, CO-CH₂-(CH₂)₉-CH₃), 2.38-2.55 (broad m, 4H, HO-CH-CH₂-CH₂-(CH₂)₆-CH₃), 2.00 (m, 2H, CO-CH₂-(CH₂)₈-CH₂-CH₃), 1.49 and 1.45 (two s, 18 H each, C(CH₃)₃), 0.76 -0.72 (m 6H, CH₃-(CH₂)₈-CO and CH₃-(CH₂)₈-CH-OH).

MALDI-MS: 1114.5

HR-FAB-MS: [M+H]⁺; calc. for C₇₂H₉₈N₄O₂Zn = 1114.6981

4.49 3-Myristoyl-17-(1-hydroxtetradecyl)-10,20-bis(3,5-di-*t*-butylphenyl)porphinato zinc [80]



$R_f = 0.43$ (CH_2Cl_2 : n-Hexane, 1:1, v/v).

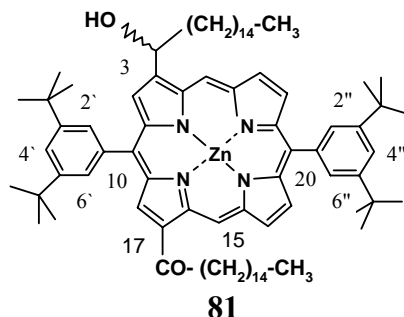
$^1\text{H-NMR}$:

$\delta = 10.99$ (s, 1H, 5-H), 10.11 (s, 1H, 15-H), 9.40 (s, 1H, 2-H), 9.21 (d, $^3J = 4.5$ Hz, 1H, 7-H), 9.15 (d, $^3J = 4.5$ Hz, 1H, 13-H), 8.87 (d, $^3J = 4.5$ Hz, 1H, 8-H), 8.87 (d, $^3J = 4.5$ Hz, 1H, 12-H), 8.83, (s, 1H, 18-H), 7.90 – 7.97 (m, 4H, 2', 6'-H and 2'', 6''-H), 7.69 (t, $^4J = 1.8$ Hz, 1H, 4''-H), 7.65 (t, $4J = 1.8$ Hz, 1H, 4'-H), 6.21 (t, $^3J = 6.9$ Hz, 1H, $\text{CH}_3\text{-(CH}_2\text{)}_{12}\text{-CH-OH}$), 3.39 (t, $^3J = 7.5$ Hz, 2H, $\text{CO-CH}_2\text{-(CH}_2\text{)}_{10}\text{-CH}_3$), 2.29-2.50 (broad m, 4H, $\text{HOCH-CH}_2\text{-CH}_2\text{-(CH}_2\text{)}_{10}\text{-CH}_3$), 2.16 (q, 2H, $\text{CO-CH}_2\text{-(CH}_2\text{)}_{10}\text{-CH}_2\text{-CH}_3$), 1.43 and 1.40 (two s, 18 H each, $\text{C(CH}_3\text{)}_3$), 0.64-0.71 (two overlapped t, 6H, $\text{CO-(CH}_2\text{)}_{12}\text{-CH}_3$ and $\text{CH}_3\text{-(CH}_2\text{)}_{12}\text{-CHOH}$)

MALDI-MS: 1170.5

HR-FAB-MS: $[\text{M}+\text{H}]^+$; calc. for $\text{C}_{76}\text{H}_{106}\text{N}_4\text{O}_2\text{Zn} = 1170.7607$

4.50 3-Palmitoyl-17-(1-hydroxyhexadecyl)-10,20-bis(3,5-di-*t*-butylphenyl)porphinato zinc [81]



$R_f = 0.47$ (CH_2Cl_2 : n-Hexane, 1:1, v/v).

$^1\text{H-NMR}$:

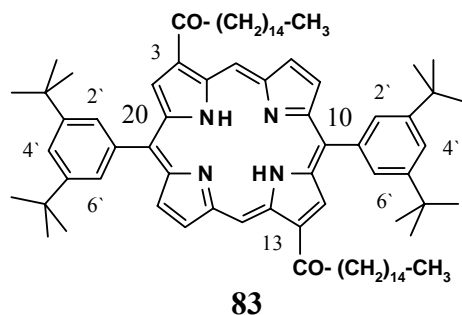
$\delta = 11.16$ (s, 1H, 5-H), 10.22 (s, 1H, 15-H), 9.52 (s, 1H, 2-H), 9.35 (d, $^3J = 4.8$ Hz, 1H, 7-H), 9.28 (d, $^3J = 4.5$ Hz, 1H, 13-H), 9.17 (d, $^3J = 4.8$ Hz, 1H, 8-H), 8.99 (d, $^3J = 4.5$ Hz, 1H, 12-

H), 8.95, (s, 1H, 18-H), 8.03-8.09 (m, 4H, 2',6'-H and 2'',6''-H), 7.81 (t, $^4J = 1.5$ Hz, 1H, 4''-H), 7.77 (t, $^4J = 1.5$ Hz, 1H, 4'-H), 6.35 (q, $^3J = 6.6$ Hz, 1H, $\text{CH}_3(\text{CH}_2)_{14}\text{CH-OH}$), 3.51 (t = 7.5 Hz, 2H, $\text{CO-CH}_2\text{-(CH}_2)_{13}\text{-CH}_3$), 2.53-2.69 (broad m, 4H, $\text{HO-CH-CH}_2\text{-CH}_2\text{-(CH}_2)_{12}\text{-CH}_3$), 2.07 (q, 2H, $\text{CO-CH}_2\text{-(CH}_2)_{12}\text{-CH}_2\text{-CH}_3$), 1.56 and 1.52 (two s, 18 H each, $\text{C}(\text{CH}_3)_3$), 0.79-0.85 (m, 6H, $\text{CO-(CH}_2)_{14}\text{-CH}_3$ and $\text{CH}_3\text{-(CH}_2)_{14}\text{-CH-OH}$).

MALDI-MS: 1226.5

HR-FAB-MS: $[\text{M}+\text{H}]^+$; calc. for $\text{C}_{80}\text{H}_{114}\text{N}_4\text{O}_2\text{Zn} = 1226.8233$

4.51 3,13-Dipalmitoyl-10,20-bis(3,5-di-*t*-butylphenyl)-21,23*H*-porphyrin [83]



$^1\text{H-NMR}$:

$\delta = 11.38$ (s, 2H, 5,15-H), 9.48 (s, 2H, 2,12-H), 9.51 (d, $^3J = 4.8$ Hz, 2H, 7,17-H), 9.17 (d, $^3J = 4.8$ Hz, 2H, 8,18-H), 8.13 (d, $^4J = 1.8$ Hz, 4H, 2',6'-H), 7.87 (t, $^4J = 1.8$ Hz, 2H, 4'-H), 3.48-3.53 (m, 4H, $\text{CO-CH}_2\text{-(CH}_2)_{13}\text{-CH}_3$), 1.55 (s, 36H, $\text{C}(\text{CH}_3)_3$), 1.24 (broad s, 28H $\text{CO-CH}_2\text{-(CH}_2)_{13}\text{-CH}_3$), 0.83-0.91 (m, 6H, $\text{CO-CH}_2\text{-(CH}_2)_{13}\text{-CH}_3$), -2.71 (s, 2H, NH)

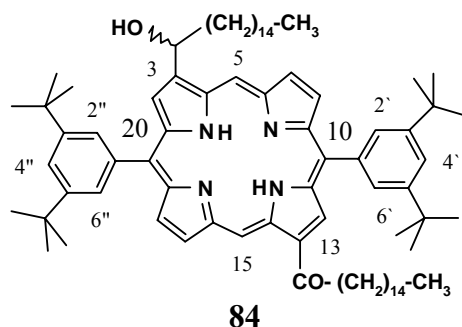
$^{13}\text{C-NMR}$:

$\delta = 14.12, 22.68, 25.28, 29.35, 29.64, 29.70, 31.77$ ($\text{C}(\text{CH}_3)_3$), 31.91, (COCH_3), 31.84, 35.15 ($\text{C}(\text{CH}_3)_3$), 42.11, 107.64 (5,15-C), 121.39, (10,20-C), 122.04 (4'-C), 128.94, 130.46 (8,18-C), 130.73 (2',6'-C), 138.93, 139.78, 140.07, 140.28, 140.71, 149.46, 150.23 151.39 (2,12-C), 200.43 ($\text{CO-(CH}_2)_{14}\text{-CH}_3$).

MALDI-MS: 1163.5

HR-FAB-MS: $[\text{M}+\text{H}]^+$; calc. for $\text{C}_{80}\text{H}_{114}\text{N}_4\text{O}_2 = 1162.8941$

4.52 (Rac)-3-(1-hydroxyhexadecyl)-13-palmitoyl-10,20-bis(3,5-di-*t*-butylphenyl)-21,23*H*-porphyrin [84]



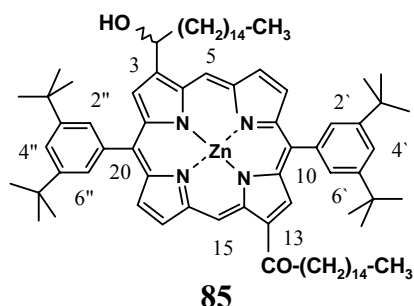
¹H-NMR:

δ = 11.41 (s, 1H, 5-H), 10.42 (s, 1H, 15-H), 9.52 (s, 1H, 2-H), 9.50 (d, ³J = 4.8 Hz, 1H, 7-H), 9.42 (d, ³J = 5.1 Hz, 1H, 17-H), 9.18 (d, ³J = 5.1 Hz, 1H, 8-H), 9.11 (d, ³J = 4.8 Hz, 1H, 18-H), 8.88 (s, 1H, 12-H), 8.09 – 8.16 (m, 4H, 2',6'-H and non-equivalent 2'',6''-H), 7.88 (t, ⁴J = 1.8 Hz, 1H, 4'-H), 7.84 (t, ⁴J = 1.8 Hz, 1H, 4''-H), 6.37 (q, ³J = 6.3 Hz, 1H, CH₃-(CH₂)₁₅-CH-OH), 3.54 (t, ³J = 7.2 Hz, 2H, CO-CH₂-(CH₂)₁₄-CH₃), 2.17 (broad s, 1H, HO-CH-(CH₂)₁₄-CH₂-CH₃), 2.10 (q, ³J = 7.5 Hz, 2H, HO-CH-CH₂-(CH₂)₁₅-CH₃), 1.61 and 1.57 (two s, 18 H each, C(CH₃)₃), 0.83-0.89 (two overlapped t, 6H, CO-CH₂-(CH₂)₁₄-CH₃ and HO-CH-(CH₂)₁₅-CH₃), -2.76 and -2.79 (two s, 2H, NH).

¹³C-NMR:

δ = 14.11, 25.30, 26.43, 29.32, 29.35, 29.61, 29.64, 29.70, 29.75, 31.76 (C(CH₃)₃), 31.89, 31.91, 35.10 and 35.14 (C(CH₃)₃), 39.80, 42.09, 69.78 (HO-CH-(CH₂)₁₄-CH₃), 107.56, 120.23, 121.16, 121.30, 122.38, 129.17, 129.65, 130.14, 130.30, 130.72, 139.27, 140.02, 149.22, 149.23, 149.34, 149.87, 200.46 (CO-(CH₂)₁₄-CH₃)

4.53 3-(1-Hydroxyhexadecyl)-13-palmitoyl-10,20-bis(3,5-di-*t*-butylphenyl)porphinato zinc [85]



The free base porphyrine **5** was metallated using zinc acetate as described above in over 80 % isolated yield. After column chromatography, the eluent was washed several times with brine to remove traces of methanol, evaporated in vacuum and was then thoroughly dried overnight (10⁻³ Torr) in order to perform self-assembly experiments.

$R_f = 0.09$.

¹H-NMR:

$\delta = 11.13$ (s, 1H, 5-H), 10.22 (s, 1H, 15-H), 9.51 (s, 1H, 2-H), 9.33 (d, $^3J = 4.5$ Hz, 1H, 7-H), 9.26 (d, $^3J = 4.5$ Hz, 1H, 17-H), 9.05 (d, $^3J = 4.5$ Hz, 1H, 8-H), 8.96 (d, $^3J = 4.5$ Hz, 1H, 18-H), 8.88 (s, 1H, 12-H), 8.08 (d, $^4J = 1.8$ Hz, 2H, 2',6'-H), 8.01 (d, $^4J = 1.8$ Hz, 2H, non-equivalent 2'',6''-H), 7.80 (t, $^4J = 1.8$ Hz, 1H, 4'-H), 7.75 (t, $^4J = 1.8$ Hz, 1H, 4''-H), 6.33 (q, $^3J = 6.6$ Hz, 1H, CH₃-(CH₂)₁₅-CH₂-OH), 3.51 (t, $^3J = 7.5$ Hz, 2H, CO-CH₂-(CH₂)₁₄-CH₃), $2.43 - 2.58$ (broad m, 4H, CO-CH₂-(CH₂)₁₃-CH₂-CH₃ and HO-CH-(CH₂)₁₄-CH₂-CH₃), 2.13 (broad s, 1H, HO-CH-(CH₂)₁₄-CH₂-CH₃), 2.06 (quint, $^3J = 7.2$ Hz, 2H, HO-CH-CH₂-(CH₂)₁₄-CH₂-CH₃), 1.54 and 1.51 (two s, 18 H each, C(CH₃)₃), $0.77-0.83$ (two overlapped t, 6H, CO-CH₂-(CH₂)₁₄-CH₃ and HO-CH-(CH₂)₁₅-CH₃)

References

- [1] Balaban, T. S. "Light-Harvesting Nanostructures" in *Encyclopedia of Nanoscience and Nanotechnology*, Nalwa, H. S. (Ed.) American Scientific Publishers, Los Angeles, **2004**, Vol. 4, pp. 505 - 559.
- [2] Blakenship, R.E. Photosynthetic Antennas and Reaction Centers: Current Understanding and Prospects for Improvement, in *Research Opportunities in Photochemical Sciences* (A. J. Nozik, Ed.). NREL/CP-450-21097; DE96007867, **1996**.
- [3] Blankenship, R. E.; Madigan, M. T.; Bauer, C. E.; (Eds). *Anoxygenic Photosynthetic Bacteria*, Kluwer: Dordrecht, **1995**.
- [4] Deisenhofer, J.; Norris, J. R. (Eds.). *The Photosynthetic Reaction Center*. Academic Press: San Diego, **1993**.
- [5] Scheer, H. (Ed.) *Chlorophylls*, CRC Press: Boca Raton, **1991**.
- [6] van Grondelle, R.; Dekker, J. P.; Gillbro, T.; Sundstrom, V. *Biochim. Biophys. Acta*. **1994**, *1187*, 1- 65.
- [7] Menger, F. M. *Proc. Natl. Acad. Sci. USA*. **2002**, *99*, 4818 – 4822.
- [8] Whitesides, G. M.; Boncheva, M. *Proc. Natl. Acad. Sci USA*. **2002**, *99*, 4769 – 4774.
- [9] Lindoy, L. F.; Atkinson, I. M. "Self-Assembly in Supramolecular Systems".
- [10] Balaban, T. S.; Bhise, A. D.; Linke-Schaetzel, M.; Roussel, C, Vanthyne, N. *Angew. Chem. Int. Ed*, **2003**, *42*, 2139 – 2144.
- [11] Nazeeruddin, M. K.; Humphry-Baker, R.; Grätzel, M.; Wöhrle, D.; Schnurpfeil, G.; Schneider, G.; Hirth, A.; Trombach, N. *J. Porphyrins Phthalocyanines*. **1999**, *3*, 230.
- [12] Nazeeruddin, M. K.; Humphry-Baker, R.; Grätzel, M.; Murrer, B. A. *Chem. Commun.*, **1998**, 719 – 720.
- [13] He, J.; Hagfeldt, A.; Lindquist, S. –E. *Langmuir*, **2001**, *17*, 2743 – 2747.
- [14] He, J.; Benkö, G.; Korodi, F.; Polivka, T.; Lomoth, R.; Akermark, B.; Sun, L.; Hagfeldt, A.; Sundström, V. *J. Am. Chem. Soc.*, **2002**, *124*, 4922 – 4932.
- [15] Ferrere, S.; Zaban, A.; Gregg, B. A. *J. Phys. Chem. B*, **1997**, *101*, 4490 – 4493.

- [16] Tian, H.; Liu, P.-H.; Zhu, W.; Gao, E.; Wuand,D. -J.; Cai, S. *J. Mater. Chem.*, **2000**, 10, 2708 – 2715.
- [17] Tian, H.; Liu, P.-H.; Meng, F. S.; Gao, E.; Cai, S. *Synth. Met.* **2001**, 121, 1557 – 1558.
- [18] Ramakrishna, G.; Ghosh, H. N. *J. Phys. Chem. B*, **2001**, 105, 7000 – 7008.
- [19] Matsumura, M.; Mitsuda, K.; Yoshizawa, N.; Tsubomura, H. *Bull. Chem. Soc. Jpn.*, **1981**, 54, 692.
- [20] Sayama, K.; Sugino, M.; Sugihara, H.; Abe, Y.; Arakawa, H. *Chem. Lett.*, **1998**, 27, 753 – 754.
- [21] Wang, Z. -S.; Li, F.-Y.; Huang, C.-H.; Wang, L.; Wei, M.; Jin, L. - P.; Li, N.- Q. *J. Phys. Chem. B*, **2000**, 104, 9676 – 9682.
- [22] Wang, Z.; Huang, Y.; Huang, C.; Zheng, J.; Cheng, H.; Tian, S. *Synth. Met.*, **2000**, 114, 201 – 207.
- [23] Wang, Z.- S.; Li, F.- Y.; Huang, C. – H. *J. Phys. Chem. B*, **2001**,105, 9210 - 9217.
- [24] Koehorst, R. B. M.; Boschloo, G. K.; Savenije, T. J.; Goossens.; Schaafsma, T. J. *J. Phys. Chem. B*, **2000**, 104, 2371 - 2377.
- [25] Cherian, S.; Wamser, J. *J. Phys. Chem. B*, **2000**, 104, 3624 – 3629.
- [26] Fungo, F.; Otero, L.; Durantini, E. N.; Silber, J. J.; Sereno, L. E. *J. Phys.Chem. B*, **2000**, 104, 7644 - 7651.
- [27] Fungo, F.; Otero, L. A.; Sereno, L.; Silber, J. J.; Durantini, E. N. *J. Mater. Chem.*, **2000**, 10, 645 – 650.
- [28] Odobel, F.; Blart, E.; Marie Lagrée, A.; Villieras, M.; Boujtita, H.; Murr, N. E.; Caramoric, S.; Bignozzi, C. A. *J. Mater. Chem.*, **2003**, 13, 502 – 510.
- [29] Gust; D.; Moore, T. A.; Moore, A. L. *Acc. Chem. Res.* **1993**, 26, 198 – 205.
- [30] Mclendon, G.; Hake, R. *Chem. Rev.* **1992**, 92, 481 – 490.
- [31] Wasielewski, M. R. *Chem. Rev.* **1993**, 92, 435 – 461.
- [32] Wagner, R. W.; Johnson, T. E.; Lindsey, J. S. *J. Am. Chem. Soc.* **1996**, 118, 11166 – 11180.

- [33] Hsiao, J.-S.; Krueger, B. P.; Wagner, R. W.; Johnson, T. E.; Delaney, J. K.; Mauzerall, D. C.; Fleming, G. R.; Lindsey, J. S.; Bocian, D. F.; Donohoe, R. J. *J. Am. Chem. Soc.* **1996**, *118*, 11181 – 11193.
- [34] Seth, J.; Palaniappan, V.; Wagner, R. W.; Lindsey, J. S.; Bocian, D. F. *J. Am. Chem. Soc.* **1996**, *118*, 11194 – 11207.
- [35] Nakano, A.; Osuka, A.; Yamazaki, I.; Yamazaki, T.; Nishimura, Y. *Angew. Chem. Int. Ed.* **1998**, *37*, 3023 – 3027.
- [36] Mongin, O.; Hoyler, N.; Gossauer, A. *Eur. J. Org. Chem.* **2000**, *7*, 1193 – 1197.
- [37] Li, J.; Diers, J.R.; Seth, J.; Yang, S. I.; Bocian, D. F.; Holten, D.; Lindsey, J. S. *J. Org. Chem.* **1999**, *64*, 9090 – 9100.
- [38] Linke, M.; Chambron, S. C.; Heitz, V.; Sauvage, S. P.; Encinas, S.; Barigelletti, F.; Flamigni, L. *J. Am. Chem. Soc.* **2000**, *122*, 11834 – 11844.
- [39] Sumida, J. P.; Liddell, P. A.; Su Lin.; MacPherson, A. N.; Seely, G. R.; Moore, A. L.; Moore, T. A.; Gust, D. *J. Phys. Chem. A* **1998**, *102*, 5512 – 5519.
- [40] Kodis, G.; Liddell, P. A.; Garza, L.; Moore, A. L.; Moore, A. T.; Gust, D. *J. Mater. Chem.* **2002**, *12*, 2100 – 2108.
- [41] Paolesse, R.; Jaquinode, L.; Della sala, F.; Nurco, D. J.; Prodi, L.; Montalti, M.; Di Natale, C.; D' Amico, C.; Di Carlo, A.; Lugli, P.; Smith, K. M. *J. Am. Chem. Soc.* **2000**, *122*, 11295 – 11302.
- [42] Kuciauskas, D.; Liddell, P. A.; Su Lin.; Johnson, T. E.; Weghorn, S. J.; Lindsey, J. S.; Moore, A. L.; Moore, T. A.; Gust, D. *J. Am. Chem. Soc.* **1999**, *121*, 8604 – 8614.
- [43] Norstan, T.; Branda, N. *J. Chem. Soc. Chem. Commun.* **1998**, 1257.
- [44] Lehn, J.-M. "Supramolecular Chemistry: Concepts and Perspectives." VCH, Weinheim, **1995**.
- [45] Drain, C. M.; Lehn, J.-M. *J. Chem. Soc. Chem. Commun.* **1994**, 2313 – 2315.
- [46] Hunter, C. A.; Hyde, R. K. *Angew. Chem. Int. Ed. Engl.* **1996**, *35*, 1936.
- [47] Berman, A.; Izraeli, E. S.; Levanon, H.; Wang, B.; Sessler, J. L. *J. Am. Chem. Soc.* **1995**, *117*, 8252 – 8257.

- [48] Jesorka, A.; Balaban, T. S.; Holzwarth, A. R.; Schaffner, K. *Angew. Chem. Int. Ed.* **1996**, *35*, 2861 – 2863.
- [49] Susumu, K.; Shimidzu, T.; Tanaka, K.; Segawa, H. *Tetrahedron Lett.* **1996**, *37*, 8399 – 8402.
- [50] Bhuiyan, A. A.; Seth, J.; Yoshida, N.; Osuka, K.; Bocian, D. F. *J. Phys. Chem, B*, **2000**, *104*, 10757 – 10764.
- [51] Balaban, A. T.; Nenitzescu, C. D. in *Friedel-Crafts and Related Reactions*, Olah, G. A. (Ed.); Wiley-Interscience: New York, **1964**, Vol 3, p 1033.
- [52] Hassner, A.; Stumer, C. *Organic Synthesis Based on Name Reactions*, Pergamon, Elsevier Science, Amsterdam, **2002**, p 17.
- [53] Balaban, T. S.; Balaban, A. T. in *Science of Synthesis – Houben-Weyl Methods of Molecular Transformations*, Vol. 14, Thomas, E. J. (Ed.), Georg Thieme Verlag, Stuttgart, **2003**, pp. 11-200.
- [54] Bogatian, M. V.; Deleanu, C.; Udrea S.; Chiraleu F.; Plaveti M.; Danila M. G.; Bogatian G. ; Balaban T. S. *Rev. Roumaine Chim.* **2003**, *48*, 717-722.
- [55] Bogatian M. V.; Campeanu V.; Serban S.; Mihai G.; Balaban T. S. *Revue Roumaine Chim.* **2001**, *46*, 115-120.
- [56] Bogatian M.; Mihai G.; Plaveti M.; Chiraleu F.; Maganu M.; Badescu V.; Balaban T. S. *Rev. Roumaine Chim.* **1998**, *43*, 315-320.
- [57] Bogatian M.; Mihai G.; Plaveti M.; Chiraleu F.; Deleanu C.; Badescu V.; Balaban T. S. *Rev. Roumanie Chim.* **1996**, *41*, 979-987.
- [58] Bogatian M.; Deleanu C.; Mihai G.; Balaban T. S. *Z. Naturforsch.* **1992**, *47b*, 1011-1015.
- [59] Balaban T. S.; Bogatian M.; Plaveti M.; Badea M.; Mihai G. *Rev. Roumaine Chim.* **1991**, *36*, 229-234.
- [60] Jeandon, C.; Bauder, C.; Callot, H. J. *Energy & Fuels* **1990**, *4*, 665-667.
- [61] Gryko, D. T.; Clausen, C.; Lindsey, J. S. *J. Org. Chem.* **1999**, *64*, 8635–8647.
- [62] HyperChem®, Hypercube Inc. Release 7, Gainesville, Florida, **2002**.
- [63] Anderson, S.; Anderson, H. L.; Bashall, A.; McPartlin, M.; Sanders, J. K. M., *Angew. Chem. Int. Ed.* **1995**, *34*, 1096-1099.
- [64] Burrel, A. K.; Officier, D.L.; Reid, D.C.W.; Wild, K.Y. *Angew. Chem. Int. Ed.* **1998**, *110*, 122-125.
- [65] Wilson, G.S.; Anderson, H.L. *Chem. Chemmun.* **1999**, 1539-1540.

- [66] Kobayashi, K.; Koyanagi, M.; Endo, K.; Masuda, H.; Aoyama, Y. *Chem. Eur. J.* **1998**, *4*, 417-424.
- [67] Bhyrappa, P.; Wilson, S.R.; Suslick, K.S. *J. Am. Chem. Soc.* **1997**, *119*, 8492-8502.
- [68] Kuroda, Y.; Kato, Y.; Ogoshi, H. *Chem. Commun.* **1997**, 469-470.
- [69] Drain, C.M.; Russell, K.C.; Lehn, J.-M. *Chem. Commun.* **1996**, 337-338.
- [70] Kral, V.; Springs, S.L.; Sessler, J.L. *J. Am. Chem. Soc.* **1995**, *117*, 8881-8882.
- [71] Desiraju, G.R. *Angew. Chem. Int. Ed.* **1995**, *34*, 2311-2327.
- [72] Sessler, J.L.; Wang, B.; Harriman, A. *J. Am. Chem. Soc.* **1995**, *117*, 704-714.
- [73] Drain, C.M.; Fischer, R.; Nolen, E.G.; Lehn, J.-M. *J. Chem. Soc. Chem. Commun.* **1993**, 243-245.
- [74] Endisch, C.; Fuhrhop, J.-H.; Buschmann, J.; Luger, P.; Siggel, U. *J. Am. Chem. Soc.* **1996**, *118*, 6671-6680.
- [75] Sessler, J.L.; Andrievsky, A.; Gale, P.A.; Lynch, V. *Angew. Chem. Int. Ed. Engl.* **1996**, *35*, 2782-2785.
- [76] Wojaczynski, J.; Latos-Grazynski, L. *Inorg. Chem.* **1996**, *35*, 4812-4818.
- [77] Susumu, K.; Segawa, H.; Shimidzu, T. *Chem. Lett.* **1995**, 929-930.
- [78] Rao, T.A.; Maiya, B.G. *J. Chem. Soc. Chem. Commun.* **1995**, 939-940.
- [79] Wojaczynski, J.; Latos-Grazynski, L. *Inorg. Chem.* **1995**, *34*, 1044-1053.
- [80] Senge, M.O.; Smith, K.M. *J. Chem. Soc. Chem. Commun.* **1994**, 923-924.
- [81] Balch, A.L.; Mazzanti, M.; Olmstead, M.M. *Inorg. Chem.* **1993**, *32*, 4737-4744.
- [82] Balch, A.L.; Latos-Grazynski, L.; Noll, B.C.; Olmstead, M.M.; Zovinka, E.P. *Inorg. Chem.* **1992**, *31*, 2248-2255.
- [83] Masuoka, N.; Itano, H.A. *BioChem.* **1987**, *26*, 3672-3680.
- [84] Godziela, G.M.; Tilotta, D.; Goff, H.M. *Inorg. Chem.* **1986**, *25*, 2142 - 2146.
- [85] Goff, H.M.; Shimomura, E.T.; Lee, Scheidt Y.J., W.R. *Inorg. Chem.* **1984**, *23*, 315-321.
- [86] Bystrova, M. I.; Mal'gosheva, I. N.; Krasnovsky, A. A. *Mol. Biol.* **1979**, *13*, 440-451.
- [87] Smith, K. M.; Kehres, L. A.; Fajer, J. *J. Am. Chem. Soc.* **1983**, *105*, 1387-1389.
- [88] Dähne L. *J. Am. Chem. Soc.* **1995**, *117*, 12855-12860.
- [89] Wang, M.; Silva, G.L.; Armitage, B.A. *J. Am. Chem. Soc.* **2000**, *122*, 9977-9986.
- [90] Thalacker, C.; Würthner, F. *Adv. Funct. Mater.* **2002**, *12*, 209-218.
- [91] Schenning, A.P.H.J.; Herrikhuyzen, J.V.; Jonkheijm, P.; Chen, Z.; Würthner, F.; Meijer, E.W. *J. Am. Chem. Soc.* **2002**, *124*, 10252-10353.
- [92] von Berlepsh H., Kirstein S., Hania R., Didraga C., Pugžlys A., Böttcher C., *J. Phys. Chem.* **2003**, *107*, 14176-14184.

- [93] Ogoshi, H.; Mizutani, T.; Hayashi, T.; Kuroda, Y. In *The Porphyrin Handbook*; Kadish, K. M., Smith, K. M., Guillard, R., Eds.; Academic Press: San Diego, **2000**; Vol. 6, pp 280-340.
- [94] Weiss, J. J. *Inclusion Phenom. Macrocyclic Chem.* **2001**, *40*, 1-22.
- [95] Keller, D.; Bustamante, C. *Chem. Phys.* **1986**, *84*, 2972-2980.
- [96] Kim, M.-H.; Ulibarri, L.; Keller, D.; Maestre, M.F.; Bustamante, C. *J. Chem. Phys.* **1986**, *84*, 2981-2990.
- [97] Pescitelli, G.; Gabriel, S.; Wang, Y.; Fleischhauer, J.; Woody, R.W.; Berova, N. *J. Am. Chem. Soc.* **2003**, *125*, 7613-7628.
- [98] Berova, N.; Nakanishi, K. in *Circular Dichroism. Principles and Applications* 2nd ed. (Eds.: N. Berova, K. Nakanishi, R. W. Woody), Wiley-VCH, New York, **2000**, pp. 337–382.
- [99] Prokhorenko, V.I.; Steensgard, D.B.; Holzwarth, A.R.; *Biophys. J.* **2003**, *85*, 3173-3186.
- [100] Didraga, C.; Klugkist, J.A.; Knoester, J. *J. Phys. Chem. B*, **2002**, *106*, 11474-11486.
- [101] Kitamoto, H. Master Thesis **2002**, Ritsumeikan University, Kusatsu, Shiga, Japan; H. Tamiaki, H. Kitamoto, manuscript in preparation.
- [102] Berova, N.; Nakanishi, K. in *Circular Dichroism. Principles and Applications* 2nd ed. (Eds.: N. Berova, K. Nakanishi, R. W. Woody), Wiley-VCH, New York, **2000**, pp. 337–382.
- [103] Balaban, T. S.; Linke-Schaetzel, M.; Bhise, A. D.; Vanthuyne, N.; Roussel, C.; Anson, C.; Buth, G.; Eichhöfer, A.; Foster, K.; Garab, G.; Gliemann, H.; Goddard, R.; Javorfi, T.; Powell, A. K.; Rösner, H.; Schimmel, T. *Chem. Eur. J.* **2005**, *11*, 2267-2275.
- [104] Jelley, E. E. *Nature* **1936**, *138*, 1009.
- [105] Scheibe, G. *Angew. Chem.* **1936**, *49*, 563-563.
- [106] Higgins, D. A.; Reid, P. J.; Barbara, P. F. *J. Phys. Chem.* **1996**, *100*, 1174-1180.
- [107] Fukumoto, H.; Yonezawa, Y. *Thin Solid Films.* **1998**, *327-329*, 748-751.
- [108] Balaban, T. S.; Tamiaki, H.; Holzwarth, A. R.; Schaffner, K. *J. Phys. Chem.* **1997**, *101*, 3424–3431.
- [109] Balaban, T. S.; Goddard, R.; Linke-Schaetzel, M.; Lehn, J.-M. *J. Am. Chem. Soc.* **2003**, *125*, 4233-4239.
- [110] Jung, T. A.; Schlittler, R. R.; Gimzewski, J.K. *Nature*, **1997**, *386*, 696.
- [111] Gimzewski, J. K.; Joacghim, C. *Science*, **1999**, *283*, 1683-1688.
- [112] Eisen, J.A.; Nelson, K.E.; Paulsen, I.T.; Heidelberg, J.F.; Wu, M.; Dodson, R.J.; Deboy, R.; Gwinn, M.L.; Nelson, W.C.; Haft, D.H.; Hockey, E.K.; Peterson, J D.; Durkin, A.S.;

- Kolonay, J.L.; Yang, F.; Holt, I.; Umayam, L.A.; Mason, T.; Brenner, M.; Shea, T.P.; Parksey, D.; Nierman, W.C.; Feldblyum, T.V.; Hansen, C.L.; Crafen, M.B.; Radune, D.; Vamathevan, J.; Khouri, H.; White, O.; Gruber, T.M.; Ketchum, K.A.; Ventre, J.C.; Tettelin, H.; Bryant, D.A.; Fraser, C.M. *Proc. Natl. Acad. Sci. USA*. **2002**, *99*, 9509–9514.
- [113] Frigaard, N.-U; Gomez Maqueo Chew, A; Li, H; Maresca, J. A; Bryant, D. A. *Photosynth. Res.* **2003**, *78*, 93.
- [114] Balaban, T. S.; Eichhofer, A.; Lehn, J.-M. *Eur. J. Org. Chem.* **2000**, 4047–4057.
- [115] Tamiaki, H.; Kimura, S.; Rimura, T. *Tetrahedron*, **2003**, *59*, 7423-7435.
- [116] Hunter, C. A; Sanders, J K.M. *J. Am. Chem. Soc.* **1990**, *112*, 5525-5534.
- [117] Balaban, T. S.; Tamiaki, H.; Holzwarth, A. R.; Schaffner, K. *J. Phys. Chem. B*. **1997**, 3424-3431
- [118] Grätzel, M. *Pure. Appl. Chem.* **2001**, *73(3)*, 459–467.
- [119] O'Regan B.; Grätzel, M. *Nature*, **1991**, *353*, 737.
- [120] Nazeeruddin, M.K.; Pechy, P.; Renouard, T.; Zakeeruddin, S.M.; Humphry-Baker, R.; Comte, P.; Liska, P.; Cevey, L.; Costa, E.; Shklover, V.; Spiccia, L.; Deacon, G.B.; Bignozzi C. A.; Grätzel, M. *J. Am. Chem. Soc.*, **2001**, *123*, 1613-1623.
- [121] Kuciauskas, D.; Freund, M. S.; Gray, H. B.; Winkler J. R.; Lewis, N. S. *J. Phys. Chem. B*, **2001**, *105*, 392-403
- [122] Sauve, G.; Cass, M. E.; Doig, S. J.; Lauermann, I.; Pomykal, K.; Lewis, N.S. *J. Phys. Chem. B*, **2000**, *104*, 3488-3491.
- [123] Nazeeruddin, M. K.; Kay, A.; Rodicio, I.; Humphry-Baker, R.; Muller, E.; Liska, P.; Vlachopoulos, N.; Grätzel, M. *J. Am. Chem. Soc.* **1993**, *115*, 6382-6390.
- [124] Argazzi, R.; Bignozzi, C. A.; Heimer, T. A.; Castellano, F. N.; Meyer, G. J. *J. Inorg. Chem.* **1994**, *33*, 5741-5749.
- [125] Nazeeruddin, M. K.; Müller, E.; Humphry-Baker, R.; Vlachopoulos, N.; Grätzel, M. *J. Chem. Soc., Dalton Trans.* **1997**, 4571.
- [126] Nazeeruddin, M. K.; Péchy, P.; Grätzel, M. *J. Chem. Soc., Chem. Commun.* **1997**, 1705-1706
- [127] Argazzi, R.; Bignozzi, C. A.; Hasselmann, G. M.; Meyer, G. J. *Inorg. Chem.* **1998**, *37*, 4533-4537.
- [128] Ruile, S.; Kohle, O.; Pettersson, H.; Grätzel, M. *New J. Chem.* **1998**, 25-31.
- [129] Zakeeruddin, S. M.; Nazeeruddin, M K.; Humphry-Baker, R.; Grätzel, M. *Inorg. Chem.* **1998**, *37*, 5251-5259.

- [130] Jing, B.; Zhang, H.; Zhang, M.; Lu, Z.; Shen, T. *J. Mater. Chem.* **1998**, *8*, 2055-2060.
- [131] Islam, A.; Hara, K.; Singh, L. P.; Katoh, R.; Yanagida, M.; Murata, S.; Takahashi, Y.; Sugihara, H.; Arakawa, H. *Chem. Lett.* **2000**, 490-491.
- [132] Sauv e, G.; Cass, M. E.; Coia, G.; Doig, S. J.; Lauermann, I.; Pomykal, K. E.; Lewis, N. *S. J. Phys. Chem. B* **2000**, *104*, 6821-6836.
- [133] Kimberly, A. M.; Sykora, M.; DeSimone, J. M.; Meyer, T. J. *Inorg. Chem.* **2000**, *39*, 71-75.
- [134] Sugihara, H.; Singh, L. P.; Sayama, K.; Arakawa, H.; Nazeeruddin, M. K.; Gr tzel, M. *Chem. Lett.* **1998**, 1005-1006.
- [135] Yanagida, M.; Singh, L. P.; Sayama, K.; Hara, K.; Katoh, R.; Islam, A.; Sugihara, H.; Arakawa, H.; Nazeerddin, Md. K.; Gr tzel, M. *J. Chem. Soc., Dalton Trans.* **2000**, 2817.
- [136] Milgrom, L. R.; O'Neill, F. in *The Chemistry of Natural Products*, 2nd edn., ch. 8 'Porphyrins', ed. Thomson, R.H, Blackie Academic & Professional, London, **1993**, pp. 329-376.
- [137] Han, W.; Durantini, E. N.; Moore, T. A.; Moore, A. L.; Gust, D.; Rez, P.; Leatherman, G.; Seely, G.; Tao, N.; Lindsay, S. M. *J. Phys. Chem. B*, **1997**, *101*, 10719-10725.
- [138] Steinberg-Yfrach, G.; Rigaud, J.-L. Durantini, E.N.; Moore, A.L.; Gust, D.; Moore, T.A. *Nature*, **1998**, *392*, 479.
- [139] Bedja, I.; Kamat, P.V.; Hotchandani, S. *J. Appl. Phys.*, **1996**, *80*, 4637.
- [140] Kay, A.; Gr tzel, M. *J. Phys. Chem.*, **1993**, *97*, 6272-6277.
- [141] Memming, R. in *Comprehensive Treatise of Electrochemistry*, Plenum Press, New York, **1983**, vol. 7, p. 529.
- [142] Gerischer, H.; Willig, F. *Top. Curr. Chem.*, **1976**, *61*, 31-84.
- [143] Kay, A.; Humphry-Baker, R.; Gr tzel, M. *J. Phys. Chem.*, **1994**, *98*, 952-959.
- [144] Tachibana, Y.; Haque, S. A.; Mercer, I. P.; Durrant, J. R.; Klug, D. R. *J. Phys. Chem. B*, **2000**, *104*, 1198-1205.
- [145] Balaban, T. S.; Boender, G.-J.; Holzwarth, A. R.; Schaffner, K.; de Groot, H.J.M. *Biochemistry*. **1995**, *34*, 15259-15266.
- [146] Chieffari, J.; Griebenow, K.; Fages, F.; Griebenow, N.; Balaban, T.S.; Holzwarth, A.R.; Schaffner, K. *J. Phys. Chem.* **1995**, *99*, 1357-1365.
- [147] Balaban, T. S.; Holzwarth, A. R.; Schaffner, K. *J. Mol. Struct.* **1995** *349* 183-186.